UNIVERSIDADE ESTADUAL DE CAMPINAS
FACULDADE DE ENGENHARIA DE ALIMENTOS

PHILIPE DOS SANTOS

PRODUÇÃO DE ÉSTERES DE AROMAS POR REAÇÕES CATALISADAS POR ENZIMAS EM DIÓXIDO DE CARBONO (CO_2) SUPERCRÍTICO

PRODUCTION OF AROMA ESTERS BY ENZYMATIC-CATALYZED REACTIONS IN SUPERCRITICAL CARBON DIOXIDE (CO_2)

CAMPINAS-SP
2017

PHILIPE DOS SANTOS

PRODUÇÃO DE ÉSTERES DE AROMAS POR REAÇÕES CATALISADAS POR ENZIMAS EM DIÓXIDO DE CARBONO (CO_2) SUPERCRÍTICO

PRODUCTION OF AROMA ESTERS BY ENZYMATIC-CATALYZED REACTIONS IN SUPERCRITICAL CARBON DIOXIDE (CO_2)

Tese de doutorado apresentada à Faculdade de Engenharia de Alimentos da Universidade Estadual de Campinas como parte dos requisitos exigidos para a obtenção do título de Doutor em Engenharia de Alimentos.

Thesis presented to the School of Food Engineering of the University of Campinas in partial fulfillment of the requirements for the degree of Doctor, in the area of Food Engineering.

Supervisor/Orientador: **PROF. DR. JULIAN MARTÍNEZ**

ESTE EXEMPLAR CORRESPONDE À VERSÃO FINAL TESE DEFENDIDA PELO ALUNO PHILIPE DOS SANTOS, E ORIENTADA PELO PROF. DR. JULIAN MARTÍNEZ

CAMPINAS-SP

2017

Agência(s) de fomento e nº(s) de processo(s): CNPq, 142373/2013-3; FAPESP, 2015/11932-7

Ficha catalográfica
Universidade Estadual de Campinas
Biblioteca da Faculdade de Engenharia de Alimentos
Claudia Aparecida Romano - CRB 8/5816

Santos, Philipe dos, 1987-
Sa59p Produção de ésteres de aromas por reações catalisadas por enzimas em dióxido de carbono (CO_2) supercrítico / Philipe dos Santos. – Campinas, SP : [s.n.], 2017.

Orientador: Julian Martínez.
Tese (doutorado) – Universidade Estadual de Campinas, Faculdade de Engenharia de Alimentos.

1. Fluido supercrítico. 2. Dióxido de carbono. 3. Lipase. 4. Acetato de eugenila. 5. Acetato de isoamila. I. Martínez, Julian. II. Universidade Estadual de Campinas. Faculdade de Engenharia de Alimentos. III. Título.

Informações para Biblioteca Digital

Título em outro idioma: Production of aroma esters by enzymatic-catalyzed reactions in supercrítical carbon dioxide (CO_2)
Palavras-chave em inglês:
Supercritical fluid
Carbon dioxide
Lipase
Eugenyl acetate
Isoamyl acetate
Área de concentração: Engenharia de Alimentos
Titulação: Doutor em Engenharia de Alimentos
Banca examinadora:
Julian Martínez [Orientador]
Ruann Janser Soares de Castro
Roberta Ceriani
Elton Franceschi
Helen Treichel
Data de defesa: 27-01-2017
Programa de Pós-Graduação: Engenharia de Alimentos

BANCA EXAMINADORA

Prof. Dr. Julian Martínez
Orientador
Faculdade de Engenharia de Alimentos – UNICAMP

Prof. Dr. Ruann Janser Soares de Castro
Membro Titular
Faculdade de Engenharia de Alimentos – UNICAMP

Prof.ª Dr.ª Roberta Ceriani
Membro Titular
Faculdade de Engenharia de Engenharia Química – UNICAMP

Prof. Dr. Elton Franceschi
Membro Titular
Universidade Tiradentes - UNIT

Prof.ª Dr.ª Helen Treichel
Membro Titular
Universidade Federal da Fronteira Sul - UFFS

Prof. Dr. Marcus Bruno Soares Forte
Membro Suplente
Faculdade de Engenharia de Alimentos – UNICAMP

Prof.ª Dr.ª Gabriela Alves Macedo
Membro Suplente
Faculdade de Engenharia de Alimentos – UNICAMP

Prof. Dr. Lúcio Cardozo Filho
Membro Suplente
Universidade Estadual de Maringá - UEM

A ata da Defesa com as respectivas assinaturas dos membros encontra-se no processo da vida acadêmica do aluno.

Dedico esse trabalho a todas as pessoas que acreditaram na minha capacidade e me incentivaram durante o desenvolvimento do mesmo. Em especial aos meus queridos pais e a minha filha Estela.

AGRADECIMENTOS

Ao professor Dr. Julian Martínez pela atenção, incentivo e todas as ideias e correções do trabalho. Muito obrigado.

À professora Drª Maria Angela de Almeida Meireles pelo apoio no desenvolvimento do trabalho, especificamente nos experimentos de cromatografia gasosa e equilíbrio de fases. Muito obrigado.

À professora Drª Camila Alves de Rezende pela paciência, ideias e o apoio no desenvolvimento do trabalho, especificamente nos experimentos de microscopia. Muito obrigado.

Ao Laboratório Nacional de Natotecnologia (LNNano), vinculado ao Centro Nacional de Pesquisa em Energia e Materiais (CNPEM), pelo apoio nos experimentos de microscopia eletrônica de varredura, que foram realizados no microscópio FESEM Quanta 650F (FEI).

Agradeço sinceramente aos membros da banca examinadora pelas correções e sugestões.

Ao Ari pela amizade, atenção e ajuda com os equipamentos que operam com fluidos supercríticos.

Ao CNPq e FAPESP pelo financiamento do trabalho.

À minha família por todo amor e incentivo durante o período de doutorado.

À minha esposa Renata por toda a compreensão e incentivo.

Aos colegas do Departamento de Engenharia de Alimentos, em especial aos amigos do Laboratório de Alta Pressão em Engenharia de Alimentos (LAPEA). Muito obrigado.

"*Todos começamos com o "realismo ingênuo", isto é, a doutrina de que as coisas são aquilo que parecem ser. Achamos que a grama é verde, que as pedras são duras e que a neve é fria. Mas a física nos assegura que o verdejar da grama, a dureza das pedras e a frieza da neve não são o verdejar da grama, a dureza das pedras e a frieza da neve que conhecemos em nossa experiência própria, e sim algo muito diferente".*

O filósofo e matemático britânico Bertrand Russell *apud* MLODINOW, L. O Andar do Bêbado: como o acaso determina nossas vidas; [tradução Alfaro D.; consultoria Jurkiewicz, S.] – Rio de Janeiro: Zahar, 2009.

RESUMO

A utilização de dióxido de carbono (CO_2) supercrítico como meio reacional ganhou atenção nos últimos anos devido ao seu caráter atóxico, não inflamável, inerte, não poluente e totalmente recuperável e reutilizável. Do mesmo modo, a descoberta de que algumas enzimas são estáveis em meio reacional não aquoso expandiu a sua aplicação em reações de síntese orgânica, como por exemplo, reações de produção de ésteres de aromas biocatalisadas por lipases em CO_2 supercrítico como meio reacional. No entanto, poucas pesquisas avaliam a produção de ésteres de aromas utilizando CO_2 supercrítico em reatores contínuos. Em vista disso, o objetivo do presente trabalho foi a avaliação técnica de reações químicas biocatalisadas utilizando CO_2 supercrítico como meio reacional em uma unidade operada em batelada e em modo contínuo. Inicialmente, foi projetada e construída uma unidade de reações químicas a alta pressão. Posteriormente, foram estudadas a estabilidade e a atividade de uma lipase imobilizada comercial em meio supercrítico. Após esta etapa, as produções de acetato de eugenila e acetato de isoamila em CO_2 supercrítico foram avaliadas, com o objetivo de verificar a influência das variáveis do processo sobre a taxa de esterificação (X; %) , produtividade (P; kg/h) e produtividade específica (SP; kg/kg.h). Por fim, foi realizado o estudo do processo de transferência de massa no reator em batelada e da produção de acetato de isoamila em modo contínuo. Os resultados obtidos evidenciaram que a exposição da enzima imobilizada comercial Lipozyme 435 ao CO_2 supercrítico reduziu a sua atividade catalítica em todas as condições experimentais testadas. Apesar da diminuição da atividade catalítica, em torno de 10% para as melhores condições, foi possível obter altos valores de taxa de esterificação e rendimento de acetato de eugenila (50% de X) e acetato de isoamila (100% de X) em condições operacionais específicas. Experimentos em modo contínuo resultaram em uma baixa conversão (aproximadamente 30%), porém altos valores de produtividade (10 g/h) em comparação com os valores obtidos para reações em batelada (0,35 g/h). Pode-se concluir que a aplicação da tecnologia supercrítica em reações químicas catalisadas por enzimas, especificamente em CO_2 supercrítico, é viável tecnologicamente.

Palavras-chave: fluido supercrítico, dióxido de carbono; lipase, acetato de eugenila, acetato de isoamila.

ABSTRACT

The use of supercritical carbon dioxide (CO_2) as reaction medium has gained attention in recent years due to their non-toxic, non-flammable, inert, non-polluting and recoverable characteristics of this solvent. Besides, the discovery that some enzymes are stable in non-aqueous reaction media has expanded the applicability of enzymes in organic synthesis reactions, such as the production of terpenic esters catalyzed by lipases in supercritical CO_2. However, few studies evaluate the production of aromatic esters using supercritical CO_2 in continuous mode. Therefore, the objective of this work is the scientific evaluation of chemical reactions catalyzed by lipases using supercritical CO_2 as reaction medium in a homemade unit that operates in batch and continuous flow modes. First, the high-pressure unit was designed and assembled. Next, the study of stability and activity of an immobilized lipase in supercritical media was performed. After this step, the production of eugenyl acetate and isoamyl acetate in supercritical CO_2 was evaluated, aiming to verify the influence of process variables on the esterification rate (X; %), productivity (P; kg/h) and specific productivity (SP; kg/kg.h). Finally, the mass transfer analyses in the batch reactor and the production of isoamyl acetate in continuous mode were performed. The results showed that the exposure of the commercial immobilized enzyme Lipozyme 435 to supercritical CO_2 reduced its catalytic activity in all experimental conditions. In spite of the decreased residual activity, about 10% in optimal condition, it was possible to obtain high esterification rate, productivity and specific productivity of eugenyl acetate (50% of X) and isoamyl acetate (100% of X) in specific operating conditions. Continuous mode experiments showed lower conversion (about 30%), but higher productivity (10 g/h) than those obtained in the batch reactor (0.35 g/h). It is possible to conclude that the application of supercritical fluid technology in chemical reactions, in particular with supercritical CO_2, is technically viable.

Keywords: supercritical fluid; carbon dioxide; lipase; eugenyl acetate, isoamyl acetate.

SUMÁRIO

CAPÍTULO 1 14

1.1 INTRODUÇÃO 15

1.2 OBJETIVOS 17

1.2.1 Objetivo geral 17

1.2.2 Objetivos específicos 17

1.3 ESTRUTURA DA TESE 18

CAPÍTULO 2 19

2.1 REVISÃO BIBLIOGRÁFICA 20

2.1.1 Ésteres de aromas 20

2.1.2 Enzimas 22

2.1.2.1 Lipases 23

2.1.5 Cinética de reação enzimática 26

2.1.4 Reatores químicos 32

2.1.5 Fluidos supercríticos 38

2.1.6 Atividade enzimática em fluidos supercríticos 41

2.1.7 Produção de ésteres de aromas em fluidos supercríticos 43

Referências Bibliográficas 48

CAPÍTULO 3 55

3.1 INTRODUCTION 59

3.2 MATERIALS AND METHODS 60

3.2.1 Materials and chemicals 60

3.2.2 Lipase activity 61

3.2.3 Apparatus and experimental procedure 61

3.2.3.1 Lipase treatment 61

3.2.3.2 Catalytic tests 63
3.2.4 Estimation of kinetic data and thermodynamic parameters 64
3.2.5 Fourier transform infrared spectroscopy (FT-IR) 65
3.2.6 Field emission scanning electron microscopy (FESEM) 66
3.2.7 Statistical analysis 67
3.3 RESULTS AND DISCUSSION 67
3.3.1 Effect of supercritical carbon dioxide on the lipase activity 67
3.3.2 Structural analysis 72
3.3.3 Effect of supercritical CO_2 on the esterefication reaction 75
3.4 CONCLUSIONS 77
3.5 ACKNOWLEDGMENTS 78
3.6 REFERENCES 78
CAPÍTULO 4 83
4.1 INTRODUCTION 87
4.2 MATERIALS AND METHODS 88
4.2.1 Materials 88
4.2.2 Characterization of the enzymes 88
4.2.3 Synthesis of eugenyl acetate in SC-CO_2 90
4.2.4 Phase behavior experiments 92
4.2.5 Analytical methods 93
4.2.6 Kinetic model 93
4.2.7 Statistical analysis 95
4.3 RESULTS AND DISCUSSION 95
4.3.1 Effect of the enzyme concentration 95
4.3.2 Effect of acetic anhydride and eugenol molar ratio 97
4.3.3 Effect of pressure and temperature of SC-CO_2 99
4.3.4 Reuse of Lipozyme 435 101

4.3.5 Kinetic experiments 103
4.4 CONCLUSIONS 106
4.5 ACKNOWLEDGEMENTS 107
4.6 APPENDIX A: Supplementary data 108
4.7 REFERENCES 109
CAPÍTULO 5 113
5.1 INTRODUCTION 117
5.2 MATERIALS AND METHODS 118
5.2.1 Materials 118
5.2.2 Particle characterization 118
5.2.3 Synthesis of isoamyl acetate in SC-CO_2 119
5.2.4 Analytical methods 122
5.2.5 Modeling of Mass Transfer in Batch Reactor 123
5.2.6 Kinetic and Reactor Modeling 125
5.2.7 Statistical Analysis 127
5.3 RESULTS AND DISCUSSION 127
5.3.1 Preliminary experiments 127
5.3.2 Fractional Factorial Design 128
5.3.3 Mass Transfer Effects in Batch Reactor 131
5.3.4 Kinetics Modeling 134
5.3.5 Production Continues Packed Bed Reactor 137
5.4 CONCLUSIONS 140
5.5 AKNOWLEDGEMENT 141
5.6 APPENDIX A: Supplementary data 141
5.7 REFERENCES 143
CAPÍTULO 6 146

6.1 DISCUSSÕES GERAIS 147

CAPÍTULO 7 152

7.1 CONCLUSÃO GERAL 153

7.2 SUGESTÕES PARA TRABALHOS FUTUROS 156

CAPÍTULO 8 157

REFERÊNCIAS BIBLIOGRÁFICAS 158

APÊNDICE 180

I Montagem da Unidade de Reação Química 181

I. I Esquema da Unidade Reações Químicas em Modo Batelada 186

I. II Esquema da Unidade Reações Químicas em Modo Contínuo 187

I. III Calculo da Carga Térmica do Sistema de Refrigeração e Aquecimento 188

I. IV Reator em Batelada 198

I. V Reator Contínuo 198

I. VI Separador 200

II Manual de Operação da Unidade de Reações Químicas 201

II. I Operação em Modo Batelada 201

II. II Operação em Modo Contínuo 203

III Normalização e Análise dos Dados de FT-IR 205

IV Ajuste não-linear do modelo de Ping-Pong Bi-Bi I 209

V Ajuste não-linear do modelo de Ping-Pong Bi-Bi II 211

VI Curvas de Calibração 218

VII Cromatogramas 221

Referências Bibliográficas 222

Memorial do Período de Doutorado 223

ANEXOS 225

I Permissão para o uso do artigo correspondente ao capítulo 3 226

II Permissão para o uso do artigo correspondente ao capítulo 4 232

CAPÍTULO 1

INTRODUÇÃO, ESTRUTURA E OBJETIVOS

1.1 INTRODUÇÃO

Ésteres de aromas derivados de cadeias curtas de ácidos, como acetatos, propionatos e butiratos são largamente utilizados na indústria de alimentos, pois possuem aromas característicos de frutas. (HARI KRISHNA *et al.*, 2001; COUTO *et al.*, 2011; DHAKE *et al.*, 2013). Tais ésteres são encontrados naturalmente em matrizes vegetais, porém a extração e purificação desses aromas exigem recursos técnicos específicos. Assim sendo, a síntese química de tais compostos torna-se viável do ponto de vista tecnológico e econômico, porém o uso indiscriminado de solventes orgânicos e catalisadores químicos tornam este processo pouco atrativo do ponto de vista ambiental, além disso, o processo químico convencional pode gerar compostos indesejáveis para futuras aplicações em produtos alimentícios ou farmacológicos. Assim sendo, a síntese enzimática se torna de grande interesse devido ao seu caráter quimio, regio, e estereosseletivo, possibilitando a síntese de enantiômeros de ésteres aromáticos de origem natural (DHAKE *et al.*, 2013). Adicionalmente, o éster de aroma obtido pode ser considerado natural, desde que o processo atenda a legislação vigente e utilize matérias-primas naturais (HARI KRISHNA *et al.*, 2001; DHAKE *et al.*, 2011a; DHAKE *et al.*, 2013).

Os processos bioquímicos para produção de ésteres de aroma podem empregar lipases (glicerol éster hidrolases, EC 3.1.1.3) (JAEGER e EGGERT, 2002) de origem animal ou microbiana como catalisadoras das reações de formação. Diversos trabalhos de obtenção de ésteres de aroma podem ser encontrados na literatura, tais como acetato de isoamila (aroma de banana) (HARI KRISHNA *et al.*, 2001; ROMERO *et al.*, 2005), butirato de isoamila (aroma de pera) (SRIVASTAVA *et al.*, 2002; MACEDO *et al.*, 2004) e acetato de cinamila (componente do óleo essencial de canela) (DHAKE *et al.*, 2011b). Além disso, estudos demonstraram a estabilidade das lipases em fluidos pressurizados, o que aumentou o potencial de uso dessas enzimas em diferentes reações (KNEZ, 2009; MONHEMI e HOUSAINDOKHT, 2012; KNEZ *et al.*, 2015; MELGOSA *et al.*, 2015). A utilização de fluidos supercríticos como meio reacional tem demonstrado vantagens frente a outros solventes, tais como alta difusividade e baixa viscosidade, as quais podem facilitar a transferência de massa de substrato para o interior do sítio ativo da enzima.

A descoberta de que algumas enzimas, tais como proteases (GUPTA e KHARE, 2006), lipases (VERMA *et al.*, 2008) e peroxidases (DORDICK *et al.*, 1987) são estáveis e ativas em solventes orgânicos ampliou imensamente o alcance das suas aplicações como catalisadores em reações de síntese orgânica. Logo, substratos insolúveis em água podem ser transformados através de catalisadores enzimáticos em meios não aquosos, abrindo novas rotas de síntese para produtos alimentícios e/ou farmacêuticos (WIMMER e ZAREVÚCKA, 2010; KNEZ *et al.*, 2015). No entanto, a preocupação mundial com a saúde do consumidor, a proteção ao meio ambiente e as preocupações com as mudanças climáticas impulsionaram a redução na utilização de solventes orgânicos em processos químicos. Portanto, há um interesse considerável em substituir os processos que usam tais solventes.

O dióxido de carbono (CO_2) supercrítico é frequentemente apresentado como um meio reacional alternativo para a síntese química (LAUDANI *et al.*, 2007; KNEZ, 2009; KNEZ *et al.*, 2015), devido ao seu caráter atóxico, não inflamável, inerte, não poluente, totalmente recuperável e de baixo custo. Além disso, o CO_2 apresenta condições críticas de pressão e temperatura relativamente amenas (7,38 MPa e 304,2 K, respectivamente), comparado a outros solventes de grau alimentício, o que permite a preservação de compostos e catalisadores termicamente instáveis (KERN, 1987; RAVENTOS *et al.*, 2002; REVERCHON e DE MARCO, 2006). No estado supercrítico, o CO_2 apresenta propriedades tanto de um gás como de um líquido, ou seja, sua densidade se aproxima de um líquido, enquanto a sua viscosidade é próxima à de um gás. Isto torna o CO_2 supercrítico um bom solvente e ao mesmo tempo um eficiente meio de transferência de massa (MATSUDA *et al.*, 2004).

Devido ao exposto, a proposta principal deste trabalho consiste em estudar as reações de obtenção de ésteres de aromas utilizando CO_2 supercrítico como meio reacional. Adicionalmente, estudaram-se tais reações em um reator em batelada e em modo contínuo, e analisou-se a influência dos parâmetros do processo sobre as reações em estudo e a atividade e estabilidade enzimática.

1.2 OBJETIVOS

1.2.1 Objetivo geral

Avaliar a viabilidade técnica de reações biocatalisadas por lipases imobilizadas comerciais utilizando CO_2 supercrítico como meio reacional em reatores batelada e contínuo

1.2.2 Objetivos específicos

- Projetar e montar uma unidade de reações à alta pressão utilizando CO_2 supercrítico;
- Avaliar a estabilidade e a atividade enzimática de uma lipase comercial em CO_2 supercrítico;
- Realizar as reações de formação de acetato de eugenila e acetato de isoamila em CO_2 supercrítico em modo batelada;
- Estudar os parâmetros que afetam a formação de ésteres de aromas, acetato de eugenila e acetato de isoamila, tais como: temperatura, pressão, concentração enzimática, concentração de substrato (reagentes) e ciclos de reutilização.
- Realizar as reações de formação de acetato de isoamila em CO_2 supercrítico em modo contínuo nas condições ótimas de conversão obtidas.

1.3 ESTRUTURA DA TESE

Nesta tese, as etapas de desenvolvimento do projeto de pesquisa são apresentadas em seis (8) capítulos. No **Capítulo 1** são expostos o tema principal do estudo, o objetivo geral e os objetivos específicos envolvidos na realização do projeto. No **Capítulo 2** encontra-se uma breve revisão teórica sobre reações químicas, enzimas, cinética enzimática e atividade enzimática em fluidos supercríticos. Os **Capítulos 3, 4 e 5** consistem em artigos publicados ou submetidos para publicação em periódicos internacionais. No **Capítulo 3** são apresentados os resultados experimentais da pesquisa de estabilidade e atividade enzimática em dióxido de carbono supercrítico. No artigo publicado são avaliados fatores de processo como, por exemplo, temperatura, pressão, ciclos de pressurização/despressurização e tempo de exposição ao CO_2 supercrítico sobre a atividade enzimática. Além disso, são apresentados dados termodinâmicos e análises estruturais da enzima imobilizada comercial Lipozyme 435. Posteriormente, com base nos resultados obtidos para estabilidade enzimática, no **Capítulo 4,** a reação de esterificação de eugenol em meio supercrítico é avaliada. Neste capítulo, reações de síntese de acetato de eugenila foram efetuadas em diferentes condições de processo, cinéticas reacionais e a eficiência de reutilização do catalisador são apresentadas. O **Capítulo 5** apresenta o estudo dos dois modelos de reator (batelada e contínuo) na produção de acetato de isoamila. Modelagem matemática, estudo da transferência de massa e cálculos de produtividade são efetuados neste artigo. Por fim, no **Capítulo 6,** uma discussão geral é realizada e no **Capítulo 7** são apresentadas, sucintamente, as principais conclusões oriundas do desenvolvimento deste projeto e sugestões para trabalhos futuros. O **Capítulo 8** apresenta as referências bibliográficas e no **Apêndice** são apresentadas informações das etapas de projeto e montagem da unidade de reações químicas a alta pressão, bem como dados e os algoritmos usados neste projeto. Por fim, os **Anexos** apresentam as licenças para utilização dos artigos publicados neste documento.

CAPÍTULO 2

REVISÃO BIBLIOGRÁFICA

2.1 REVISÃO BIBLIOGRÁFICA

2.1.1 Ésteres de aromas

Ésteres de ácidos carboxílicos são compostos naturais utilizados na indústria alimentícia que contribuem na formação dos aromas em alimentos. Os ésteres de baixa massa molecular representam uma importante classe de aromas, sendo que muitos deles são responsáveis por odores de frutas e são constituídos principalmente por compostos derivados de ácidos de cadeia curta como acetatos, propionatos e butiratos (HARI KRISHNA *et al.*, 2001; DHAKE *et al.*, 2013).

A demanda mundial de aromas e fragrâncias de grau alimentício, incluindo suas misturas, óleos essenciais e outros extratos aromáticos naturais, representou uma movimentação de cerca de 23,5 milhões de dólares em 2014, um aumento de 4,23% por ano em relação a 2012 (DHAKE *et al.*, 2013). Mais recentemente, a revista especializada em aromas de grau alimentício Markets & Markets (MARKETS, September 2015) prevê um crescimento no mercado de aromas alimentícios a uma taxa de crescimento anual composta (*Compound Annual Growing Rate* - CAGR) de 5,4% entre 2015 e 2020. O grupo Freedonia, em seu relatório intitulado "*World Flavors & Fragrances"* (GROUP, 2012), prevê uma aumento na demanda de aromas e fragrâncias de 4,4% ao ano, atingindo cerca de US$ 26 bilhões ao final de 2016. Apesar dessa perspectiva de crescimento, as indústrias produtos de insumos alimentícios e de alimentos vêm sendo influenciadas pelo aumento da exigência dos consumidores por produtos naturais e com apelos nutricionais, tais como produtos com baixo índice de gordura, sódio e açúcar e a busca por alimentos com corantes naturais, atividade antioxidante, e contendo pré e probióticos.

Os ésteres de aromas estão presentes em óleos essenciais e são conhecidos pelas suas propriedades flavorizantes e aromatizantes. Atualmente são utilizados pelas indústrias farmacêuticas e alimentícias como aditivos e melhoradores de *flavour*. A maioria dos ésteres de aromas utilizados na indústria é de origem natural e muitos deles são difíceis de isolar a partir de uma matriz vegetal, tornando os processos de extração e purificação inviáveis do ponto de vista econômico. Por outro lado, a síntese química convencional conduz à formação de produtos indesejáveis para o uso na indústria alimentícia e farmacêutica. Assim, a síntese enzimática se torna de grande interesse

devido ao seu caráter quimio, regio e estereosseletivo, possibilitando a síntese de enantiômeros de ésteres aromáticos de origem natural (DHAKE *et al.*, 2013).

Vários ésteres de aromas têm sido obtidos através da extração a partir de fontes naturais ou por meio da síntese química a um custo elevado, devido ao grau de pureza e à estereospecificidade requeridos. Os ésteres produzidos por síntese química não podem ser considerados aromas naturais, portanto são menos valorizados no mercado que os ésteres de fontes naturais. No entanto, ésteres obtidos através de processos biotecnológicos podem ser considerados naturais (HARI KRISHNA *et al.*, 2001; DHAKE *et al.*, 2011b; DHAKE *et al.*, 2013). Porém, algumas condições devem ser garantidas para assegurar que o produto final seja considerado natural, tais como: a matéria-prima ou os substratos utilizados devem ser naturais; e devem-se empregar somente processos físicos ou biotecnológicos para o isolamento ou purificação dos produtos formados, por exemplo, extração, destilação e concentração (MACEDO, 1997). Pode-se encontrar na literatura vários estudos de síntese enzimática de ésteres de aromas, tais como acetato de isoamila (aroma de banana) (HARI KRISHNA *et al.*, 2001; ROMERO *et al.*, 2005), butirato de isoamila (aroma característico de pera) (SRIVASTAVA *et al.*, 2002; MACEDO *et al.*, 2004) e acetato de cinamila (componente do óleo essencial de canela) (DHAKE *et al.*, 2011c).

A Figura 1 mostra a reação de formação de ésteres a partir do anidrido acético com doador do grupo acetil (ROMERO *et al.*, 2005; DHAKE *et al.*, 2013).

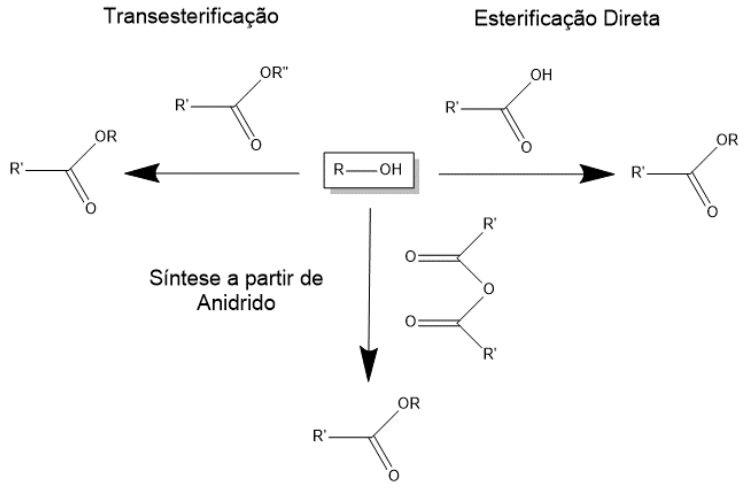

Figura 1 – Reação de formação de ésteres a partir do anidrido acético com doador do grupo acetil. Adaptado de Romero *et al*. (2005)

O ácido acético tem sido tradicionalmente usado como doador acil para a formação de ésteres (esterificação direta) de aromas (RAZAFINDRALAMBO *et al.*, 1994). Por outro lado, vários trabalhos científicos relatam uma inibição da atividade enzimática pela alta concentração de ácido (HARI KRISHNA *et al.*, 2001), provavelmente devido a uma diminuição do pH no sistema reacional. Além disso, o ácido acético pode ser um inibidor da lipase, pois reage com os resíduos do aminoácido serina no sítio ativo da enzima (HUANG *et al.*, 1998). Alternativamente, a síntese de ésteres pode ser realizada por transesterificação com acetatos e por acilação com anidrido acético (ROMERO *et al.*, 2005).

2.1.2 Enzimas

Enzimas são proteínas com sítios ativos capazes de catalisar uma determinada reação química. Elas são consideradas catalisadores naturais que aceleram a velocidade das reações, que em certos casos podem alcançar valores 10^{12} vezes maiores do que as reações não catalisadas. Além disso, são altamente versáteis na catálise de vários tipos de reações que ocorrem sob condições brandas. O intervalo de massa molecular de enzimas varia de 8 até 4.600 kDa, dependendo do número de subunidades de aminoácidos em sua estrutura (DAMODARAN *et al.*, 2008).

As principais enzimas são compostas por subunidades de aminoácidos, entre 62 a 2.500 resíduos de aminoácidos, combinados com ligações peptídicas. Os resíduos de aminoácidos formam ligações entre si através do grupo amino do aminoácido com o grupo carboxílico de outro aminoácido, gerando cadeias polipeptídicas extensas que formam uma estrutura espacial complexa. As ligações entre os aminoácidos são classificadas como estrutura primária, e quando organizadas, essas cadeias podem tomar formas diferentes, devido à mobilidade da cadeia como, por exemplo, as estruturas em forma de folha, fita ou hélice (Estrutura secundária). Por fim, o arranjo dos elementos na estrutura secundária e as interações das cadeias laterais de aminoácidos definem a estrutura tridimensional, ou estrutura terciária da enzima (COPELAND, 2002; DAMODARAN *et al.*, 2008).

As enzimas podem ser classificadas em seis classes principais, com base na natureza da reação: 1 - Oxidoredutases; 2 - Transferases; 3 - Hidrolases; 4 - Liases; 5 – Isomerases e 6 – Ligases (KNEZ, 2009). Dentre tais classes, pode-se destacar as

enzimas da classe transferases, que são aplicadas na síntese de ésteres aromáticos e as hidrolases, entre as quais se destacam as lipases, devido à gama de reações catalisadas em sistemas orgânicos com baixo teor de água e à alta estabilidade nesses ambientes.

2.1.2.1 Lipases

As lipases (glicerol éster hidrolases, EC 3.1.1.3) são pertencentes ao grupo das hidrolases e são responsáveis por catalisar a reação de hidrólise de ésteres de gliceróis e cadeias longas de ácidos graxos, liberando moléculas de álcool e ácido (JAEGER *et al.*, 1999). As lipases também são capazes de catalisar reações de esterificação, transesterificação e lactonização (esterificação intramolecular) (MACEDO, 1997). Estas enzimas são encontradas naturalmente em tecidos animais, vegetais e em micro-organismos, apresentando um papel fundamental no metabolismo de lipídios destes seres vivos (VILLENEUVE *et al.*, 2000). A Figura 2 ilustra reações catalisadas por lipases.

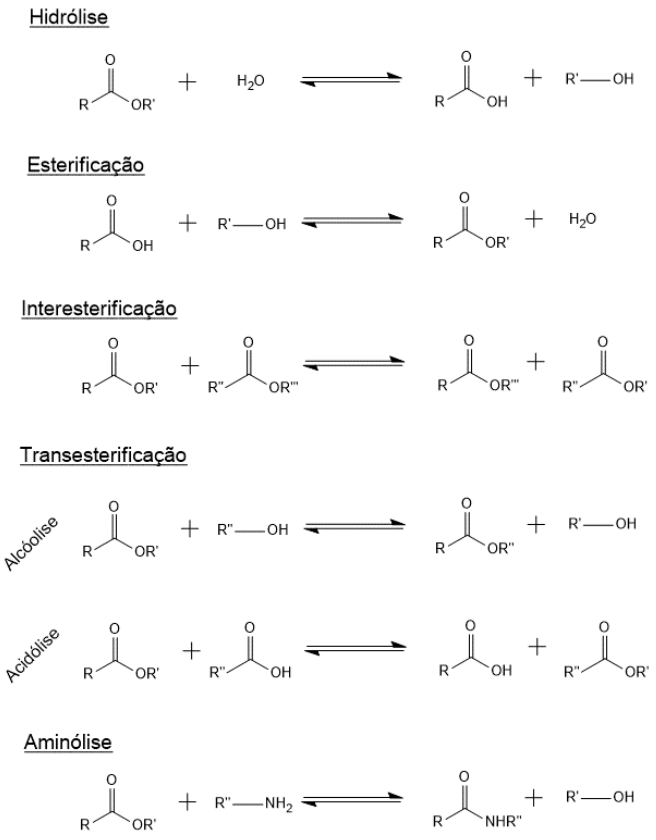

Figura 2 – Reações catalisadas por lipases. Adaptado de Macedo (1997).

A estrutura cristalina da lipase proveniente do micro-organismo *Candida antartica* foi resolvida em 1994 por Uppenberg *et al*. (1994), e apresenta uma estrutura α/β hidrolase constituída de 317 aminoácidos e uma massa molecular de 33 kDa. A estrutura secundária é constituída por sete folhas centrais que são flanqueadas em ambos os lados por 10 α-hélices. Segundo Skjot *et al*. (2009), duas estruturas hélices têm papéis importantes na atividade da lipase, a α5 (resíduo de aminoácido 139-150) e a α10 (resíduo 266-289), pois ambas interagem diretamente com o sítio ativo da enzima.

O sítio ativo (cavidade catalítica) das lipases geralmente é formado por três resíduos de aminoácidos, chamados de tríade catalítica, um resíduo nucleofílico (serina), um resíduo ácido catalítico (aspartato) e um resíduo de histidina (JAEGER *et al.*, 1999). A Figura 3 apresenta a rota reacional de hidrólise ou esterificação de uma lipase em sua cavidade catalítica.

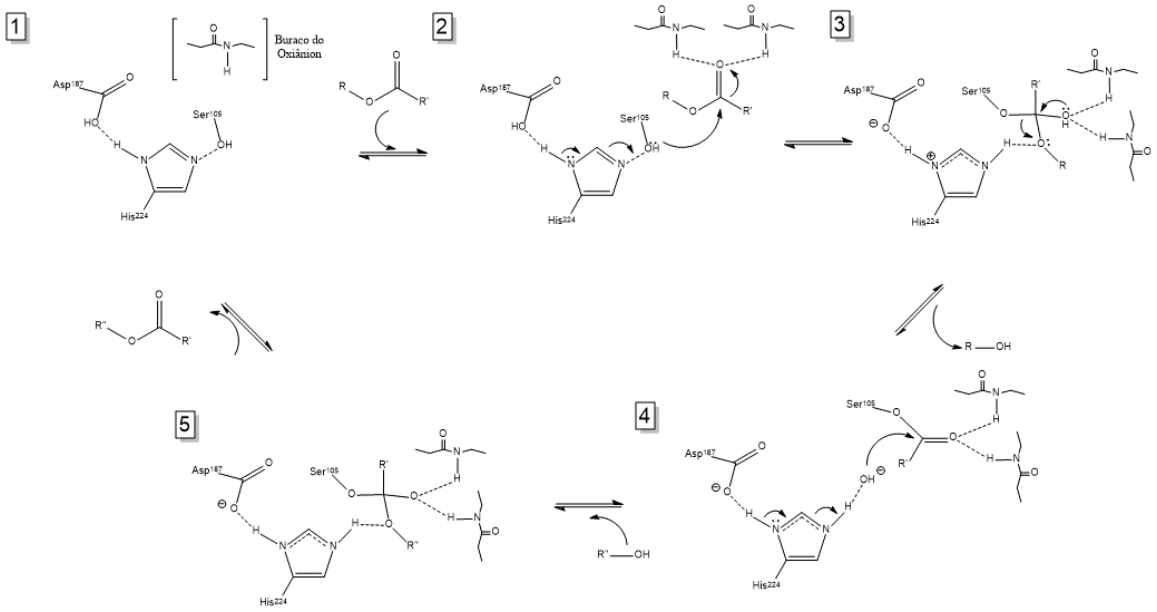

Figura 3 – Mecanismo reacional da lipase. [1] Tríade catalítica e o buraco oxiânion. [2] Ativação da serina nucleofílica e ataque ao átomo da carbonila. [3] Intermediário tetraédrico estabilizado pela interação entre grupos NH de peptídeos. [4] Intermediário covalente. [5] Quebra da ligação éster entre a serina e o componente acil e a liberação do produto. Adaptado de Jaeger *et al*., (1999) e Li *et al*., (2010).

A hidrólise de ésteres ou esterificação de álcoois, dependendo dos radicais R e R’ do substrato, ocorre em duas grandes etapas. Primeiramente, a reação se inicia com o ataque nucleofílico ao carbono do grupo éster, ligação C=O, através do átomo de

oxigênio presente no grupo hidroxila da serina (Ser). Assim, um intermediário tetraédrico, caracterizado pela carga negativa do oxigênio da carbonila e o arranjo tetraédrico do átomo de carbono, é formado e estabilizado por ligações de hidrogênio com os grupos amidas dos resíduos pertencentes ao chamado cavidade do oxiânion. As cargas formadas são neutralizadas através da orientação do anel imidazol da histidina (His) pela transferência de um próton do grupo hidroxila da serina, no qual é facilitada pela presença do ácido catalítico e o aspartato (Asp), por sua vez, estabiliza a carga positiva formada na histidina. O intermediário tetraédrico formado é desfeito, pelo retorno da ligação C=O, e consequentemente ocorre a clivagem da ligação éster, a liberação de uma molécula de álcool ou ácido, dependendo do radical R do substrato, e a formação do intermediário covalente acil enzima (JAEGER *et al.*, 1999).

A etapa seguinte é a desacetilação, em que uma molécula de água hidrolisa ou uma molécula de álcool esterifica o intermediário covalente (acil enzima). No caso de hidrólise, a água é ativada devido ao sítio ativo da histidina, sendo que os íons $OH^{(-)}$ resultantes atacam o átomo de carbono da carbonila do grupo acila covalentemente ligado a serina. Então, um componente acila (ácido carboxílico) é liberado através da doação de um próton da histidina para o átomo de oxigênio ativo do resíduo da serina. Após a difusão do produto, a enzima retorna às condições iniciais, podendo recomeçar o ciclo catalítico (JAEGER *et al.*, 1999).

A determinação da estrutura da lipase foi realizada através de técnicas de cristalografia em meios aquosos homogêneos, revelando que a tríade catalítica ou sítio ativo frequentemente está protegido por uma estrutura, "tampa" (*lid*), hidrofóbica, composta pelos resíduos de aminoácidos 139-150 (α5-hélice) e 266-289 (α10-hélice). Devido à presença de tal "tampa", pode-se encontrar a lipase em duas diferentes conformações. A primeira conformação é caracterizada pela presença da "tampa" polipeptídica que isola o sítio ativo da enzima, e nessa conformação a lipase é considerada inativa. Por sua vez, na segunda conformação, em contato com uma interface hidrofóbica, ocorre a abertura da "tampa" polipeptídica, resultando consequentemente na ativação da enzima (VERGER, 1997; REIS *et al.*, 2009). Segundo Paiva, Balcão e Malcata (2000), a abertura do sítio ativo ocorre devido a uma reestruturação na conformação da lipase, na qual se cria uma região nucleofílica em torno do resíduo de serina. A "tampa" helicoidal se move, encobrindo seu lado hidrofóbico em uma cavidade polar e expondo seu lado hidrofílico. Tal exposição faz com que a superfície apolar em torno do sítio ativo seja expandida, aumentando assim a

afinidade do complexo peptídico tridimensional com os substratos apolares (lipídios). Esse fenômeno é conhecido como ativação interfacial.

Devido ao fenômeno de ativação interfacial, grande parte das reações catalisadas por lipases são realizadas em meio aquoso, em emulsão água-óleo ou em solventes orgânicos, como hexano. Acreditava-se que as lipases eram estáveis somente em tais meios reacionais (DHAKE *et al.*, 2013). Porém, há pouco tempo descobriu-se que as lipases são estáveis em fluídos pressurizados, tais como dióxido de carbono, propano e butano, possibilitando ainda mais seu uso em reações de esterificação, interesterificação, transesterificação e aminólise (KNEZ, 2009).

2.1.5 Cinética de reação enzimática

O estudo cinético de reações enzimáticas geralmente é realizado a fim de qualificar e quantificar os fatores que influenciam a atividade de uma enzima, avaliando o aumento ou diminuição das velocidades ou taxas de reação. Esta velocidade pode ser influenciada por diversos fatores, tais como temperatura, concentração de substratos (reagentes), quantidade de enzima, presença de inibidores, pH da solução, etc.

Os bioquímicos Leonor Michaelis e Maud Leonola Menten, com base no trabalho do químico francês Victor Henri, propuseram um mecanismo capaz de explicar a dependência da velocidade de reação catalisada por uma enzima em relação à quantidade de substrato. O mecanismo descrito por Michaelis e Menten é dividido em duas etapas: primeiramente o substrato, em excesso, reage com a enzima formando o complexo enzima-substrato (ES); posteriormente, na segunda etapa ocorre a quebra do complexo formado e a liberação do produto (P) e da enzima na forma ativa (E), conforme mostra a Equação (1) (COPELAND, 2002).

$$S + E \underset{k-1}{\overset{k1}{\rightleftarrows}} ES \xrightarrow{k2} P + E \qquad (1)$$

As constantes cinéticas de formação e dissociação do complexo ES são representadas por k_1 (formação), k_{-1} (dissociação) e k_2 (dissociação). A taxa de formação de cada complexo pode ser expressa de acordo com as Equações (2) a (5).

$$\frac{d[S]}{dt} = -k_1[S][E] + k_{-1}[ES] \quad (2)$$

$$\frac{d[E]}{dt} = -k_1[S][E] + k_{-1}[ES] + k_2[ES] \quad (3)$$

$$\frac{d[ES]}{dt} = k_1[S][E] - k_{-1}[ES] - k_2[ES] \quad (4)$$

$$\frac{d[P]}{dt} = k_2[ES] \quad (5)$$

Para resolver as equações diferenciais 2 a 5, as dependências das mudanças das concentrações de cada complexo com o tempo devem ser conhecidas, o que é uma tarefa experimentalmente complicada, especialmente para [E] e o complexo [ES]. A Figura 4 mostra o resultado de uma simulação numérica para a solução dessas equações diferenciais. Podem-se observar três fases distintas: 1) Período de formação do complexo [ES] e diminuição da concentração de enzima livre [E]; 2) Neste período a concentração do complexo [ES] é aproximadamente constante e as taxas de formação de [P] e consumo de [S] são máximos; 3) A última fase é determinada pela diminuição da concentração do complexo [ES] devido ao esgotamento do substrato excedente [S], além da diminuição da taxa de formação de [P] (COPELAND, 2002).

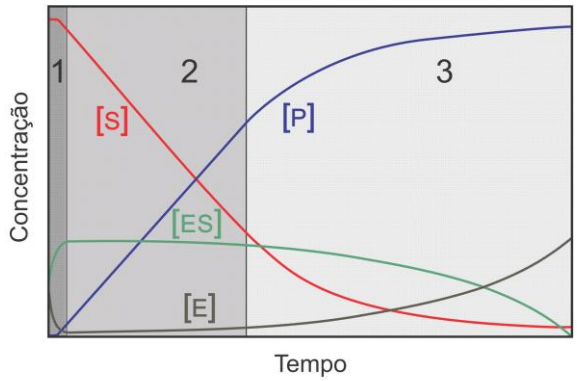

Figura 4 – Mecanismo da cinética de Michaelis-Menten; (1) Fase de estado pré-estacionário; (2) Fase de estado estacionário; (3) Fase de taxa decrescente (COPELAND, 2002).

Os parâmetros k_1, k_{-1} e k_2 representam as constantes de velocidade de cada etapa, sendo que k_2 determina o número máximo de moléculas de substrato convertidas em produto por molécula de enzima por unidade de tempo. Michaelis e Menten consideraram que a concentração de substrato é muito maior que a concentração da enzima. Assim, a constante de dissociação do complexo ES (k_2) é muito menor que a constante de formação (k_1) e a de redissociação (k_{-1}) do complexo ES, ou seja, $k_1 \approx k_{-1} > k_2$. Além disso, Michaelis e Menten consideraram que a concentração total de enzima no sistema era constante durante a catálise e igual à soma das concentrações de enzima-substrato (ES) e de enzima livre (E) (SEGEL, 1993; COPELAND, 2002).

Observa-se na Figura 4 que o complexo [ES] permanece praticamente constante durante um tempo considerável (Equação 6). Nesta fase a formação e dissociação do complexo [ES] se mantêm em equilíbrio por um determinado tempo, ou seja, em um estado estacionário. Como consequência, a decomposição do substrato [S] e a formação do produto [P] ocorrem de forma linear e de ordem zero.

$$\frac{d[ES]}{dt} = k_1[S][E] - k_{-1}[ES] - k_2[ES] = 0 \qquad (6)$$

Logo, através da Equação (6) é possível obter:

$$[ES] = \frac{k_1[S][E]}{k_{-1} + k_2} \qquad (7)$$

Sabe-se que a concentração total de enzima no meio reacional é determinada pelo balanço de massa:

$$[E]_0 = [E] + [ES] \qquad (8)$$

Substituindo (7) em (8):

$$[EA] = \frac{k_1[S][E]_0}{k_{-1} + k_2 + k_1[S]} \qquad (9)$$

Para obter a taxa de produção de [P], substitui-se (9) em (5), assim:

$$v = \frac{d[P]}{dt} = k_2[EA] = \frac{k_2[S][E]_0}{\frac{k_{-1} + k_2}{k_1} + [S]} \quad (10)$$

Onde a relação entre as constantes é a constante cinética de Michaelis-Menten (K_m), e a relação $k_2[E]_0$ é a velocidade máxima de reação, onde toda a enzima livre participa da formação de [P].

$$K_m = \frac{k_{-1} + k_2}{k_1} \quad (11)$$

$$V_{max} = k_2[E]_0 \quad (12)$$

Logo a Equação (10) pode ser escrita como:

$$v = \frac{V_{max}[S]}{K_m + [S]} \quad (13)$$

A Equação (13) é a expressão geral da teoria de cinética enzimática em estado estacionário, universalmente conhecida como equação de Michaelis-Menten ou Henri-Michaelis-Menten. O parâmetro K_m pode ser interpretado como a concentração de substrato [S] que proporciona a metade da velocidade máxima, ou seja, $V_{max}/2$. Isto equivale a dizer que K_m representa a concentração de substrato na qual metade dos sítios ativos das enzimas no meio reacional está ligada (saturada) por moléculas de substrato (SEGEL, 1993; ROBERTS, 2010).

O modelo de Henri-Michaelis-Menten permite expressar o comportamento da velocidade da reação em função da variação da concentração de apenas um substrato [S]. No entanto, na grande maioria das reações enzimáticas, dois ou três substratos estão envolvidos na cinética reacional. Ainda assim, o modelo de Henri-Michaelis-Menten revela ser válido para aspectos mais amplos, desde que a dependência de um único substrato seja estudada e os outros substratos e cofatores sejam mantidos em excesso (saturados). Desta forma, são obtidas as constantes cinéticas do substrato [S], mas nenhuma informação é fornecida sobre o mecanismo de multi-substratos. Uma análise

abrangente de tais reações complexas requer as variações mútuas de todos os substratos participantes.

A Figura 5 ilustra o esquema na nomenclatura de Cleland para uma reação de multi-substrato (dois substratos) catalisada por uma enzima. Os substratos são denominados como A e B, os produtos P e Q, estados diferentes da enzima são denominados E e F, complexos enzimáticos transitórias com os substratos e produtos formados, EA e EP, conforme as Equações 14, 15 e 16. A reação catalítica ocorre nos complexos centrais transitórios EAB e EQP. O número de substratos e de produtos que participam da reação denominam os termos uni, bi ou tri, ou seja, dois substratos reagindo para formar um produto a denominação será bi-uni, ou dois substratos reagindo para formar dois produtos, a denominação será bi-bi. Além disso, no mecanismo cinético todos os substratos devem se ligar antes que os produtos possam ser liberados (chamados mecanismos sequenciais), e ainda a ligação dos substratos pode ser tanto na ordem aleatória ou ordenados. No mecanismo de chamado de *ping-pong* produtos são liberados antes da ligação com todos os substratos envolvidos (SEGEL, 1993). Por exemplo, para uma reação com dois substratos e a liberação de dois produtos de forma ordenada, tem-se um mecanismo ordenado bi-bi, conforme mostra a Figura 5.

$$E + A \underset{k-1}{\overset{k1}{\rightleftarrows}} EA \tag{14}$$

$$EA + B \underset{k-2}{\overset{k2}{\rightleftarrows}} EAB - EPQ \underset{k-3}{\overset{k3}{\rightleftarrows}} EQ + P \tag{15}$$

$$EQ \underset{k-4}{\overset{k4}{\rightleftarrows}} E + Q \tag{16}$$

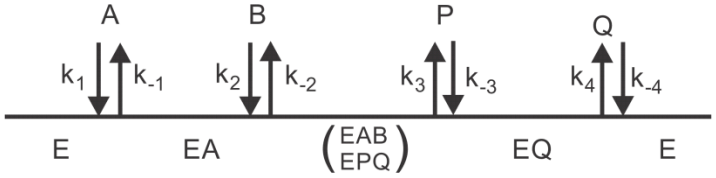

Figura 5 - Esquema na nomenclatura de Cleland para uma reação de multi-substrato (dois substratos) catalisada por uma enzima (SEGEL, 1993).

Diversos estudos de esterificação enzimática para a produção de ésteres aromáticos têm demonstrado a robustez do modelo de multi-substrato (ROMERO *et al.*, 2007; OLIVEIRA *et al.*, 2009; COUTO *et al.*, 2011; ZHANG *et al.*, 2013). Além disso, vários autores têm aplicado o mecanismo *ping-pong bi-bi* para esterificação de ésteres. A Figura 6 apresenta o mecanismo *ping-pong bi-bi* na síntese enzimática de acetato de isoamila a partir de anidrido acético

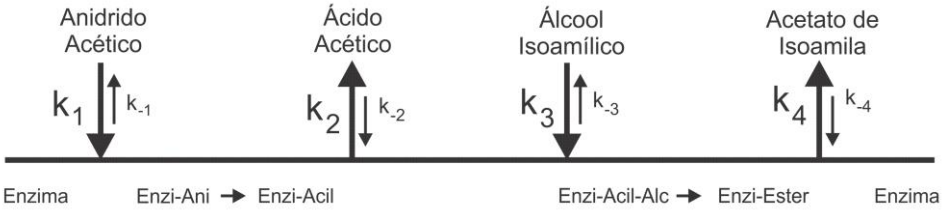

Figura 6 - Mecanismo *ping-pong bi-bi* na síntese enzimática de acetato de isoamila a partir de anidrido acético (ROMERO *et al.*, 2007).

Pode-se observar na Figura 6 que o doador do grupo acetil (anidrido acético, A) é o primeiro substrato e se ligar com a enzima livre, formando um complexo não covalente enzima-anidrido (EA), que é transformado por uma reação de isomerização em outro complexo intermediário enzima-acetil, liberando o primeiro produto, o ácido acético. Em uma segunda etapa, o álcool isoamílico se liga com o complexo enzima-acetil para formar um complexo ternário enzima-acetil-álcool. Este complexo também é transformado por uma reação de isomerização em um complexo enzima-éster, resultando na liberação do segundo produto, acetato de isoamila, enquanto a enzima recupera sua conformação inicial (ROMERO *et al.*, 2005; ROMERO *et al.*, 2007). A taxa de reação para este tipo de mecanismo, assumindo que não há inibição de ambos os substratos e produtos, é dada pela Equação (17).

$$v = \frac{V_{\max}[A][B]}{K_m^B[A] + K_m^A[B] + [A][B]} \tag{17}$$

onde: v é a taxa inicial de reação; $V_{\max}$é máxima taxa de reação; K_m^A e K_m^B são as constantes de Michaelis-Menten para os dois substratos, anidrido acético (A) e álcool isoamílico (B).

2.1.4 Reatores químicos

Há diversos modelos de reatores químicos. Porém, uma característica especifica dos reatores que diferencia um modelo do outro é a natureza da mistura no seu interior. Pode se compreender melhor a diferença entre os modelos através do(s) balanço(s) de massa no reator, que são de fundamental importância para a discussão de desempenho do modelo de reator químico (ROBERTS, 2010).

Consideremos um volume de controle arbitrário (V), no qual a temperatura e as concentrações das espécies variam de ponto a ponto, com reações químicas ocorrendo que resultam na formação da espécie i na taxa G_i. A espécie i escoa para o interior do sistema a uma vazão molar $F_{i,0}$ (mols de i/tempo) e sai do sistema a uma vazão molar F_i, conforme a Figura 7.

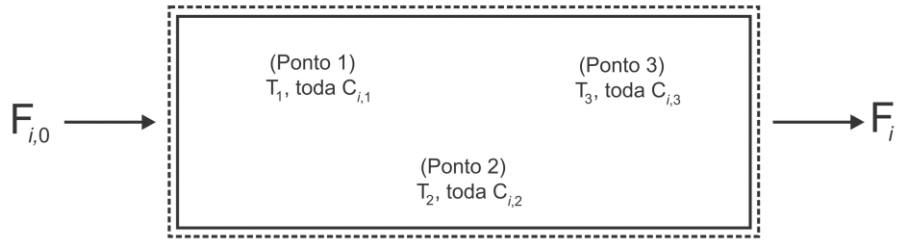

Figura 7 – Volume de controle arbitrário (V) (ROBERTS, 2010).

O balanço em base molar para a espécie i, para este volume de controle, pode ser escrito como a diferença entre taxas de entrada e saída da espécie i mais a taxa de geração por reações químicas da espécie i no volume de controle menos a taxa de acúmulo do componente i, conforme a Equação (18) (BIRD *et al.*, 2006).

$$F_{i,0} - F_i + G_i = \frac{dN_i}{dt} \tag{18}$$

Para uma reação catalítica heterogênea a taxa de geração do componente i pode ser expressa como:

$$G_i = \iiint_V r_i \rho_c dV \tag{19}$$

Na Equação (19) a variável ρ_c é a massa específica aparente do catalisador (massa/volume do reator), r_i é a taxa líquida na qual a espécie i é formada por todas as reações que estejam ocorrendo e V é o volume do reator. A taxa r_i é uma função da temperatura e das concentrações das espécies em cada ponto i no interior do reator. Como essa taxa de reação nunca é conhecida como uma função explícita da posição, a integração direta da Equação (19) não pode ser efetuada. Assim tornam-se necessários outros meios ou casos específicos de reatores, nos quais seja possível determinar essa taxa de geração ou a taxa líquida de formação (r_i). Um caso específico são os reatores em batelada ideais (ROBERTS, 2010).

Reator em batelada é definido como um reator no qual não há escoamento de massa através das fronteiras do sistema, uma vez que os reagentes são previamente carregados em seu interior. O início da reação é considerado em um instante preciso no tempo, normalmente tomado com $t = 0$. Este tempo pode corresponder, por exemplo, ao instante em que um catalisador é adicionado ou quando o último reagente é adicionado ao meio reacional. Ao longo do tempo, o número de mols de cada reagente diminui e o número de mols de cada produto aumenta. Consequentemente, as concentrações das espécies no reator irão variar. A temperatura também pode mudar com o tempo, caso a reação seja endotérmica ou exotérmica ($\Delta H_r \neq 0$). A reação continua ocorrendo até que atinja o equilíbrio químico, até que o reagente limite seja completamente consumido, ou até que uma ação seja tomada, por exemplo, resfriamento, remoção do catalisador ou adição de um inibidor químico (ROBERTS, 2010).

Esse modelo de reator frequentemente é agitado mecanicamente para assegurar que o material em seu interior seja bem misturado. Além disso, a agitação proporciona o aumento do coeficiente de transferência de calor entre o meio reacional e as superfícies de transferência de calor no reator, e o coeficiente de transferência de massa entre as fases. Em reatores multifásicos, a agitação pode manter suspenso um catalisador sólido ou criar área superficial entre duas fases líquidas, ou entre uma fase líquida e uma fase gasosa.

Para um reator em batelada, não há escoamento entre as fronteiras do sistema, logo a Equação (18) torna-se:

$$G_i = \frac{dN_i}{dt} \tag{20}$$

Substituindo (19) em (20):

$$\iiint_V r_i \rho_c dV = \frac{dN_i}{dt} \tag{21}$$

Um caso limite de comportamento de reatores em batelada pode ser considerado quando a agitação do meio reacional no interior do reator é vigorosa, como por exemplo, se a mistura dos elementos fluidos no seu interior for muito intensa. Assim, a temperatura e as concentrações das espécies serão as mesmas em cada ponto no interior do reator, em qualquer tempo t. Um reator em batelada que satisfaça essa condição é chamado de reator batelada ideal (ROBERTS, 2010). Para um reator batelada ideal, a taxa líquida de formação (r_i) e a massa específica aparente do catalisador não são funções da posição no reator, de forma que a Equação (21) pode ser escrita como:

$$r_i \rho_c V = \frac{dN_i}{dt} \tag{22}$$

O volume V na Equação (22) é a porção do volume total do reator na qual a reação realmente acontece. Isso não representa necessariamente o volume geométrico total do reator. Por exemplo, considerando uma reação que ocorra em um líquido que preenche parcialmente um vaso, se nenhuma reação ocorrer no espaço preenchido pelo gás acima do líquido, então V representa o volume do líquido e não o volume geométrico, que inclui o espaço preenchido pelo gás (ROBERTS, 2010). Se V for constante, independentemente do tempo, pode-se escrever a Equação 22 em termos da concentração da espécie i (C_i) na forma:

$$\frac{dC_i}{dt} = C_{cat} r_i \tag{23}$$

onde C_{cat} é a concentração mássica do catalisador (massa de catalisador/volume de reação).

Segundo Roberts (2010), a suposição de volume constante é válida para a maioria dos reatores industriais em batelada. A massa específica é aproximadamente constante para a grande maioria dos líquidos, mesmo se a temperatura variar moderadamente ao longo da reação. Consequentemente, a suposição de volume constante é razoável para reações em batelada que ocorrem em fase líquida. Além disso, se um vaso rígido estiver cheio de um fluido compressível, o volume desse fluido será constante porque as dimensões do vaso são fixas e não variam com o tempo.

Outro reator considerado ideal que tem sido aplicado em processos químicos é o reator de escoamento pistonado ideal (*Plug Flow Reactor* - PFR). Frequentemente, esse tipo de reator é representado como um reator tubular, conforme a Figura 8.

Segundo Roberts (2010), o reator de escoamento pistonado ideal tem duas características principais que o definem: 1) Não há mistura na direção do escoamento (z), ou seja, as concentrações dos reagentes (substratos) diminuem na direção do escoamento. Consequentemente, a taxa de reação (r_i) varia apenas na direção do escoamento. Além disso, caso a reação seja endotérmica ou exotérmica ($\Delta H_r \neq 0$), a temperatura também irá variar na direção do escoamento; 2) Não há variação de concentração e de temperatura na direção normal ao escoamento. Isso significa que não há variação radial ou angular da concentração ou da temperatura de qualquer espécie em uma dada posição axial z, consequentemente, a taxa de reação r_i não varia em qualquer seção transversal na direção do escoamento (ROBERTS, 2010).

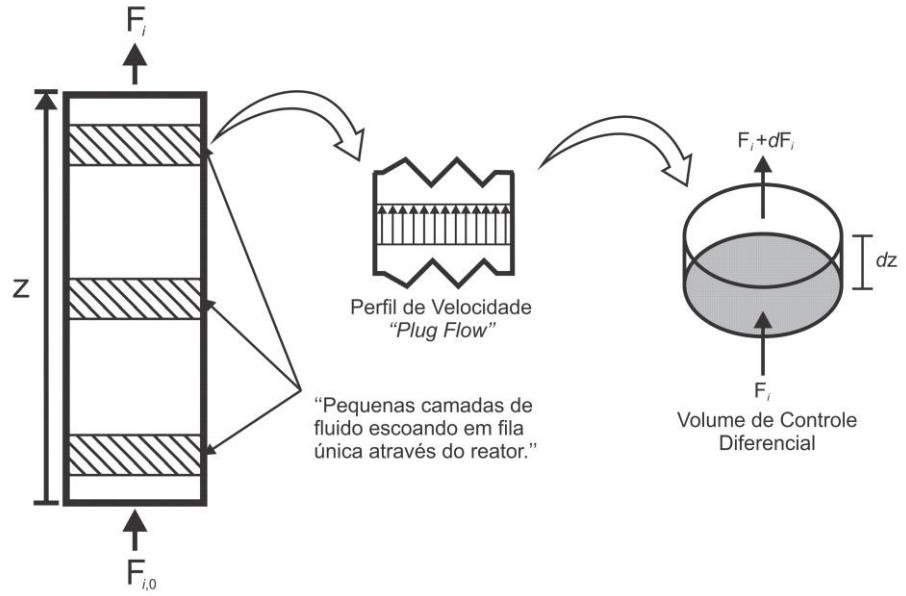

Figura 8 - Reator de escoamento pistonado ideal (*Plug Flow Reactor* - PFR); Esquerda: Volume de controle todo o reator tubular; Centro: Perfil de velocidade "*Plug Flow*"; Direita: Novo volume de controle, diferencial. Adaptado de Roberts (2010)

Pode-se imaginar um reator de escoamento pistonado como uma série de pequenos reatores em batelada com dimensão dz que escoam em fila única. Cada pequeno reator em batelada mantém sua integridade à medida que ocorre o escoamento da entrada do reator para a sua saída. Além disso, não há transferência de massa ou energia entre as camadas adjacentes do fluido. Para que um reator real se aproxime das condições idealizadas, a velocidade do fluido não pode variar na direção normal ao escoamento, ou seja, para um reator tubular isto implica em um perfil de velocidade sem variações nas direções radial e angular, conforme mostra a Figura 8. Para reatores tubulares, este perfil de velocidade plano é aproximado quando o escoamento é altamente turbulento, isto é, com altos valores do número de Reynolds (Re > 3000) (FORNEY *et al.*, 2001; BIRD *et al.*, 2006).

Analisando o comportamento de um reator de escoamento pistonado e tomando como volume de controle todo o reator tubular, podemos considerar que após um período de pré-estabilização, a variação do número de mols ao longo do tempo não muda, isto é, o processo está em estado estacionário ($dN_i/dt = 0$) (ROBERTS, 2010). Além disso, para esse modelo de reator, a taxa de reação (r_i) depende da posição no reator (z). Logo, a taxa de reação é função de V, conforme a Equação (24).

$$F_{i,0} - F_i + \iiint_V r_i dV = 0 \quad (24)$$

Como a integração tripla da Equação (24) é trabalhosa, pode-se simplesmente mudar o volume de controle escolhido, de maneira que no novo balanço de material a taxa de reação r_i não dependa de V. Para um reator tubular, o volume de controle é uma fatia através do reator, perpendicular à direção z, com uma espessura diferencial dz, conforme a Figura 8. O balanço de material para esse volume de controle pode ser expresso conforme a Equação (25).

$$F_{i,0} - (F_i + dF_i) + r_i dV = 0 \quad (25)$$

onde: F_i é a vazão molar do elemento i que entra do volume de controle; $F_i + dF_i$ é a vazão molar do elemento i que sai do volume de controle.

Rearranjando a Equação (25), obtém-se a equação de projeto para um reator de escoamento pistonado ideal (PFR), na forma diferencial.

$$dV = \frac{dF_i}{r_i} \quad (26)$$

Aplicando o conceito de tempo espacial para reações catalisadas heterogeneamente, com um fluido de massa específica constante escoando ao longo do reator, temos o tempo espacial, que é a relação entre a massa de catalisador (m) e a velocidade desse fluido no reator (v) (ROBERTS, 2010).

$$\tau = \frac{m}{v} \quad (27)$$

Utilizando as Equações (26) e (27) e rearranjando-as, podemos expressar a equação de projeto de um reator PFR em função do tempo espacial e da concentração do substrato *i*.

$$d\tau = \frac{-dC_i}{r_i} \tag{28}$$

$$\frac{dC_i}{dz} = -r_i \frac{\rho_c}{u_s} \tag{29}$$

A equação de projeto de um reator PFR em função da concentração de substrato tem sido utilizada para descrever matematicamente reatores contínuos para a produção de ésteres de aromas catalisada por enzimas imobilizadas utilizando fluidos supercríticos com solvente (MARTY *et al.*, 1994; COUTO *et al.*, 2011). Couto et al. (2011) utilizaram a Equação (29) para modelar matematicamente a síntese em modo contínuo de acetato de geranila. Os autores utilizaram o modelo de Ping-Pong Bi-Bi para descrever os parâmetros cinéticos para a lipase Novozym 435, e concluíram que os modelos matemáticos descreveram adequadamente o processo de síntese em um reator tubular contínuo operando com etano e CO_2 supercríticos como solventes.

2.1.5 Fluidos supercríticos

Uma substância pura atinge o seu estado supercrítico quando sua temperatura e pressão são superiores aos seus valores críticos. O ponto crítico (PC) de cada substância é caracterizado por sua temperatura, pressão e volume críticos. Abaixo deste ponto, a substância pode existir nos estados líquido, sólido ou vapor e acima deste ponto o composto existe somente no estado de agregação supercrítico (KERN, 1987; SANDLER, 2006). Segundo Sandler (2006), este fluido pode ser considerado tanto como um líquido expandido como um gás comprimido. A Figura 9 apresenta um diagrama de fases para um composto puro.

A curva, no diagrama de fases, representa a pressão e temperatura onde dois estados de agregação coexistem, sendo que no ponto triplo (PT) as três fases coexistem. A linha de coexistência entre gás e líquido é chamada de curva de saturação líquido-gás. Percorrendo tal linha chega-se ao ponto crítico (PC), onde as densidades das fases líquida e gasosa se igualam, não sendo possível diferenciar o estado de agregação liquido ou gás (SANDLER, 2006).

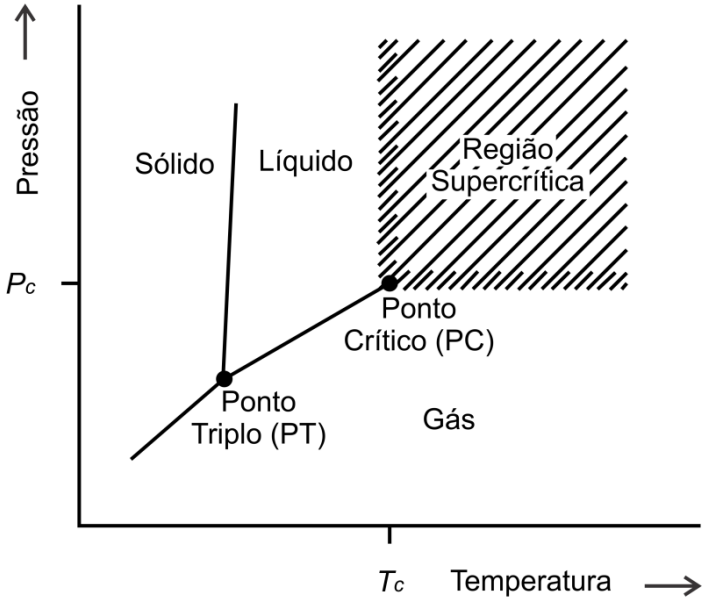

Figura 9 - Diagrama de fases para uma substância pura. Fonte: adaptado de Brunner (1987).

Dentre os fluidos supercríticos utilizados em processos industriais, o dióxido de carbono (CO_2) se destaca por não ser tóxico, inflamável e poluente, ser totalmente recuperável, de baixo custo e inerte, e as suas condições críticas são relativamente seguras quando comparado a outros solventes, tornando-o apropriado para o trabalho com compostos voláteis ou termolábeis, como as enzimas (KERN, 1987; RAVENTOS *et al.*, 2002; REVERCHON e DE MARCO, 2006). O CO_2 possui a temperatura crítica de 304,2 K e a pressão crítica 7,38 MPa. Uma vez atingido o estado supercrítico, este fluido apresenta propriedades tanto de um gás como de um líquido, ou seja, sua densidade se aproxima de um líquido, enquanto a viscosidade é próxima à de um gás normal (KERN, 1987).

A capacidade de solvatação do CO_2 no estado de agregação supercrítico depende de sua densidade. Logo, quanto maior a densidade, menores os espaços entre as moléculas e maior a interação entre elas. O CO_2 tem a capacidade de dissolver compostos não polares e levemente polares. Por outro lado, seu poder de solvatação decresce com o aumento da massa molecular do soluto (BRUNNER, 1994).

Resumidamente, reações químicas em meio supercrítico operadas em modo contínuo, especificamente utilizando CO_2, ocorrem em três etapas: a mistura dos substratos com CO_2, a reação química e a separação dos produtos e do CO_2. A primeira etapa consiste em ajustar pressão e temperatura do processo a fim de obter a maior

solvatação dos substratos da reação e/ou a maior estabilidade do catalisador. O solvente escoa para dentro do reator e através do leito empacotado com o catalisador. Após um tempo de residência preestabelecido para a reação química, a mistura produtos/CO_2 segue para a terceira etapa, na qual a pressão é reduzida abaixo do valor da pressão crítica do CO_2. Desta maneira, o CO_2 altera seu estado de agregação de supercrítico para gás, diminuindo seu poder de solvatação, e consequentemente ocorre a separação dos produtos da reação. Assim, os produtos são recuperados e o gás é redirecionado a um reciclo (RAVENTOS *et al.*, 2002; MARTINEZ, 2008). A Figura 10 ilustra um processo de reação química em modo contínuo com fluído supercrítico.

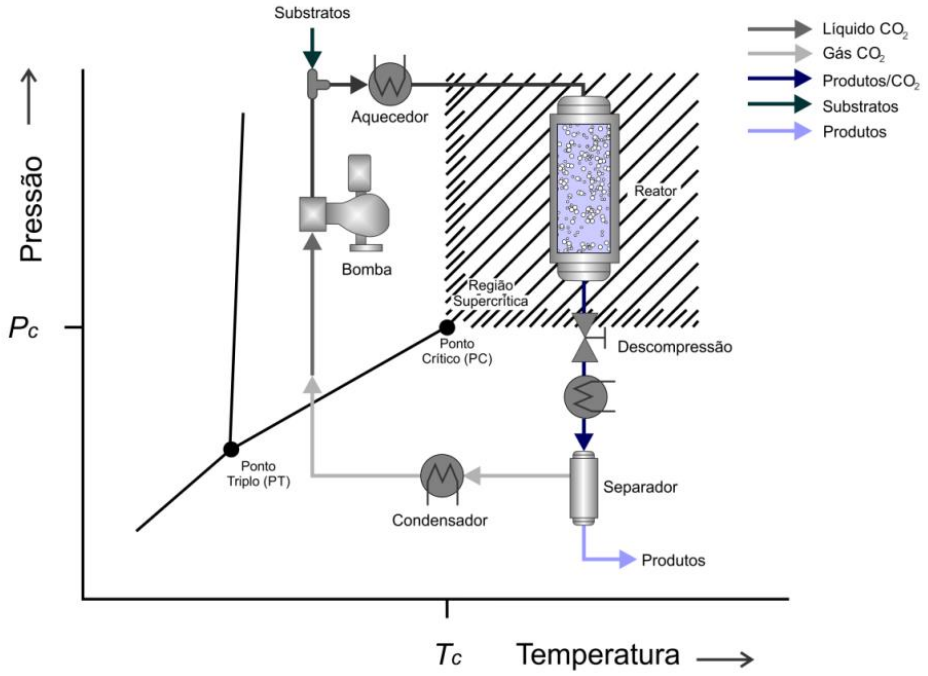

Figura 10 – Representação do processo de reação química em modo contínuo em meio supercrítico. Fonte: adaptado de Rosa *et al*. (2008).

O reciclo conduz o CO_2 gasoso até um condensador, onde o gás é liquefeito. Em seguida, o CO_2 líquido tem sua pressão aumentada acima da pressão do ponto crítico, por consequência do trabalho de uma bomba, e sua temperatura elevada até a uma temperatura de operação desejada por um aquecedor (ROSA *et al.*, 2008).

2.1.6 Atividade enzimática em fluidos supercríticos

Assim como em todos os processos catalíticos, a estabilidade do catalisador é uma informação crucial para o processo. Portanto, devem se conhecer os fatores que influenciam sua estabilidade. As enzimas utilizadas como biocatalisadores requerem condições operacionais restritas. Isto é, reações em meio supercrítico a elevadas pressões e temperaturas, bem como em meios com baixo pH, podem conduzir à desnaturação e inativação enzimática (KNEZ, 2009). A Tabela 1 apresenta diversos trabalhos científicos sobre os efeitos das condições do CO_2 supercrítico na atividade residual de diferentes lipases imobilizadas.

Tabela 1 – Efeito da exposição de CO_2 sub/supercrítico sobre a atividade enzimática residual de lipases imobilizadas. *P* (pressão), *T* (temperatura), Ciclos (ciclos de pressurização e despressurização).

Enzima	Condições (*P* e *T*)	Tempo*	Ciclos	Atividade Residual (%)	Referência
Lipozyme[3]	13 MPa e 40 °C	144 h	1	90	(MARTY *et al.*, 1990)
Lipozyme[3]	13 MPa e 40 °C	144 h	1	90-80[a]	(MARTY *et al.*, 1992)
Lipozyme[3]	15 MPa e 50 °C	12 h	1-15	96	(DUMONT *et al.*, 1992)
Lipozyme IM[1]	30 MPa e 40 °C	4-24 h	1	≈100	(HABULIN *et al.*, 1996)
Lipozyme IM[1]	30 MPa e 40 °C	4-24 h	1	≈100	(KNEZ *et al.*, 1998)
Lipozyme IM20[4]	8,6-8,9 MPa e 35-37 °C	1-6h	1	100[8]	(AUCOIN e LEGGE, 2001)
Novozym 435[2]	8 MPa e 40 °C	1 h	1	≈96	(LANZA *et al.*, 2004)
Lipozyme IM[1]	11,4 MPa e 35 °C	1 h	1	96,6	(OLIVEIRA *et al.*, 2006b)
Novozym 435[2]	7,15 MPa e 35 °C	1 h	1	98,7	(OLIVEIRA *et al.*, 2006b)
Lipase YLL[5]	7,15 MPa e 35 °C	1 h	1	≈89,8	(OLIVEIRA *et al.*, 2006a)
Lipozyme RM IM[6]	10 MPa e 50 °C	3 h	1	≈100	(MELGOSA *et al.*, 2015)
Lipozyme 435[7]	10 MPa e 50 °C	3 h	1	≈97	(MELGOSA *et al.*, 2015)

*Tempo de exposição ao fluido sub/supercrítico; [1]Lipase de *Mucor miehei* imobilizada em resina de troca aniônica macroporosa (Novozymes); [2]Lipase comercial de *Candida antarctica* imobilizada em resina aniônica macroporosa (Novozymes). [3]Lipase de *Mucor miehei* imobilizada em resina (Novo Industri);[4]Lipase comercial de *Mucor miehei* imobilizada em resina de troca aniônica macroporosa (Novo Nordish); [5]Lipase produzida de *Yarrowia lipolytica* e imobilizada pelos autores; [6]Lipase comercial de *Mucor miehei* imobilizada em Duolite A584 (Sigma Aldrich); [7]Lipase comercial de *Candida antarctica* imobilizada em Lewatit VP OC 1600 (Novozymes); [a]Adição de água (0 a 2 µL/mg de enzima). -[8]Não houve influência significativa da exposição ao CO_2.

De maneira geral, pode se verificar que a atividade residual das lipases imobilizadas, principalmente as enzimas comerciais, como a Lipozyme 435, Novozyme 435 e Lipozyme IM, demonstrou estabilidade à exposição do CO_2 supercrítico em diferentes condições de pressão e temperatura, com atividades residuais próximas ou até iguais 100%. Segundo Gießauf *et al*. (1999), a estabilidade e a atividade de uma enzima exposta ao CO_2 supercrítico dependem da espécie da enzima, da atividade de água na solução e das condições de pressão e temperatura. Porém, o fator mais importante na inativação enzimática é provavelmente a despressurização, sendo que a atividade decresce com o acréscimo do número de pressurizações/despressurizações.

Outro fator importante na estabilidade do catalisador é a pressão do processo, que pode acarretar a desnaturação e inativação enzimática, através de efeitos diretos e/ou indiretos. O efeito direto da pressão sobre a inativação é pequeno, pois a estrutura da enzima é pouco alterada, ocorrendo pequenas mudanças em locais específicos. Segundo Francisco *et al*. (2007), pressões acima de 600 MPa podem causar efeitos irreversíveis na estrutura da enzima, levando a sua inativação. Por outro lado, o efeito indireto da pressão é maior, e ocorre devido à alteração das propriedades do solvente supercrítico, que influenciam a velocidade da reação e a solubilidade dos reagentes (KNEZ, 2009).

As temperaturas críticas da maioria dos solventes utilizados como fluidos supercríticos em meios reacionais estão no mesmo intervalo de maior estabilidade e atividade das enzimas. Geralmente, tais condições não são prejudiciais para trabalhar com solutos termicamente instáveis. Por outro lado, a água supercrítica (pressão crítica de 22,1 MPa) não pode ser utilizada como meio para as reações biocatalíticas devido às elevadas temperaturas envolvidas, maiores que 647,1 K (WEINGÄRTNER e FRANCK, 2005), que inativam completamente as enzimas (KNEZ, 2009).

Os reagentes, bem como os produtos finais, também podem causar inibição da enzima, bloqueando o seu sítio ativo e acarretando uma diminuição de sua atividade. Muitas reações enzimáticas são propensas à inibição por substrato e/ou produto, fazendo com que muitas reações biocatalisadas sejam realizadas com a menor concentração de substrato e produto possível, o que diminui a eficiência do processo. Pode-se controlar a inibição por substrato através da adição contínua dos reagentes em uma baixa concentração, mas a inibição por produto é um processo complicado, pois é difícil remover gradualmente o produto utilizando sistemas de separação tradicionais. Assim sendo, a utilização de fluidos supercríticos torna esse processo viável do ponto de vista

técnico, pois o poder de solvatação ajustável do solvente permite a separação contínua do produto (FRANCISCO *et al.*, 2007; KNEZ, 2009).

2.1.7 Produção de ésteres de aromas em fluidos supercríticos

A principal vantagem de utilizar um fluido supercrítico como meio reacional é a capacidade de ajuste das propriedades deste meio através da alteração de pressão e/ou temperatura, modificando assim sua viscosidade e densidade, e consequentemente favorecendo a transferência de massa dos substratos até os sítios ativos das enzimas. Além disso, uma mudança nas condições de pressão e temperatura pode facilitar a separação dos produtos em uma etapa posterior à reação química. As enzimas, como biocatalisadores, exibem alta tolerância ao substrato e não é necessária a presença de grandes quantidades de água (solvente) para catalisar as reações. Estes atributos proporcionam flexibilidade no uso de fluidos supercríticos como meios de reações (KNEZ, 2009; WIMMER e ZAREVÚCKA, 2010)

A Tabela 2 apresenta uma visão geral de trabalhos científicos de produção de ésteres de aromas em CO_2 supercrítico utilizando enzimas imobilizadas (lipases) como catalisadores. As informações apresentadas são: tipo de enzima utilizada, condições ótimas de pressão e temperatura, conversão máxima ou taxa inicial de reação e tipo de reator utilizado. No entanto, vale ressaltar que outros solventes supercríticos e subcríticos têm sido investigados como meios de reação, tais como propano (HABULIN e KNEZ, 2001; KNEZ e HABULIN, 2002; HILDEBRAND *et al.*, 2009), butano (KRMELJ *et al.*, 1999), metano (VARMA e MADRAS, 2010b), etano (VARMA e MADRAS, 2010b) e etileno (VARMA e MADRAS, 2010b).

Tabela 2 – Ésteres de aroma produzidos em CO_2 supercrítico, destacando as condições de processo (Pressão – P, Temperatura – T e o tipo de reator) e a enzima (lipase) utilizada. MC (máxima conversão), TIR (Taxa inicial de reação).

Produto	Enzima	Condições (P/T)	MC/ TIR	Reator	Referência
Acetato de Isoamila	Novozyme 435[1] Lipozyme RM-IM[5]	8-30 MPa/40°C	100%	HPB e PBR	(ROMERO *et al.*, 2005)
Acetato de Isoamila	Lipase Pâncreas Suíno[2]	ρ*/ 40-50°C	6 %	HPB	(SRIVASTAVA *et al.*, 2002)
Acetato de Isoamila	Lipase Pâncreas Suíno[2] Novozym 435[1] Lipolase 100T[6]	7.5-10 MPa/ 50-55ºC	≈ 45%	HPB	(KUMAR *et al.*, 2005)
Propionato de Isoamila	Lipase Pâncreas Suíno[2]	ρ* e 40-50°C	60 %	HPB	(SRIVASTAVA *et al.*, 2002)
Propionato de Isoamila	Novozym 435[1] Lipolase 100T[6]	ρ*/50ºC	≈ 65 %	HPB	(VARMA e MADRAS, 2010a)
Propionato de Isoamila	Lipase Pâncreas Suíno[2] Novozym 435[1] Lipolase 100T[6]	7.5-10 MPa/ 50-55ºC	≈ 45 %	HPB	(KUMAR *et al.*, 2005)
Propionato de Isobutila	Novozym 435[1] Lipolase 100T[6]	ρ*/50ºC	≈ 95 %	HPB	(VARMA e MADRAS, 2010a)
Propionato de Isopropila	Novozym 435[1] Lipolase 100T[6]	ρ*/50ºC	≈ 40 %	HPB	(VARMA e MADRAS, 2010a)
Butirato de Isoamila	Lipase Pâncreas Suíno[2]	ρ* /40-50°C	38 %	HPB	(SRIVASTAVA *et al.*, 2002)
Butirato de Isoamila	Lipase Pâncreas Suíno[2] Novozym 435[1] Lipolase 100T[6]	7.5-10 MPa/ 50-55ºC	≈ 40 %	HPB	(KUMAR *et al.*, 2005)
Pentanoato de Isoamila	Lipase Pâncreas Suíno[2] Novozym 435[1] Lipolase 100T[6]	7.5-10 MPa/50-55ºC	≈ 35 %	HPB	(KUMAR *et al.*, 2005)
Octanoato de Isoamila	Lipase Pâncreas Suíno[2]	ρ* / 40-50°C	77 %	HPB	(SRIVASTAVA *et al.*, 2002)
Laurato de isoamila	Novozyme 435[1]	11 MPa/40-45°C	37 %	HPB	(VARMA e MADRAS, 2007)
Estearato de Isoamila	Novozyme 435[1]	11 MPa/40-45°C	53 %	HPB	(VARMA e MADRAS, 2007)
Hexanoato de Isoamila	Lipase Pâncreas Suíno[2] Novozym 435[1] Lipolase 100T[6]	7.5-10 MPa/ 50-55ºC	≈ 35 %	HPB	(KUMAR *et al.*, 2005)
Heptanoato de Isoamila	Lipase Pâncreas Suíno[2] Novozym 435[1] Lipolase 100T[6]	7.5-10 MPa/ 50-55ºC	≈ 35 %	HPB	(KUMAR *et al.*, 2005)
Octanoato de Isoamila	Lipase Pâncreas Suíno[2] Novozym 435[1] Lipolase 100T[6]	7.5-10 MPa/ 50-55ºC	≈ 40 %	HPB	(KUMAR *et al.*, 2005)
Butirato de Butila	Novozyme 435[1]	6 MPa/ 45-50°C	≈ 80 %	HPB	(VARMA e MADRAS, 2008)
Acetato de Decila	Novozyme 435[1]	10 MPa/ 35°C	100 %	HPB-VV	(OLIVEIRA *et al.*, 2009)
Acetato de Decila	Novozym 435[1]	10 MPa/ 35°C	50 mmol/min.g	HPB-VV	(RIBEIRO *et al.*, 2010)
Acetato de Terpenila	Lipozyme RM IM[5] *Candida rugosa* tipo VII (Sigma)[3]	10 MPa/ 50°C	53 %	HPB	(LIAW e LIU, 2010)
Acetato de Terpenila	Candida rugosa tipo VII (Sigma)[3]	10 MPa/ 50°C	95,1 %	HPB	(LIU e HUANG, 2010)

Tabela 3 – (*Continuação*).

Octanoato de Cetila	Novozyme 435[1] Lipozyme RM-IM[5] Lipase IM-77[7]	10,2 MPa/ 63,7°C	99,5 %	HPB	(KUO *et al.*, 2012)
Lactato de Butila	Novozyme 435[1]	40 MPa/ 55°C	99 %	HPB	(KNEZ *et al.*, 2012)
Acetato de Geranila	Lipozyme RM-IM[5]	14 MPa/ 40°C	30%	HPB	(CHULALAKSANANUKUL *et al.*, 1993)
Acetato de Geranila	Novozym 435[1]	10 MPa/ 40°C	73%	HPB-VV	(PERES *et al.*, 2003)
Acetato de Geranila	Novozyme 435[1]	10 MPa e 35°C	99 %	PBR	(COUTO *et al.*, 2011)
Butirato de Geranila	Novozym 435[1]	ρ* /50-55°C	≈ 47 %	HPB	(VARMA e MADRAS, 2010b)
Laureato de Citronelila	Novozyme 435[1]	10 MPa e 60°C	87 %	HPB	(HABULIN *et al.*, 2008)
Laureato de Citronelila	Lipase de *Rhizopus oryzae*[4]	8 MPa e 45°C	91 %	HPB	(DHAKE *et al.*, 2011a)
Butirato de Citronelila	Lipase de *Rhizopus oryzae*[4]	8 MPa e 45°C	98 %	HPB	(DHAKE *et al.*, 2011a)
Laureato de Citronelila	Lipase de *Rhizopus oryzae*[4]	8 MPa e 45°C	99 %	HPB	(DHAKE *et al.*, 2011a)
Acetato de Butila	Imobilizada Cal B[9]	12MPa/ 333 K	501 umol/min.g	PBR	(ESCANDELL *et al.*, 2015)
Laureato de Butila	*Candida Antarctica* Lipase B[10]	30 MPa/ 40°C	≈ 100 %	PBR	(STEYTLER *et al.*, 1991)
Propianato de Butila	Novozym 525F[8]	8 MPa/ 50ºC	≈ 100 %	REMR	(HERNÁNDEZ *et al.*, 2006)
Propianato de Butila	Novozym 525F[8]	8 MPa/ 50ºC	≈ 100 %	REMR	(DE LOS RÍOS *et al.*, 2007)
Acetato de Hexila	Lipozyme IM-77[7]	18.2 MPa/ 46.7ºC	77.3 %	HPB	(YU *et al.*, 2003)
Acetato de Hexila	Novozym 435[1]	14 MPa/ 40ºC	76%	HPB	(DIAZ *et al.*, 2010)
Propionato de Hexila	Novozym 435[1]	14 MPa/ 40ºC	70 %	HPB	(DIAZ *et al.*, 2010)
Butirato de Hexila	Novozym 435[1]	14 MPa/ 40ºC	91 %	HPB	(DIAZ *et al.*, 2010)
Caproato de Hexila	Novozym 435[1]	14 MPa/ 40ºC	87 %	HPB	(DIAZ *et al.*, 2010)
Caprilato de Hexila	Novozym 435[1]	14 MPa/ 40ºC	91 %	HPB	(DIAZ *et al.*, 2010)
Palmitato de Etila	Novozym 435[1] Lipolase 100T[6] Lipase Pâncreas Suíno[2]	ρ*/ 55°C	74 %	HPB	(KUMAR *et al.*, 2004)

HPB – *High pressure batch reactor*; PBR – *Packed-bed reactor*; HPB-VV – *High pressure batch with varible volume reactor*; REMR – *High pressure recirculating enzimatic membrane reactor*; ρ* - Densidade Constante; [1] Lipase imobilizada comercial de *Candida antarctica*; [2]Lipase proveniente de pâncreas suíno; [3]Lipase imobilizada comercial de *Candida rugosa* tipo VII. [4] Lipase de *Rhizopus oryzae* imobilizada pelos autores. [5]Lipase imobilizada comercial de *Rhizomucor mehei*; [6] Lipase não imobilizada comercial de *Aspergillus niger*; [7]Lipase imobilizada comercial de *Rhizomucor miehei;* [8]Lipase livre comercial de *Candida antarctica* em solução aquosa; [9]Solução comercial de *Candida antartica* Lipase B (CalB) imoblizada pelos autores;[10] Lipase B de *Candida antarctica* na forma livre;

A influência de pressão e temperatura em reações enzimáticas depende do comportamento da atividade enzimática e das propriedades físicas do solvente. O aumento da temperatura de processo pode acarretar em um acréscimo ou uma diminuição na taxa de reação, uma vez que a atividade enzimática pode ser afetada negativamente ou positivamente pela temperatura (MELGOSA *et al.*, 2015). Além disso, o aumento dessa variável ocasiona mudanças nas propriedades físicas do solvente, tais como viscosidade, tensão superficial e poder de solvatação, que aumentam com a elevação da temperatura, causando uma diminuição das resistências à transferência de massa entre o meio reacional e o catalisador ou entre as fases, quando existir distinção (RANDOLPH *et al.*, 1988).

A pressão, por sua vez, também está ligada ao comportamento da atividade enzimática e às propriedades do solvente supercrítico. Além disso, a pressão de processo pode influenciar no coeficiente de partição e na constante dielétrica, os quais controlam indiretamente a estabilidade e a especificidade da enzima (MATSUDA *et al.*, 2004; GUTHALUGU *et al.*, 2006; SOVOVÁ *et al.*, 2008). A associação entre os fatores pressão e temperatura também pode influenciar a produção de ésteres de aromas, pois a solubilidade dos substratos e produtos dessas reações depende da densidade do solvente supercrítico, que pode ser controlada por alterações dessas variáveis.

Romero *et al.* (2005), avaliaram os efeitos da pressão e da temperatura sobre a produção de acetato de isoamila em SC-CO_2 utilizando lipase imobilizada Novozym 435. Os autores observaram que o incremento na pressão não influenciou a conversão de esterificação, enquanto o incremento na temperatura diminuiu a taxa de reação e a extensão de esterificação, sendo que a condição ótima de produção foi 40 °C e 10 MPa. Dhake *et al.* (2011a) avaliaram a influência da temperatura e da pressão na produção de acetato de citronelol, butirato de citronelol e do laurato de citronelol utilizando lipase proveniente do micro-organismo *Rhizopus oryzae* em SC-CO_2 como meio reacional. Os autores observaram que um aumento de temperatura e pressão gerou uma diminuição no rendimento de esterificação devido à diminuição da atividade da enzima, sendo que o rendimento máximo de esterificação foi observado na condição mais branda entre as testadas, 45 °C e 8 MPa.

A utilização de CO_2 supercrítico como meio de reação tem sido amplamente aplicada para produzir ésteres de aromas, tornando este solvente interessante para a síntese enzimática devido à sua alta difusividade, baixa viscosidade e fácil separação de substâncias que não reagiram (HABULIN *et al.*, 2008). No entanto, muitos compostos

polares têm baixa solubilidade, uma vez que SC-CO_2 tem baixa constante dielétrica e baixa polaridade. A adição de uma pequena quantidade de compostos polares (por exemplo, metanol, etanol, acetona) como cossolventes em SC-CO_2 pode aumentar a solubilidade e, consequentemente, a taxa de conversão dos substratos (LIAQUAT e APENTEN, 2000; GUTHALUGU *et al.*, 2006; SOVOVÁ *et al.*, 2008). Alguns autores têm aplicado cossolventes com sucesso em meios reacionais, tais como Habulin *et al.* (2008) e Liu e Huang (2010).

Nota-se, na Tabela 2, que a maioria dos trabalhos citados utiliza reatores em modo batelada para a produção dos respectivos ésteres de aromas, uma vez que esse modelo de reator possibilita o estudo de diversas variáveis e obtenção de parâmetros cinéticos com a baixa utilização de substratos e catalisadores. Por outro lado, a produtividade desse modo de operação geralmente é baixa devido a limitações volumétricas. Assim, do ponto de vista industrial, os reatores de leito empacotado são preferíveis para a produção desses ésteres (SRIVASTAVA *et al.*, 2002; ROMERO *et al.*, 2005). Um bom exemplo da aplicação desses modelos de reatores foi publicado por Couto *et al.* (2011). Estes autores estudaram a síntese enzimática de acetato de geranila em SC-CO_2 utilizando a lipase imobilizada Novozyme 435 como catalisador. Os resultados obtidos demonstraram a utilidade de um reator em batelada para obtenção de dados cinéticos e concluíram que a produção de acetato de geranila pode ser realizada diversas vezes consecutivas em um reator de leito empacotado, sem uma perda considerável na atividade da enzima.

Logo, esta proposta de trabalho surge como uma alternativa para a produção de ésteres de aromas frente aos métodos tradicionais. O processo proposto torna o produto final livre de solventes tóxicos e não gera qualquer resíduo ao meio ambiente. Além disso, impulsionado pela crescente demanda de produtos de alta qualidade, o cenário futuro apresenta perspectivas de um aumento no número de aplicações potenciais do CO_2 supercrítico como meio reacional.

Deste modo, a justificativa da realização deste trabalho considera que a validação e o estudo de reações enzimáticas em CO_2 supercrítico como meio reacional em batelada e em modo contínuo fornecerão informações qualitativas e quantitativas importantes para a aplicação em escala industrial, contribuindo para a produção limpa de compostos aromáticos que possam suprir a necessidade das indústrias alimentícias e farmacêuticas.

Referências Bibliográficas

AUCOIN, M. e LEGGE, R. Effects of supercritical CO2 exposure and depressurization on immobilized lipase activity. **Biotechnology Letters,** v. 23, n. 22, p. 1863-1870, 2001.

BIRD, B.; STEWART, W. e LIGHTFOOT, E. **Transport Phenomena, Revised 2nd Edition**. John Wiley & Sons, Inc., 2006. ISBN 0470115394.

BRUNNER, G. **Gas Extraction: An Introduction to Fundamentals of Supercritical Fluids and the Application to Separation Processes**. 1. Steinkopff-Verlag Heidelberg, 1994. 387

CHULALAKSANANUKUL, W.; CONDORET, J.-S. e COMBES, D. Geranyl acetate synthesis by lipase-catalyzed transesterification in supercritical carbon dioxide. **Enzyme and Microbial Technology,** v. 15, n. 8, p. 691-698, 1993.

COPELAND, R. A. Enzymes: A Practical Introduction to Structure, Mechanism, and Data Analysis. In: (Ed.). **Enzymes**: John Wiley & Sons, Inc., 2002. p.42-75. ISBN 9780471220633.

COUTO, R.; VIDINHA, P.; PERES, C.; RIBEIRO, A. S.; FERREIRA, O.; OLIVEIRA, M. V.; MACEDO, E. A.; LOUREIRO, J. M. e BARREIROS, S. Geranyl Acetate Synthesis in a Packed-Bed Reactor Catalyzed by Novozym in Supercritical Carbon Dioxide and in Supercritical Ethane. **Industrial & Engineering Chemistry Research,** v. 50, n. 4, p. 1938-1946, 2011.

DAMODARAN, S.; PARKIN, K. L. e FENNEMA, O. R. **Fennema's food chemistry**. Boca Raton :: CRC Press/Taylor & Francis 2008.

DE LOS RÍOS, A. P.; HERNÁNDEZ-FERNÁNDEZ, F. J.; GÓMEZ, D.; RUBIO, M.; TOMÁS-ALONSO, F. e VÍLLORA, G. Understanding the chemical reaction and mass-transfer phenomena in a recirculating enzymatic membrane reactor for green ester synthesis in ionic liquid/supercritical carbon dioxide biphasic systems. **The Journal of Supercritical Fluids,** v. 43, n. 2, p. 303-309, 2007.

DHAKE, K. P.; DESHMUKH, K. M.; PATIL, Y. P.; SINGHAL, R. S. e BHANAGE, B. M. Improved activity and stability of Rhizopus oryzae lipase via immobilization for citronellol ester synthesis in supercritical carbon dioxide. **J Biotechnol,** v. 156, n. 1, p. 46-51, 2011a.

DHAKE, K. P.; DESHMUKH, K. M.; PATIL, Y. P.; SINGHAL, R. S. e BHANAGE, B. M. Improved activity and stability of Rhizopus oryzae lipase via immobilization for citronellol ester synthesis in supercritical carbon dioxide. **Journal of Biotechnology,** v. 156, n. 1, p. 46-51, 2011b.

DHAKE, K. P.; TAMBADE, P. J.; QURESHI, Z. S.; SINGHAL, R. S. e BHANAGE, B. M. HPMC-PVA Film Immobilized Rhizopus oryzae Lipase as a Biocatalyst for Transesterification Reaction. **ACS Catalysis,** v. 1, n. 4, p. 316-322, 2011c.

DHAKE, K. P.; THAKARE, D. D. e BHANAGE, B. M. Lipase: A potential biocatalyst for the synthesis of valuable flavour and fragrance ester compounds. **Flavour and Fragrance Journal,** v. 28, n. 2, p. 71-83, 2013.

DIAZ, M. D. R.; GÓMEZ, J. M.; DÍAZ-SUELTO, B. e GARCÍA-SANZ, A. Enzymatic synthesis of short-chain esters in n-hexane and supercritical carbon dioxide: Effect of the acid chain length. **Engineering in Life Sciences,** v. 10, n. 2, p. 171-176, 2010.

DUMONT, T.; BARTH, D.; CORBIER, C.; BRANLANT, G. e PERRUT, M. Enzymatic reaction kinetic: Comparison in an organic solvent and in supercritical carbon dioxide. **Biotechnology and Bioengineering,** v. 40, n. 2, p. 329-333, 1992.

ESCANDELL, J.; WURM, D. J.; BELLEVILLE, M. P.; SANCHEZ, J.; HARASEK, M. e PAOLUCCI-JEANJEAN, D. Enzymatic synthesis of butyl acetate in a packed bed reactor under liquid and supercritical conditions. **Catalysis Today,** v. 255, p. 3-9, 2015.

FORNEY, L. J.; PENNEY, W. R. e VO, H. X. Scale-up in plug-flow reactors: Laminar feed. **AIChE Journal,** v. 47, n. 1, p. 31-38, 2001.

FRANCISCO, J. D. C.; GOUGH, S. e DEY, E. Use of Lipases in the Synthesis of Structured Lipids in Supercritical Carbon Dioxide. In: POLAINA, J. e MACCABE, A. (Ed.). **Industrial Enzymes**: Springer Netherlands, 2007. cap. 20, p.341-354. ISBN 978-1-4020-5376-4.

GIEßAUF, A.; MAGOR, W.; STEINBERGER, D. J. e MARR, R. A study of hydrolases stability in supercritical carbon dioxide (SC-CO2). **Enzyme and Microbial Technology,** v. 24, n. 8–9, p. 577-583, 1999.

GROUP, T. F. World Flavors & Fragrances: Industry Study with Forecasts for 2016 & 2021. Cleveland, OH, 2012. Disponível em: < http://www.freedoniagroup.com/DocumentDetails.aspx?Referrerid=FM-Bro&StudyID=2952 >.

GUTHALUGU, N. K.; BALARAMAN, M. e KADIMI, U. S. Optimization of enzymatic hydrolysis of triglycerides in soy deodorized distillate with supercritical carbon dioxide. **Biochemical Engineering Journal,** v. 29, n. 3, p. 220-226, 2006.

HABULIN, M. e KNEZ, Ž. Activity and stability of lipases from different sources in supercritical carbon dioxide and near-critical propane. **Journal of Chemical Technology & Biotechnology,** v. 76, n. 12, p. 1260-1266, 2001.

HABULIN, M.; KRMELJ, V. e KNEZ, Ž. Synthesis of Oleic Acid Esters Catalyzed by Immobilized Lipase. **Journal of Agricultural and Food Chemistry,** v. 44, n. 1, p. 338-342, 1996.

HABULIN, M.; ŠABEDER, S.; SAMPEDRO, M. A. e KNEZ, Ž. Enzymatic synthesis of citronellol laurate in organic media and in supercritical carbon dioxide. **Biochemical Engineering Journal,** v. 42, n. 1, p. 6-12, 2008.

HARI KRISHNA, S.; DIVAKAR, S.; PRAPULLA, S. G. e KARANTH, N. G. Enzymatic synthesis of isoamyl acetate using immobilized lipase from Rhizomucor miehei. **Journal of Biotechnology,** v. 87, n. 3, p. 193-201, 2001.

HERNÁNDEZ, F. J.; DE LOS RÍOS, A. P.; GÓMEZ, D.; RUBIO, M. e VÍLLORA, G. A new recirculating enzymatic membrane reactor for ester synthesis in ionic liquid/supercritical carbon dioxide biphasic systems. **Applied Catalysis B: Environmental,** v. 67, n. 1–2, p. 121-126, 2006.

HILDEBRAND, C.; DALLA ROSA, C.; FREIRE, D. M. G.; DESTAIN, J.; DARIVA, C.; OLIVEIRA, D. D. e OLIVEIRA, J. V. Fatty acid ethyl esters production using a non-commercial lipase in pressurized propane medium. **Food Science and Technology (Campinas),** v. 29, p. 603-608, 2009.

HUANG, S. Y.; CHANG, H. L. e GOTO, M. Preparation of Surfactant-Coated Lipase for the Esterification of Geraniol and Acetic Acid in Organic Solvents. **Enzyme and Microbial Technology,** v. 22, n. 7, p. 552-557, 1998.

JAEGER, K. E.; DIJKSTRA, B. W. e REETZ, M. T. Bacterial biocatalysts: molecular biology, three-dimensional structures, and biotechnological applications of lipases. **Annu Rev Microbiol,** v. 53, p. 315-51, 1999.

KERN, D. Q. **Processos de Transmissão de Calor**. Guanabara Koogan S.A., 1987.

KNEZ, Ž. Enzymatic reactions in dense gases. **The Journal of Supercritical Fluids,** v. 47, n. 3, p. 357-372, 2009.

KNEZ, Ž. e HABULIN, M. Compressed gases as alternative enzymatic-reaction solvents: a short review. **The Journal of Supercritical Fluids,** v. 23, n. 1, p. 29-42, 2002.

KNEZ, Ž.; HABULIN, M. e KRMELJ, V. Enzyme catalyzed reactions in dense gases. **The Journal of Supercritical Fluids,** v. 14, n. 1, p. 17-29, 1998.

KNEZ, Ž.; KAVČIČ, S.; GUBICZA, L.; BÉLAFI-BAKÓ, K.; NÉMETH, G.; PRIMOŽIČ, M. e HABULIN, M. Lipase-catalyzed esterification of lactic acid in supercritical carbon dioxide. **The Journal of Supercritical Fluids,** v. 66, p. 192-197, 2012.

KRMELJ, V.; HABULIN, M.; ZNEZ, Ž. e BAUMAN, D. Lipase-catalyzed synthesis of oleyl oleate in pressurized and supercritical solvents. **Lipid / Fett,** v. 101, n. 1, p. 34-38, 1999.

KUMAR, R.; MADRAS, G. e MODAK, J. Enzymatic synthesis of ethyl palmitate in supercritical carbon dioxide. **Industrial & engineering chemistry research,** v. 43, n. 7, p. 1568-1573, 2004.

KUMAR, R.; MODAK, J. e MADRAS, G. Effect of the chain length of the acid on the enzymatic synthesis of flavors in supercritical carbon dioxide. **Biochemical Engineering Journal,** v. 23, n. 3, p. 199-202, 2005.

KUO, C.-H.; JU, H.-Y.; CHU, S.-W.; CHEN, J.-H.; CHANG, C.-M.; LIU, Y.-C. e SHIEH, C.-J. Optimization of Lipase-Catalyzed Synthesis of Cetyl Octanoate in Supercritical Carbon Dioxide. **Journal of the American Oil Chemists' Society,** v. 89, n. 1, p. 103-110, 2012.

LANZA, M.; PRIAMO, W.; OLIVEIRA, J.; DARIVA, C. e DE OLIVEIRA, D. The effect of temperature, pressure, exposure time, and depressurization rate on lipase activity in SCCO2. **Applied Biochemistry and Biotechnology,** v. 113, n. 1-3, p. 181-187, 2004.

LI, C.; TAN, T.; ZHANG, H. e FENG, W. Analysis of the conformational stability and activity of Candida antarctica lipase B in organic solvents: insight from molecular dynamics and quantum mechanics/simulations. **J Biol Chem,** v. 285, n. 37, p. 28434-41, 2010.

LIAQUAT, M. e APENTEN, R. Synthesis of low molecular weight flavor esters using plant seedling lipases in organic media. **Journal of food science,** v. 65, n. 2, p. 295-299, 2000.

LIAW, E. T. e LIU, K. J. Synthesis of terpinyl acetate by lipase-catalyzed esterification in supercritical carbon dioxide. **Bioresour Technol,** v. 101, n. 10, p. 3320-4, 2010.

LIU, K.-J. e HUANG, Y.-R. Lipase-catalyzed production of a bioactive terpene ester in supercritical carbon dioxide. **Journal of Biotechnology,** v. 146, n. 4, p. 215-220, 2010.

MACEDO, G. A. **Síntese de ésteres de aroma por lipases microbianas em meio livre de solvente orgânico**. 1997. 143 (Doutorado). Faculdade de Engenharia de Alimentos, Universidade Estadual de Campinas, Campinas.

MACEDO, G. A.; PASTORE, G. M. e RODRIGUES, M. I. Optimising the synthesis of isoamyl butyrate using Rhizopus sp. lipase with a central composite rotatable design. **Process Biochemistry,** v. 39, n. 6, p. 687-693, 2004.

MARKETS, M. A. Food Flavors Market by Type (Chocolate, Vanilla, Fruits & Nuts, Others), Origin (Natural, Synthetic), Application (Beverages, Savory & Snacks, Bakery & Confectionery, Dairy & Frozen Products, Others), & by Region - Global Forecast to 2020. September 2015. Disponível em: < http://www.marketsandmarkets.com/Market-Reports/food-flavors-market-93115891.html >.

MARTINEZ, J. L. **Supercritical fluid extraction of nutraceuticals and bioactive compounds.** . Boca Raton-FL: CRC Press, 2008.

MARTY, A.; CHULALAKSANANUKUL, W.; CONDORET, J. S.; WILLEMOT, R. M. e DURAND, G. Comparison of lipase-catalysed esterification in supercritical carbon dioxide and in n-hexane. **Biotechnology Letters,** v. 12, n. 1, p. 11-16, 1990.

MARTY, A.; CHULALAKSANANUKUL, W.; WILLEMOT, R. M. e CONDORET, J. S. Kinetics of lipase-catalyzed esterification in supercritical CO2. **Biotechnology and Bioengineering,** v. 39, n. 3, p. 273-280, 1992.

MARTY, A.; COMBES, D. e CONDORET, J. S. Continuous reaction-separation process for enzymatic esterification in supercritical carbon dioxide. **Biotechnol Bioeng,** v. 43, n. 6, p. 497-504, 1994.

MATSUDA, T.; HARADA, T. e NAKAMURA, K. Organic synthesis using enzymes in supercritical carbon dioxide. **Green Chemistry,** v. 6, n. 9, p. 440-444, 2004.

MELGOSA, R.; SANZ, M. T.; G. SOLAESA, Á.; BUCIO, S. L. e BELTRÁN, S. Enzymatic activity and conformational and morphological studies of four commercial lipases treated with supercritical carbon dioxide. **The Journal of Supercritical Fluids,** v. 97, p. 51-62, 2015.

OLIVEIRA, D.; FEIHRMANN, A. C.; DARIVA, C.; CUNHA, A. G.; BEVILAQUA, J. V.; DESTAIN, J.; OLIVEIRA, J. V. e FREIRE, D. M. G. Influence of compressed fluids treatment on the activity of Yarrowia lipolytica lipase. **Journal of Molecular Catalysis B: Enzymatic,** v. 39, n. 1–4, p. 117-123, 2006a.

OLIVEIRA, D.; FEIHRMANN, A. C.; RUBIRA, A. F.; KUNITA, M. H.; DARIVA, C. e OLIVEIRA, J. V. Assessment of two immobilized lipases activity treated in compressed fluids. **The Journal of Supercritical Fluids,** v. 38, n. 3, p. 373-382, 2006b.

OLIVEIRA, M. V.; REBOCHO, S. F.; RIBEIRO, A. S.; MACEDO, E. A. e LOUREIRO, J. M. Kinetic modelling of decyl acetate synthesis by immobilized lipase-catalysed transesterification of vinyl acetate with decanol in supercritical carbon dioxide. **The Journal of Supercritical Fluids,** v. 50, n. 2, p. 138-145, 2009.

PAIVA, A. L.; BALCÃO, V. M. e MALCATA, F. X. Kinetics and mechanisms of reactions catalyzed by immobilized lipases. **Enzyme and Microbial Technology,** v. 27, n. 3–5, p. 187-204, 2000.

PERES, C.; GOMES DA SILVA, M. D. e BARREIROS, S. Water activity effects on geranyl acetate synthesis catalyzed by novozym in supercritical ethane and in supercritical carbon dioxide. **J Agric Food Chem,** v. 51, n. 7, p. 1884-8, 2003.

RANDOLPH, T. W.; BLANCH, H. W. e PRAUSNITZ, J. M. Enzyme-caytalyzed oxidation of cholesterol in supercritical carbon dioxide. **AIChE Journal,** v. 34, n. 8, p. 1354-1360, 1988.

RAVENTOS, M.; DUARTE, S. e ALARCON, R. Application and possibilities of supercritical CO2 extraction in food processing industry: An overview. **Food Science and Technology International,** v. 8, n. 5, p. 269-284, 2002.

RAZAFINDRALAMBO, H.; BLECKER, C.; LOGNAY, G.; MARLIER, M.; WATHELET, J.-P. e SEVERIN, M. Improvement of enzymatic synthesis yields of

flavour acetates: The example of the isoamyl acetate. **Biotechnology Letters,** v. 16, n. 3, p. 247-250, 1994.

REIS, P.; HOLMBERG, K.; WATZKE, H.; LESER, M. E. e MILLER, R. Lipases at interfaces: a review. **Adv Colloid Interface Sci,** v. 147-148, p. 237-50, 2009.

REVERCHON, E. e DE MARCO, I. Supercritical fluid extraction and fractionation of natural matter. **The Journal of Supercritical Fluids,** v. 38, n. 2, p. 146-166, 2006.

RIBEIRO, A. S.; OLIVEIRA, M. V.; REBOCHO, S. F.; FERREIRA, O.; VIDINHA, P.; BARREIROS, S.; MACEDO, E. A. e LOUREIRO, J. M. Enzymatic production of decyl acetate: kinetic study in n-hexane and comparison with supercritical CO2. **Industrial & Engineering Chemistry Research,** v. 49, n. 16, p. 7168-7175, 2010.

ROBERTS, G. W. **Reações químicas e reatores químicos**. Rio de Janeiro: LTC, 2010. 414

ROMERO, M. D.; CALVO, L.; ALBA, C. e DANESHFAR, A. A kinetic study of isoamyl acetate synthesis by immobilized lipase-catalyzed acetylation in n-hexane. **Journal of Biotechnology,** v. 127, n. 2, p. 269-277, 2007.

ROMERO, M. D.; CALVO, L.; ALBA, C.; HABULIN, M.; PRIMOŽIČ, M. e KNEZ, Ž. Enzymatic synthesis of isoamyl acetate with immobilized Candida antarctica lipase in supercritical carbon dioxide. **The Journal of Supercritical Fluids,** v. 33, n. 1, p. 77-84, 2005.

ROSA, P.; MEIRELES, M. A. A.; BEATRIZ, D.-R.; LOUW, F.; MOTONOBU, G.; ANDRES, M.; MASAAKI, T.; SUSANA, L.; RICHARD, L. S.; COR, P.; HERMINIA, D. N. e JUAN CARLOS, P. Supercritical and Pressurized Fluid Extraction Applied to the Food Industry. In: (Ed.). **Extracting Bioactive Compounds for Food Products**: Boca Raton: CRC Press, 2008. p.269-401. (Contemporary Food Engineering). ISBN 978-1-4200-6237-3.

SANDLER, S. I. **Chemical, biochemical and engineering thermodynamics**. 4ª. Wiley Series, 2006. 495

SEGEL, I. H. **Enzyme Kinetics**. New York: Wiley-Interscience, 1993.

SKJOT, M.; DE MARIA, L.; CHATTERJEE, R.; SVENDSEN, A.; PATKAR, S. A.; OSTERGAARD, P. R. e BRASK, J. Understanding the plasticity of the alpha/beta hydrolase fold: lid swapping on the Candida antarctica lipase B results in chimeras with interesting biocatalytic properties. **Chembiochem,** v. 10, n. 3, p. 520-7, 2009.

SOVOVÁ, H.; ZAREVÚCKA, M.; BERNÁŠEK, P. e STAMENIĆ, M. Kinetics and specificity of Lipozyme-catalysed oil hydrolysis in supercritical CO2. **Chemical Engineering Research and Design,** v. 86, n. 7, p. 673-681, 2008.

SRIVASTAVA, S.; MODAK, J. e MADRAS, G. Enzymatic Synthesis of Flavors in Supercritical Carbon Dioxide. **Industrial & Engineering Chemistry Research,** v. 41, n. 8, p. 1940-1945, 2002.

STEYTLER, D.; MOULSON, P. e REYNOLDS, J. Biotransformations in near-critical carbon dioxide. **Enzyme and microbial technology,** v. 13, n. 3, p. 221-226, 1991.

UPPENBERG, J.; HANSEN, M. T.; PATKAR, S. e JONES, T. A. The sequence, crystal structure determination and refinement of two crystal forms of lipase B from Candida antarctica. **Structure,** v. 2, n. 4, p. 293-308, 1994.

VARMA, M. e MADRAS, G. Effect of Chain Length of Alcohol on the Lipase-Catalyzed Esterification of Propionic Acid in Supercritical Carbon Dioxide. **Applied Biochemistry and Biotechnology,** v. 160, n. 8, p. 2342-2354, 2010a.

VARMA, M. N. e MADRAS, G. Synthesis of isoamyl laurate and isoamyl stearate in supercritical carbon dioxide. **Appl Biochem Biotechnol,** v. 141, n. 1, p. 139-48, 2007.

VARMA, M. N. e MADRAS, G. Kinetics of synthesis of butyl butyrate by esterification and transesterification in supercritical carbon dioxide. **Journal of Chemical Technology & Biotechnology,** v. 83, n. 8, p. 1135-1144, 2008.

VARMA, M. N. e MADRAS, G. Kinetics of enzymatic synthesis of geranyl butyrate by transesterification in various supercritical fluids. **Biochemical Engineering Journal,** v. 49, n. 2, p. 250-255, 2010b.

VERGER, R. 'Interfacial activation' of lipases: facts and artifacts. **Trends in Biotechnology,** v. 15, n. 1, p. 32-38, 1997.

VILLENEUVE, P.; MUDERHWA, J. M.; GRAILLE, J. e HAAS, M. J. Customizing lipases for biocatalysis: a survey of chemical, physical and molecular biological approaches. **Journal of Molecular Catalysis B: Enzymatic,** v. 9, n. 4–6, p. 113-148, 2000.

WEINGÄRTNER, H. e FRANCK, E. U. Supercritical Water as a Solvent. **Angewandte Chemie International Edition,** v. 44, n. 18, p. 2672-2692, 2005.

WIMMER, Z. e ZAREVÚCKA, M. A Review on the Effects of Supercritical Carbon Dioxide on Enzyme Activity. **International Journal of Molecular Sciences,** v. 11, n. 1, p. 233-253, 2010.

YU, Z.-R.; CHANG, S.-W.; WANG, H.-Y. e SHIEH, C.-J. Study on synthesis parameters of lipase-catalyzed hexyl acetate in supercritical CO2 by response surface methodology. **Journal of the American Oil Chemists' Society,** v. 80, n. 2, p. 139-144, 2003.

ZHANG, D.-H.; LI, C. e ZHI, G.-Y. Kinetic and thermodynamic investigation of enzymatic l-ascorbyl acetate synthesis. **Journal of Biotechnology,** v. 168, n. 4, p. 416-420, 2013.

CAPÍTULO 3

ATIVIDADE ENZIMÁTICA EM FLUIDO SUPERCRÍTICO

ACTIVITY OF IMMOBILIZED LIPASE FROM *CANDIDA ANTARCTICA* (LIPOZYME 435) AND ITS PERFORMANCE ON THE ESTERIFICATION OF OLEIC ACID IN SUPERCRITICAL CARBON DIOXIDE

Philipe dos Santos[1], Camila Alves Rezende[2] and Julian Martínez[1].

[1] Faculdade de Engenharia de Alimentos, Departamento de Engenharia de Alimentos e [2] Instituto de Química, Universidade de Campinas, UNICAMP, Rua Monteiro Lobato, 80, CEP:13083-862,Campinas, SP, Brasil

Os resultados desse capítulo foram publicados no periódico "*The Journal of Supercritical Fluids*".
Vol. 107, p. 170-178, 2016

ISSN: 0896-8446
DOI: 10.1016/j.supflu.2015.08.011

Activity of immobilized lipase from *Candida antarctica* (Lipozyme 435) and its performance on the esterification of oleic acid in supercritical carbon dioxide

Philipe dos Santos[1], Camila A. Rezende[2] and Julian Martínez[1]*

[1]School of Food Engineering, Food Engineering Department and [2]Institute of Chemistry, University of Campinas, UNICAMP, 13083-862 Campinas, SP, Brazil.

*Corresponding author at: Tel.: +55 19 35214033; fax: +55 19 35214027. E-mail address: julian@fea.unicamp.br

Highlights

- Activity of Lipozyme 435 decreased with an increase of pressure, exposure time and temperature of SC-CO_2.
- FT-IR analyses suggested a change in the secondary structure of the immobilized lipase.
- FESEM images did not present morphological alterations on the macroporous anionic resin (support).
- High yields and esterification rates of oleic acid under SC-CO_2 were obtained.
- Esterification percentage in supercritical CO_2 was 65% higher than in n-hexane medium.

SF-CO_2 Home-made Unit Batch Reactor

Lipozyme 435 Activity

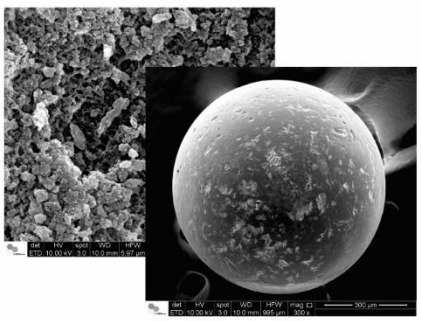

FESEM

Abstract: The factors influencing the stability of a catalyst are crucial information for the catalytic processes. The main objective of this work was to evaluate the activity of the enzyme Lipozyme 435 in processes with supercritical carbon dioxide (SC-CO_2) as reaction medium. The effect of temperature (40-60°C), pressure (10-20 MPa), exposure time (1-6 h) and depressurization steps (1-3) on the activity of the enzyme were evaluated. The kinetic data of inactivation and thermodynamic parameters were also determined. Infrared spectroscopy analysis and field scanning electron microscopy (FESEM) were carried out to investigate the structure of Lipozyme 435. The results obtained showed that the activity of Lipozyme 435 decreased with an increase of pressure, exposure time, temperature of SC-CO_2 and the number of pressurization/depressurization cycles. The thermodynamic parameters showed the stability of immobilized lipase under the tested conditions, and the kinetic data of inactivation revealed a half-life of 11 hours for the lipase exposed to SC-CO_2 (40ºC/10MPa) for 1 hour. FT-IR analyses suggested a change in the secondary structure of the immobilized lipase, considering the first amide band, while the FESEM images did not present morphological alterations on the macroporous anionic resin used as a support for the enzyme that could affect its activity. The study of the esterification of oleic acid with methanol showed that it is possible to obtain high yields (Y, g/g*h) and esterification rates (X, %) under certain process conditions (10 MPa and 40 °C). Moreover, the esterification percentage in supercritical CO_2 was 67% higher than in n-hexane medium.

Key-words: Lipozyme 435; enzyme activity; half-time; esterification; high pressure.

3.1 INTRODUCTION

Lipases (glycerol ester hydrolases, EC 3.1.1.3) belong to the hydrolase group and are responsible for catalyzing the hydrolysis of glycerol esters and long-chain fatty acids, producing alcohol and acid [1]. They are also useful in esterification, transesterification and lactonization (intramolecular esterification). Most of these reactions are carried out in aqueous or organic solvent media [2].

However, a large number of studies showed recently that lipases are stable in pressurized fluids, which increased their potential use in esterification reactions, interesterification, transesterification and aminolysis [3]. Among the supercritical fluids used in industrial processes, carbon dioxide (CO_2) is the most common, due to its advantages, such as low cost, nontoxicity, non-flammability, inertness, full recovery and moderate critical properties (P_c = 7.38 MPa, T_c= 304.2 K), when compared to other green solvents. Therefore, reactions in supercritical CO_2 can be carried out with low energy cost for pressurization, and at temperatures that do not damage the enzymes [4, 5, 6].

The main advantage of using a supercritical fluid as a reaction medium is the ability to tune its properties, such as density and the viscosity, by changing its pressure and/or temperature, thus favoring the mass transfer of the substrate to the enzyme active sites. Furthermore, the change in temperature and pressure may improve the separation of the products at a later reaction stage. These attributes provide flexibility in the use of supercritical fluids as media for enzyme catalyzed processes [3, 7].

As in all catalytic processes, the stability of the catalyst is a critical parameter, and therefore it is important to determine the factors that affect it. The enzymes used as biocatalysts require strict operating conditions. Thus, reactions in supercritical media at high pressures and temperatures, as well as in high pH, can lead to denaturation and enzyme inactivation [3]. According Gießauf *et al.* [8], the stability and the activity of an enzyme exposed to supercritical CO_2 depend on the enzyme type, water activity in the enzyme and in the reaction medium, pressure and temperature conditions. However, the most important factor in enzyme deactivation is probably the depressurization process, since enzymatic activity decreases with the increase in the number of pressurization and depressurization cycles.

The critical temperatures of most supercritical fluids used as reaction media are close to those of higher stability and activity of the enzymes. Generally, these temperatures are not harmful to thermally unstable solutes. On the other hand, supercritical water (critical pressure 22.1 MPa) cannot be used as a medium for biocatalytic reactions due to the high temperatures involved, which are greater than 647.1 K [9] and would inactivate completely the enzymes [3].

Another important factor in the catalyst stability is the pressure of the process, which can lead to denaturation and enzyme inactivation, through direct and/or indirect effects. The direct effect of pressure on the inactivation is small, since the structure of the enzyme is just slightly altered, with small changes occurring at specific locations. According to Francisco, Gough and Dey [10], pressures up to 600 MPa can cause irreversible effects on the enzyme structure, leading to its inactivation. On the other hand, the indirect effect of the pressure is more significant and occurs due to the change of the properties of the supercritical solvent, which affect the reaction rate and the solubility of the reagents [3].

The objective of this work was to investigate the application of enzymes in reactions using supercritical carbon dioxide and to evaluate the influence of process conditions on the activity of a commercial lipase (Lipozyme 435). Moreover, the half-time, decimal reduction times and thermodynamic parameters were calculated. Infrared spectroscopy analysis (FT-IR) and field emission scanning electron microscopy (FESEM) analyses were performed to assess the possible structure changes on the support of immobilized enzyme after treatment under supercritical conditions.

3.2 MATERIALS AND METHODS

The work was carried out in the Laboratory of High Pressure in Food Engineering – DEA/UNICAMP (LAPEA) located in Campinas-SP/Brazil.

3.2.1 Materials and chemicals

The commercial lipase from *Candida antarctica* (Lipozyme 435, food grade [11]) immobilized on a macroporous anionic resin was kindly supplied by Novozymes

Brazil (Araucária-PR/Brazil). The reagents oleic acid, ethanol, methanol, acetone, sodium hydroxide, arabic gum and other chemicals (analytical grade) were obtained from Êxodo Científica (Campinas-SP/Brazil). Olive oil (Gallo, Abrantes/Portugal) with low acidity (maximum acidity ≤ 0.5 %) was acquired in a local market in Campinas-SP/Brazil. Carbon dioxide (99.9%) was purchased from White Martins S.A. (Campinas-SP/Brazil).

3.2.2 Lipase activity

The enzymatic activity was measured through the volumetric method, which is based on the titrimetric determination of the free acids released from triacylglycerols by lipase catalyzed hydrolysis [12, 13]. About 5 mL of olive oil emulsion, water and arabic gum (7%), 2 mL of phosphate buffer pH 7.0 (0.1M) and 10 mg of enzyme were incubated for one hour in a shaker incubator (TE-421, Tecnal, Piracicaba-SP/Brazil) at 40 °C and 140 orbitals per minute (OPM). The hydrolysis reaction was stopped by adding 15 mL of acetone/ethanol (1:1, v/v) and the released free acids were titrated with a 0.05 M KOH solution, using phenolphthalein as an indicator. A unit of activity (U) was defined as the amount of enzyme needed to release 1 μmol of free acids per minute. All lipase activity experiments were replicated at least three times.

3.2.3 Apparatus and experimental procedure

3.2.3.1 Lipase treatment

The experimental homemade apparatus used in all treatments of enzyme with supercritical CO_2 consists basically of a CO_2 pump (Maximator M-111, Zorge/Germany), a solvent reservoir, a cooling (SOLAB SL152/18, Êxodo Científica, Hortolândia/SP, Brazil) and a heating thermostatic bath (Marconi S.A., Campinas-SP/Brazil), manometers (Zurich, São Paulo-SP/Brazil), a magnetic stirrer (IKA, RCT Basic, Staufen/Germany), thermocouples, control valves (Autoclave Engineers, Erie/PA, USA), a micrometric valve (Autoclave Engineers, Erie/PA, USA) and a stainless steel vessel of 100 mL. Figure 1 shows the schematic flow diagram of the high-pressure stirred-bath reactor unit.

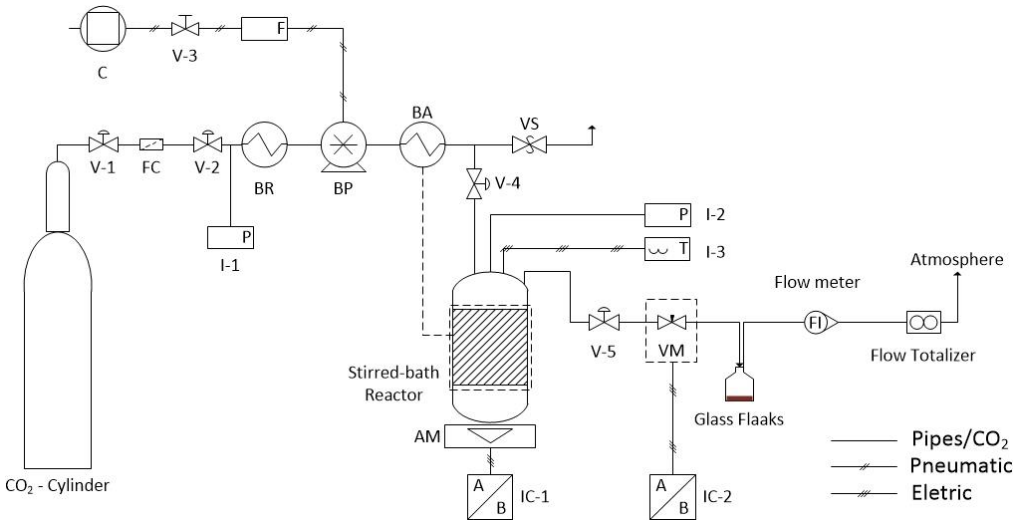

Figure 2. Diagram of the homemade unit for high-pressure stirred-batch reactor containing: V-1, V-2, V-3, V-4 and V-5 – Control valves; VM – Micrometer valves; VS – Safety valve (P_{max} = 30 MPa); C - Compressor; F - Compressed air filter; FC – CO_2 Filter; BR – Cooling bath; BP - Pump (Booster); BA – Heating bath; I-1 and I-2– Pressure indicators; I-3 - Temperature indicators; IC-1 – Indicators and controllers of magnetic stirrer; IC-2 – Indicators and controllers of temperature of micrometer valve; AM – Magnetic stirrer.

An amount of 0.4 g of immobilized lipase was introduced inside the high-pressure stirred-bath reactor and the temperature was adjusted. Next, the reactor was pressurized with CO_2 at a rate 10 MPa.min^{-1} and pressure and temperature were maintained constant for a pre-established exposure time. After the end of exposure time, the system was depressurized at 1 MPa.min^{-1}, and the lipase activity was measured as described in Section 2.2. The process variables evaluated were pressure (10 to 20 MPa), exposure time (1 to 6 hours) and number of pressurization/depressurization cycles (1 to 3). According to the studies realized by Oliveira *et al.* [14] for Novozyme 435 and by Melgosa *et al.* [11] for Lipozyme 435 and RM IM, an increase on the temperature of supercritical process causes a higher decrease on the residual activity of enzyme. Based on the literature survey, experiments were carried out at temperature range of 40 to 60°C. The residual activity (%) in the lipase was defined as the ratio between the activity of the untreated enzyme (U_0) and that of the lipase treated with supercritical CO_2 (U), as stated in Equation 1.

$$Residual\ Activity\ (\%) = \left(\frac{U}{U_0}\right) x\ 100 \qquad (1)$$

3.2.3.2 Catalytic tests

Many lipase-catalyzed esterification reactions in supercritical CO_2 have been studied [15-17]. Therefore, a simple esterification reaction was selected as model to evaluate the activity of Lipozyme 435 in supercritical CO_2: the esterification of oleic acid with methanol. First, the reaction mixture formed by oleic acid and methanol was introduced in the batch reactor, at molar ratio of 1:1 (equimolar) and 3:1 (alcohol:acid). Then, a determined amount (160 mg) of immobilized lipase was added. Finally, CO_2 was pumped into the batch reactor up to the working pressure and stirred at 600 rpm. After the end of reaction time, the system was depressurized at 1 MPa.min^{-1}, and the total of oleic acid was measured.

The amount of consumed oleic acid was measured through the volumetric method, using a 0.05 N KOH solution in water with phenolphthalein as an indicator [18]. All experiments were replicated at least three times. From the residual amount of oleic acid, the mass balance and the reaction stoichiometry, it was possible to determine the esterification rate or conversion ($X, \%$), which was obtained by the ratio between the products (n_p) and substrates (n_s), in mol, using Equation 2:

$$X(\%) = \left(\frac{n_p}{n_s}\right) x\ 100 \qquad (2)$$

The reaction yield (Y) was expressed as the ratio between the mass of the product (m_p) and the one of catalyst (m_c) per unit time (t), as shown in Equation 3:

$$Y\ (g/g * h) = \frac{m_p}{m_c * t} \qquad (3)$$

The reaction of esterification of oleic acid was also performed in n-hexane for comparison with the process in supercritical CO_2. Oleic acid and methanol were dissolved in 100 mL of hexane. The reaction was carried out at atmospheric pressure and temperature, stirring rate and substrate molar ratio (0.1 M - equimolar) equal to those used in the reactions in supercritical CO_2. The amount of consumed oleic acid was measured by the volumetric method, using a 0.05 N KOH solution in ethanol with phenolphthalein as indicator.

3.2.4 Estimation of kinetic data and thermodynamic parameters

The kinetic data of the lipase inactivation was calculated as described by Weemaes *et al.* [19], considering that, in the range of experiments, the inactivation kinetics behaves as a 1st-order model, as shown in Equation 4. According to Naudi *et al.* [20] and Ortega *et al.* [21] it is assumed in this model that the enzyme activity decreases log-linearly with time.

$$\frac{dU}{dt} = -k_d * [U] \tag{4}$$

Integrating Equation 4 leads to:

$$\frac{U}{U_0} = \exp(-k_d * t) \tag{5}$$

The experimental k_d values were determined by the slope of the plot of -ln(U/U_0) against the sample treatment time, wherein U is the enzyme activity at each experimental time and U_0 is the activity of the untreated enzyme, as described previously [22-24].

The half-life ($t_{1/2}$) of the lipase was calculated taking into account the time needed for the activity to be reduced to half of its original value, according Equation 6:

$$t_{\frac{1}{2}} = \frac{ln(2)}{k_d} \tag{6}$$

The decimal reduction time (D), which is defined as the treatment time needed for 90% inactivation of initial activity at a given condition, was calculated with Equation 7:

$$D = \frac{2.3026}{k_d} \tag{7}$$

The enzyme deactivation energy ($\Delta E^{\#}$) was calculated from the Arrhenius equation, which relates the dependence of the constant rate of inactivation with the temperature. The value of deactivation energy was obtained from the regression of the logarithm of the constant rate (k_d) versus the inverse of the absolute temperature ($1/T$) [25].

$$k_d = k_0 exp\left(-\frac{\Delta E^{\#}}{RT}\right) \quad (8)$$

where the constant k_0 represents the probability of a reaction to take place and comprises components for the collision frequency and the orientation of the colliding particles, and R is the gas constant (8,314 J mol^{-1} K^{-1}) [26].

The energies and entropies of deactivation were estimated from the absolutes rates (k_d) using Equation 9 [20].

$$k_d = \frac{\kappa T}{h} * exp\left(\frac{\Delta S^{\#}}{R}\right) * exp\left(-\frac{\Delta H^{\#}}{RT}\right) \quad (9)$$

where h is the Plack constant (6.6262x10^{-34} J s), κ is the Boltzmann constant (1.3806x10^{-23} J K^{-1}), $\Delta S^{\#}$ and $\Delta H^{\#}$ are the activation entropy and enthalpy, respectively.

The values of $\Delta H^{\#}$ and $\Delta S^{\#}$ were obtained from the slope and the intercept of the regression of $\ln(k_d/T)$ versus the absolute temperature ($1/T$), respectively. The values of Gibbs free energy of deactivation ($\Delta G^{\#}$) were calculated using Equation 10 [21].

$$\Delta G^{\#} = \Delta H^{\#} - T\Delta S^{\#} \quad (10)$$

3.2.5 Fourier transform infrared spectroscopy (FT-IR)

Infrared spectroscopy analysis was carried out to evaluate the possible chemical alterations in the peptide bond of lipase caused by the exposure to supercritical CO_2. Fourier transform-infrared spectroscopy was carried out using a CARY 630 FTIR Spectrometer Agilent Technologies in the 400-4000 cm^{-1} range and with a resolution of

4 cm^{-1}. Untreated and treated immobilized Lipozyme 435 samples were mixed with KBr in pellets, which were prepared by pressing in a mold. The equipment was available at the Institute of Chemistry (IQ/UNICAMP) located in Campinas-SP/Brazil.

The normalization of IR spectra was carried out by dividing each spectral intensity by the square root of the sum of squares intensities on the corresponding spectrum, as shown in Equation 11 [27]. The MATLAB software (2014Ra, MathWorks, Natick, MA, USA) was used for normalization.

$$SN_{i,j} = \frac{S_{i,j}}{\sqrt{\sum_{j=1}^{n}\left(S_{i,j}\right)^2}} \quad j = 1, 2, 3, \dots, n. \tag{11}$$

where: n is the number of wavenumbers in the scanning spectral region; $S_{i,j}$ is the spectral absorbance of sample i at the j^{th} wavenumber and SN_i is the normalized spectral absorbance of sample i at the j^{th} wavenumber.

The *toolbox* in MATLAB routine developed by the Departament of Analytical Chemistry and Pharmaceutical Technology (FABI) –Vrije Universiteit Brussel [28] was used for signal processing and baseline corrections by the Multiplicative Scatter Correction method (MSC) [29, 30].

3.2.6 Field emission scanning electron microscopy (FESEM)

The morphology of the immobilized lipase before and after the SC-CO_2 treatment was analyzed using a scanning electron microscope equipped with a field emission gun (FESEM - FEI Quanta 650). Prior to analysis, the samples were coated with gold in a SCD 050 sputter coater (Oerlikon-Balzers, Balzers, Liechtenstein). Both equipment were available at the National Laboratory of Nanotechnology (LNNano) located in Campinas-SP/Brazil. Analyses of the samples were performed under vacuum, using a 10 kV acceleration voltage and a large number of images was obtained on different areas of the samples (20-25 images per sample) to guarantee the reproducibility of the results.

3.2.7 Statistical analysis

The results were statistically evaluated by analysis of variance (ANOVA), applied using the software Statistica for Windows 6.0 (Statsoft Inc., USA) in order to detect significant differences in the enzyme activity, esterification rate and yield. The significant differences at level of 5 % ($p \leq 0.05$) were analyzed by the Tukey test.

3.3 RESULTS AND DISCUSSION

3.3.1 Effect of supercritical carbon dioxide on the lipase activity

The experimental results obtained for the enzyme activity of Lipozyme 435 treated in supercritical CO_2 are presented in Table 1. It can be observed that the enzyme activity decreased with the increase of pressure at the same treatment times. The lowest residual activity (about 30%) was obtained at 20 MPa and 6 hours. Instead, the treatment condition with lowest influence on the enzymatic activity was the one carried out at 10 MPa for 1 hour, in which 90% of the initial activity was preserved at the end of the process.

Table 1. Final activity and residual activity of the immobilized lipase Lipozyme 435 after treatment in supercritical CO_2 at constant temperature (40°C).

		Enzyme Activity (U/g)	
Initial Activity		14.8 ± 1.0^{a}	
Pressure (MPa)	Time (h)	Enzyme Activity (U/g)	Residual Activity (%)
10	1	13.4 ± 1.3^{ab}	90.3
15	1	10.7 ± 0.5^{abc}	72.1
20	1	7.9 ± 0.8^{bcd}	53.3
10	3.5	11.1 ± 0.1^{abc}	75.1
15	3.5	8.0 ± 1.7^{bcd}	54.0
20	3.5	6.6 ± 1.0^{cd}	44.4
10	6	9.9 ± 1.5^{bcd}	67.1
15	6	6.0 ± 0.2^{cd}	40.7
20	6	4.8 ± 0.9^{d}	32.3

Results are expressed as mean ± standard deviation of the values performed in triplicates; Time (h) – Exposure time; Residual activity is defined as absolute value of (final activity/initial activity) x 100; Different indexes (a, b, c, d) in the same column indicate that the means differ significantly by Tukey's test ($p \leqslant 0.05$).

The enzymatic activity generally decreases after treatment with supercritical CO_2 at different pressures and exposure times. The results obtained in this work are consistent with data reported by other authors [11, 14, 31, 32]. According to Monhemi e Housaindokht [33], supercritical CO_2 causes irreversible changes in the structure of enzymes, resulting in their inactivation. Furthermore, the decrease of the lipase activity treated with supercritical CO_2 has been related to the interactions between enzyme and solvent, which lead to the formation of covalent complexes with the free amino groups forming carbamates on the enzyme surface [14, 34, 35]. According to Oliveira *et al.* [14] and Kamat, Barrera and Beckman [35], these carbamates are possibly responsible for the removal of the histidine residues present at the active site of the enzyme, thus resulting in a decrease of its activity or even in its complete inactivation.

Another possible cause for the decreased lipase activity in supercritical CO_2 has been assigned to the hydrophilicity of the solvent, which would distort the essential interactions of water with the biocatalyst, thus promoting the inactivation or the denaturation of the enzyme. Recent results have shown that supercritical CO_2 has a hydrophilic nature, which can be increased with decreasing pressure [36]. Therefore, supercritical CO_2 removes the water present in the enzyme microenvironment, causing its inactivation [14]. Habulin *et al.* [37] showed that the water amount in the lipase decreased from 1.44% (before the treatment) to 0.88% after the treatment with supercritical CO_2. According to Silveira *et al.* [38], a small amount of water in the lipase can bind to specific protein sites, protecting it from the adsorption of CO_2 molecules, which is the main cause of enzyme inactivation under dry supercritical CO_2.

Some authors also suggested that the stability of a biocatalyst in supercritical CO_2 depends on intrinsic characteristics of the enzyme and of the process parameters during its exposure to CO_2 at high pressure [14, 39]. According to Steinberger, Gamse, and Maar [39], high temperatures and cycles of pressurization/depressurization may cause enzyme inactivation. Considering this results, an investigation of the enzyme stability at different process temperatures (40, 50 and 60 °C) and undergoing different numbers of pressurization/depressurization cycles was carried out, keeping pressure (10 MPa) and exposure time (1 h) constant. These results are presented on Table 2 and Table 3.

Table 2. Final activity and residual activity of the immobilized lipase Lipozyme 435 after treatment in supercritical CO_2 at different temperatures.

Pressure (MPa)	Temperature (°C)	Enzyme Activity (U/g)	Residual Activity (%)
10	40	13.4 ± 1.3^{a}	90.3
	50	11.0 ± 0.5^{ab}	74.3
	60	8.4 ± 0.5^{b}	56.7

Results are expressed as mean ± standard deviation of the values performed in triplicates; Residual activity is defined as absolute value of (final activity/initial activity) x 100; Different indexes (a, b) in the same column indicate that the means differ significantly by Tukey's test ($p \leqslant 0.05$).

It can be observed in Table 2 that the activity of the enzyme decreased with increasing temperature, therefore the lowest residual activity was observed at 60 °C. At milder conditions, 40 and 50 °C, the residual enzyme activity was not different at the level of 5% of significance. The highest value of residual activity was obtained at the lower temperature. Investigating the influence of temperature on the activity of two commercial immobilized lipases submitted to supercritical CO_2, Oliveira *et al.*[14] observed that at higher temperatures, up to 70 °C, the activity losses were at least 8%. Liu *et al.* [13] evaluated the effect of sub and supercritical CO_2 treatment, including pressure, exposure time and temperature on the residual activity of two commercial enzymes (*Candida antarctica* Lipase B (CALB) and lipase PS in solution). Differently from this work, the authors observed an increase of activity for both lipases after treatment with sub- and supercritical CO_2, in which the highest residual activities obtained were 105% and 116% for CALB and lipase PS, respectively, at the same conditions (10 MPa, 40 °C and 30 minutes of exposure time). According to the authors, the improvement of the activity may be due to changes in the tertiary structure promoted during the exposure of the enzyme to supercritical CO_2.

Data on Table 3 show that the enzyme activity decreases continuously with the increasing number of cycles, and after three cycles the enzymatic activity decreased to about 64% of that obtained with only one cycle of depressurization/pressurization. An advantage of immobilized enzymes over non-immobilized enzymes is the possibility to reuse them many times. However, as any catalyst, their catalytic ability decreases with utilization cycles [40], as confirmed by the data in Table 3. The number of tested cycles was not large enough to obtain a definitive conclusion about the influence of the number of cycles on residual enzyme activity. However, the results are consistent with those found by Oliveira *et al.* [14], who obtained a decrease in the residual activity of about 10% after 5 cycles of depressurization/pressurization and Melgosa *et al.* [11], who reported a decrease of 22% after 3 cycles. Knez *et al.* [40] studying the

esterification of lactic acid and n-butanol with a commercial lipase (Novozym 435), showed that after one cycle of pressurization/depressurization, 67.8% of conversion was achieved, while after three cycles the conversion rate decreased to approximately 11.4%. Besides, according to Knez [3], the pressurization step has small influence on the enzyme activity, but depressurization is usually the step that most affects the residual activity, in which the high expansion rate of the fluid can cause changes in the structure and even the inactivation of the enzyme.

Table 3. Activity of Lipozyme 435 undergoing pressurization and depressurization cycles in supercritical CO_2.

Number of cycles	Enzyme Activity (U/g)
1	13.4 ± 1.1^{a}
2	6.6 ± 1.0^{b}
3	4.9 ± 1.0^{b}

Results are expressed as mean ± standard deviation of the values performed in triplicates; Different indexes (a,b) in the same column indicate that the means differ significantly by Tukey's test ($p \leqslant 0.05$).

In general, a decrease in the residual activity of lipase treated with supercritical CO_2 was observed in all the experiments, wherein the main factors were pressure and the number of pressurization and depressurization cycles. Based on these results, the half-life and the decimal reduction time of lipase treated with supercritical CO_2 were calculated at three different pressures, and these values are presented in Table 4.

Table 4. Experimental values of half-life and decimal reduction time for the lipase Lipozyme 435 treated with supercritical CO_2 at 40 °C and three different pressures.

Pressure (MPa)	$t_{1/2}$ (h)	D (h)	R^2 (%)
10	11.6	38.4	98.1
15	6.1	20.2	99.0
20	6.8	22.6	97.7

Where: D: Decimal reduction (h) and $t_{1/2}$: Half-time (h).

As can be noted, reduction of 48% in the half-life of the enzyme is achieved from 10 to 15 MPa. The same behavior was observed for the decimal reduction values, for which the time necessary to obtain a 90% reduction in the enzyme activity at 10 MPa was 38 h, while for samples under other conditions, the decimal reduction time was approximately 20 hours. All regression coefficients (R^2) were greater than 0.95, indicating a good linear fit [24].

The thermodynamic parameters were determined by irreversible deactivation in two-stage theory, as shown by Ortega *et al.* [21] and Tran and Chang [25]. According to these authors, at moderate temperatures the rate-limiting step for the irreversible heat deactivation of enzymes is the formation of an unfolded enzyme state (U), as the reaction of Equation 12:

$$N \leftrightarrow T_n^{\#} \leftrightarrow U \rightarrow I \quad (12)$$

where N is the native conformation of the lipase (folded), $T_n^{\#}$ is the transition state to irreversible inactivated state of lipase. Thus, $\Delta H^{\#}$ and $\Delta G^{\#}$ are the heat and the entropy change for the $N \leftrightarrow T_n^{\#}$ reaction, respectively.

Table 5 shows the thermodynamic parameters associated with the formation of the transition state ($T_n^{\#}$).

Table 5. Estimated thermodynamic parameters for the lipase Lipozyme 435 treated with CO_2 at 40-60 °C and 10 MPa.

Thermodynamic parameter	Values
$\Delta E^{\#}$ (kJ mol^{-1})[a]	7.90
$\Delta H^{\#}$ (kJ mol^{-1})[b]	5.22
$\Delta G^{\#}$ (kJ mol^{-1})[c]	39.36 – 41.54
$\Delta S^{\#}$ (J mol^{-1}.K^{-1})	-109.02

[a] Regression coefficients (R^2) of 99.79%; [b] Regression coefficients (R^2) of 99.97%; [c] The temperature range was 40-60 °C.

It can be noted that the values obtained for entropy ($\Delta S^{\#}$) were negative. A possible explanation for this behavior is the compaction of the enzyme and the support. According to Naidu *et al.* [20], Ortega *et al.* [21] and Dannenberg and Kessler [41], the negative values of $\Delta S^{\#}$ can appear due to the aggregation of charged particles around the enzyme molecule during the exposure of proteins to high temperatures. Moreover, the values obtained for $\Delta S^{\#}$ were lower than those reported by Tran and Chang [25], which found an entropy range from -28.22 to -25.11 J mol^{-1}K^{-1} for the immobilized lipase from *Burkholdeira sp;* The enthalpy for the change $N \leftrightarrow T_n^{\#}$ reaction ($\Delta H^{\#}$) was also lower than the ones obtained by other research papers, such as Tran and Chang [25] and Owusu *et al.* [42].

According to Kristjansson and Kinsella [43], the Gibbs free energy ($\Delta G^{\#}$) can be related to the forces to stabilize the native structural state of the protein, such as the hydrophobic interaction, hydrogen bonds, disulfide bridges and electrostatic

interactions, wherein high values indicate a greater stability. The values obtained for $\Delta G^{\#}$ in this work were lower than those reported by Tran and Chang [25] (88.35 to 90.13 kJ mol^{-1}), which were estimated for immobilized lipase from *Burkholdeira sp*. at temperature ranges from 45 to 85 °C. In turn, the deactivation energy ($\Delta E^{\#}$) obtained to the immobilized lipase treated with SC-CO_2 at 10 MPa and 40-60 °C was 7.90 kJ mol^{-1}. This value is also lower than the obtained by Chiou and Wu [44] for immobilized lipase from *Candida rugosa*, which was between 36.82 and 24.69 kJ mol^{-1} for free, wet and dry lipase. According to Tran and Chang [25], the higher values of deactivation energy imply that a larger temperature change is required to deactivate the enzyme. Therefore, observing the behavior of $\Delta G^{\#}$ and $\Delta E^{\#}$ and comparing them with literature data, it can be stated that the immobilized lipase treated with SC-CO_2 in this work is less stable than those obtained by other works with lipases [25, 44, 45]. This instability was described by many researches through molecular dynamic simulation [33, 38, 46, 47].

3.3.2 Structural analysis

In order to analyze changes in the enzyme structure or in the support (macroporous anionic resin) due to the application of supercritical CO_2, infrared spectroscopy analysis and field scanning electron microscopy (FESEM) were carried out. The infrared spectroscopy spectra of Lipozyme 435 before and after treatment under two different pressure conditions are shown in Figure 2, and the infrared band of the amide regions of Lipozyme 435 are shown in Table 6.

Table 6. Infrared band of amide regions for the Lipozyme 435 untreated treated with supercritical CO_2.

	Amide I (cm^{-1})	Amide II (cm^{-1})	Amide III (cm^{-1})
Range*	1600 to 1700	≈1560**	1200 to 1400
Untreated	1648±1	1551±n	1387±n
10 MPa and 1 hour	1648±1	1551±7	1387±1
20 MPa and 6 hour	1648±n	1551±8	1388±1

Results are expressed as mean ± amplitude of the values performed in duplicate; n – there was not variation between samples. *Range of amide bands cited in literature for the lipase; **Around 1560 cm^{-1}.

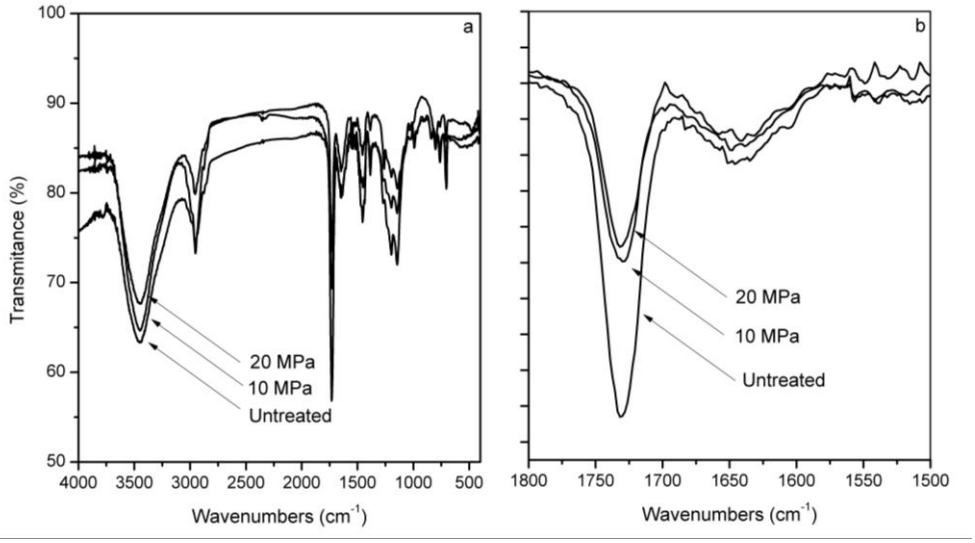

Figure 2. FT-IR spectra of immobilized lipase (Lipozyme 435) untreated and treated with supercritical CO_2 at 10 MPa for 1h and 20 MPa for 6 hour: (a) complete IR spectra and (b) Normalized IR spectra in the 1800-1500 cm^{-1} range. CO_2 temperature was kept constant at 40 °C.

Analyzing the wavenumber range between 1900 and 1200 cm^{-1}, which are mainly assigned to the peptide group vibrations [48, 49], two distinct amino bands can be observed, as shown in Figure 2 (b) and in Table 6. The first amide band (amide I), which is observed from 1600 to 1700 cm^{-1}, is associated to the carbonyl stretching of the peptide [48]. The second amide band (amide II) is responsible for the N–H bending with a contribution from the C–N stretching vibrations around 1550 cm^{-1} [48]. A third amide band was also observed at 1387 cm^{-1}. According to Collins *et al.* [48], the amide III bands (observed between 1200 and 1400 cm^{-1}) are due to in-phase combination of the N–H deformation vibration with C–N, including a minor contribution from C–O and C–C stretching. In general, after the pre-processing of the spectra (baseline correction and normalization), it was possible to observe a significant difference between the intensities of the amide I characteristic peak from the immobilized lipase before and after treatments with supercritical CO_2 at 10 and 20 MPa. In other words, the treatment with supercritical CO_2 probably caused a conformational change in the secondary structure of the immobilized lipase in the amide I band, by the formation of covalent complexes with the free amino groups on the peptides forming carbamates on the enzyme, consequently decreasing the activity of the immobilized lipase.

The main objective of FESEM analysis was to investigate possible morphological changes on the support of immobilized lipase caused by the treatment with supercritical CO_2. Changes such as increase in porosity or the presence of

obstructed pores could affect the efficiency of the enzyme. Figure 3 shows the micrographs from Lipozyme 435 before and after treatments at different magnifications (scale bars from 300 µm to 1 µm).

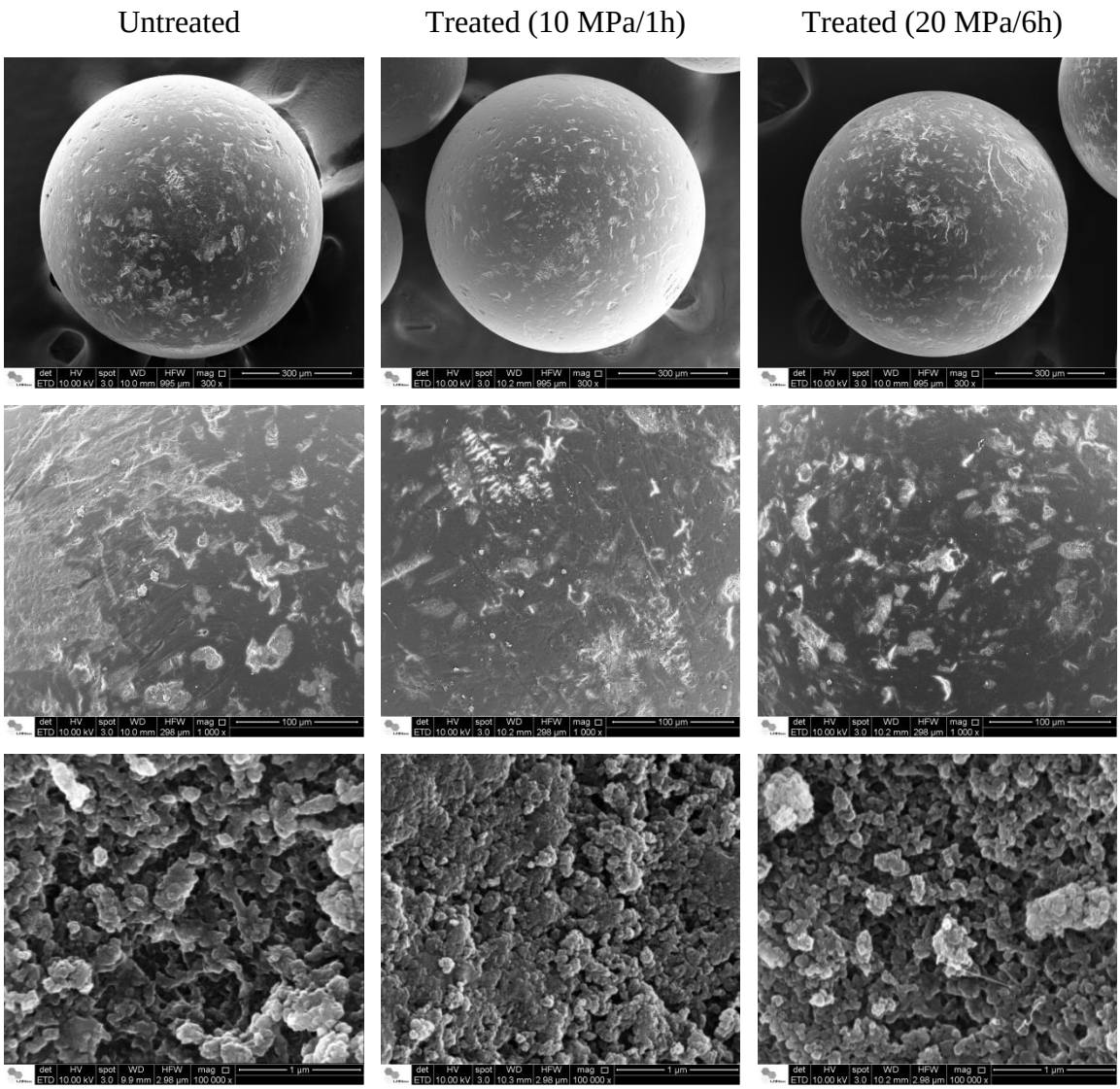

Figure 3. FESEM micrographs of Lipozyme 435 untreated and treated with supercritical CO_2 at 10 MPa and 20MPa for 1 and 6 hour, respectively. First line: scale bar of 300µm; Second line: scale bar of 100 µm; Third line: scale bar of 1 µm.

At lower magnification (first line in Figure 3) it is possible to observe that the resin particles acting as a support for Lipozyme 435 are almost perfect spheres, both before and after the treatment with supercritical CO_2. This suggests that the high pressures applied inside the reactor did not cause morphological alterations in the macroporous anionic resin of Lipozyme 435. Higher magnification images (second in Figure 3) show scratched areas on the particle surfaces due to abrasive wear. These

scratched areas are equally distributed in all the analyzed samples, untreated or treated, possibly due to collision among the particles during transport, manipulation and the flow inside the reactor. These changes cannot be assigned to the supercritical CO_2 treatment, since the scratches were already observed in untreated particles. In the third line of Figure 3, amplifications inside the scratched areas are presented (scale bar of 1 μm), and they show that the porosity pattern in the particle internal region (just beneath the surface) is also kept unchanged after the treatments with supercritical CO_2. Some authors reported that the treatment with supercritical CO_2 can cause deformations such as plasticization and swelling [50], formation of cracks, holes and fissures [14, 49] in the particle surfaces, leading to increased porosity [11, 14]. For instance, Melgosa *et al* [11] showed a rough and cracked surface with an apparent increase in porosity for Lipozyme 435 after the treatment. Morphological changes in the resin support were not observed in the present work.

3.3.3 Effect of supercritical CO_2 on the esterefication reaction

In spite of the decreased residual activity of the immobilized lipase after the treatment with supercritical CO_2, the enzyme can still catalyze reactions in supercritical media efficiently, as demonstrated by several studies [40, 51-55]. Therefore, the study of the esterification reaction of oleic acid (Figure 4) using immobilized Lipozyme 435 as a catalyst was carried out in supercritical CO_2.

Figure 4 shows the effect of pressure (Figure 4(A)) and temperature (Figure 4(B)) on the yield and rate of oleic acid esterification. It can be observed that an increase in pressure from 10 to 20 MPa caused a small increase in the esterification rate, from approximately 71% to 75%. The same behavior was observed for the esterification yield, in which the highest value was obtained at 20 MPa, approximately 7.0 kg/kg.h. This behavior may be related to the higher solubilization of the substrate due to the increased density of supercritical CO_2 [40, 56]. At the higher operating pressure (30 MPa), small decreases in the rate and in the esterification yield were noted. According to Knez *et al.* [40] and Knez *et al.* [57], these decreases may be assigned to dilution effects of the substrates due to the largest amount of CO_2 pumped into the reactor.

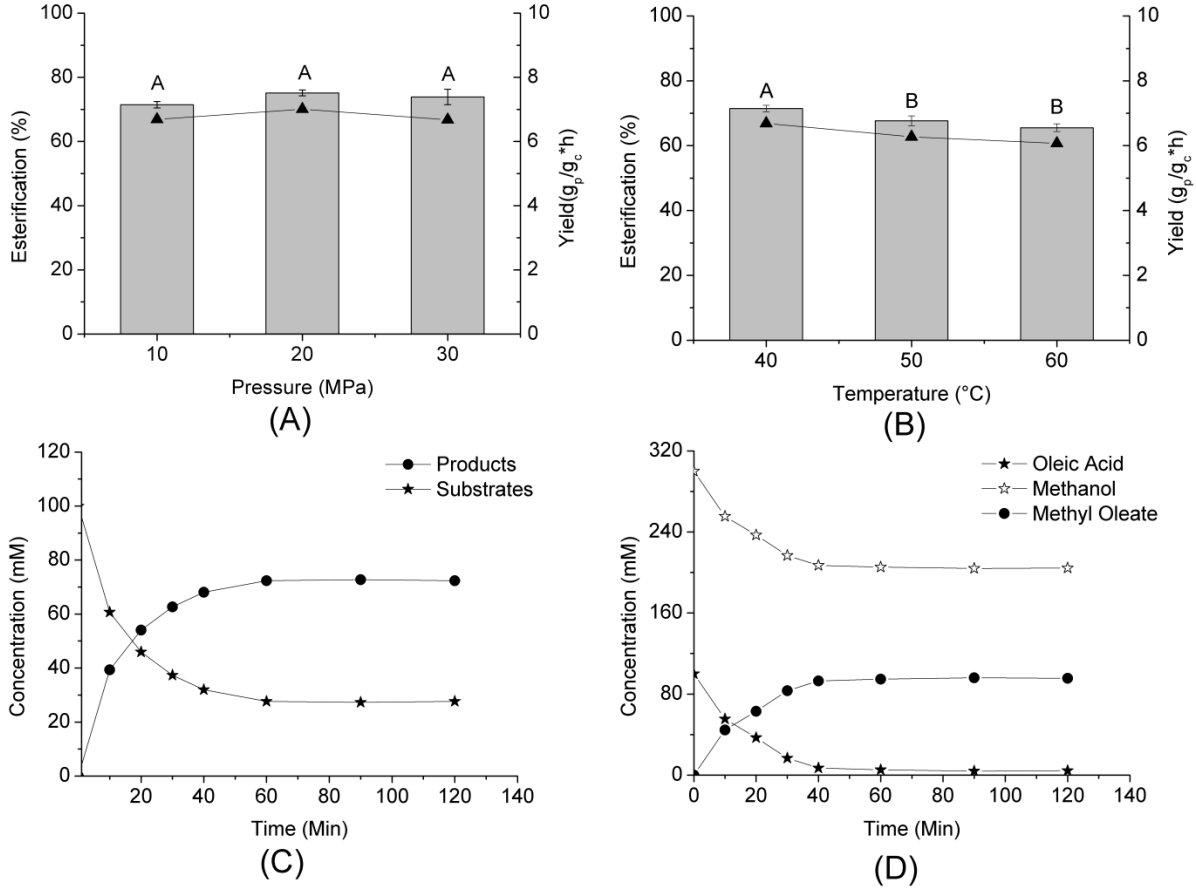

Figure 4. Effect of pressure (A) and temperature (B) on the yield (▲) and esterification (bar chart) of oleic acid after 2 hours of reaction using supercritical CO_2 as a reaction medium. Esterification kinetic of acid oleic at 40 °C and 10 MPa (C) and at molar ratio alcohol:acid 3:1; Reaction conditions: Equimolar reaction at 0,1 M (alcohol:acid) for (A), (B) and (C); 160 mg of enzyme; 600 rpm; 40 °C for different pressures and 10 MPa for different temperatures; (—) Empirically drawn lines; Different indexes on the bar chart indicate that the means differ significantly by Tukey's test ($p \leqslant 0.05$).

The increase of process temperature from 40 to 50 °C caused a decrease in the esterification rate and yield from approximately 71.5 to 67.7% and from 6.7 to 6.2 kg/kg.h, respectively. The same behavior was observed when temperature was increased from 50 to 60 ºC. These decreasing values can be explained by changes in the physical properties of the solvent, such as limitations in mass transfer, viscosity, surface tension and solvating power of the substrates (due to lower density) [3]. Moreover, this effect may not be related to enzyme denaturation because, according to Knez [3], most proteins denature at temperatures above 60 °C.

Esterification kinetics of oleic acid was performed in order to validate the results obtained in the best condition (40 °C and 10 MPa). In Figure 4(C), a typical kinetic curve of an equimolar reaction is presented. The substrate consumption, which occurs

simultaneously, increases the product concentration in such a way that the concentrations of both substrates were the same at the same time, when it was possible to obtain about 74% esterification. Laudani *et al.* [18] studied the synthesis of n-octyl oleate by esterification of free fatty acid (FFA) with 1-octanol using the immobilized lipase (Lipozyme RM IM) and found about 88% of esterification when the molar ratio between alcohol:fatty acid increased from 1:1 to 3:2. Based on this result, an esterification procedure was carried out with molar ratio alcohol:fatty acid of 3:1. It can be observed in Figure 4(D) that the consumption of alcohol was not complete when the molar ratio was increased. On the other hand, all the oleic acid was consumed in the reaction. After two hours, an esterification rate of 95% was achieved. In general, the results showed that the immobilized lipase Lipozyme 435 has good ability for the esterification of oleic acid in supercritical media, with values for esterification yield up to 74%.

Finally, esterification reactions of oleic acid were carried out in n-hexane for comparison with the results obtained at supercritical conditions. The experiments were conducted with identical amount of enzyme, concentration of reagents and temperature (160 mg, 0.1 M (equimolar) and 40 °C, respectively). The comparison was made in the same reaction time, one hour. The esterification percentage was 43.0 ± 1.5%, while in supercritical CO_2 (10 MPa and 40°C) it was about 72%, achieving an increase of 67%. According to Laudani *et al.* [18], the higher diffusivity and lower viscosity and surface tension of supercritical CO_2 are responsible for the decrease of the interphase transport limitations, consequently increasing the reaction rate and esterification percentage of oleic acid.

3.4 CONCLUSIONS

The exposure of the lipase Lipozyme 435 to supercritical CO_2 under different process conditions reduces their residual activity. The best condition obtained for residual activity was 40 °C, 10 MPa and one hour of exposure time, when the residual activity was about 90% of the original value. Higher half-life and lower decimal reduction time were also obtained at this condition. Furthermore, the residual activity of the lipase decreases with the increasing number of cycles of pressurization/depressurization. The infrared spectroscopy analysis showed that the

treatment with supercritical CO_2 caused a conformational change in the secondary structure of the immobilized lipase in the first amide band, and the images obtained by FESEM demonstrated that high pressure treatment did not cause morphological alterations on the structure of the macroporous anionic resin support of Lipozyme 435.

The study of the oleic acid esterification with methanol was conducted to demonstrate that, although there is an inactivation of the enzyme with supercritical CO_2, it is still possible to obtain high yields and esterification rates under certain process conditions. The esterification percentage in supercritical CO_2 was 67% higher than in n-hexane media. Moreover, CO_2 is considered a green solvent and has the possibility to combine the reaction and separation of products at the end of process with a single stage. The results obtained by this work may be relevant in the selection of process conditions that cause lower activity losses for future studies with Lipozyme 435.

3.5 ACKNOWLEDGMENTS

The authors wish to thank CAPES, CNPq (Ph.D. fellowship: 142373/2013-3) and FAPESP (Project 2013/02203-6) for the financial support and LME/LNNano/CNPEM for the technical support during the electron microscopy work.

3.6 REFERENCES

[1] K.E. Jaeger, T. Eggert, Lipases for biotechnology, Current opinion in biotechnology, 13 (2002), 390-397.
[2] K.P. Dhake, D.D. Thakare, B.M. Bhanage, Lipase: A potential biocatalyst for the synthesis of valuable flavour and fragrance ester compounds, Flavour and Fragrance Journal, 28 (2013), 71-83.
[3] Ž. Knez, Enzymatic reactions in dense gases, The Journal of Supercritical Fluids, 47 (2009), 357-372.
[4] M. Raventós, S. Duarte, R. Alarcón, Application and Possibilities of Supercritical CO2 Extraction in Food Processing Industry: An Overview, 8 (2002), 269-284.
[5] G. Brunner, Supercritical fluids: technology and application to food processing, Journal of Food Engineering, 67 (2005), 21-33.
[6] E. Reverchon, I. De Marco, Supercritical fluid extraction and fractionation of natural matter, The Journal of Supercritical Fluids, 38 (2006), 146-166.
[7] Z. Wimmer, M. Zarevúcka, A Review on the Effects of Supercritical Carbon Dioxide on Enzyme Activity, 11 (2010), 233-253.

[8] A. Gießauf, W. Magor, D.J. Steinberger, R. Marr, A study of hydrolases stability in supercritical carbon dioxide (SC-CO2), Enzyme and Microbial Technology, 24 (1999), 577-583.
[9] H. Weingärtner, E.U. Franck, Supercritical Water as a Solvent, Angewandte Chemie International Edition, 44 (2005), 2672-2692.
[10] J. da Cruz Francisco, S. Gough, E. Dey, Use of Lipases in the Synthesis of Structured Lipids in Supercritical Carbon Dioxide, in: J. Polaina, A. MacCabe (Eds.) Industrial Enzymes, Springer Netherlands, 2007, pp. 341-354.
[11] R. Melgosa, M.T. Sanz, Á. G. Solaesa, S.L. Bucio, S. Beltrán, Enzymatic activity and conformational and morphological studies of four commercial lipases treated with supercritical carbon dioxide, The Journal of Supercritical Fluids, 97 (2015), 51-62.
[12] M. Stoytcheva, G. Montero, R. Zlatev, J. A. Leon, V. Gochev, Analytical Methods for Lipases Activity Determination: A Review, Current Analytical Chemistry, 8 (2012), 400-407.
[13] Y. Liu, D. Chen, S. Wang, Effect of sub- and super-critical CO2 pretreatment on conformation and catalytic properties evaluation of two commercial enzymes of CALB and Lipase PS, Journal of Chemical Technology & Biotechnology, 88 (2013), 1750-1756.
[14] D. Oliveira, A.C. Feihrmann, A.F. Rubira, M.H. Kunita, C. Dariva, J.V. Oliveira, Assessment of two immobilized lipases activity treated in compressed fluids, The Journal of Supercritical Fluids, 38 (2006), 373-382.
[15] M.A. Jackson, I.K. Mbaraka, B.H. Shanks, Esterification of oleic acid in supercritical carbon dioxide catalyzed by functionalized mesoporous silica and an immobilized lipase, Applied Catalysis A: General, 310 (2006), 48-53.
[16] M. Habulin, S. Šabeder, M.A. Sampedro, Ž. Knez, Enzymatic synthesis of citronellol laurate in organic media and in supercritical carbon dioxide, Biochemical Engineering Journal, 42 (2008), 6-12.
[17] K.P. Dhake, K.M. Deshmukh, Y.P. Patil, R.S. Singhal, B.M. Bhanage, Improved activity and stability of *Rhizopus oryzae* lipase via immobilization for citronellol ester synthesis in supercritical carbon dioxide, Journal of Biotechnology, 156 (2011), 46-51.
[18] C.G. Laudani, M. Habulin, Ž. Knez, G.D. Porta, E. Reverchon, Lipase-catalyzed long chain fatty ester synthesis in dense carbon dioxide: Kinetics and thermodynamics, The Journal of Supercritical Fluids, 41 (2007), 92-101.
[19] C.A. Weemaes, L.R. Ludikhuyze, I. Van den Broeck, M.E. Hendrickx, Effect of pH on Pressure and Thermal Inactivation of Avocado Polyphenol Oxidase: A Kinetic Study, Journal of Agricultural and Food Chemistry, 46 (1998), 2785-2792.
[20] G.S.N. Naidu, T. Panda, Studies on pH and thermal deactivation of pectolytic enzymes from *Aspergillus niger*, Biochemical Engineering Journal, 16 (2003), 57-67.
[21] N. Ortega, S. de Diego, M. Perez-Mateos, M.D. Busto, Kinetic properties and thermal behaviour of polygalacturonase used in fruit juice clarification, Food Chemistry, 88 (2004), 209-217.
[22] T. Yoshimura, M. Furutera, M. Shimoda, H. Ishikawa, M. Miyake, K. Matsumoto, Y. Osajima, I. Hayakawa, Inactivation Efficiency of Enzymes in Buffered System by Continuous Method with Microbubbles of Supercritical Carbon Dioxide, Journal of Food Science, 67 (2002), 3227-3231.
[23] T. Yoshimura, M. Shimoda, H. Ishikawa, M. Miyake, I. Hayakawa, K. Matsumoto, Y. Osajima, Inactivation Kinetics of Enzymes by Using Continuous Treatment with Microbubbles of Supercritical Carbon Dioxide, Journal of Food Science, 66 (2001), 694-697.

[24] F. Gui, Z. Wang, J. Wu, F. Chen, X. Liao, X. Hu, Inactivation and reactivation of horseradish peroxidase treated with supercritical carbon dioxide, Eur Food Res Technol, 222 (2006), 105-111.
[25] D.-T. Tran, J.-S. Chang, Kinetics of enzymatic transesterification and thermal deactivation using immobilized *Burkholderia* lipase as catalyst, Bioprocess Biosyst Eng, 37 (2014), 481-491.
[26] H. Bisswanger, Enzyme Kinetics: Section 2.6–2.12, in: Enzyme Kinetics, Wiley-VCH Verlag GmbH & Co. KGaA, 2008, pp. 124-193.
[27] I. Masserschmidt, C. Cuelbas, R. Poppi, J. De Andrade, C. De Abreu, C. Davanzo, Determination of organic matter in soils by FTIR/diffuse reflectance and multivariate calibration, Journal of Chemometrics, 13 (1999), 265-273.
[28] Vrije Universiteit Brussel - Departament of Analytical Chemistry and Pharmaceutical Technology. Selection and representativity of the calibration sample subset. Available from: http://www.vub.ac.be/fabi/publiek/index.html.
[29] Å. Rinnan, F.v.d. Berg, S.B. Engelsen, Review of the most common pre-processing techniques for near-infrared spectra, TrAC Trends in Analytical Chemistry, 28 (2009), 1201-1222.
[30] A.M.d. Souza, R.J. Poppi, Teaching experiment of chemometrics for exploratory analysis of edible vegetable oils by mid infrared spectroscopy and principal component analysis: a tutorial, part I, Química Nova, 35 (2012), 223-229.
[31] M. Habulin, Ž. Knez, Activity and stability of lipases from different sources in supercritical carbon dioxide and near-critical propane, Journal of Chemical Technology & Biotechnology, 76 (2001), 1260-1266.
[32] M. Lanza, W.L. Priamo, J.V. Oliveira, C. Dariva, D. De Oliveira, The effect of temperature, pressure, exposure time, and depressurization rate on lipase activity in $SCCO_2$, Applied Biochemistry and Biotechnology - Part A Enzyme Engineering and Biotechnology, 113 (2004), 181-187.
[33] H. Monhemi, M.R. Housaindokht, How enzymes can remain active and stable in a compressed gas? New insights into the conformational stability of *Candida antarctica* lipase B in near-critical propane, The Journal of Supercritical Fluids, 72 (2012), 161-167.
[34] Ž. Knez, M. Habulin, Compressed gases as alternative enzymatic-reaction solvents: a short review, The Journal of Supercritical Fluids, 23 (2002), 29-42.
[35] S. Kamat, J. Barrera, J. Beckman, A.J. Russell, Biocatalytic synthesis of acrylates in organic solvents and supercritical fluids: I. Optimization of enzyme environment, Biotechnology and Bioengineering, 40 (1992), 158-166.
[36] H. Nakaya, O. Miyawaki, K. Nakamura, Determination of log P for pressurized carbon dioxide and its characterization as a medium for enzyme reaction, Enzyme and Microbial Technology, 28 (2001), 176-182.
[37] M. Habulin, S. Šabeder, M. Paljevac, M. Primožič, Ž. Knez, Lipase-catalyzed esterification of citronellol with lauric acid in supercritical carbon dioxide/co-solvent media, The Journal of Supercritical Fluids, 43 (2007), 199-203.
[38] R.L. Silveira, J. Martínez, M.S. Skaf, L. Martínez, Enzyme Microheterogeneous Hydration and Stabilization in Supercritical Carbon Dioxide, The Journal of Physical Chemistry B, 116 (2012), 5671-5678.
[39] D.-J. Steinberger, T. Gamse, R. Maar, Enzyme inactivation and prepurification effects of supercritical carbon dioxide (SC-CO2), in: Proceedings of the Fifth Conference on Supercritical Fluids and their Applications, A. Bertucco (Ed.), Verona, Italy, 1999, pp. p. 339.

[40] Ž. Knez, S. Kavčič, L. Gubicza, K. Bélafi-Bakó, G. Németh, M. Primožič, M. Habulin, Lipase-catalyzed esterification of lactic acid in supercritical carbon dioxide, The Journal of Supercritical Fluids, 66 (2012), 192-197.
[41] F. Dannenberg, H.-G. Kessler, Reaction Kinetics of the Denaturation of Whey Proteins in Milk, Journal of Food Science, 53 (1988), 258-263.
[42] R.K. Owusu, A. Makhzoum, J.S. Knapp, Heat inactivation of lipase from psychrotrophic *Pseudomonas fluorescens* P38: Activation parameters and enzyme stability at low or ultra-high temperatures, Food Chemistry, 44 (1992), 261-268.
[43] M.M. Kristjansson, J.E. Kinsella, Protein and enzyme stability: structural, thermodynamic, and experimental aspects, Advances in food and nutrition research, 35 (1991), 237-316.
[44] S.-H. Chiou, W.-T. Wu, Immobilization of *Candida rugosa* lipase on chitosan with activation of the hydroxyl groups, Biomaterials, 25 (2004), 197-204.
[45] A.T. Olusesan, L.K. Azura, B. Forghani, F.A. Bakar, A.K. Mohamed, S. Radu, M.Y. Manap, N. Saari, Purification, characterization and thermal inactivation kinetics of a non-regioselective thermostable lipase from a genotypically identified extremophilic *Bacillus subtilis* NS 8, New biotechnology, 28 (2011), 738-745.
[46] M.R. Housaindokht, M.R. Bozorgmehr, H. Monhemi, Structural behavior of Candida antarctica lipase B in water and supercritical carbon dioxide: A molecular dynamic simulation study, The Journal of Supercritical Fluids, 63 (2012), 180-186.
[47] V.S. Chaitanya, S. Senapati, Self-assembled reverse micelles in supercritical CO2 entrap protein in native state, Journal of the American Chemical Society, 130 (2008), 1866-1870.
[48] S.E. Collins, V. Lassalle, M.L. Ferreira, FTIR-ATR characterization of free *Rhizomucor meihei* lipase (RML), Lipozyme RM IM and chitosan-immobilized RML, Journal of Molecular Catalysis B: Enzymatic, 72 (2011), 220-228.
[49] E. Jenab, F. Temelli, J.M. Curtis, Y.-Y. Zhao, Performance of two immobilized lipases for interesterification between canola oil and fully-hydrogenated canola oil under supercritical carbon dioxide, LWT-Food Science and Technology, 58 (2014), 263-271.
[50] M. Habulin, M. Primozic, Z. Knez, Supercritical fluids as solvents for enzymatic reactions, Acta chimica slovenica, 54 (2007), 667-677.
[51] M.D. Romero, L. Calvo, C. Alba, M. Habulin, M. Primožič, Ž. Knez, Enzymatic synthesis of isoamyl acetate with immobilized *Candida antarctica* lipase in supercritical carbon dioxide, The Journal of Supercritical Fluids, 33 (2005), 77-84.
[52] C.-H. Kuo, H.-Y. Ju, S.-W. Chu, J.-H. Chen, C.-M. Chang, Y.-C. Liu, C.-J. Shieh, Optimization of Lipase-Catalyzed Synthesis of Cetyl Octanoate in Supercritical Carbon Dioxide, J Am Oil Chem Soc, 89 (2012), 103-110.
[53] M. Varma, G. Madras, Synthesis of isoamyl laurate and isoamyl stearate in supercritical carbon dioxide, Appl Biochem Biotechnol, 141 (2007), 139-147.
[54] M. Varma, G. Madras, Effect of Chain Length of Alcohol on the Lipase-Catalyzed Esterification of Propionic Acid in Supercritical Carbon Dioxide, Appl Biochem Biotechnol, 160 (2010), 2342-2354.
[55] M.N. Varma, G. Madras, Kinetics of synthesis of butyl butyrate by esterification and transesterification in supercritical carbon dioxide, Journal of Chemical Technology & Biotechnology, 83 (2008), 1135-1144.
[56] M.V. Oliveira, S.F. Rebocho, A.S. Ribeiro, E.A. Macedo, J.M. Loureiro, Kinetic modelling of decyl acetate synthesis by immobilized lipase-catalysed transesterification of vinyl acetate with decanol in supercritical carbon dioxide, The Journal of Supercritical Fluids, 50 (2009), 138-145.

[57] Z. Knez, C.G. Laudani, M. Habulin, E. Reverchon, Exploiting the pressure effect on lipase-catalyzed wax ester synthesis in dense carbon dioxide, Biotechnol Bioeng, 97 (2007), 1366-1375.

CAPÍTULO 4

ESTERIFICAÇÃO DE EUGENOL EM FLUIDO SUPERCRÍTICO

SYNTHESIS OF EUGENYL ACETATE BY ENZYMATIC REACTIONS IN SUPERCRITICAL CARBON DIOXIDE

Philipe dos Santos[1], Giovani L. Zabot[2], M. Angela A. Meireles[1], Marcio A. Mazutti[3], and Julian Martínez[1]*

[1] Faculdade de Engenharia de Alimentos, Departamento de Engenharia de Alimentos, UNICAMP, Rua Monteiro Lobato, 80, CEP:13083-862, Campinas, SP, Brasil; [2] Departamento de Engenharia Mecânica, Universidade Federal de Santa Maria, UFSM, CEP: 96506- 302, Cachoeira do Sul, RS, Brasil e [3] Departamento de Engenharia Química, Universidade Federal de Santa Maria, UFSM, CEP: 97105-900, Santa Maria, RS, Brasil.

Os resultados desse capítulo foram publicados no periódico
"*Biochemical Engineering Journal*"
Vol. 114, p. 1-9, 2016

ISSN: 1369-703X
DOI: doi:10.1016/j.bej.2016.06.018

Synthesis of Eugenyl Acetate by Enzymatic Reactions in Supercritical Carbon Dioxide

Philipe dos Santos[1], Giovani L. Zabot[2], M. Angela A. Meireles[1], Marcio A. Mazutti[3], and Julian Martínez[1]*

[1] School of Food Engineering, Food Engineering Department, University of Campinas, UNICAMP, 13083-862, Campinas, SP, Brazil. [2] Academic Center, Federal University of Santa Maria, UFSM, 96506-302, Cachoeira do Sul, RS, Brazil. [3] Chemical Engineering Department, Federal University of Santa Maria, UFSM, 97105-900, Santa Maria, RS, Brazil. *Corresponding author at: Tel.: +55 19 35214033; fax: +55 19 35214027. E-mail address: julian@unicamp.br

Highlights

- Optimal condition for the synthesis of eugenyl acetate in SC-CO_2 was determined at 60 ºC/10 MPa;
- The phase behavior of the reaction system and the synthesis in organic medium also were studied;
- The conversion and yield of eugenyl acetate decreased with the increasing number of cycles;
- The affinity of acetic anhydride to the enzyme was larger than that of eugenol;
- The second step of the reaction kinetics required more energy that the first step.

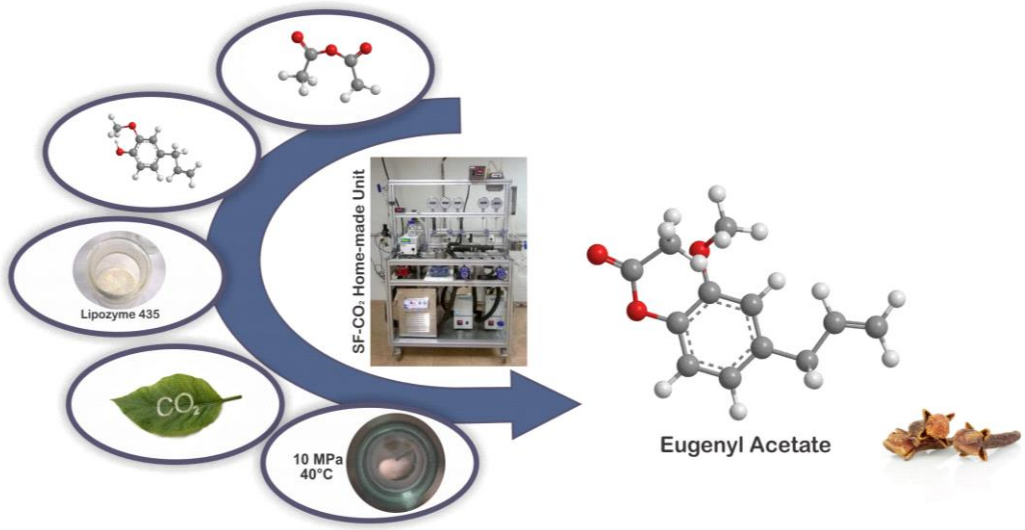

Abstract: Supercritical carbon dioxide (SC-CO_2) as reaction medium has gained attention in the production of terpenic esters catalyzed by lipases. Therefore, this work investigated the production of eugenyl acetate by esterification of eugenol and acetic anhydride in SC-CO_2 using two commercial lipases (Lipozyme 435 and Novozym 435) as catalysts. The influence of enzyme concentration (1 to 10% weight/weight), substrates' molar ratio (1:1 to 5:1), temperature (40 to 60 ºC) and pressure of SC-CO_2 (10 to 30 MPa) on the esterification rate (X; %) and specific productivity (SP; kg of product/kg of catalyst x hour) were evaluated. A home-made high-pressure stirred-batch reactor (100 mL) was used in the experiments. The use of Novozym 435 achieved higher conversion and specific productivity of eugenyl acetate than Lipozyme 435. An excess of acetic anhydride (5:1 M/M) and high enzyme concentration (10%) achieved higher esterification rates than the lowest conditions (1% and 1:1 M/M). The optimal temperature and pressure for the synthesis of eugenyl acetate in SC-CO_2 were 50 and 60 ºC at 10 MPa, respectively. The phase behavior of the reaction system and the synthesis in organic medium were also studied. Kinetic experiments were performed at 40, 50 and 60 ºC and indicated that the reaction follows the simple Ping-Pong Bi-Bi mechanism and the affinity of acetic anhydride to enzyme was larger than that of eugenol.

Key-words: eugenol; Lipozyme 435; Novozym 435; esterification; supercritical.

4.1 INTRODUCTION

Low molecular weight esters represent an important class of aroma, consisting of compounds derived from short chain acids such as acetates, propionates and butyrates, which are often responsible for fruity aroma [1-3]. These esters, known for their flavoring properties, are present in essential oils of natural matter, which are technically difficult to extract, isolate and purify. Furthermore, conventional chemical synthesis leads to the formation of undesirable products to the food and pharmaceutical industries. Therefore, biocatalyzed chemical synthesis becomes of great interest due to the high chemo-, regio- and stereo-selectivity of the enzymes, which provide possible in vitro synthesis of naturally existing single enantiomers of specific compounds[2]. Moreover, the esters can be considered as natural [2-4], since the process meets the required conditions by the legislation. For example, the substrates or raw materials used in process are natural and only physical or biotechnological processes must be employed for the isolation and purification of the formed products [5].

Lipases (glycerol ester hydrolases, EC 3.1.1.3) belong to the hydrolase group and are responsible for catalyzing the hydrolysis of glycerol esters and long-chain fatty acids, producing alcohol and acid [6]. In many research works, lipases have been employed as catalysts for the synthesis of esters, such as isoamyl acetate (banana flavor) [3, 7], isoamyl butyrate (pear flavor) [8, 9] and cinamyl acetate (a compound of cinnamon essential oil) [10]. Besides, a recent research showed that lipases are stable in pressurized fluids, which increased their potential use in esterification reactions [11]. Among the supercritical fluids (SC) used in industrial processes, carbon dioxide (CO_2) is the most common due to its advantages, such as low cost, nontoxicity, non-flammability, inertness, full recovery and moderate critical properties (P_c = 7.38 MPa, T_c = 304.2 K) when compared to other green solvents. Therefore, reactions in supercritical CO_2 can be carried out with low energy cost for pressurization, and at temperatures that do not damage the enzymes [12, 13]. Moreover, if SC-CO_2 cannot improve reaction rate, the adjustable solvent power of the fluid allows the design of a production process with integrated downstream separation of products and unreacted substrates [11].

Eugenyl acetate is an aroma ester generally found in the essential oil of clove buds (*Syzygium aromaticum*). Besides eugenyl acetate, clove oil is rich in

eugenol, beta-carophyllene, alfa-humulene and other minor compounds. The European Food Safety Authority (EFSA) evaluated and considered the application of eugenyl acetate safe as aromatic substance in food products. Actually, eugenyl acetate is listed on the database of the European Union as authorized substance to be used by the food industry [14]. Besides the flavoring property of eugenyl acetate, several works have reported other properties of industrial interest, such as antioxidant capacity [15], antimicrobial [16] and anticancer properties [17].

In this context, the aim of the present work was to investigate the synthesis of eugenyl acetate through enzymatic reactions in SC-CO_2 media. The effects of enzyme and substrates' concentration, temperature, pressure and number of reuse cycles of the enzymes were evaluated for two commercial immobilized lipases. The differences between two commercial immobilized lipases from *C. antartica* were shown. Moreover, experiments were performed to determine the kinetic parameters, and finally the phase behavior of the reaction system and the synthesis in organic medium were studied.

4.2 MATERIALS AND METHODS

4.2.1 Materials

Two commercial lipases from *Candida antarctica* (Lipozyme 435 and Novozym 435), both immobilized on a macroporous anionic resin, were kindly supplied by Novozymes Brazil (Araucária-PR/Brazil). The reagents eugenol and eugenyl acetate were obtained from Sigma Aldrich. Acetic anhydride, *n*-hexane and ethyl acetate were supplied by Synth (Diadema-SP/Brazil). All chemicals were analytical grade. Carbon dioxide (99.9%) was purchased from White Martins S.A. (Campinas-SP/Brazil).

4.2.2 Characterization of the enzymes

The activity of the immobilized enzymes was determined as the initial rate of the esterification reaction of oleic acid (Sigma Aldrich) with propanol (Sigma Aldrich) at a molar ratio of 3:1, with hexane (Synth) as reaction medium and enzyme

concentration of 5% (w/w) in the substrates. The mixture was kept at 50 °C in a shaker incubator (TE-421, Tecnal, Piracicaba-SP/Brazil) at 150 orbitals per minute (OPM) for 30 min. Then, the oleic acid content was determined by titration with KOH 0.1 M in ethanol (Synth). A unit of activity (U) was defined as the amount of enzyme needed to consume 1 μmol of oleic acid per minute. All determinations of lipase activity were replicated at least three times. The residual activity (%) of the lipase was defined as the ratio between the activity of the untreated enzyme (U_0) and that of the lipase treated with SC-CO_2 (U), as stated in Equation 1.

$$Residual\ Activity\ (\%) = \left(\frac{U}{U_0}\right) x\ 100 \quad (1)$$

The protein content of the enzymes was determined by the Lowry method [18], but the original method is not suitable for immobilized lipase forms, so a preliminary desorption step was executed as according to the method proposed by Petry *et al.* [19]. A known amount of immobilized lipase (0.1–0.2 g) was stirred in 2–4 mL of the extraction buffer/solvent, 10% formic acid in 45% acetonitrile (in water), for 2 h, at room temperature (22-25 ºC). The material was washed three times with the same buffer/solvent for 10 min in each step, and finally with distillated water. The supernatant and washings were collected for protein analysis by the Lowry method [18], described as follows.

A standard curve was prepared with bovine serum albumin (BSA) powder (Sigma Aldrich). Samples, supernatant and washings were diluted in order to fit within the BSA standard curve range (0.02-0.6 mg/mL). 50 μL of sample and 450 μL of distilled water were placed in each tube. Next, 5 mL of biuret reagent was added to each tube and mixed thoroughly with a vortex. The biuret reagent was prepared by mixing three solutions: solution A: cupric sulfate at 1%; solution B: sodium potassium tartrate at 1%; solution C: 2% sodium carbonate in 0.1 M of NaOH with ratio of 1:1:50 (A:B:C). The mixture was then let incubating for 10 minutes prior to the addition of 500 μL per tube of 1.0 N Folin & Ciocalteu's reagent (Dinâmica, Diadema/SP), and the samples were mixed immediately. Color was developed for 30 minutes in the dark at room temperature and the absorbance was measured at 650 nm. All absorbance determinations were made using a UV–vis spectrophotometer (Hach, DR/4000U, Colorado, USA). All experiments were replicated at least three times.

The water content of immobilized lipases was determined by Karl Fischer titration using a model 701 Metrohm apparatus (Herisau, Switzerland) equipped with a 5 mL burette and an extractor, which was operated at 120 °C and a nitrogen (White Martins S.A., Campinas-SP/Brazil) flow rate of 50 x 10^{-9} mL/min. The Karl Fischer reagent used in the titration was from Merck (Darmstadt, Germany).

The mean particle size distributions of Lipozyme 435 and Novozym 435 were determined based on the static light scattering method using a Multi-Angle Static Light-Scattering Mastersizer (Malvern Instruments, Worcestershire, UK). The real densities of immobilized enzymes were measured by helium pycnometry, whereas bulk density was measured by weighing a known volume of solid material. Finally, the ratio between real and bulk density determined the porosity of the packed enzyme bed.

4.2.3 Synthesis of eugenyl acetate in SC-CO_2

The experimental homemade apparatus used in all reaction experiments consists in a CO_2 booster (Maximator M-111, Zorge/Germany), a solvent reservoir, a cooling (Solab SL152/18, Êxodo Científica, Hortolândia/SP, Brazil) and a heating thermostatic (Marconi S.A., Campinas-SP/Brazil) baths. Manometers (Zurich, São Paulo-SP/Brazil), a magnetic stirrer (IKA, RCT Basic, Staufen/Germany), thermocouples, control valves (Autoclave Engineers), a micrometric valve (Autoclave Engineers, Erie/PA, USA) and a stainless steel vessel of 100 mL. Figure 1 shows the schematic flow diagram of the high-pressure stirred-bath reactor unit.

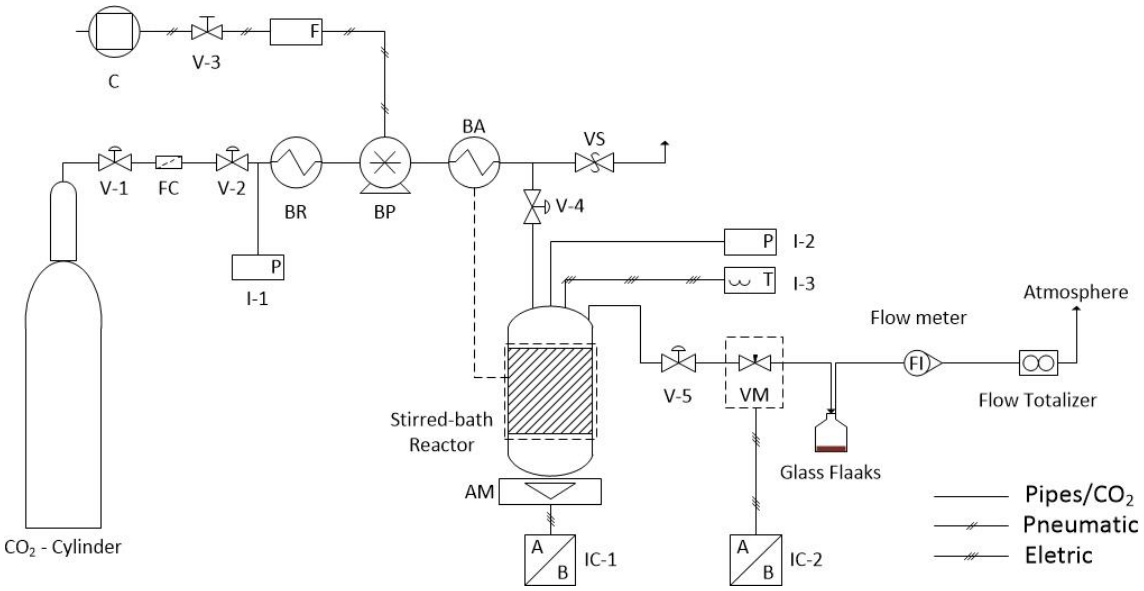

Figure 1. Diagram of the homemade unit for high-pressure stirred-batch reactor containing: V-1, V-2, V-3, V-4 and V-5– Control valves; VM – Micrometer valves; VS – Safety valve (Pmax = 30 MPa); C- Compressor; F-Compressed air filter; FC – CO_2 Filter ; BR – Cooling bath; BP- Pump (Booster); BA – Heating bath; I-1 and I-2– Pressure indicators; I-3 - Temperature indicators; IC-1 – Indicators and controllers of magnetic stirrer; IC-2 – Indicators and controllers of temperature of micrometer valve; AM – Magnetic stirrer.

First, an amount of immobilized lipase was placed inside the high-pressure stirred-bath reactor. After 30 min of thermal stabilization and to remove the residual superficial water in the catalyst and the wall reactor, the reaction mixture formed by eugenol and acetic anhydride was introduced in the stirred-batch reactor. Next, the reactor was pressurized with CO_2 at a rate of 10 MPa.min^{-1}. After the end of the established reaction time (1 hour), the system was depressurized at 1 MPa.min^{-1}. In all experiments the stirring rate was fixed at 600 rpm. The evaluated process variables were pressure (10 to 30 MPa), temperature (40 to 60 °C), enzyme concentration (1 to 10 %), concentration of substrates (molar ratio from 1:1 to 5:1 of acetic anhydride : eugenol) and the reuse of the enzyme (1, 2 and 3 times). In the kinetic experiments each point of the curve at the same process condition represents the mean of the performed experiments at the established reaction time. All experiments were replicated at least three times.

From the amount of eugenol and eugenyl acetate after the reaction, the mass balance and the reaction stoichiometry, it was possible to determine the esterification rate or conversion (X, %), which was obtained by the molar ratio between the products (n_p) and substrates (n_s), using Equation 2:

$$X(\%) = \left(\frac{n_p}{n_s}\right) x\ 100 \quad (2)$$

The specific productivity of eugenyl acetate (SP) was expressed as the mass ratio between product (m_p) and catalyst (m_c) per unit time (t), as shown in Equation 3:

$$SP\ (kg/kg * h) = \frac{m_p}{m_c * t} \quad (3)$$

The esterification of eugenol was also performed in *n*-hexane for comparison with SC-CO_2. The reaction was carried out at atmospheric pressure and temperature, substrate molar ratio (5:1 acetic anhydride/eugenol) and concentration of enzyme (1%) equal to those used in the reactions in SC-CO_2 at the best condition of conversion and specific productivity. The reaction volume was completed to 100 mL of hexane and the mixture was incubated in a shaker incubator (TE-421, Tecnal, Piracicaba-SP/Brazil) under agitation of 150 orbitals per minute (OPM). After one hour an aliquot of 1.5 mL was filtered (Chormafil Xtra PA-20/25, Macherey-Nagel, Düren/Germany) and analyzed by gas chromatography (see Section 2.5.) to determine the concentrations of eugenol and eugenyl acetate. The experiments were replicated three times.

4.2.4 Phase behavior experiments

The solubility of substrates in SC-CO_2 depends on CO_2 density, which can be tuned by changes in temperature and/or pressure, and an increase in solubility of substrates in SC-CO_2 can lead to an increase in the reaction rate. On the other side, a decrease on reaction rate can occur due to formation of two phases (liquid and gas) [20]. Therefore, phase behavior experiments were performed through a static method without sampling in a high-pressure variable-volume view cell. Basically, the apparatus consists of a view cell with two sapphire windows for visual observations, a magnetic stirrer to promote the agitation in the mixture, an absolute pressure transducer (Novus, TP-Model 520, Brazil), a “PT 100” type thermocouple inside the cell, a CO_2 pump (Thermo Separation Products, Model Constametric 3200 P/F, Waltham/USA) that was coupled to

a cooling ultra-thermostatic bath (Marconi S.A., Model MA-184, Campinas-SP/ Brazil) and a metallic jacket on the cell coupled with a heating thermostatic bath (Polyscience, Illinois/USA). The equilibrium cell includes a movable piston, which allows pressure control inside the cell.

Phase behavior was visually observed through the pressure manipulation using the pump with CO_2 as pneumatic fluid. First, the amount of substrates and enzyme were introduced inside the view cell. The cell was closed and loaded with a determined amount of CO_2. After the desired temperature was reached, the pressure was increased until the observation of a single phase. From this point, the pressure was slowly decreased until the apparition of a new phase. Three temperatures were evaluated (40, 50 and 60 °C) with enzyme concentration and substrates' molar ratio of 1% and 5:1 (acetic anhydride/eugenol), respectively, which are the same used in the reaction experiments.

4.2.5 Analytical methods

After the reaction the reactant (eugenol) and product (eugenyl acetate) contents were determined using a gas chromatograph with a flame ionization detector (GC-FID). The method was based according to Zabot *et al*. [21]. A GC–FID chromatograph (Shimadzu, CG17A, Kyoto/Japan) equipped with a capillary column of fused silica DB-5 (J&W Scientific, 30 m × 0.25 mm × 0.25 μm, Folsom,/USA) was used. Each sample was filtered (Chormafil Xtra PA-20/25, Macherey-Nagel, Düren/Germany) and diluted to 5 mg/ml in ethyl acetate, and 1 μL was injected into the chromatograph. The sample split ratio was 1:20. The carrier gas (Helium, 99.9% purity, White Martins, Campinas,/Brazil) flowing at 1.1 mL/min. The injector and the detector temperatures were 220 and 240 °C, respectively. The column was heated from 60 °C to 246 °C at 3 °C/min. At these conditions the retention times of eugenol and eugenyl acetate peaks were 24 and 32 min, respectively. Quantification was performed using external standard calibration curves (R^2 = 0.999 to eugenol and R^2 = 0.996 to eugenyl acetate).

4.2.6 Kinetic model

The experimental data of conversion versus time were adjusted with a second-order model, as shown in Equation 4. The quality of this adjustment was evaluated from the determination coefficient (R^2) using the MATLAB software (2014Ra, MathWorks, Natick, MA, USA)

$$X(\%) = at^2 + bt + c \tag{4}$$

where X is the conversion (%), t is time (h) and a, b and c are adjustable parameters.

Through the analytical derivative of the adjusted model for eugenol conversion, the eugenol conversion rate at each time t was calculated, as shown in Equation 5.

$$v = C_{e,0}\left(\frac{dX}{dt}\right) \tag{5}$$

where v is the reaction rate at the time t (mol/l.s), $C_{e,0}$ is the initial ($t = 0$) concentration of eugenol (mol/l) and dX/dt is the analytical derivative of the conversion calculated with Equation 4.

Next, the reaction rate was adjusted with the Ping-Pong Bi-Bi model without inhibition, as described by Equation (6).

$$v = \frac{V_{\max}[A][B]}{K_m^B[A] + K_m^A[B] + [A][B]} \tag{6}$$

where $V_{\max}$ is the maximum reaction rate (mol/l.g.s), $[A]$ and $[B]$ are the acetic anhydride and eugenol concentrations (mol/l), respectively, and K_m^A and K_m^B are the Michaelis-Mentem constants for acetic anhydride and eugenol (mol/l).

The Ping-Pong Bi-Bi model was fitted to the calculated reaction rate (v) using a minimum of constrained nonlinear multivariable function algorithm from the MATLAB software. The objective function was defined as sum of the squares, as shown in Equation (7).

$$f_{obj} = \sum_{i=1}^{n} \left[v_{exp} - v_{sim} \right]^2 \quad 7)$$

where v_{exp} is the experimental reaction rate (mol/l.s), v_{sim} is the simulated reaction rate (mol/l.s) and n is the total of experimental points.

The activation energies were obtained from the slope of the straight line of $ln\left(\frac{k_B T}{h K_m}\right)$ *vs* reciprocal of absolute temperature (1/T), as described by the Arrhenius Equation (8) and the Eyring absolute rate equation [22, 23].

$$\ln\left(\frac{k_B T}{h K_m}\right) = -\frac{E_a}{RT} + \ln(A) \quad 8)$$

where K_m is the Michaelis-Menten constant, h is the Planck constant (6.6256 x 10^{-34} J.s), k_B is Boltzman constant (1.3805 x 10^{-24} J/K), A is the frequency factor, E_a is the activation energy and R is the molar gas constant (8.314 J/K.mol).

4.2.7 Statistical analysis

The results of conversion and specific productivity of eugenyl acetate were statistically evaluated by ANOVA, using the software Statistica for Windows 6.0 (Statsoft Inc., USA) in order to detect significant differences. The significant differences at level of 5% ($p < 0.05$) were analyzed by the Tukey test.

4.3 RESULTS AND DISCUSSION

4.3.1 Effect of the enzyme concentration

In industrial applications the process variables should be controlled to obtain the maximum specific productivity with minimum cost, specifically in biocatalyzed processes where high esterification and low enzyme concentrations should be achieved. Therefore, the effects of enzyme concentration and substrates' molar ratio

on the conversion and specific productivity of eugenyl acetate using Lipozyme 435 and Novozym 435 were evaluated. In these experiments the temperature and pressure of supercritical CO_2 were fixed at 40°C and 10 MPa, respectively. In these conditions the immobilized lipases has been showed the highest residual activity [24-26]. Moreover, the stirring rate was fixed in a higher value to ensure that the reaction was kinetically controlled and the inter-particle diffusion effect and external mass transfer was negligible [27, 28]. The results are shown in Table 1.

Table 1. Effect of enzyme concentration and substrates' molar ratio on the conversion and specific productivity of eugenyl acetate using two different lipases in SC-CO_2.

Enzyme (%)[1]	Molar Ratio[2]	Conversion (%)		Specific productivity (kg/kg.h)	
		Lipozyme 435	Novozym 435	Lipozyme 435	Novozym 435
1	1:1	4.42 ± 0.18^{eA}	1.63 ± 0.02^{eB}	3.29 ± 0.02^{abA}	1.21 ± 0.04^{cdB}
1	3:1	6.50 ± 0.25^{deB}	15.60 ± 0.69^{cdA}	2.59 ± 0.10^{bcB}	6.73 ± 0.45^{bA}
1	5:1	19.34 ± 1.34^{aB}	33.23 ± 0.26^{aA}	6.22 ± 0.41^{aB}	10.09 ± 0.07^{aA}
5	1:1	12.27 ± 2.53^{bcA}	5.11 ± 0.54^{eB}	1.89 ± 0.39^{cdA}	0.78 ± 0.08^{dB}
5	3:1	15.70 ± 0.27^{abB}	19.61 ± 0.85^{cA}	1.37 ± 0.02^{deB}	1.71 ± 0.07^{cA}
5	5:1	18.50 ± 1.20^{aB}	26.58 ± 0.36^{bA}	1.13 ± 0.12^{deB}	1.62 ± 0.02^{cA}
10	1:1	10.34 ± 0.95^{cdB}	14.45 ± 2.92^{dA}	0.80 ± 0.07^{eA}	1.11 ± 0.21^{cdA}
10	3:1	16.30 ± 0.01^{abB}	19.37 ± 0.99^{cA}	0.72 ± 0.01^{eB}	0.84 ± 0.04^{dA}
10	5:1	20.27 ± 1.00^{aA}	19.51 ± 0.49^{cA}	0.64 ± 0.03^{eA}	0.60 ± 0.01^{dA}

Experiments were carried out at fixed conditions of time (1 hour), stirring (600 rpm), pressure (10 MPa) and temperature (40 °C). [1]Enzyme concentration expressed by weight of substrates, w/w (%); [2] Acetic anhydride/eugenol molar ratio (M/M). Different indexes (a,b,c,d) in the same column (lowercase) or in the same line (uppercase) indicate that the means differ significantly by Tukey's test ($p \leq 0.05$). For example: Lowercases compares the means at different experimental conditions at the same enzyme and uppercases compares the means at different enzymes at the same experimental condition.

The ANOVA results show that the effect of enzyme concentration on the conversion was statistically significant ($p < 0.05$ and $F_{cal} = 37.97$) using immobilized lipase Lipozyme 435, and not significant for Novozym 435 ($p = 0.362$ and $F_{cal} = 1.14$). It can be observed that, for Lipozyme 435, the highest conversion of eugenyl acetate was obtained with high concentration of the enzyme (10%) at the three evaluated substrate molar ratios, but for Novozym 435 this behavior was not observed in any condition. Moreover, at the highest substrate molar ratio 5:1 (acetic anhydride/eugenol) for Lipozyme 435, the concentration of lipase did not affect the conversion. The same behavior was found to the specific productivity of eugenyl acetate, but the magnitude of the specific productivity decreases with the amount of enzyme increase, even with increase of reaction rate.

The increase of enzyme loading results in higher reaction rate, as exposed on Table 1. Although the reaction time was kept constant at one hour, the highest rate and specific productivity for both commercial lipases were obtained with 1% enzyme and 5:1 molar ratio. Eventually, with longer reaction time some experimental runs would overlap for larger enzyme content. However, in the industrial point of view it is interesting to use lower amount of catalyst (enzyme), which results in reduced cost. Other works using SC-CO_2 as reaction medium obtained similar results [29, 30]. Chiaradia *et al.* [16], studying the eugenyl acetate esterification in a solvent-free system found a significant effect of the enzyme (Novozym 435) concentration on the conversion, and concluded that lower concentrations can be used without affecting the reaction conversion. It should be emphasized that the conversion increased with the substrates concentration, but in the same molar ratio, 5:1, the increase of enzyme concentration not affected the reaction rate (conversion), from 5.5 to 10%. Probably because in these conditions the quantity of substrates was the controller reaction rates instead the enzyme concentration. Furthermore the values obtained to reaction rate in these experiments were not large enough to compensate the amount of immobilized lipase used in the reaction, thus the lowest values of specific productivity were obtained.

4.3.2 Effect of acetic anhydride and eugenol molar ratio

Acetic acid has been traditionally used as acyl donor to flavor ester reactions (direct esterification) [31]. Moreover, several works have reported an inhibition of enzyme by high concentration of acid [3], probably due to the decrease of pH in the reaction system. In addition, acetic acid can be a lipase inhibitor, reacting with serine in the active site of the enzyme [32]. Alternatively, the synthesis of esters can be performed by transesterification with acetates and by acylation with acetic anhydride [7]. Table 1 shows the conversions and specific productivities obtained with three acetic anhydride concentrations and three different enzyme loadings.

A positive effect of molar ratio on the conversion and specific productivity of eugenyl acetate was observed, and the ANOVA results showed that the acetic anhydride/eugenol molar ratio was statistically significant in the conversion using both immobilized lipases, Lipozyme ($p < 0.05$ and $F_{cal} = 104.20$) and Novozym 435 ($p < 0.05$ and $F_{cal} = 447.40$). In fact, the major effect on the conversion was that of acetic

anhydride/eugenol molar ratio. The same behavior was observed by Chiaradia *et al.* [16], who concluded that the molar ratio of acetic anhydride/eugenol presented a positive effect, followed by the effect of temperature on eugenyl acetate production in a solvent-free system using Novozym 435. It is also observed on Table 1 that the conversion and specific productivity of eugenyl acetate using Novozym 435 was higher than that of Lipozyme 435 at all experimental conditions, except under the lowest molar ratio with 1 and 5% of enzyme, in which is probably attributed to experimental errors. In order to explain the reasons why Novozym 435 outperformed Lipozyme 435 in the eugenol conversion, the characterization of both lipases was performed and the results are exposed on Table 2.

Table 2. Characteristics of two different immobilized lipases from *Candida antarctica*.

Characteristic	Novozym 435	Lipozyme 435
Enzymatic Activity (U/g)	167.1±0.39	173.9±0.36
Protein Content (mg/g of particle)	85.4±5.41	108.2±6.38
Specific Enzymatic Activity (U/mg)	1.95 ± 0.07	1.60 ± 0.01
Water Content (g/g, %)	1.62±0.04	2.71±0.06
Bulk Density (g/cm³)	0.35±0.01	0.35±0.01
Real Density (g/cm³)	0.96±0.01	1.21±0.06
Porosity (ad.)	0.64±0.01	0.71±0.01
Mean Diameter (μm)	350.3±2.5	452.4±12.6

According to the enzyme supplier, Lipozyme 435 is food grade while Novozym 435 is analytic or technical grade, information also reported by Melgosa *et al.* [24]. This can be confirmed by the specific enzymatic activity (SA), which represents the ratio between the enzymatic activity and protein content. The SA of Lipozyme 435 was 1.6 U/mg while Novozym 435 achieved SA about 18% higher, 1.9 U/mg. The water content of Novozym 435 was similar to that found by Habulin *et al.* [33] (1.44%) and lower than the obtained by Yadav and Devi [34] (3%), but the titrable water content for Lipozyme 435 was about four times higher than that reported by Melgosa *et al.* [24] (0.7 ± 0.2%).

Particle size, porosity and density are important characteristics of catalysts, which can influence mass transfer and intraparticle diffusion of substrates and products, and consequently the reaction rate and specific productivity. The measured bulk density for both immobilized lipases was the same as reported by the enzyme supplier, and closer to that reported by Yadav and Devi [34] for Novozym 435 (0.45 g/cm³). However, the real density of Lipozyme was higher than that of Novozym 435. In fact,

the immobilization material is the same for both lipases (macroporous resin of poly-methyl methacrylate (Lewatit VP OC 1600)) [24, 35], but since Lipozyme 435 contains more protein with lower SA, these proteins may also have been immobilized during the immobilization process, increasing the real density of the particles. Moreover, the mean particle diameter of Lipozyme is higher than that of Novozym 435. According to Yadav and Devi [34] the bead size range of Novozym 435 is 0.3–0.9 mm, and the same particle distribution was observed for both immobilized lipases. Despite the higher specific enzymatic activity of Novozym 435, the study of the effects of SC-CO_2 pressure and temperature on the conversion and specific productivity of eugenyl acetate was performed with Lipozyme 435 because few papers dealing with enzymatic reactions using a food grade immobilized lipase (Lipozyme 435) are found in literature.

4.3.3 Effect of pressure and temperature of SC-CO_2

Based on the results shown on Table 1, the effects of temperature and pressure were evaluated at the conditions that achieved high conversion and specific productivity. Thus, the enzyme concentration and acetic anhydride/eugenol molar ratio were kept constant at 1% and 5:1, respectively. According to Oliveira *et al.* [25] for Novozym 435 and Melgosa *et al.* [24] for Lipozyme 435 and Lipozyme RM IM, the increase of temperature in a supercritical reaction process causes a decrease of the residual activity of enzymes. The same behavior was reported to pressure by several works [24, 25, 36]. Indeed, according to Knez, Habulin and Primožič [37] the pressure-induced deactivation of enzymes occurs mostly above 150 MPa. Based on the literature survey, the experiments were performed at temperatures from 40 to 60 °C and pressures from 10 to 30 MPa. Table 3 shows the effects of temperature and pressure on the conversion and specific productivity of eugenyl acetate using the Lipozyme 435 as catalyst.

Table 3. Effect of temperature and pressure on the conversion and specific productivity of eugenyl acetate using Lipozyme 435.

Temperature (°C)[1]	Pressure (MPa)[2]	Conversion (%)	Yield (kg/kg.h)
40	10	19.34 ± 1.34^{c}	6.22 ± 0.41^{b}
40	20	20.76 ± 0.25^{c}	6.38 ± 0.08^{b}
40	30	22.80 ± 0.08^{c}	7.01 ± 0.02^{b}
50	10	32.26 ± 1.25^{a}	9.77 ± 0.36^{a}
50	20	21.17 ± 0.85^{c}	6.23 ± 0.26^{b}
50	30	24.77 ± 3.80^{bc}	7.53 ± 1.15^{b}
60	10	30.75 ± 0.74^{ab}	9.47 ± 0.23^{a}
60	20	20.17 ± 1.85^{c}	6.05 ± 0.35^{b}
60	30	24.70 ± 0.26^{bc}	7.51 ± 0.19^{b}

Experiments were carried out at fixed conditions of time (1 hour), agitation (600 rpm), enzyme concentration (1 %) and acetic anhydride/eugenol molar ratio (5:1). [1]Temperature and [2]Pressure of SC-CO_2. Different indexes (a, b, c, d) in the same column (lowercase) indicate that the means differ significantly by Tukey's test ($p < 0.05$).

The ANOVA analyses showed that the effects of pressure and temperature were statistically significant ($p < 0.05$ and $F_{cal} > F_{tab}$) on the conversion and specific productivity of eugenyl acetate. A positive effect of pressure at 40 ºC and a negative effect at 50 and 60 ºC can be observed on Table 3. The positive effect can be related to the increase of CO_2 density with pressure, which improves its solvation power in the reaction medium [20]. In turn, the negative effect on the conversion can be connected with the dilution of the substrates caused by the greater amount of CO_2 pumped into the reactor, causing an increase in the molar ratio between SC-CO_2 and substrates [20, 38]. Knez *et al.* [38] studied the effect of pressure on the conversion of free fatty acid into fatty acid ester using lipase from *Rhizomucor miehei* (Lipozyme RM IM) in dense CO_2. According to the authors, at pressures above 10 MPa the conversion decreased due to the dilution effect caused by larger CO_2 amount, which reduced the substrates' molar fraction in the reaction bulk, slowing down the esterification.

The effect of temperature from 40 to 50 °C was positive for the conversion, from 19 to 32% at 10 MPa, from 20 to 21% at 20 MPa and from 22 to 24% at 30 MPa. Besides, the increase of temperature from 50 to 60 ºC caused a decrease on the conversion, which can be related to the changes in the physical properties of the solvent, such as limitations in mass transfer, viscosity, surface tension and due to the decrease of the solvation power of the substrates at lower solvent density. The esterification of eugenol was also carried out in *n*-hexane for comparison with the results obtained at supercritical conditions. The conversion in *n*-hexane was 15.3 ± 1.8%, whereas in SC-CO_2 (10 MPa and 40 °C) it was near 19%. According to Laudani *et al*. [39], the higher diffusivity and lower viscosity and surface tension of SC-CO_2 are responsible for the

reduction of interphase transport limitations, thus increasing the reaction rate and esterification of eugenol.

Researches dealing with esterification reactions in supercritical media have shown that the conversion can be influenced by the solubility of substrates in SC-CO_2, which depends on the system's temperature and pressure. The solubilities of eugenyl acetate and eugenol in SC-CO_2 were reported by Cheng *et al.* [40], Souza *et al*. [41] and Guan *et al*. [42], who showed that the solubility of these compounds increase with CO_2 density. However, few publications dealing with phase equilibrium of the whole enzymatic esterification system have been found in the literature. Phase equilibrium experiments of the system eugenol/acetic anhydride/Lipozyme 435/SC-CO_2 were performed to observe the behavior at each experimental condition exposed on Table 3, and the results are shown in Appendix A (Supplementary data, Figure S1).

At 10 MPa and 60 °C the reaction mixture contained solid (enzyme), liquid and gas phases, and at the other conditions the equilibrium between solid and supercritical phase was observed. The transition from three-phase (solid-liquid-gas) to two-phase (solid-supercritical) system at 40, 50 and 60 ºC was observed at pressures around 8.0-8.2, 9.1-9.3 and 11-13 MPa, respectively. At the end of all phase equilibrium experiments a white and opaque solid material was observed on the view cell. This material can be observed in Figure S1 (Appendix A: Supplementary data) at conditions of 50-60 ºC and 20-28 MPa, where the reaction bulk became more opaque. This solid material may be a small particle displaced from the support of the immobilized lipase. Moreover, this can help elucidating the decrease of conversion at high temperature and pressure observed in the reactions using Lipozyme 435.

4.3.4 Reuse of Lipozyme 435

The main advantage of immobilized lipases over the free form is that the enzyme can be reused many times in the process, thus reducing the cost of catalyst. Several works have shown that the enzyme activity decreases continuously with the increasing number of cycles, so the reusability of Lipozyme 435 was analyzed at 10 MPa and 40º C, as shown on Table 4.

Table 4. Influence of reuse cycles of Lipozyme 435 on the conversion and specific productivity of eugenyl acetate in SC-CO_2 at 10 MPa and 40 ºC.

Number of Cycles	Conversion (%)	Specific productivity (kg/kg.h)
1	19.34 ± 1.34	6.22 ± 0.41
2	17.60 ± 0.29	5.45 ± 0.60
3	13.10 ± 0.06	4.43 ± 0.02

Experiments were carried out at fixed conditions of time (1 hour), agitation (600 rpm), enzyme concentration (1%) and acetic anhydride/eugenol molar ratio (5:1).

The substrates and products were extracted from the high-pressure vessel at 2 hours with a CO_2 flow rate of 2.84 x 10^{-4} kg/s, which was enough to remove all the compounds from the reactor, as established by previous experiments. The data on Table 4 show that the conversion and specific productivity of eugenyl acetate decreased continuously with the increasing number of cycles. The catalytic ability of the lipase CALB (*Candida antarctica* lipase B) in immobilized form decreases with the increase of the utilization cycles [20] or depressurization/pressurization cycles [24, 25]. The reduction of enzyme activity after SC-CO_2 exposure has been related to several reasons. One of them is the water content needed to preserve the conformation of enzyme, and thus its optimal activity [24, 43]. Therefore, the effect of the number of depressurization/pressurization cycles on the residual activity (%) and water content (%) of Lipozyme 435 treated with SC-CO_2 was evaluated. Each cycle was carried out at 40 °C, 10 MPa, 1 hour of exposure time, and the depressurization rate was fixed at 1 MPa.min^{-1}. The results are presented in Figure 2.

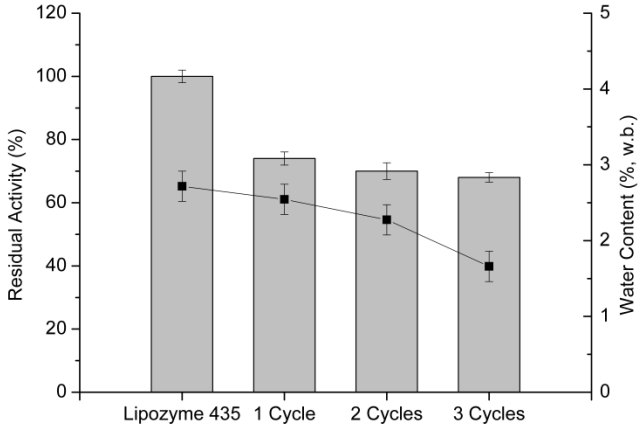

Figure 2. Effect of the number of depressurization/pressurization cycles on the residual activity (bar chart, %) and water content (■, %) of Lipozyme 435 treated with SC-CO_2 at 10 MPa and 40 ºC.

It can be noted that the residual enzyme activity and the water content decreased with the increase of the number of depressurization/pressurization cycles. The initial titrable water content of Lipozyme 435 was 2.71 ± 0.06%, and after exposure to SC-CO_2 it decreased to 2.54 ± 0.20, 2.27 ± 0.22 and 1.66 ± 0.19%, for 1, 2 and 3 cycles respectively. These results of residual activity are in accordance with those reported by Melgosa *et al.* [24] for Lipozyme RM IM and Lipozyme 435, in which several depressurization/pressurization steps led to activity loss of both immobilized lipases. Moreover, the authors did not report the water content of the Lipozyme 435 after treatment with SC-CO_2, because of the low values found. Habulin *et al.* [33] related the decrease of residual activity to the extraction of essential water from the immobilized lipase Novozym 435, in which the water content fell from 1.44% for the untreated enzyme to 0.88% for lipase treated with SC-CO_2.

4.3.5 Kinetic experiments

The kinetics of the production of eugenyl acetate was investigated at 10 MPa, with 1% (w/w) of enzyme, 5:1 molar ratio and stirring at 600 rpm. The results are shown in Figure 3 (A) for conversion (%) and (B) for specific productivity (kg/kg.h). It can be observed that, at longer times, the conversion increased for the reaction at the three tested temperatures, 40, 50 and 60 ºC. However, the specific productivity of eugenyl acetate decreased with time for all temperatures. This behavior can be explained observing Equation (3), which suggests that the increase of reaction time decreases its specific productivity. To keep the specific productivity at similar values for all reaction times the conversion should be twice the obtained at the previous point. Based on the kinetics experiments and the phase behavior the optimal conditions of eugenyl acetate synthesis were 50 and 60°C at 10MPa. Although it appears a two-phase region (liquid and gas) at 60°C and 10 MPa, the reaction rate was about equal to the experiments at 50°C and 10 MPa.

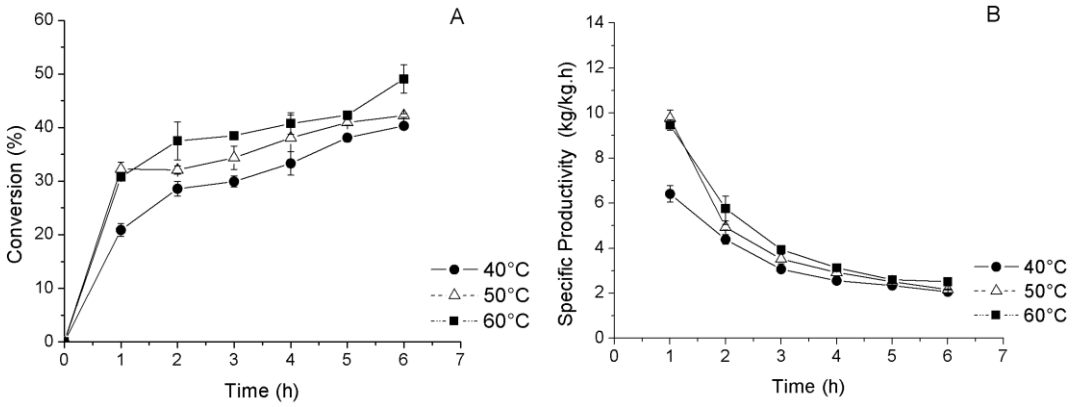

Figure 3. Kinetics of eugenyl acetate conversion (A) and specific productivity (B) in SC-CO_2 at 40, 50 and 60 ºC. Experiments were carried out at fixed conditions of pressure (10 MPa), agitation (600 rpm), enzyme concentration (1%) and acetic anhydride/eugenol molar ratio (5:1).

The kinetics of many reactions have been successfully described by the Ping-Pong Bi-Bi model, such as hydrolysis, esterification and transesterification, using organic solvents [22, 44] or supercritical fluids [29, 30] as reaction media. In the kinetic study it is first necessary to determine possible inhibitions caused by any substance involved in the reaction [44]. In this work, the substrates are eugenol and acetic anhydride, and the products are eugenyl acetate and acetic acid. A second route of eugenol esterification can occur between acetic acid and eugenol, resulting in eugenyl acetate and water. This second route and the effect of acetic acid on the kinetics were not considered. The reaction routes are shown in Appendix A (Supplementary data, Figure S2). However, acetic acid is an important inactivating compound, causing an indirect inhibition by the decrease of pH in the reaction medium, changing the isoelectric point of proteins and thus inactivating the enzyme. Moreover, acetic acid can also act as a direct inhibitor of the enzyme, forming a dead-end complex. According to Romero *et al.* [44], this effect has little importance when the initial concentration of substrates is low. Figure 4 shows the Lineweaver-Burk plot of reciprocal of the reaction rates versus reciprocal concentrations of acetic anhydride [A] and eugenol [B] at 40 ºC and 10 MPa (A) and the effect of substrates on the reaction rate (B).

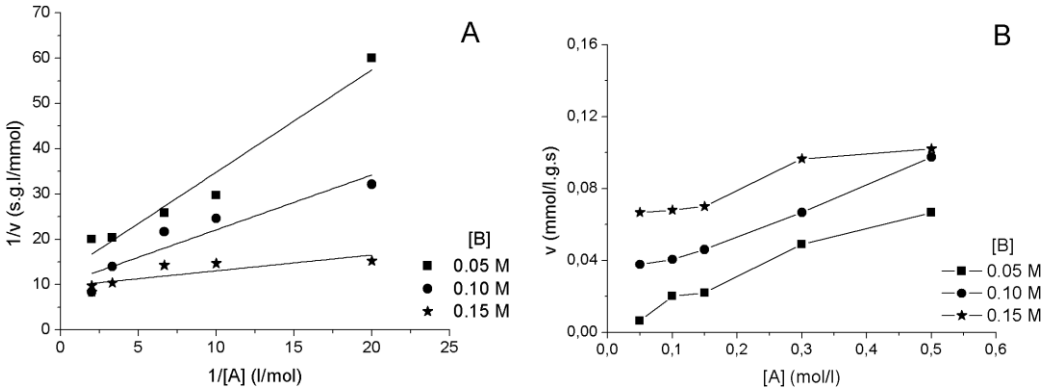

Figure 4. (A) Lineweaver-Burk plot of reciprocal of the reaction rates versus reciprocal acetic anhydride [A] concentration at different eugenol [B] concentrations. (B) Effect of acetic anhydride [A] concentration on the reaction rate at different eugenol [B] concentrations. Experiments were carried out at fixed conditions of agitation (600 rpm), enzyme concentration (1 %), time (1 hour), temperature (40 °C) and pressure (10 MPa).

The variation of the concentrations of the substrates acetic anhydride [A] and eugenol [B] caused an increase on the reaction rate, as shown in Figure 4 (B). Moreover, in the plot of Figure 4 (A) the esterification of eugenol followed the classical Michaelis-Menten kinetics. However, the three fitting straight lines in Figure 4 (A) were not parallel to each other, suggesting that the enzymatic reaction did not follow a simple Ping-Pong Bi-Bi mechanism within the range of tested concentrations [22, 45]. The kinetic parameters were obtained by fitting the model to the experimental data using a subroutine (*fminsearch*) of the software MATLAB [29]. The values calculated by the Lineweaver-Burk plot of reciprocal of the reaction rates versus reciprocal concentrations were used as initial guess. Table 5 shows the kinetic parameters adjusted with the model for the production of eugenyl acetate in SC-CO_2.

The affinity of the enzyme to the substrates can be determined by the value of $1/K_m$, which indicates that the affinity of the enzyme to acetic anhydride is larger than to eugenol. This suggests that acetic anhydride is the acyl donor that binds to the active sites of lipase. Similar behavior also was observed by Romero *et al.* [41], investigating the esterification of isoamyl alcohol and acetic anhydride using immobilized lipase in *n*-hexane. According to the authors, the Ping-Pong Bi-Bi mechanism can be divided in two steps: a) First, the acyl donor binds the enzyme, forming an enzyme-anhydride complex (EA). Through a unimolecular isomerization reaction, the EA complex is transformed to an enzyme-acyl complex (EC) and the first product (acetic acid) is released; b) The second substrate (eugenol) binds to the enzyme-

acyl complex (EC) forming a ternary complex, enzyme-acyl-eugenol. Again, through a unimolecular isomerization reaction the ternary complex is transformed to an enzyme-ester complex, finally releasing the second product (eugenyl acetate) and the enzyme in its initial conformation.

Table 5. Kinetic parameters for the production of eugenyl acetate in SC-CO_2 at 40, 50 and 60 ºC using Lipozyme 435.

Parameter	40° C	50 °C	60° C
V_{max} (µmol/g.s)	3.6	4.2	4.5
K_m^A (µM)	17.0	17.5	14.0
K_m^B (µM)	260.2	190.0	147.5
R^2 (%)[1]	97.1	97.5	94.9
f_{obj}[2]	8.0 x 10^{-14}	0.7 x 10^{-14}	3.0 x 10^{-14}

[1] Lack of fit to Equation (4); [2] Values for adjustment of Ping-Pong Bi-Bi model (Equation 6).

It can be noted on Table 5 that the affinity of both substrates (K_m^A and K_m^B) to the lipase and the maximum reaction rate increased from 40 to 60 ºC, suggesting a positive effect of temperature on the esterification rate. Furthermore, the activation energy for both steps could be determined by the Arrhenius equation (Equation 8) and the absolute values of the reaction rate. The activation energy for the first step was 5.8 kJ/mol. However, the activation energy for the second step was about four times higher, 21.4 kJ/mol. This confirms that the second step of the reaction has required more energy than the first step, so it was the rate-limiting reaction.

4.4 CONCLUSIONS

The synthesis of eugenyl acetate in SC-CO_2 using the immobilized lipases Novozym 435 and Lipozyme 435 was investigated at several conditions. Emphasis was given to the differences between the enzymes, the number of the utilization cycles and the effect of temperature and pressure, and the esterification kinetics was also studied. The specific enzymatic activity (SA) obtained for Novozym 435 was about 18% higher than that achieved by Lipozyme 435. Differences were also observed in the particle size distribution and water content of the immobilized lipases. Novozym 435 achieved higher conversion and specific productivity of eugenyl acetate than Lipozyme 435.

The influence of temperature and pressure was verified in reactions conducted with 1% of enzyme and substrate molar ratio of 5:1, and the optimal condition for the synthesis of eugenyl acetate in SC- CO_2 was determined at 50 and 60 ºC at 10 MPa, in which the study of phase behavior identified that the reaction mixture contained solid (enzyme), liquid and gas phases. The conversion and specific productivity of eugenyl acetate decreased with the increasing number of cycles, and the residual enzyme activity and the water content decreased with the increase of the number of depressurization/pressurization cycles. The results suggested that the reaction mechanism could be described to follow the simple Ping-Pong Bi-Bi mechanism within the range of studied concentrations. The affinity of acetic anhydride to the enzyme was larger than that of eugenol, and the affinity of both substrates to the lipase and the maximum reaction rate increased with temperature. The second step of the reaction kinetics required more energy that the first step, so it was identified as the rate-limiting reaction.

4.5 ACKNOWLEDGEMENTS

The authors wish to thank CAPES (Project 2952/2011), CNPq (Ph.D. fellowship: 142373/2013-3) and FAPESP (Projects 2013/02203-6, 2015/11932-7 and 2009/54137-1) for the financial support.

4.6 APPENDIX A: Supplementary data

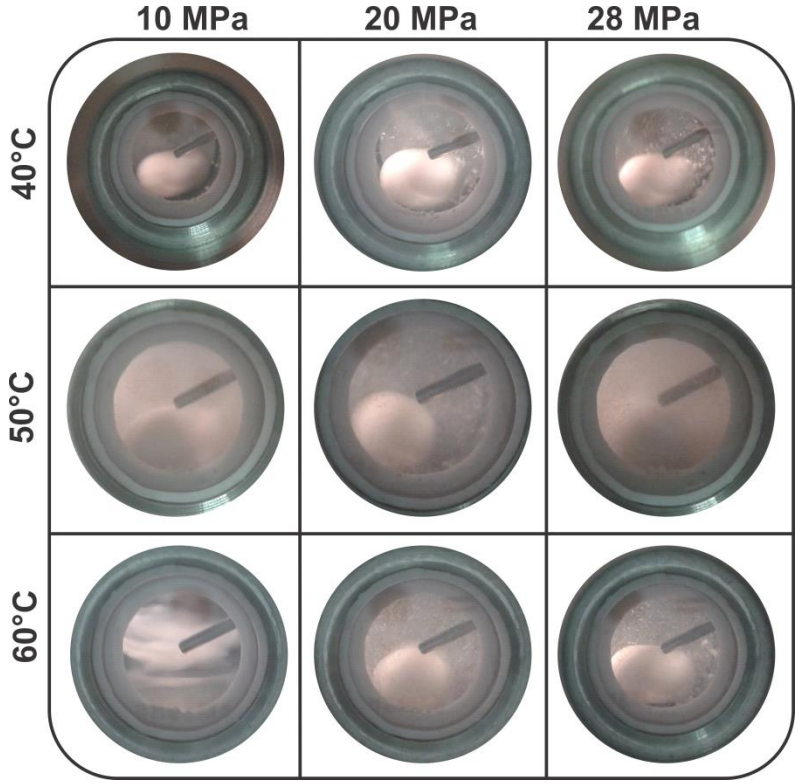

Figure S1. Phase behavior of the system eugenol/acetic anhydride/Lipozyme 435/SC-CO_2 Temperatures: 40, 50 and 60°C. Pressures: 10, 20 and 28 MPa.

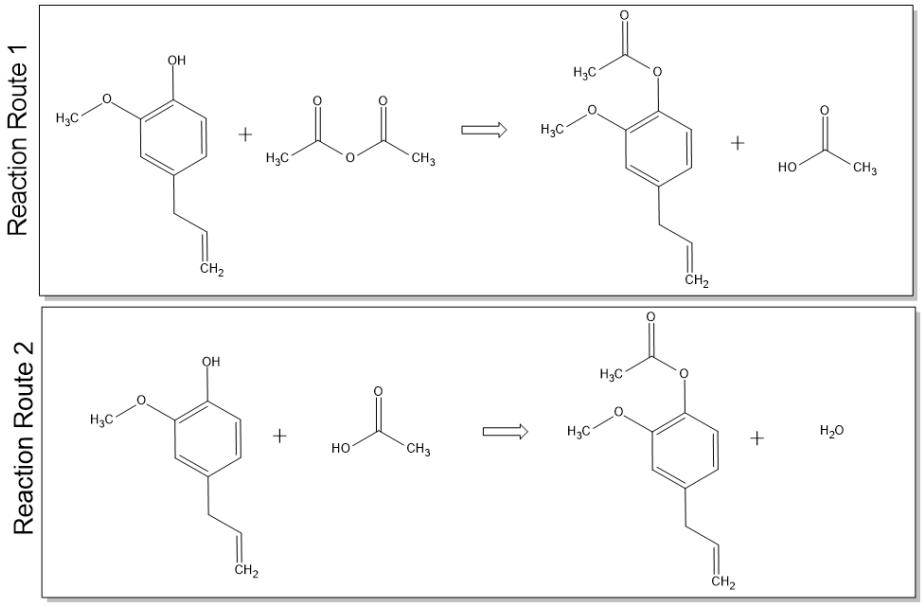

Figure S2. Routes of eugenyl acetate synthesis from eugenol and acetic anhydride (Reaction Route 1) or acetic acid (Reaction Route 2).

4.7 REFERENCES

[1] R. Couto, P. Vidinha, C.l. Peres, A.S. Ribeiro, O. Ferreira, M.V. Oliveira, E.n.A. Macedo, J.M. Loureiro, S. Barreiros, Geranyl Acetate Synthesis in a Packed-Bed Reactor Catalyzed by Novozym in Supercritical Carbon Dioxide and in Supercritical Ethane, Industrial & Engineering Chemistry Research, 50 (2011) 1938-1946.
[2] K.P. Dhake, D.D. Thakare, B.M. Bhanage, Lipase: A potential biocatalyst for the synthesis of valuable flavour and fragrance ester compounds, Flavour and Fragrance Journal, 28 (2013) 71-83.
[3] S. Hari Krishna, S. Divakar, S.G. Prapulla, N.G. Karanth, Enzymatic synthesis of isoamyl acetate using immobilized lipase from *Rhizomucor miehei*, Journal of Biotechnology, 87 (2001) 193-201.
[4] K.P. Dhake, K.M. Deshmukh, Y.P. Patil, R.S. Singhal, B.M. Bhanage, Improved activity and stability of *Rhizopus oryzae* lipase via immobilization for citronellol ester synthesis in supercritical carbon dioxide, Journal of Biotechnology, 156 (2011) 46-51.
[5] G.A. Macedo, Síntese de ésteres de aroma por lipases microbianas em meio livre de solvente orgânico, Faculdade de Engenharia de Alimentos, Universidade Estadual de Campinas, Campinas, 1997, pp. 143.
[6] K.E. Jaeger, T. Eggert, Lipases for biotechnology, Current opinion in biotechnology, 13 (2002) 390-397.
[7] M.D. Romero, L. Calvo, C. Alba, M. Habulin, M. Primožič, Ž. Knez, Enzymatic synthesis of isoamyl acetate with immobilized *Candida antarctica* lipase in supercritical carbon dioxide, The Journal of Supercritical Fluids, 33 (2005) 77-84.

[8] S. Srivastava, J. Modak, G. Madras, Enzymatic Synthesis of Flavors in Supercritical Carbon Dioxide, Industrial & Engineering Chemistry Research, 41 (2002) 1940-1945.
[9] G.A. Macedo, G.M. Pastore, M.I. Rodrigues, Optimising the synthesis of isoamyl butyrate using *Rhizopus* sp. lipase with a central composite rotatable design, Process Biochemistry, 39 (2004) 687-693.
[10] K.P. Dhake, P.J. Tambade, Z.S. Qureshi, R.S. Singhal, B.M. Bhanage, HPMC-PVA Film Immobilized *Rhizopus oryzae* Lipase as a Biocatalyst for Transesterification Reaction, ACS Catalysis, 1 (2011) 316-322.
[11] Ž. Knez, Enzymatic reactions in dense gases, The Journal of Supercritical Fluids, 47 (2009) 357-372.
[12] M. Raventós, S. Duarte, R. Alarcón, Application and Possibilities of Supercritical CO2 Extraction in Food Processing Industry: An Overview, 8 (2002) 269-284.
[13] E. Reverchon, I. De Marco, Supercritical fluid extraction and fractionation of natural matter, The Journal of Supercritical Fluids, 38 (2006) 146-166.
[14] E.F.S.A. European Food Safety Authority, Scientific Opinion on the safety and efficacy of allylhydroxybenzenes (chemical group 18) when used as flavourings for all animal species. EFSA Panel on Additives and Products or Substances used in Animal Feed (FEEDAP), EFSA Journal, 9 (2011).
[15] K.-G. Lee, T. Shibamoto, Antioxidant property of aroma extract isolated from clove buds [Syzygium aromaticum (L.) Merr. et Perry], Food Chemistry, 74 (2001) 443-448.
[16] V. Chiaradia, N. Paroul, R.L. Cansian, C.V. Júnior, M.R. Detofol, L.A. Lerin, J.V. Oliveira, D. Oliveira, Synthesis of Eugenol Esters by Lipase-Catalyzed Reaction in Solvent-Free System, Appl Biochem Biotechnol, 168 (2012) 742-751.
[17] H. Carrasco A., L. Espinoza C., V. Cardile, C. Gallardo, W. Cardona, L. Lombardo, K. Catalán M., M. Cuellar F., A. Russo, Eugenol and its synthetic analogues inhibit cell growth of human cancer cells (Part I), Journal of the Brazilian Chemical Society, 19 (2008) 543-548.
[18] O.H. Lowry, N.J. Rosebrough, A.L. Farr, R.J. Randall, Protein measurement with the Folin phenol reagent, The Journal of biological chemistry, 193 (1951) 265-275.
[19] I. Petry, A. Ganesan, A. Pitt, B.D. Moore, P.J. Halling, Proteomic methods applied to the analysis of immobilized biocatalysts, Biotechnol Bioeng, 95 (2006) 984-991.
[20] Ž. Knez, S. Kavčič, L. Gubicza, K. Bélafi-Bakó, G. Németh, M. Primožič, M. Habulin, Lipase-catalyzed esterification of lactic acid in supercritical carbon dioxide, The Journal of Supercritical Fluids, 66 (2012) 192-197.
[21] G.L. Zabot, M.N. Moraes, A.J. Petenate, M.A.A. Meireles, Influence of the bed geometry on the kinetics of the extraction of clove bud oil with supercritical CO_2, The Journal of Supercritical Fluids, 93 (2014) 56-66.
[22] D.-H. Zhang, C. Li, G.-Y. Zhi, Kinetic and thermodynamic investigation of enzymatic l-ascorbyl acetate synthesis, Journal of Biotechnology, 168 (2013) 416-420.
[23] A.C. Sehgal, R. Tompson, J. Cavanagh, R.M. Kelly, Structural and catalytic response to temperature and cosolvents of carboxylesterase EST1 from the extremely thermoacidophilic archaeon *Sulfolobus solfataricus* P1, Biotechnol Bioeng, 80 (2002) 784-793.
[24] R. Melgosa, M.T. Sanz, Á. G. Solaesa, S.L. Bucio, S. Beltrán, Enzymatic activity and conformational and morphological studies of four commercial lipases treated with supercritical carbon dioxide, The Journal of Supercritical Fluids, 97 (2015) 51-62.
[25] D. Oliveira, A.C. Feihrmann, A.F. Rubira, M.H. Kunita, C. Dariva, J.V. Oliveira, Assessment of two immobilized lipases activity treated in compressed fluids, The Journal of Supercritical Fluids, 38 (2006) 373-382.

[26] P. Santos, C.A. Rezende, J. Martínez, Activity of immobilized lipase *from Candida antarctica* (Lipozyme 435) and its performance on the esterification of oleic acid in supercritical carbon dioxide, The Journal of Supercritical Fluids, 107 (2016) 170-178.
[27] H. Veny, M.K. Aroua, N.M.N. Sulaiman, Kinetic study of lipase catalyzed transesterification of jatropha oil in circulated batch packed bed reactor, Chemical Engineering Journal, 237 (2014) 123-130.
[28] M. Hajar, F. Vahabzadeh, Production of a biodiesel additive in a stirred basket reactor using immobilized lipase: Kinetic and mass transfer analysis, Korean Journal of Chemical Engineering, 33 (2016) 1220-1231.
[29] M.N. Varma, G. Madras, Kinetics of enzymatic synthesis of geranyl butyrate by transesterification in various supercritical fluids, Biochemical Engineering Journal, 49 (2010) 250-255.
[30] M.V. Oliveira, S.F. Rebocho, A.S. Ribeiro, E.A. Macedo, J.M. Loureiro, Kinetic modelling of decyl acetate synthesis by immobilized lipase-catalysed transesterification of vinyl acetate with decanol in supercritical carbon dioxide, The Journal of Supercritical Fluids, 50 (2009) 138-145.
[31] H. Razafindralambo, C. Blecker, G. Lognay, M. Marlier, J.-P. Wathelet, M. Severin, Improvement of enzymatic synthesis yields of flavour acetates: The example of the isoamyl acetate, Biotechnol Lett, 16 (1994) 247-250.
[32] S.Y. Huang, H.L. Chang, M. Goto, Preparation of Surfactant-Coated Lipase for the Esterification of Geraniol and Acetic Acid in Organic Solvents, Enzyme and Microbial Technology, 22 (1998) 552-557.
[33] M. Habulin, S. Šabeder, M. Paljevac, M. Primožič, Ž. Knez, Lipase-catalyzed esterification of citronellol with lauric acid in supercritical carbon dioxide/co-solvent media, The Journal of Supercritical Fluids, 43 (2007) 199-203.
[34] G.D. Yadav, K.M. Devi, Enzymatic synthesis of perlauric acid using Novozym 435, Biochemical Engineering Journal, 10 (2002) 93-101.
[35] Y. Mei, L. Miller, W. Gao, R.A. Gross, Imaging the Distribution and Secondary Structure of Immobilized Enzymes Using Infrared Microspectroscopy, Biomacromolecules, 4 (2003) 70-74.
[36] M. Lanza, W. Priamo, J. Oliveira, C. Dariva, D. de Oliveira, The effect of temperature, pressure, exposure time, and depressurization rate on lipase activity in SCCO2, Appl Biochem Biotechnol, 113 (2004) 181-187.
[37] Ž. Knez, M. Habulin, M. Primožič, Enzymatic reactions in dense gases, Biochemical Engineering Journal, 27 (2005) 120-126.
[38] Ž. Knez, C.G. Laudani, M. Habulin, E. Reverchon, Exploiting the pressure effect on lipase-catalyzed wax ester synthesis in dense carbon dioxide, Biotechnology and Bioengineering, 97 (2007) 1366-1375.
[39] C.G. Laudani, M. Habulin, Ž. Knez, G.D. Porta, E. Reverchon, Lipase-catalyzed long chain fatty ester synthesis in dense carbon dioxide: Kinetics and thermodynamics, The Journal of Supercritical Fluids, 41 (2007) 92-101.
[40] K.-W. Cheng, S.-J. Kuo, M. Tang, Y.-P. Chen, Vapor–liquid equilibria at elevated pressures of binary mixtures of carbon dioxide with methyl salicylate, eugenol, and diethyl phthalate, The Journal of Supercritical Fluids, 18 (2000) 87-99.
[41] A.T. Souza, M.L. Corazza, L. Cardozo-Filho, R. Guirardello, M.A.A. Meireles, Phase Equilibrium Measurements for the System Clove (*Eugenia caryophyllus*) Oil + CO2, Journal of Chemical & Engineering Data, 49 (2004) 352-356.
[42] W. Guan, S. Li, C. Hou, R. Yan, J. Ma, Determination and correlation of solubilities of clove oil components in supercritical carbon dioxide, CIESC Journal, 58 (2007) 1077-1081.

[43] K. Rezaei, E. Jenab, F. Temelli, Effects of Water on Enzyme Performance with an Emphasis on the Reactions in Supercritical Fluids, Critical Reviews in Biotechnology, 27 (2007) 183-195.
[44] M.D. Romero, L. Calvo, C. Alba, A. Daneshfar, A kinetic study of isoamyl acetate synthesis by immobilized lipase-catalyzed acetylation in n-hexane, Journal of Biotechnology, 127 (2007) 269-277.
[45] I.H. Segel, Enzyme Kinetics, Wiley-Interscience, New York, 1993.

CAPÍTULO 5

ESTERIFICAÇÃO DE ÁLCOOL ISOAMÍLICO EM FLUIDO SUPERCRÍTICO

PRODUCTION OF ISOAMYL ACETATE BY ENZYMATIC REACTIONS IN BATCH AND PACKED BED REACTOR OPERATED WITH SUPERCRITICAL CO_2

Philipe dos Santos[1], M. Angela A. Meireles[1] and Julian Martínez[1]*

[1] Faculdade de Engenharia de Alimentos, Departamento de Engenharia de Alimentos, UNICAMP, Rua Monteiro Lobato, 80, CEP:13083-862, Campinas, SP, Brasil.

Os resultados desse capítulo foram submetidos ao periódico "*Journal of Molecular Catalysis B: Enzymatic*"

Production of Isoamyl Acetate by Enzymatic Reactions in Batch and Packed Bed Reactor operated with Supercritical CO_2

Philipe dos Santos[1], M. Angela A. Meireles[1], and Julian Martínez[1]*

[1] School of Food Engineering, Food Engineering Department, University of Campinas, UNICAMP, 13083-862, Campinas, SP, Brazil.

*Corresponding author at: Tel.: +55 19 35214033; fax: +55 19 35214027. E-mail address: julian@unicamp.br

Highlights

- Substrate's molar ratio, enzyme amount and agitation were statistically significant in the conversion of isoamyl alcohol;
- Temperature and pressure had small influence on the reaction;
- The kinetic model was able to describe the esterification of isoamyl alcohol;
- The reaction kinetics is independent of particle diameter and agitation;
- The continuous packed bed reactor is the best option to synthesize isoamyl acetate in SC-CO_2 media.

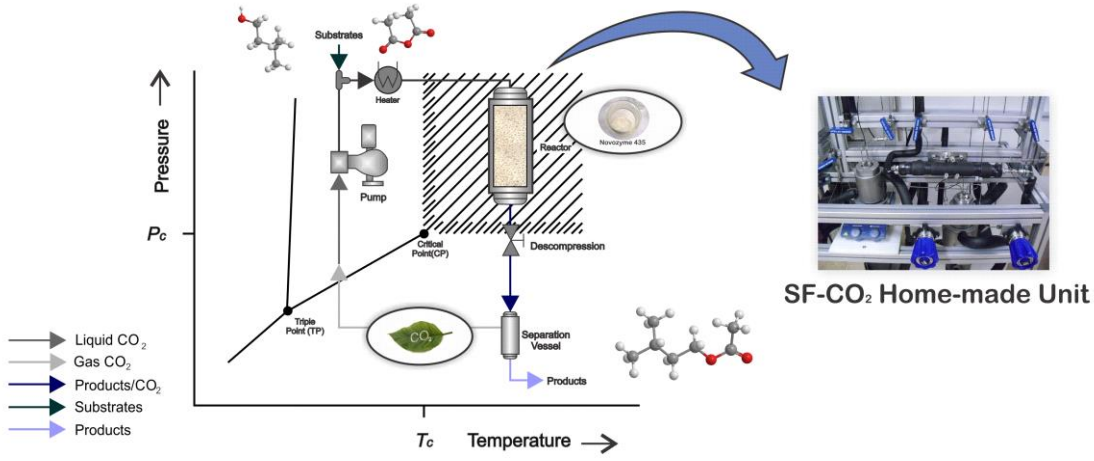

Abstract: Batch reactors (BRs) are probably the most widely used reactor designs for biocatalysis in supercritical fluids, but for industrial scale applications packed bed reactors (PBRs) are frequently preferred. The objective of this work was to investigate and compare BR and PBR in the synthesis of isoamyl acetate through enzymatic reactions in SC-CO_2 media. Experiments were performed to determine the kinetic parameters and to evaluate the internal and external mass transfer effects. The results indicate that the reaction is kinetically controlled, independently of particle diameter and agitation, therefore intra-particle diffusion and external mass transfer resistance are unimportant. The kinetic Ping-Pong Bi-Bi model described well the esterification of isoamyl alcohol with acetic anhydride at the evaluated conditions, indicating that the affinity of the enzyme to acetic anhydride is larger than to isoamyl alcohol. The PBR achieved the highest productivity of isoamyl acetate, although its conversion was lower than that obtained by the BR. In summary, PBR is the best option to synthesize isoamyl acetate in SC-CO_2 media.

Key-words: isoamyl alcohol; lipase; mass transfer; Thiele modulus; effectiveness factor.

5.1 INTRODUCTION

The demand for flavors and fragrances, including essential oils, other natural aromatic extracts and their blends is forecasted to increase 4.4% per year and reach $26.5 billion in 2016 [1]. Though, according to Markets & Markets [2], the food flavor market is projected to grow at a CAGR (Compound Annual Growing Rate) of 5.4 % from 2015 to 2020. Natural flavors have attracted the attention of manufacturers of food ingredients due to the increasing consumer demand for fresh and natural products. Low molecular weight esters [3-5], which are present in essential oils of natural matter and known by their flavoring properties, are technically difficult to extract, isolate and purify. Furthermore, conventional chemical synthesis leads to the formation of undesirable products for food and pharmaceutical industries. Therefore, biocatalyzed chemical synthesis has becomes attractive due to the high chemo-, regio- and stereo-selectivity of the enzymes [4]. Moreover, the esters produced through this route can be considered natural, since the process meets the required conditions to such attribute. For instance, the substrates or raw materials used in the process are natural and only physical or biotechnological processes must be employed for the isolation and purification of the formed products [4-6].

Lipases (glycerol ester hydrolases, EC 3.1.1.3) [7] have been employed as catalysts for the synthesis of esters, such as isoamyl acetate (banana flavor) [5, 8], isoamyl butyrate (pear flavor) [9, 10] and cinnamyl acetate (a compound of cinnamon essential oil) [11]. Besides, researches have shown that lipases are stable in pressurized fluids, which increases their potential application in esterification reactions [12]. Carbon dioxide (CO_2) is the most common supercritical solvent due to its low cost, nontoxicity, non-flammability, inertness, full recovery and moderate critical properties (Pc = 7.38 MPa, Tc = 304.2 K) when compared to other green solvents. Therefore, reactions in supercritical CO_2 can be carried out with low energy cost for pressurization, and at temperatures that do not damage the enzymes [13, 14].

Batch reactors (BRs) are probably the most used for synthesis with biocatalyst in supercritical fluids [8, 10, 15]. Nonetheless, their productivity is relatively low due to volumetric limitations (size). Packed bed reactors (PBRs) are often preferred at industrial scale [3]. BRs require a depressurization step to collect the products. According to Santos, Rezende and Martínez [15] and Melgosa *et al.* [16], this step can

lead to a decrease of lipase activity and make its reuse inviable. The PBR configuration coupled to a high-pressure separator may be an alternative to avoid the depressurization step, since the reaction mixture is collected in the separator and the catalyst remains packed inside the reactor.

In this context, the objective of the present work was to investigate the synthesis of isoamyl acetate through enzymatic reactions in SC-CO_2 media in a batch and packed bed reactors. First, the effects of enzyme and substrate's concentration, temperature, pressure and agitation were evaluated using a commercial immobilized lipase (Novozym 435). Next, experiments were performed to determine the kinetic parameters and to assess the internal and external mass transfer effects. Finally, the production of isoamyl acetate was carried out in a packed bed reactor and compared with that performed in the BR.

5.2 MATERIALS AND METHODS

5.2.1 Materials

A commercial lipase from *Candida antarctica* (Novozym 435), immobilized on a macroporous anionic resin (Lewatit VP OC 1600, supplied by Bayer), which consists of poly (methyl methacrylate-*co*-divinylbenzene) [17], was kindly supplied by Novozymes Brazil (Araucária-PR/Brazil). Isoamyl acetate was obtained from Sigma-Aldrich (Brazil). Isoamyl alcohol, acetic anhydride, acetic acid and *n*-hexane were supplied by Synth (Diadema-SP/Brazil). All chemicals were analytical grade. Carbon dioxide (99.9%) was purchased from White Martins S.A. (Campinas-SP/Brazil).

5.2.2 Particle characterization

Samples of the immobilized lipase Novozym 435 were classified in three groups to check the influence of particle diameter (D_p) on the mass transfer coefficient: Group 1 - Particles retained on mesh sieves from 10 to 32 (D_p = 486 ± 2 μm); Group 2 - Particles retained on mesh sieves from 35 to 42 (D_p = 400 ± 1 μm); and Group 3 - Particles retained on mesh sieves from 48 to 170 (D_p = 308 ± 3μm). The mean particle

diameter of each group and the mean diameter of Novozym 435 (350 ± 2.5 μm) were determined through the static light scattering method using a Multi-Angle Static Light-Scattering Mastersizer 2000 (Malvern Instruments, Worcestershire, UK).

The average particle diameter was determined by laser diffraction on a Mastersizer 2000 (Malvern Instruments, Malvern, United Kingdom). The calculation of the mean particle diameter was based of the mean diameter of a sphere of the same volume, as shown in Equation 1. The samples were analyzed in quintuplicate, by wet method, dispersed in water.

$$D_p = \frac{\sum n_i d_i^4}{\sum n_i d_i^3} \quad (1)$$

where d_i is the diameter of the particle *i* and n_i is the number of analyzed particles.

The real density of the immobilized enzyme (0.96 ± 0.01 g/cm³) was determined by helium pycnometry, whereas bulk density (0.35 ± 0.01 g/cm³) was measured by weighing a known volume of solid material. Finally, the porosity of the packed enzyme bed (0.64 ± 0.01) was determined from the ratio between real and bulk densities.

5.2.3 Synthesis of isoamyl acetate in SC-CO_2

The experimental homemade apparatus used in the BR experiments consists of a CO_2 pump (Maximator M-111, Zorge/Germany), a solvent reservoir, a cooling (Solab SL152/18, Êxodo Científica, Hortolândia/SP, Brazil) and a heating thermostatic (Marconi S.A., Campinas-SP/Brazil) bath, manometers (Zurich, São Paulo-SP/Brazil), a magnetic stirrer (IKA, RCT Basic, Staufen/Germany), thermocouples, control valves (Autoclave Engineers), a micrometric valve (Autoclave Engineers, Erie/PA, USA) and a 100 mL stainless steel vessel, with an inner diameter of 40 mm and length of 90 mm. Figure 1 shows the schematic flow diagram of the high-pressure BR unit [15].

First, an amount of immobilized lipase was placed inside the stainless steel vessel. After 20 min of thermal stabilization, the reaction mixture formed by isoamyl alcohol and acetic anhydride was introduced. Next, the vessel was pressurized with CO_2 at a rate of 10 MPa/min. After the end of the established reaction time, the system was depressurized at 1 MPa/min. In order, to evaluate the main effects of some process variables in conversion, productivity and specific productivity of isoamyl acetate, a factorial design of 2^{5-1} runs plus 3 central points was applied, totalizing 19 experiments. The evaluated process variables were pressure (10 to 30 MPa), temperature (40 to 60 °C), agitation (100 to 700 rpm), substrates' molar ratio (1:1 to 5:1) and enzyme concentration (1 to 10%). All experiments were replicated two times.

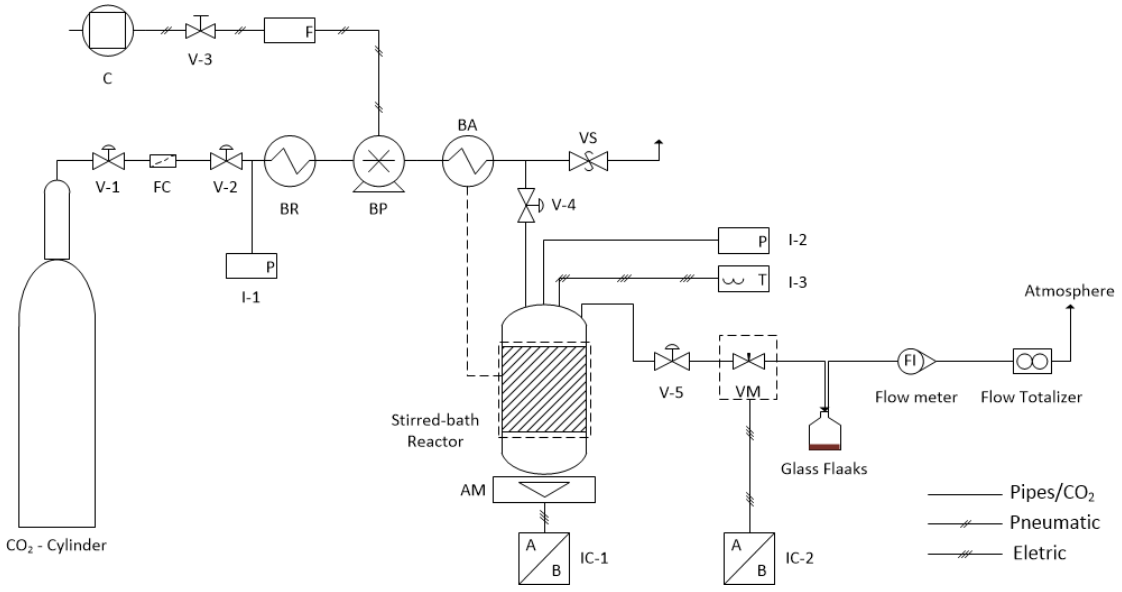

Figure 1. Diagram of the homemade unit for the high-pressure batch reactor [15] containing: V-1, V-2, V-3, V-4 and V-5– Control valves; VM – Micrometer valves; VS – Safety valve (P_{max} = 35 MPa); C- Compressor; F-Compressed air filter; FC – CO_2 Filter ; BR – Cooling bath; BP- Pump (Booster); BA – Heating bath; I-1 and I-2– Pressure indicators; I-3 - Temperature indicators; IC-1 – Indicators and controllers of magnetic stirrer; IC-2 – Indicators and controllers of temperature of micrometer valve; AM – Magnetic stirrer. With permission from Elsevier.

The esterification of isoamyl alcohol was also performed in *n*-hexane for comparison with the process in supercritical CO_2. The reaction was carried out at atmospheric pressure, temperature of 40° C, with substrate's molar ratio (1:1 acetic anhydride/isoamyl alcohol) and enzyme concentration (3%) equal to those used in the reactions in supercritical CO_2. The reaction volume was completed to 100 mL with *n*-hexane and the mixture was incubated in a shaker incubator (TE-421, Tecnal,

Piracicaba-SP/Brazil) under agitation of 250 orbitals per minute (OPM). After a determined time, a 1.5 mL aliquot was filtered (Chormafil Xtra PA-20/25, Macherey-Nagel, Düren/Germany) and analyzed by gas chromatography (see Section 2.4) to determine the concentrations of substrates and products. The experiments were replicated two times.

The packed bed reactor unit consists of the same SC-CO_2 pumping system of the high-pressure BR, which is connected to two liquid pumps for feeding the substrates and a mixer. The tubular PBR was assembled in stainless steel AISI 317 with an inner diameter of 3.37 mm and length of 0.33 m. The PBR unit is also composed of a 250 mL high-pressure separator, manometers (Zurich, São Paulo-SP/Brazil), thermocouples, control valves (Autoclave Engineers) and a micrometric valve (Autoclave Engineers, Erie/PA, USA). Figure 2 shows the schematic flow diagram of the high-pressure PBR.

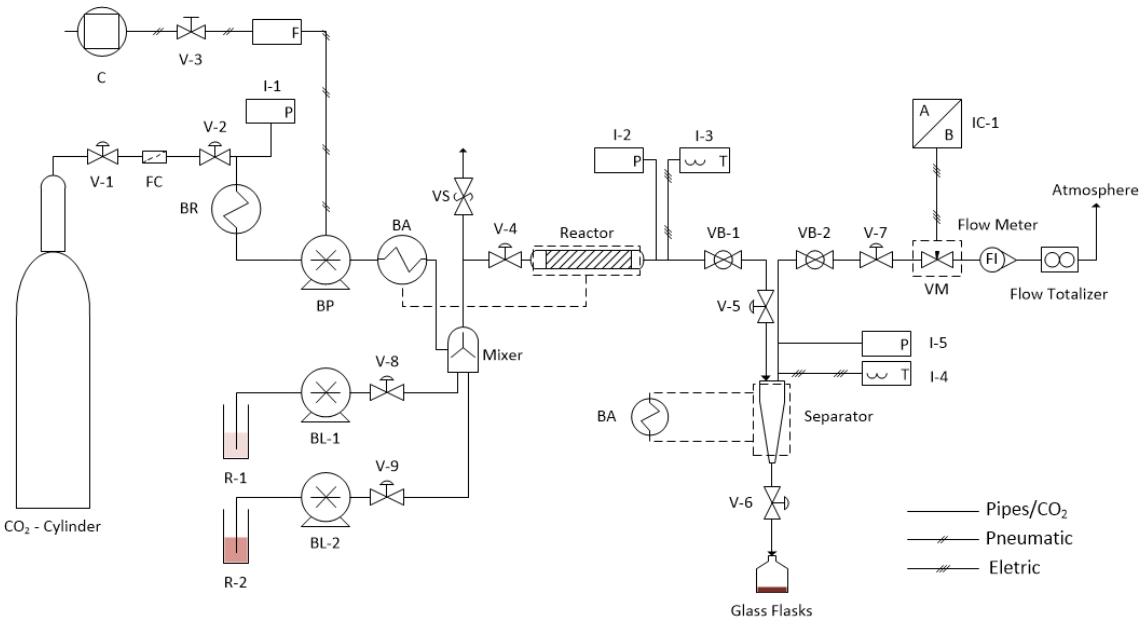

Figure 2. Diagram of the homemade unit for the high-pressure packed bed reactor, containing: V-1, V-2, V-3, V-4, V-5, V-6, V-7, V-8 and V-9 – Control valves; VM – Micrometer valves; VB-1 and VB-2 – Back-pressure valves; VS – Safety valve (P_{max} = 35 MPa); C- Compressor; F-Compressed air filter; FC – CO_2 Filter ; BR – Cooling bath; BP- Pump (Booster); BA – Heating bath; I-1, I-2 and I-5– Pressure indicators; I-3 and I-4 – Temperature indicators; IC-1 – Indicators and controllers of temperature of micrometer valve; BL-1 and BL-2 – Liquid pump; R-1 and R-2 – Substrate reservoirs.

The PBR experimental procedure was the following: an amount of immobilized lipase was placed inside the high-pressure PBR. The system was pressurized with CO_2 at a rate of 10 MPa.min^{-1}, after 30 min of thermal stabilization and

to withdraw the residual superficial water in the catalyst and on the reactor's wall. The reaction mixture formed by isoamyl alcohol and acetic anhydride was pumped into the reactor. Samples were collected in time intervals in the high-pressure separator. The evaluated process variables were the flow rates of isoamyl alcohol, acetic anhydride, SC-CO_2, and based on the BR results the temperature and pressure of SC-CO_2 were fixed at 40 °C and 15.0 MPa.

From the amounts of isoamyl alcohol and isoamyl acetate quantified after the reaction, the mass balance and the reaction stoichiometry, it was possible to determine the esterification rate or conversion ($X, \%$), which is defined as the molar ratio between the formed products (n_p) and the consumed substrates (n_s), as shown in Equation 2:

$$X(mol/mol,\ \%) = \left(\frac{n_p}{n_s}\right)\ x\ 100 \tag{2}$$

The productivity (P) was calculated as the ratio between the mass of isoamyl acetate (m_p) produced in a period of time (t), as shown in Equation 3:

$$P\ (kg/h) = \frac{m_p}{t} \tag{3}$$

The specific productivity (SP) was expressed as the mass ratio between product (m_p) formed and catalyst (m_c) per unit time (t), as shown in Equation 4:

$$SP\ (kg/kg * h) = \frac{m_p}{m_c * t} \tag{4}$$

5.2.4 Analytical methods

After the reaction, the substrate (isoamyl alcohol) and product (isoamyl acetate) contents were determined using a gas chromatograph with a flame ionization detector (GC-FID, Shimadzu, CG17A, Kyoto/Japan) equipped with a capillary column ZB-Wax plus (Phenomenex, 30 m × 0.18 mm × 0.18 μm). Each sample was filtered (Chormafil Xtra PA-20/25, Macherey-Nagel, Düren/Germany) and diluted to 5 mg/mL

in hexane, and 1 μL was injected into the chromatograph. The sample split ratio was 1:100. The carrier gas (Helium, 99.9% purity, White Martins, Campinas/Brazil) flow rate was 1.0 mL/min. The injector and the detector temperatures were 150 and 200 °C, respectively. The column was heated from 35 °C to 90 °C at 5 °C/min and from 90 °C to 150 at 5 °C/min, each one with a hold time of 5 min. The retention times of isoamyl alcohol and isoamyl acetate peaks were 11.1 and 8.1 min, respectively. Quantification was performed using external standard calibration curves (R^2 = 0.999 to isoamyl alcohol and R^2 = 0.996 to isoamyl acetate).

5.2.5 Modeling of Mass Transfer in Batch Reactor

The dimensionless numbers Reynolds (Re_p), Schmidt (Sc) and Sherwood (Sh) were calculated by Equations 5, 6 and 7, respectively, as showed by Hajar and Vahabzadeh [18].

$$Re_p = \frac{D_p u_{pL} \rho_L}{\mu_L} \tag{5}$$

$$Sc = \frac{\mu_L}{\rho_L \mathcal{D}_{AL}} \tag{6}$$

$$Sh = \frac{K_{SL} D_p}{\mathcal{D}_{AL}} \tag{7}$$

where D_p is the particle diameter (m), u_{pL} is the particle velocity relative to the bulk liquid (m.s^{-1}), ρ_L is the density of the liquid mixture in the reaction (kg.m^{-3}) and μ_L is the viscosity of the liquid mixture (Pa.s).

The particle velocity relative to the bulk solution was calculated from the linear (m.s^{-1}), angular velocity (rad.s^{-1}) and the reactor radius (m). The density and viscosity of the liquid mixture in the reactor were considered equal to those of pure CO_2, due to the low concentrations of substrates and products in the bulk solution. The solvent densities were obtained according to Angus *et al.* [19] and the viscosities were calculated by the correlation proposed by Heidaryan *et al.* [20]. Both properties were obtained at the reaction's pressure and temperature. The diffusivity of isoamyl alcohol

in SC-CO_2 ($\mathcal{D}_{AL}$) was calculated with Equation 8, proposed by Wilke and Chang [21, 22]:

$$\mathcal{D}_{AL} = \frac{7.4 * 10^{-8} T \left(\phi_{af} MW_{CO_2}\right)^{1/2}}{\mu_{CO_2} V_{al}^{0.6}} \quad (8)$$

where T is the reaction temperature (K), ϕ_{af} is the association factor of the solvent (equal to 1 for CO_2; dimensionless), MW_{CO_2} is the molecular weight of CO_2 ($g.mol^{-1}$), μ_{CO_2} is the viscosity of CO_2 (Pa.s) and V_{al} is the molar volume of isoamyl alcohol ($m^3.mol^{-1}$).

The mass transfer coefficient (K_{SL}) was determined by the following correlation (Equation 9) between the dimensionless numbers [23].

$$Sh = 2 + 0.6\left(Re_p^{0.5} Sc^{0.33}\right) \quad (9)$$

The mass transfer coefficients and the Damköhler dimensionless number (Equation 10) were used to describe the external mass transfer effect.

$$Da = \frac{v'}{K_{SL} a_c S_0} \quad (10)$$

where v' is the reaction rate ($mol.m^{-3}.s^{-1}$), a_c is the specific external surface area of the catalyst ($m^2.m^{-3}$) and S_0 is the initial concentration of isoamyl alcohol ($mol.m^{-3}$).

The specific external surface area of the catalyst was determined from the volumetric diameter (d_v), the mass (m_p), the volume (V_p), the real density (ρ_p) and the sphericity (ϕ) of the catalyst particles, as shown in Equations 11 and 12.

$$d_v = \left(\frac{6V_p}{\pi}\right)^{1/3} \quad (11)$$

$$a_c = \frac{\pi d_v^2}{\phi \pi \, d_v^3/6} \quad (12)$$

To compare the mass transfer rate to the reaction rate, the external effectiveness factor (η_E) was determined with Equation 13.

$$\eta_E = \left[\frac{1}{2Da}\left(\sqrt{1+4Da}-1\right)\right] \tag{13}$$

The occurrence of internal mass transfer diffusion was evaluated by the Thiele modulus (Φ), calculated with Equation 14.

$$\Phi = \frac{v'}{\mathcal{D}_{Ap}S_0}\left(\frac{r_p}{3}\right)^2 \tag{14}$$

where $\mathcal{D}_{Ap}$ is the effective diffusivity of isoamyl alcohol within the catalyst pores ($m^2.s^{-1}$) and r_p is the particle radius (m).

The effective diffusivity of isoamyl alcohol was determined by Equation 15.

$$\mathcal{D}_{Ap} = \frac{\mathcal{D}_{AL}\varepsilon_p\sigma_p}{\tau} \tag{15}$$

where ε_p is the porosity of the particle, σ_p is the constriction factor and τ is the tortuosity of the catalyst. ε_p was determined from the correlation between real and bulk densities of the catalyst particle. The values of τ and σ_p were 6 and 1, respectively [24].

The internal effectiveness factor (η_I) in terms of the Thiele modulus (Φ) was determined from Equation 16 [18, 25]:

$$\eta_I = \frac{1}{\Phi}\left[\frac{1}{\tanh(3\Phi)}-\frac{1}{3\Phi}\right] \tag{16}$$

5.2.6 Kinetic and Reactor Modeling

The specific reaction rate (v) was adjusted with the Ping-Pong Bi-Bi model without inhibition, as described by Equation 17.

$$v = \frac{V_{max}\left([A][B] - \frac{[P][Q]}{K_{eq}}\right)}{K_m^B[A] + K_m^A[B] + [A][B]} \quad (17)$$

where $V_{\max}$ is the maximum reaction rate (mol.g^{-1}.s^{-1}), $[A]$ and $[B]$ are the acetic anhydride and isoamyl alcohol concentrations (mol.m^{-3}), respectively, $[P]$ and $[Q]$ are the concentrations of acetic acid and isoamyl acetate, respectively. The parameters K_m^A and K_m^B are the Michaelis-Mentem constants for acetic anhydride and isoamyl alcohol (mol.m^{-3}) and K_{eq} is the equilibrium constant.

The mathematic model for the batch reactor (BR) considers that the reaction is isothermal ($\Delta H_r = 0$) and the internal and external mass transfer resistances are negligible (see Section 3.3), thus the material balance for a compound i in the reactor yields Equation 18:

$$\frac{dC_i}{dt} = -C_{cat}v \quad (18)$$

where: C_{cat} is the amount of catalyst introduced into the reactor (g.m^{-3}), C_i is the concentration of compound i (mol.m^{-3}) and v is the specific reaction rate (mol.g^{-1}.s^{-1}).

The kinetic parameters ($V_{\max}$, K_m^A, K_m^B and K_{eq}) in Equation 17 were estimated by combining the solution of the ordinary differential equation with the optimization method. The proposed kinetic model was solved using the software MATLAB (2014Ra, MathWorks, Natick, MA, USA). The fourth-order Runge-Kutta method with the time step defined by the MATLAB function "ode45" was used to solve Equation 18. The subroutine of Powell [26] was used to estimate the kinetic parameters. This routine is an iterative adjustment method that works with a range of values of the parameters defined by the user in a limited number of iterations. Within this range, the subroutine searches the parameter values that minimize the objective function (f_{obj}), which was defined as the sum of squared errors, as stated in Equation 19.

$$f_{obj} = \sum_{t=0}^{n}\left[C_{i_{exp}}(t) - C_{i_{sim}}(t, V_{max}, K_m^A, K_m^B, K_{eq})\right]^2 \quad (19)$$

where $C_{i_{exp}}$ is the experimental concentration of compound i, $C_{i_{sim}}$ is the calculated concentration of compound i and n is the total of experimental points.

5.2.7 Statistical Analysis

The conversion results were statistically evaluated by analysis of variance (ANOVA), applied using the software Statistica for Windows 6.0 (Statsoft Inc., USA) in order to measure the main effects of the variables. In the mass transfer analyses and the results obtained by conversion, productivity and specific productivity of isoamyl acetate, the significant differences at the level of 5% ($p < 0.05$) were analyzed throuugh Tukey's test.

5.3 RESULTS AND DISCUSSION

5.3.1 Preliminary experiments

Preliminary experiments were carried out to evaluate the advantages of SC-CO_2 media over organic solvents at atmospheric pressure. The experiments were conducted with identical amount of enzyme (3%, m/m), concentration of reagents (0.1 M, equimolar) and temperature (40 ^{o}C) and the comparison was made at the same reaction time (3 h). The conversion of isoamyl alcohol obtained in *n*-hexane was 51.5 ± 3.0%, whereas in SC-CO_2 it was 79.0 ± 3.4 %, evidencing the benefits of SC-CO_2 as reaction media. According to Laudani *et al.* [27], the higher diffusivity and lower viscosity and surface tension of SC-CO_2 are responsible for the decrease of interphase transport limitations, thus increasing the reaction rate and esterification percentage. Moreover, according to Hari Krishna *et al*. [5], the use of solvents with log P > 4.0 (nonpolar) is generally recommended, where P is the partition coefficient of a given solvent between water and octanol in a two-phase system. However, the lowest esterification percentage was obtained using *n*-hexane, which has log P > 3.0, and SC-CO_2 (log P < 2.0) [28] led to the highest reaction rate, in an opposite behavior to those obtained by other works [5, 29, 30]. Nakaya, Miyawaki and Nakamura [28] suggest that

log P cannot be the only factor to be considered for selecting a medium to biocatalytic reactions. Others parameters, such as solubilities of water, substrate, and product and water content should be taken into account.

5.3.2 Fractional Factorial Design

Experiments were performed to evaluate the effects of five process parameters on the synthesis of isoamyl acetate in SC-CO_2: pressure, temperature, agitation, substrate's molar ratio and enzyme concentration. Moreover, based on the work of Romero *et al.* [8], all experiments were carried out at a fixed time (1 hour). Table 1 shows the experimental design and the results obtained for conversion, productivity and specific productivity of isoamyl acetate. Table 2 shows the main effects estimated for the experimental design. As observed on Tables 1 and 2, the main effect was enzyme concentration, followed by substrate's molar ratio, agitation, temperature and pressure.

As can be seen on Table 2, the effect of enzyme concentration (% weight of enzyme/weight of substrates) in conversion is strong (the highest positive effect) and statistically significant ($p \leq 0.05$). An increase in enzyme concentration led to an increase in the conversion of isoamyl alcohol and to a decrease in the specific productivity. This behavior can be explained by the increase of available enzyme to catalyze the reaction. According to Hajar and Vahabzadeh [18], the collision probability between substrates and enzyme increases with the enzyme concentration, since the enzyme content does not change the equilibrium position of a reaction. The use of SC-CO_2 as reaction medium achieved similar results in the synthesis of isoamyl acetate [8], decyl acetate [31] and geranyl butyrate [32]. Eventually, with longer reaction time some experimental runs would overlap for larger enzyme content. However, in the industrial point of view, it is interesting to use a lower amount of catalyst, which results in reduced cost.

Table 1. Fractional factorial design (2^{5-1}) to evaluate the main effect of isoamyl acetate synthesis in SC-CO_2 media.

Assay	Pressure (MPa)	Temperature (°C)	Agitation (rpm)	Substrates Ratio (M/M)[1]	Enzyme Concentration (g/g, %)[2]	Conversion (mol/mol, %)	Productivity (g/h)	Specific Productivity (g/g*h)
1	10	40	100	1	10	60.4 ± 1.4	0.8 ± 0.02	4.1 ± 0.1
2	30	40	100	1	1	53.5 ± 0.9	0.7 ± 0.01	36.6 ± 0.6
3	10	60	100	1	1	52.2 ± 2.1	0.7 ± 0.03	35.8 ± 1.4
4	30	60	100	1	10	85.2 ± 5.3	1.1 ± 0.10	5.8 ± 0.5
5	10	40	700	1	1	72.6 ± 0.8	0.9 ± 0.01	49.7 ± 0.5
6	30	40	700	1	10	96.7 ± 1.8	1.3 ± 0.02	6.6 ± 0.1
7	10	60	700	1	10	98.0 ± 3.4	1.3 ± 0.04	6.7 ± 0.2
8	30	60	700	1	1	50.9 ± 1.8	0.7 ± 0.02	34.8 ± 1.2
9	10	40	100	5	1	85.5 ± 2.7	1.1 ± 0.04	18.6 0.6
10	30	40	100	5	10	99.0 ± 0.3	1.3 ± 0.01	2.2 ± 0.1
11	10	60	100	5	10	94.3 ± 0.6	1.2 ± 0.01	2.1 ± 0.1
12	30	60	100	5	1	72.5 ± 1.8	0.9 ± 0.02	15.8 ± 0.4
13	10	40	700	5	10	99.2 ± 4.9	1.3 ± 0.06	2.2 ± 0.1
14	30	40	700	5	1	87.7 ± 4.0	1.1 ± 0.05	19.1 ± 0.9
15	10	60	700	5	1	78.0 ± 5.7	1.0 ± 0.10	17.0 ± 1.7
16	30	60	700	5	10	100.0 ± 6.0	1.3 ± 0.08	2.2 ± 0.1
17	20	50	400	3	5.5	99.1 ± 5.3	1.3 ± 0.07	5.9 ± 0.3
18	20	50	400	3	5.5	100.0 ± 6.0	1.3 ± 0.08	6.0 ± 0.4
19	20	50	400	3	5.5	98.4 ± 5.6	1.3 ± 0.07	5.9 ± 0.3

Experiments were carried out at fixed conditions of time (1 hour); [1]Acetic anhydride/Isoamyl alcohol molar ratio (M/M); [2]Enzyme concentration expressed by weight of substrates, g/g (%).

As well as the catalyst amount, the concentrations of substrates and products in the reaction bulk are important factors that affect the cost of the process. According to Romero *et al*. [33], the solvent separation and recovery of products are usually achieved through evaporation and extraction with immiscible solvent, which is reused after cleaning and reconditioned to reduce costs and avoid environmental damages. Therefore, the volume of substrates loaded in the reaction bulk must be optimized to reduce the costs related to product recovery and solvent recycling. The substrate's molar ratio between isoamyl alcohol and acetic anhydride was investigated from 1:1 to 1:5 (M/M).

Table 2. Effect estimates to conversion (mol/mol, %) for the fractional factorial design.

Effects	Effect	Standard Error	$t(13)$[1]	p-value	Conf. limit (-95%)[2]	Conf. limit (+95%)[2]
Main Effects	83.32	2.81	29.59	0.001	77.24	89.41
Pressure	0.64	6.13	0.10	0.918	-12.61	13.90
Temperature	-2.93	6.13	-0.47	0.640	-16.19	10.32
Agitation	10.06	6.13	1.63	0.125	-3.19	23.32
Ratio Substrates	18.35	6.13	2.98	0.010	5.09	31.60
Enzyme Concentration	22.46	6.13	3.66	0.002	9.20	35.72

[1]Degrees of freedom; [2]Conf. - confidence.

Acetic acid has been traditionally used as acyl donor in flavor ester reactions, but several works [5, 8] have reported an inhibition of the enzyme by high acid concentration. Therefore, the synthesis of esters can be performed by transesterification with acetates and by acylation with acetic anhydride. The effect of substrate's molar ratio (or acetic anhydride concentration, since the isoamyl alcohol concentration was fixed (equimolar at 0.1 M)) was positive and statistically significant ($p \leq 0.05$) in the conversion of isoamyl alcohol in SC-CO_2. This can be due to the increase of the concentration of one of the substrates, which pushed the equilibrium of the reaction in the forward direction. The same results were observed by Chiaradia *et al.* [34], who concluded that the molar ratio acetic anhydride/eugenol has positive effect on the production of eugenyl acetate in a solvent-free system using Novozym 435. Recently, Santos *et al.* [35] showed similar results for the synthesis of eugenyl acetate with Lipozyme 435 as catalyst and SC-CO_2 as solvent. A discussion about inhibition and reaction mechanisms is addressed in Section 3.4.

The effect of agitation or the intensity of liquid mixing was positive but not statistically significant ($p \leq 0.05$). Despite this behavior, the increase of the liquid

mixing intensity can be correlated with the increase in the dispersion of substrate molecules in the bulk phase, thus increasing the interfacial area and the probability of effective collisions between substrate molecules and enzyme particles [18, 36, 37]. A deeper discussion based on mass transfer effects is presented in Section 3.3.

It is observed on Table 2 that the effects of SC-CO_2 conditions were opposite, since temperature had a negative effect and pressure showed a positive effect on the esterification of isoamyl alcohol. The negative effect of temperature can be related to the changes in the physical properties of the solvent, such as limitations in mass transfer, viscosity, surface tension and the decrease of the solvation power of the substrates at lower solvent density. In turn, the positive effect of pressure can be due to the increase of CO_2 density with pressure, which improves its solvation power in the reaction medium [38]. However, the effects of temperature and pressure were not statistically significant at $p \leq 0.05$ in the conversion of isoamyl alcohol.

Based on the results shown on Tables 1 and 2, the effects of pressure and temperature were not studied and these variables were fixed at 15 MPa and 40 °C for the investigation of mass transfer effects, kinetics modeling and in the production of isoamyl acetate in the continuous reactor. According to Romero *et al.* [8], the highest esterification of isoamyl alcohol in SC-CO_2 was obtained at these conditions. Moreover, in the study of mass transfer effects and kinetics modeling, the enzyme concentration was fixed at 3% (g of enzyme/g of substrates) in an equimolar reaction, which represents about 6.3 gram of enzyme per gram of alcohol, almost equal to that used by Romero *et al.* [8]. Furthermore, the evaluation of agitation and particle diameter, and the effects of substrate's molar ratio are exposed in Sections 3.3 and 3.4, respectively. It should be emphasized that the central point experiment resulted in the highest conversion with lower enzyme amount and substrate's molar ratio, which can indicate an optimal condition for the synthesis of isoamyl acetate.

5.3.3 Mass Transfer Effects in Batch Reactor

The effects of particle diameter and mixture agitation in the BR were evaluated and the mass transfer coefficients (K_{SL}), and the internal (η_I) and external (η_E) effectiveness factors are exposed in Figure 3 and Table 3, respectively. The mass transfer coefficients (K_{SL}) increased with agitation and decreased with the increase of

the catalyst particle diameter. Higher agitation in the bulk phase led to a rise in the dispersion of substrates, products and catalyst particles in the bulk phase, thus increasing the probability of collisions of substrate molecules and enzyme particles [18, 36, 37]. Besides, a decrease in particle diameter caused an increase in the mass transfer coefficients from 1.8 x 10^{-2} to 2.3 x 10^{-2} cm.s^{-1} for particle diameters of 486 and 308 µm, respectively, at 700 rpm. If fact, in smaller particles the mass transfer resistance is reduced, so the mass transfer coefficients are higher. K_{SL} ranged from 7.0 x 10^{-3} cm.s^{-1} at 486 µm and 100 rpm to 2.3 x 10^{-2} cm.s^{-1} at 308 µm and 700 rpm. This coefficient and the reaction rate allowed the determination of the Damkohler number and the external (η_E) effectiveness factor, shown on Table 3.

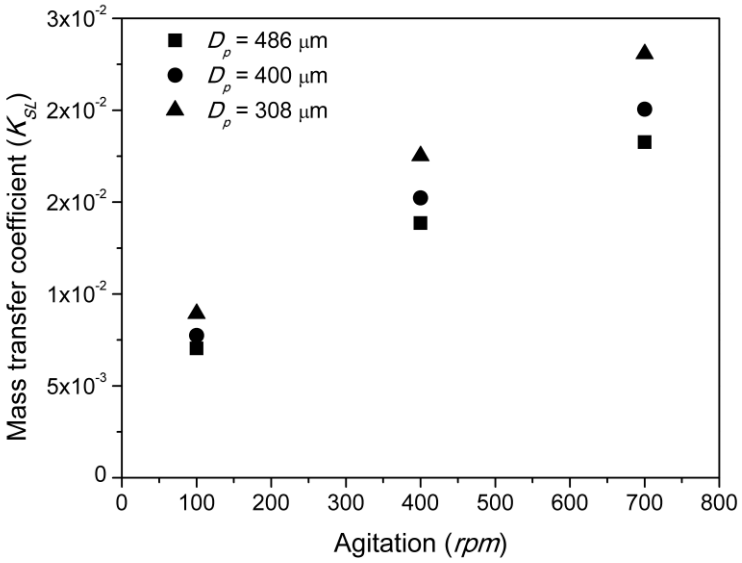

Figure 3. Mass transfer coefficients (K_{SL}) as function of Novozym 435 particle diameter and agitation, used to the synthesis of isoamyl acetate in the batch stirred reactor.

The Damkohler number, which represents the relationship between reaction rate and mass transfer coefficient, ranged from 2.4 x 10^{-3} to 6.3 x 10^{-3}. According to Hajar and Vahabzaseh [18], for Da between 0.3 x 10^{-4} and 2.3 x 10^{-3} the mass transfer resistances are negligible. Moreover, the external (η_E) effectiveness factors, which ranged between 0.9938 and 0.9976, also show that the mass transfer effects in the bulk phase were unimportant.

It can be seen on Table 3 that equal amounts of enzyme led to different conversions or yields of isoamyl acetate. According to Oliveira *et al.* [31], the specific enzyme content increases as particle size decreases, being the enzyme located in an external shell of the particle. These authors showed that, the enzyme content for the different size groups of Novozym 435 particles depends on the particle diameter, and smaller particles have higher specific enzyme content than larger ones. Therefore, the higher enzyme content in the same amount of immobilized enzyme particles led to a higher conversion, thus explaining the behavior observed for the conversion exposed on Table 3. Other works show the same enzymatic content for different particle diameters [39-41]. On the other side, Romero *et al.* [42] stated that, based on the enzyme supplier, the enzyme activity was not improved when using different particle or pore sizes, so it can be assumed that there are not internal mass transfer limitations.

Table 3. Conversion, internal (η_I) and external (η_E) effectiveness factors for particle size of Novozym 435 and agitation in the batch stirred reactor.

Diameter (μm)	Agitation (rpm)	Conversion (%)	Effectiveness Factor	
			Internal(η_I)	External (η_E)
486	100	69.7 ± 0.2^{b}	0.9997	0.9938
	400	74.4 ± 3.6^{ab}	0.9997	0.9967
	700	78.2 ± 1.8^{ab}	0.9996	0.9973
400	100	71.7 ± 5.6^{b}	0.9999	0.9942
	400	82.7 ± 6.6^{ab}	0.9998	0.9966
	700	86.5 ± 1.8^{ab}	0.9998	0.9973
308	100	70.8 ± 6.0^{b}	1.0000	0.9951
	400	85.6 ± 5.5^{ab}	0.9999	0.9969
	700	89.2 ± 0.7^{a}	0.9999	0.9976

Experiments were carried out at fixed time (1 hour), pressure (15 MPa), temperature (40 °C), enzyme concentration (3 g of enzyme/g of substrates (%)), and substrates' concentration (0.1 M, equimolar). Different indexes (a, b) in the same column (lowercase) indicate that the means differ significantly by Tukey's test ($p \leq 0.05$).

The occurrence of internal mass transfer resistance was evaluated by calculating the Thiele modulus and the internal effectiveness factor (η_I). The Thiele modulus ranged between 0.0088 and 0.024. The same range was observed by Hajar and Vahabzaseh [18], who evaluated the mass transfer in a stirred basket reactor used for biodiesel production. η_I was calculated from the Thiele modulus and the obtained values indicate that the intra-particle diffusion is negligible. Therefore, the reaction kinetics is independent of particle diameter and agitation. Thus, the kinetic experiments were performed at 600 rpm with the mean particle diameter (350 ± 2.5 μm).

5.3.4 Kinetics Modeling

The kinetics of many reactions, such as hydrolysis, esterification and transesterification using organic solvents [42, 43] or supercritical fluids [3, 31] as reaction media have been successfully described by the Ping-Pong Bi-Bi model. In the kinetic study, it is first necessary to determine possible inhibitions caused by any substance involved in the reaction [42]. The substrates in this work are isoamyl alcohol and acetic anhydride, and the products are isoamyl acetate and acetic acid. However, an alternative esterification route can occur between acetic acid and isoamyl alcohol, resulting in isoamyl acetate and water. This route and the effect of acetic acid on the kinetics were not considered. The reaction routes are shown in Appendix A (Supplementary data, Figure S1). However, acetic acid is an important inactivating compound, causing an indirect inhibition by the decrease of pH in the reaction medium, which modifies the isoelectric point of proteins and thus inactivates the enzyme. Moreover, acetic acid can also act as a direct inhibitor of the enzyme, forming a dead-end complex. According to Romero *et al.* [42], this effect has little importance when the initial concentration of substrates is low.

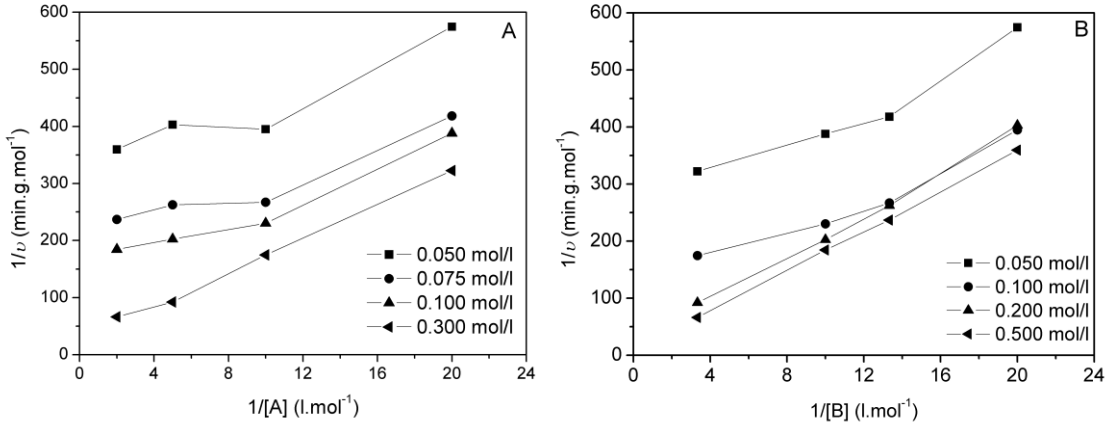

Figure 4. Lineweaver-Burk plot of the reciprocal of the reaction rates versus reciprocal concentrations of acetic anhydride [A] and at different concentrations of isoamyl alcohol [B]. The experiments were carried out at 40 ºC and 15 MPa.

Figure 4 (A and B) shows the Lineweaver-Burk plot of the reciprocal of the reaction rates versus reciprocal concentrations of acetic anhydride [A] and at different

concentrations of isoamyl alcohol [B], at 40 ºC and 15 MPa. The variation of the concentrations of the substrates acetic anhydride [A] and isoamyl alcohol [B] caused an increase in the reaction rate. Moreover, in the plot of Figure 4 (A and B), the esterification of isoamyl alcohol followed the classical Michaelis-Menten kinetics. However, the four straight lines in Figure 4 are parallel, suggesting that the enzymatic reaction follows a simple Ping-Pong Bi-Bi mechanism without inhibition, within the range of tested concentrations. Romero *et al.* [42] confirmed an inhibition by acetic anhydride using the Lineweaver-Burk plot, where the lines curved up at low values of the inverse of acetic anhydride concentration. Furthermore, the authors affirmed that isoamyl alcohol was not a Novozym 435 inhibitor. Several authors observed a positive effect of the excess of isoamyl alcohol using acetic acid as acyl donor [5, 44, 45].

The values of the kinetic parameters ($V_{\max}$, K_m^A, K_m^B and K_{eq}), calculated from the Lineweaver-Burk plot of the reciprocal of the reaction rates versus reciprocal concentrations, were used to define the range for the initial guess of the kinetic parameters. Table 4 shows the kinetic parameters adjusted with the model for the production of isoamyl acetate in SC-CO_2, and Figure 5 shows the experimental and simulated curves of conversion versus reaction time for an equimolar mixture in SC-CO_2 (40 °C and 15 MPa).

Table 4. Kinetic parameters adjusted for the production of isoamyl acetate in SC-CO_2 with Novozym 435 at 40°C and 15 MPa.

Parameter	Value
V_{max} (mol.g^{-1}.min^{-1})	10.5
K_m^A (mol.L^{-1})	154.2
K_m^B (mol.L^{-1})	584.4
K_{eq} (ad.)	11.7
f_{obj}	0.0017

The value of $1/K_m$ indicates that the affinity of the enzyme to acetic anhydride is larger than to isoamyl alcohol. Similar behavior was also observed by Romero *et al.* [42], who investigated the esterification of isoamyl alcohol and acetic anhydride using immobilized lipase in *n*-hexane. According to these authors, the Ping-Pong Bi-Bi mechanism can be divided into two steps: a) First, the acyl donor binds the enzyme, forming an enzyme-anhydride complex (EA). Through a unimolecular isomerization reaction, the EA complex is converted into an enzyme-acyl complex (EC)

and the first product (acetic acid) is released; b) Isoamyl alcohol binds to the enzyme-acyl complex (EC) forming a ternary complex, enzyme-acyl-alcohol. Again, through a unimolecular isomerization reaction, the ternary complex is transformed into an enzyme-ester complex, finally releasing isoamyl acetate and the enzyme in its initial conformation.

As can be seen in Figure 5, the modeled curve fitted well the experimental data. This suggests that the kinetic model represented by Equation 18 describes the esterification of isoamyl alcohol with acetic anhydride at the performed experimental conditions. Couto *et al.* [3] studied the esterification of geraniol with acetic acid (100 mM, equimolar) in SC-CO_2 with Novozym 435 as a catalyst. These authors determined the parameters of ordered sequential Ping-Pong Bi-Bi to model for the reaction in SC-CO_2 in a batch reactor (BR) and concluded that no additional terms should be added, since the results obtained with the simplified form were satisfactory. Also, according to these authors [3], care should be taken when using the kinetic parameters out of the range of operating conditions employed in the experiments, because the inhibition by any of the substrates or products may arise. In fact, the kinetic parameters obtained in this work are valid only within the range of performed experimental conditions.

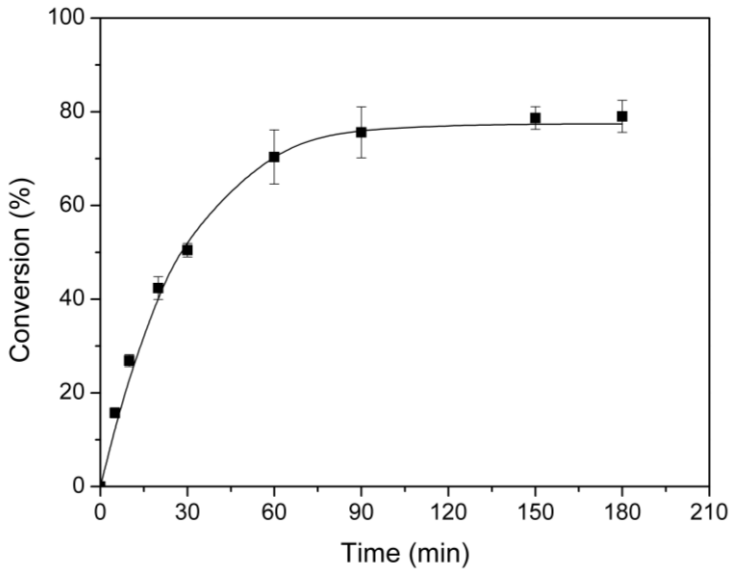

Figure 5. Experimental (■) and simulated (–) conversion data versus reaction time for an equimolar (0.3 M) mixture in SC-CO_2 (40 °C and 15 MPa). Enzyme amount of 3 g of enzyme/g of substrates (% weight of enzyme/weight of substrates) and agitation of 600 rpm.

5.3.5 Production Continues Packed Bed Reactor

A comparison between BR and PBR reactors was performed in terms of operation time, conversion (%), productivity (g/h) and specific productivity (g/g.h) of isoamyl acetate, as shown on Table 5. Some process conditions of the PBR were fixed, such as temperature and pressure of the separator and reactor at 60 ± 1°C and 8.0 ± 0.5 MPa, and 40 ± 3 °C and 15.0 ± 0.1 MPa, respectively, and the amount of immobilized lipase at approximately 1.69 ± 0.06 g. In the tests, the flow rate of substrates and SC-CO_2 were evaluated.

First, a study of the PBR was performed with an excess of isoamyl alcohol. According to Romero *et al.* [8], who studied the synthesis of isoamyl acetate with SC-CO_2, an excess of alcohol led to an esterification extent slightly higher than 100% (114% after 2 h reaction time), since part of the produced acetic acid reacted with the excess of isoamyl alcohol. Moreover, the authors obtained 100 % of isoamyl alcohol esterification for 30 days in PBR, at equimolar conditions. However, in all studied conditions with an excess of isoamyl alcohol (assays 1 to 3), equimolar (assays 1 and 2), or with an excess of acetic anhydride (assays 4 to 6), conversions higher than 100% were not observed to packed bed reactor. The highest conversion with an excess of isoamyl alcohol, equimolar and, with an excess of acetic anhydride were about 63% (assay 3), 83% (assay 5) and 100%, respectively.

Table 5. Comparison between batch stirred (BSR) and continuous packed bed (PBR) reactors for the synthesis of isoamyl acetate synthesis in SC-CO_2 at 40 °C and 15 MPa.

A*	Reactor Model	Q_s (mol/min)[3]	Q_{CO2} (kg/s)[4]	Time (h)[5]	C (%)	P (g/h)	SP (g/g.h)
-	BSR[1]	-	-	3	79.8	0.35	5.17
1	PBR[2]	0.0018/0.001	2.6×10^{-4}	1	33.2	4.67	2.76
2	PBR[2]	0.0018/0.001	1.3×10^{-4}	1	59.9	8.42	4.98
3	PBR[2]	0.00098/0.0005	1.3×10^{-4}	1	63.1	4.83	2.86
4	PBR[2]	0.0037/0.002	1.3×10^{-4}	1	36.1	10.43	6.17
5	PBR[2]	0.001/0.001	1.3×10^{-4}	1	83.8	6.55	3.87
6	PBR[2]	0.001/0.002	1.3×10^{-4}	1	100	7.81	4.62

*Number of the assay (A); [1]Batch stirred reactor (BSR) at substrate's molar ratio of 1:1 at 0.1 M, 600 rpm and enzyme concentration of 3 % (g of enzyme/g of substrates); [2]Continuous packed-bed reactor (PBR); [3]Flow rate of substrates isoamyl alcohol/acetic anhydride; [4]Flow rate of SC-CO_2; [5]Operation time.

Table 5 also shows that the increase of SC-CO_2 flow rate led to a decrease in the conversion at the same molar flow rate of substrates (assays 1 and 2), from about

60 to 33.2% at 2.6 x 10^{-4} and 1.3 x 10^{-4} kg/s of CO_2, respectively. This behavior is related to the residence time of the substrates into the PBR. At 2.6 x 10^{-4} kg/s the residence time was 5.6 seconds, whereas at 1.3 x 10^{-4} kg/s the residence time was about 11 seconds. Furthermore, the substrates are diluted in the SC-CO_2 stream and the time spent by the mixture in the reactor controls the contact between enzyme and substrates, and therefore the conversion of isoamyl alcohol. Moreover, according to Laudani *et al.* [46], at higher SC-CO_2 flow rate the water removal is more efficient, leading to a decrease in its activity [47, 48]. The same behavior was observed when the flow rates of the substrates (isoamyl alcohol/acetic anhydride) increased. The conversion of isoamyl alcohol decreased from 63.1 to 36.1% at 0.00098/0.0005 and 0.0037/0.002 mol of substrates per min, respectively. Furthermore, the highest SC-CO_2 and substrate flow rates led to an inefficient separation of the reaction mixture.

Each PBR assay shown on Table 5 was conducted at different CO_2/substrates molar ratio, which might have resulted in the formation of two phases in the PBR, causing a decrease in the conversion and/or inhibition of the catalyst by the concentration of a reagent or a product. The possible formation of two phases at the inlet and outlet sections (considering the conversion of substrates) of the PBR was investigated for the conditions shown on Table 5. The simulation was performed with the commercial simulator Aspen Plus (Aspen Technology) and the estimation was carried out using the Peng–Robinson equation of state with the Huron–Vidal mixing rule. At the inlet section only the substrates (acetic anhydride and isoamyl alcohol) and CO_2 were considered, and in the outlet section the concentrations of CO_2, substrates and products formed according to each condition of conversion were included in the simulation. The results for the inlet section are exposed in Figure 6 and those of the outlet section are presented in Appendix A (Supplementary data, Figure S2).

As can be seen in Figure 6 and in Appendix A (Supplementary data, Figure S2), a single pressurized liquid phase may exist in the inlet and outlet sections of the PBR at 15 MPa and 40 °C. Romero *et al.* [8] estimated the phase equilibrium for the synthesis of isoamyl acetate in SC-CO_2 using the Peng–Robinson equation of state with the Huron–Vidal mixing rule and concluded that the phase equilibrium does not change significantly as the reaction occurs with a CO_2/substrates molar ratio of 3.2. On the other hand, it can be observed in Figure 6 that the dew point line was dislocated when the CO_2/substrates molar ratio decreased, unlike the bubble point line, which remained apparently unchanged. Furthermore, the simulation showed that there may be two

phases in the high-pressure separator (HPS). Such behavior was expected, since the HPS was projected to separate the products and substrates from SC-CO_2 through phase change of the solvent (flash evaporation).

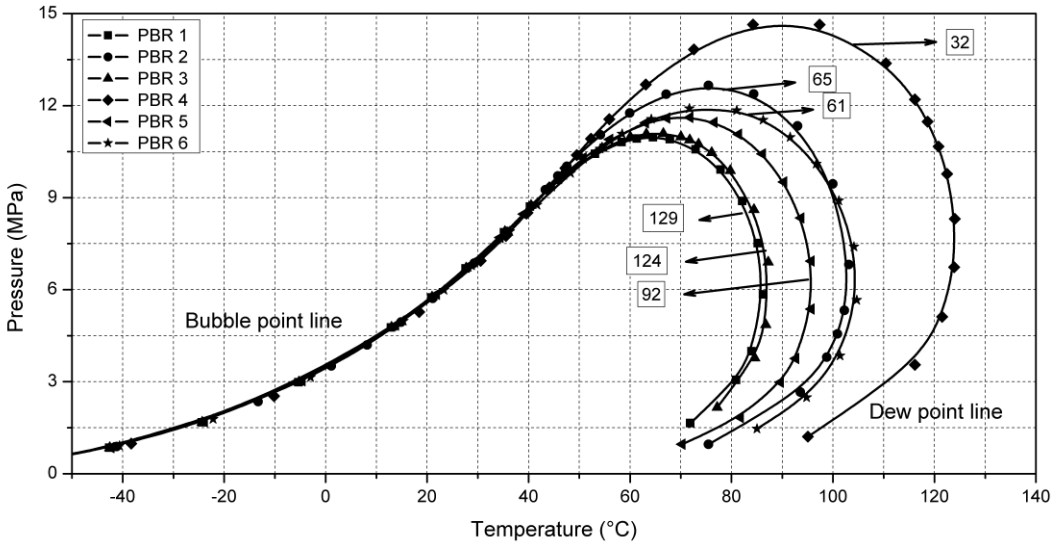

Figure 6. Phase equilibrium of the reaction mixture (isoamyl alcohol and acetic anhydride) pumped into the packed bed reactor (PBR) in the assays shown on Table 5. The numbers in the boxes represent the CO_2/substrates molar ratios.

From the results for conversion (%), productivity (g/h) and specific productivity (g/g.h) of isoamyl acetate, it can be stated that the PBR led to higher productivity of isoamyl acetate than the BR, despite the lower conversion. In summary, the PBR proved to be the best option to synthesize isoamyl acetate in SC-CO_2 media. Lozano *et al.* [49] applied active membranes (with CALB) for continuous butyl butyrate synthesis in a cross-flow reactor with SC-CO_2 as the reaction medium. The active membrane showed an excellent operational behavior, with practically no activity loss during the reaction time. Laudani *et al.* [46] showed that the continuous synthesis is preferable instead of batch reactions for large-scale production of *n*-octyl oleate in dense CO_2.

The present work showed an alternative process to obtain isoamyl acetate, which has been produced in industrial scale by batch reactors linked with distillation columns [50] or through reactive distillation [50, 51]. The proposed process applies a mild technique in terms of temperature and solvent, and the catalyst can be totally removed from the reaction medium in a single step (depressurization and decantation or

centrifugation) instead of the conventional techniques. The major catalyst used by the industrial production has been sulfuric acid, which requires neutralization and separation from the final mixture. Moreover, the catalyst employed in the conventional processes cannot be considered natural like the enzymes applied in this work. The final product obtained in the current work cannot be regarded as natural either, because the acyl donor (acetic anhydride) is not natural material like acetic acid, which can be obtained by microbiological processes and used in this reaction. Moreover, the proposed method can be applied to the esterification of fusel oil, which is a by-product obtained from bioethanol distilleries, composed of a mixture of higher alcohols, such as isoamyl alcohol [52].

5.4 CONCLUSIONS

The preliminary results of this work showed that the conversion of isoamyl alcohol in *n*-hexane was lower than in SC-CO_2, evidencing the benefits of using SC-CO_2 as the reaction medium. The effects of substrates molar ratio, enzyme amount and agitation were statistically significant in the conversion of isoamyl alcohol, whereas temperature and pressure had small influence on the reaction. The effects of particle diameter and agitation of the mixture in the batch reactor were evaluated, and the results showed that the resistances to mass transfer in the bulk phase were unimportant and the intra-particle diffusion is negligible. Therefore, the reaction kinetics is independent of particle diameter and agitation. The Lineweaver-Burk plot suggests that the enzymatic reaction follows a simple Ping-Pong Bi-Bi mechanism without inhibition, within the range of tested concentrations. The kinetic model described the esterification of isoamyl alcohol with acetic anhydride, and the kinetic parameters indicate that the affinity of the enzyme to acetic anhydride is larger than to isoamyl alcohol.

The packed bed reactor presented higher productivity of isoamyl acetate than the batch reactor, despite the lower conversion, and proved to be the best option to synthesize isoamyl acetate in SC-CO_2 media. However, further researches should be performed in order to evaluate the economic viability of the process and perform the scale-up of isoamyl acetate synthesis in PBR. Indeed, a purification step to remove the acetic acid and isoamyl alcohol from the products should be also evaluated.

5.5 AKNOWLEDGEMENT

The authors wish to thank CAPES (Project 2952/2011), CNPq (Ph.D. fellowship: 142373/2013-3) and FAPESP (Projects 2015/11932-7 and 2009/54137-1) for the financial support.

5.6 APPENDIX A: Supplementary data

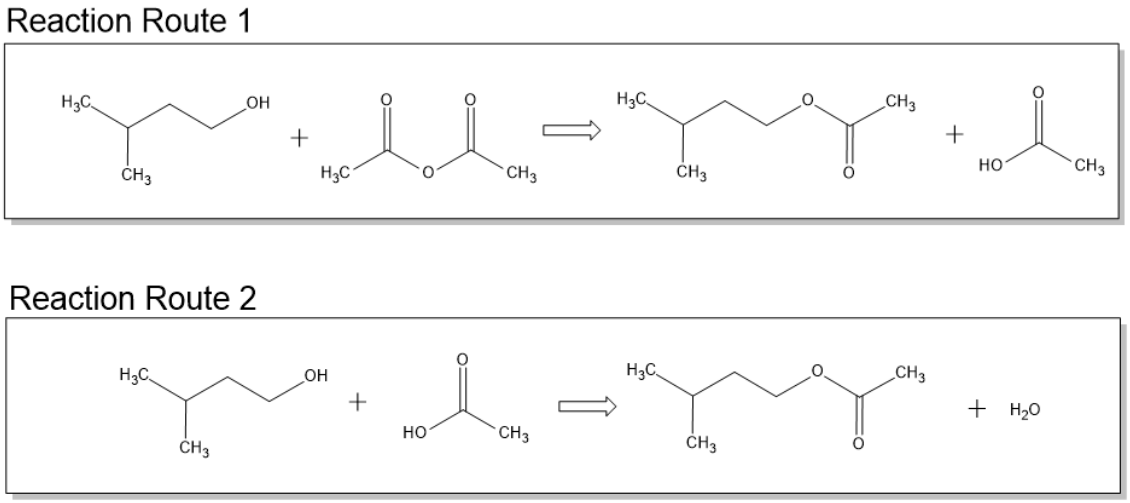

Figure S1. Routes of isoamyl acetate synthesis from isoamyl alcohol and acetic anhydride (Reaction Route 1) or acetic acid (Reaction Route 2).

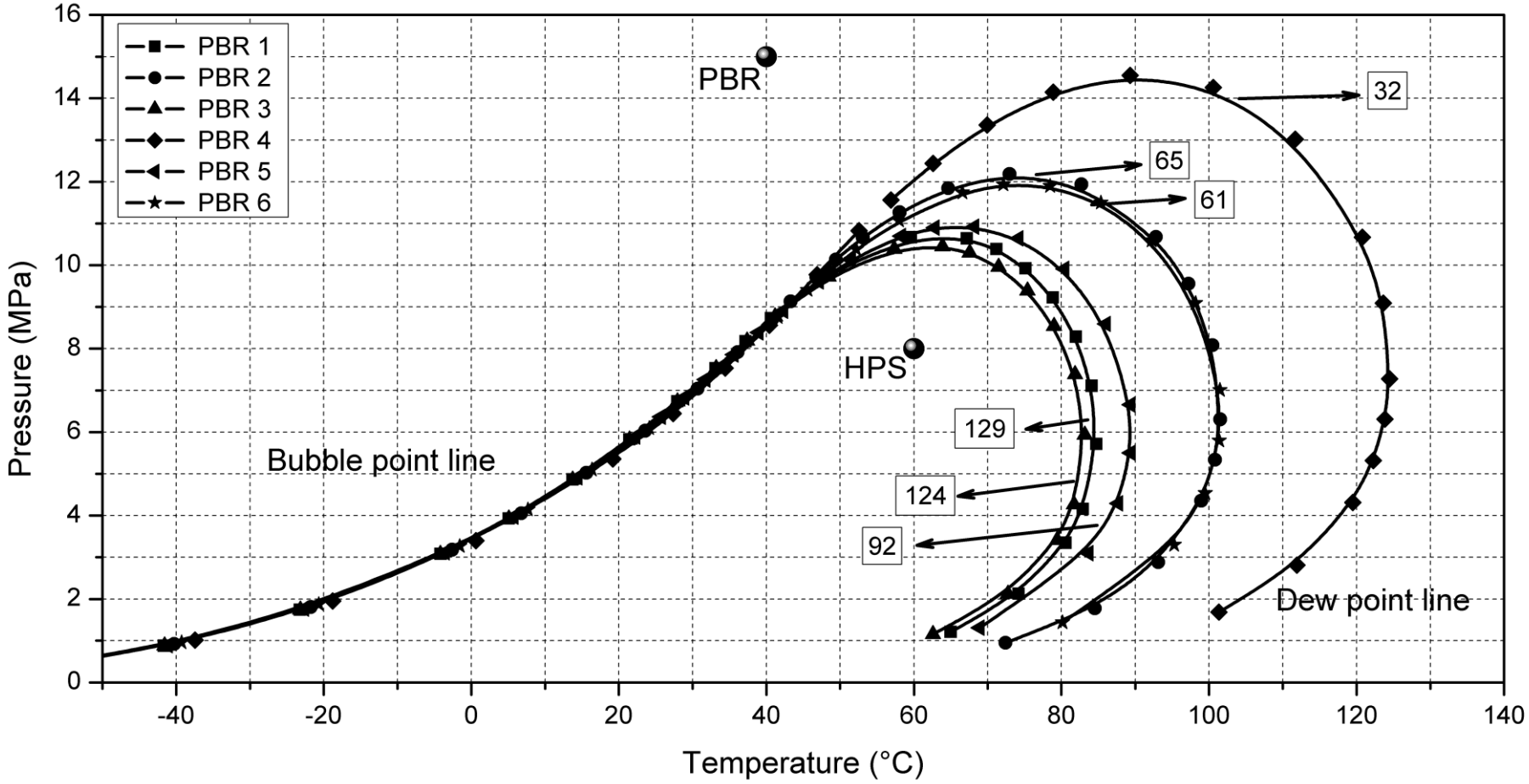

Figure S2. Phase equilibrium of the reaction mixture in the outlet section of the PBR (packed bed reactor) for the assays shown on Table 5. The simulation (Aspen Plus) was made with the Peng-Robinson equation of state with Huron–Vidal mixing rule. The points PBR and HPS represent the operational conditions of packed-bed reactor and high-pressure separator, respectively.

5.7 REFERENCES

[1] T.F. Group, in World Flavors & Fragrances: Industry Study with Forecasts for 2016 & 2021, Cleveland, OH (2016).
[2] Markets & Markets, in Food Flavors Market by Type (Chocolate, Vanilla, Fruits & Nuts, Others), Origin (Natural, Synthetic), Application (Beverages, Savory & Snacks, Bakery & Confectionery, Dairy & Frozen Products, Others), & by Region - Global Forecast to 2020, Markets And Markets, (September 2015).
[3] R. Couto, P. Vidinha, C. Peres, A.S. Ribeiro, O. Ferreira, M.V. Oliveira, E.A. Macedo, J.M. Loureiro, S. Barreiros, Industrial & Engineering Chemistry Research, 50 (2011) 1938-1946.
[4] K.P. Dhake, D.D. Thakare, B.M. Bhanage, Flavour and Fragrance Journal, 28 (2013) 71-83.
[5] S. Hari Krishna, S. Divakar, S.G. Prapulla, N.G. Karanth, Journal of biotechnology, 87 (2001) 193-201.
[6] K.P. Dhake, K.M. Deshmukh, Y.P. Patil, R.S. Singhal, B.M. Bhanage, Journal of biotechnology, 156 (2011) 46-51.
[7] K.-E. Jaeger, T. Eggert, Current Opinion in Biotechnology, 13 (2002) 390-397.
[8] M.D. Romero, L. Calvo, C. Alba, M. Habulin, M. Primožič, Ž. Knez, The Journal of Supercritical Fluids, 33 (2005) 77-84.
[9] G.A. Macedo, G.M. Pastore, M.I. Rodrigues, Process Biochemistry, 39 (2004) 687-693.
[10] S. Srivastava, J. Modak, G. Madras, Industrial & Engineering Chemistry Research, 41 (2002) 1940-1945.
[11] K.P. Dhake, P.J. Tambade, Z.S. Qureshi, R.S. Singhal, B.M. Bhanage, ACS Catalysis, 1 (2011) 316-322.
[12] Ž. Knez, The Journal of Supercritical Fluids, 47 (2009) 357-372.
[13] G. Brunner, Journal of Food Engineering, 67 (2005) 21-33.
[14] E. Reverchon, I. De Marco, The Journal of Supercritical Fluids, 38 (2006) 146-166.
[15] P. Santos, C.A. Rezende, J. Martínez, The Journal of Supercritical Fluids, 107 (2016) 170-178.
[16] R. Melgosa, M.T. Sanz, Á. G. Solaesa, S.L. Bucio, S. Beltrán, The Journal of Supercritical Fluids, 97 (2015) 51-62.
[17] B. Chen, J. Hu, E.M. Miller, W. Xie, M. Cai, R.A. Gross, Biomacromolecules, 9 (2008) 463-471.
[18] M. Hajar, F. Vahabzadeh, Korean Journal of Chemical Engineering, 33 (2016) 1220-1231.
[19] S. Angus, B. Armstrong, K.M.D. Reuck, International Thermodynamic Tables of the Fluid State: Carbon Dioxide, Pergamon Press, Oxford (1976).
[20] E. Heidaryan, T. Hatami, M. Rahimi, J. Moghadasi, The Journal of Supercritical Fluids, 56 (2011) 144-151.
[21] P.R. Sassiat, P. Mourier, M.H. Caude, R.H. Rosset, Analytical Chemistry, 59 (1987) 1164-1170.
[22] K.K. Liong, P.A. Wells, N.R. Foster, Industrial & Engineering Chemistry Research, 31 (1992) 390-399.
[23] P.M. Doran, in Bioprocess engineering principles, Academic Press, Waltham, MA (2013).
[24] H.-P. Dong, Y.-J. Wang, Y.-G. Zheng, Journal of Molecular Catalysis B: Enzymatic, 66 (2010) 90-94.

[25] H. Veny, M.K. Aroua, N.M.N. Sulaiman, Chemical Engineering Journal, 237 (2014) 123-130.
[26] M.J.D. Powell, in Subroutine BOBQYA, Department of Applied Mathematics and Theorical Physics, Cambrige University, (2009).
[27] C.G. Laudani, M. Habulin, Ž. Knez, G.D. Porta, E. Reverchon, The Journal of Supercritical Fluids, 41 (2007) 92-101.
[28] H. Nakaya, O. Miyawaki, K. Nakamura, Enzyme and Microbial Technology, 28 (2001) 176-182.
[29] R.H. Valivety, G.A. Johnston, C.J. Suckling, P.J. Halling, Biotechnology and Bioengineering, 38 (1991) 1137-1143.
[30] H. Hirata, K. Higuchi, T. Yamashina, Journal of biotechnology, 14 (1990) 157-167.
[31] M.V. Oliveira, S.F. Rebocho, A.S. Ribeiro, E.A. Macedo, J.M. Loureiro, The Journal of Supercritical Fluids, 50 (2009) 138-145.
[32] M.N. Varma, G. Madras, Biochemical Engineering Journal, 49 (2010) 250-255.
[33] M.D. Romero, L. Calvo, C. Alba, A. Daneshfar, H.S. Ghaziaskar, Enzyme and Microbial Technology, 37 (2005) 42-48.
[34] V. Chiaradia, N. Paroul, R.L. Cansian, C.V. Junior, M.R. Detofol, L.A. Lerin, J.V. Oliveira, D. Oliveira, Applied biochemistry and biotechnology, 168 (2012) 742-751.
[35] P. Santos, G.L. Zabot, M.A.A. Meireles, M.A. Mazutti, J. Martínez, Biochemical Engineering Journal, 114 (2016) 1-9.
[36] N. Chaibakhsh, M.B.A. Rahman, F. Vahabzadeh, S. Abd-Aziz, M. Basri, A.B. Salleh, Biotechnology and Bioprocess Engineering, 15 (2010) 846-853.
[37] M. Basri, M.A. Kassim, R. Mohamad, A.B. Ariff, Journal of Molecular Catalysis B: Enzymatic, 85–86 (2013) 214-219.
[38] Ž. Knez, S. Kavčič, L. Gubicza, K. Bélafi-Bakó, G. Németh, M. Primožič, M. Habulin, The Journal of Supercritical Fluids, 66 (2012) 192-197.
[39] L.F. García-Alles, V. Gotor, Biotechnology and bioengineering, 59 (1998) 684-694.
[40] J.L. Van Roon, M. Joerink, M.P. Rijkers, J. Tramper, P. Schroën, G. Catharina, H.H. Beeftink, Biotechnology progress, 19 (2003) 1510-1518.
[41] B. Chen, E.M. Miller, L. Miller, J.J. Maikner, R.A. Gross, Langmuir, 23 (2007) 1381-1387.
[42] M.D. Romero, L. Calvo, C. Alba, A. Daneshfar, Journal of biotechnology, 127 (2007) 269-277.
[43] D.-H. Zhang, C. Li, G.-Y. Zhi, Journal of biotechnology, 168 (2013) 416-420.
[44] A. Güvenç, N. Kapucu, Ü. Mehmetoğlu, Process Biochemistry, 38 (2002) 379-386.
[45] L. Gubicza, A. Kabiri-Badr, E. Keoves, K. Belafi-Bako, Journal of biotechnology, 84 (2000) 193-196.
[46] C.G. Laudani, M. Habulin, Ž. Knez, G.D. Porta, E. Reverchon, The Journal of Supercritical Fluids, 41 (2007) 74-81.
[47] D. Oliveira, A.C. Feihrmann, A.F. Rubira, M.H. Kunita, C. Dariva, J.V. Oliveira, The Journal of Supercritical Fluids, 38 (2006) 373-382.
[48] M. Habulin, Ž. Knez, Journal of Chemical Technology & Biotechnology, 76 (2001) 1260-1266.
[49] P. Lozano, G. Víllora, D. Gómez, A.B. Gayo, J.A. Sánchez-Conesa, M. Rubio, J.L. Iborra, The Journal of Supercritical Fluids, 29 (2004) 121-128.
[50] B. Saha, A. Alqahtani, H. Teo, International Journal of Chemical Reactor Engineering, 3 (2005).

[51] P. Patidar, S.M. Mahajani, Chemical Engineering Journal, 207–208 (2012) 377-387.
[52] M.C. Ferreira, A.J.A. Meirelles, E.A.C. Batista, Industrial & Engineering Chemistry Research, 52 (2013) 2336-2351.

CAPÍTULO 6

DISCUSSÕES GERAIS

6.1 DISCUSSÕES GERAIS

O uso de enzimas em solventes não aquosos, como solventes orgânicos e fluidos pressurizados, ampliou a gama de reações químicas passíveis de catálise. Assim, substratos insolúveis em água podem ser utilizados em processos de transformação que utilizam enzimas, possibilitando a obtenção de novos produtos alimentícios ou farmacêuticos. Porém, sabe-se que existe uma tendência mundial em reduzir a produção de resíduos tóxicos, devido à poluição e às mudanças climáticas. Associado a esses fatores, a crescente exigência dos consumidores a produtos ditos naturais, orgânicos ou verdes, levam a indústria química e alimentícia a buscar e desenvolver novos processos que se adequem a essas tendências.

O presente trabalho buscou utilizar um novo processo, considerado de baixo impacto ambiental, pois utiliza dióxido de carbono supercrítico como solvente, no lugar de solventes orgânicos altamente tóxicos, por exemplo, hexano. Além disso, o trabalho procurou associar tecnologias distintas, como a tecnologia supercrítica e o conhecimento de reações de produção de ésteres de aromas por via enzimática.

O primeiro passo do presente trabalho foi projetar e construir a unidade de reações químicas a alta pressão. Durante esse processo visou-se montar um equipamento versátil com a possiblidade de operação em dois modos de produção, batelada e contínuo. Além disso, o equipamento foi projetado com a possiblidade de futuras modificações referentes ao modo de operação e à geometria dos reatores. A unidade de reações pode ser utilizada para outros fins, como por exemplo, experimentos de inativação microbiana, impregnação de polímeros com materiais bioativos e tratamento de resíduos industriais. Outra possibilidade de uso da unidade de reação é o acoplamento do processo de extração com os reatores químicos. Os dados gerais do projeto e construção da unidade de reação são apresentados no Apêndice desta tese.

A literatura reporta a estabilidade de várias enzimas em fluidos pressurizados, especialmente as lipases em CO_2 supercrítico, que demonstram uma baixa perda de atividade quando submetidas a altas pressões. Além disso, a estabilidade do catalisador em reações químicas é de fundamental importância, pois representa um ponto crítico que deve ser controlado a fim de obter altos valores de produtividade e conversão. Assim, na segunda etapa desse trabalho, foi realizado o estudo da estabilidade da lipase imobilizada comercial, Lipozyme 435, em CO_2 supercrítico.

Nesta etapa verificou-se que as condições de processo afetam negativamente a atividade de lipase de maneira irreversível. Porém, demonstrou-se que, apesar da inativação pós-processo de pressurização e despressurização, é possível utilizar a lipase como catalisadora de reações em CO_2 supercrítico como meio reacional. Nesta etapa, determinou-se que a condição de maior atividade enzimática residual foi de 40 °C e 10 MPa para um único ciclo de pressurização/despressurização. Os resultados obtidos nesta etapa foram relevantes na seleção de condições específicas de processo, nas quais a enzima Lipozyme 435 mantém a sua maior atividade residual em CO_2 supercrítico.

Com base nos resultados obtidos na etapa anterior, as condições mais adequadas de processo foram utilizadas como testes preliminares de esterificação de eugenol e anidrido acético em acetato de eugenila, que foi objeto de estudo da segunda etapa desse trabalho. Nesta etapa, foram avaliadas as seguintes condições de processo: quantidade de catalisador, razão de substratos, temperatura e pressão do CO_2 supercrítico, variedade da enzima imobilizada comercial e ciclos de reutilização. Verificou-se que a atividade enzimática específica obtida para Novozym 435 foi aproximadamente 18% maior do que a obtida para a Lipozyme 435, além de apresentar maiores taxas de esterificação de eugenol. Porém, todos os demais experimentos de esterificação de eugenol foram realizados com a Lipozyme 435. Verificou-se, ainda, que a melhor condição para esterificação de eugenol em acetato de eugenila foi de razão molar de 1:5 de eugenol para anidrido acético, 1% em massa de catalisador, 50 a 60 °C e 10 MPa.

Estudos sobre reações de esterificação utilizando CO_2 supercrítico como meio reacional reportam que a conversão pode ser influenciada pela solubilidade dos substratos no meio, que depende das condições de temperatura e pressão, sendo que as mesmas definem o equilíbrio de fases do sistema. Apesar dos altos valores de esterificação demonstrados, o estudo do comportamento de fases revelou uma região de duas fases (liquido/gás) em uma das condições ótimas de esterificação (60 °C e 10 MPa). Outro fato reportado na literatura e observado nesta etapa do projeto foi que o aumento no número de ciclos de pressurização e despressurização diminuiu a quantidade de água livre na enzima e em seu suporte, consequentemente reduzindo a sua atividade e capacidade de esterificação do eugenol.

O mecanismo de reação enzimática foi investigado com base no modelo de Ping-Pong Bi-Bi. Verificou-se que a atividade enzimática não apresentou inibição pelos reagentes e nem pelos produtos, nas condições de concentrações testadas. Além disso, o

mecanismo ordenado sugeriu que a afinidade da enzima pelo anidrido acético é maior do que pelo eugenol, sendo que essa afinidade pode ser controlada através da temperatura do processo. Por fim, calculou-se a energia de ativação para as duas etapas do mecanismo enzimático, a etapa de ligação do anidrido e do eugenol, e a segunda etapa apresentou maior energia de ativação, mostrando ser a etapa limitante do processo de esterificação.

A partir do estudo cinético da esterificação de anidrido acético com eugenol surgiram novos questionamentos, como seria o mecanismo de reação enzimática o fator limitante no processo de esterificação, ou outros fatores poderiam ser predominantes na reação, como os processos de transferência de massa convectiva no fluido e difusiva nas partículas sólidas de catalisadores. Assim, a terceira etapa deste trabalho investigou os processos de transferência de massa em uma reação biocatalisada em meio supercrítico. Ademais, foi avaliada a modelagem matemática, cinética de reação e produção em modo contínuo para a reação de produção do éster de aroma acetato de isoamila.

O estudo da esterificação de álcool isoamílico ocorreu em quatro passos distintos. Inicialmente foi realizado um planejamento experimental com o objetivo de avaliar as variáveis de processo temperatura, pressão, razão de substratos, concentração de catalisador e agitação do meio reacional em um reator em modo batelada. Verificou-se que os fatores predominantes no processo foram a razão molar entre substratos, a concentração de enzima imobilizada e a agitação do meio. Por outro lado, as variáveis temperatura e pressão não foram significativas ao nível de 5%. Logo, a condição de 3% (massa de enzima/massa de substrato), razão equimolar de substrato (1:1), temperatura e pressão de 40 °C e 15 MPa, respectivamente, foram fixadas na avaliação dos efeitos de transferência de massa em um reator em batelada.

No segundo passo, os efeitos do diâmetro do suporte do catalisador e da intensidade de mistura (agitação) do meio reacional foram avaliados frente ao coeficiente de transferência de massa e ao fator de efetividade interno e externo. Notou-se um aumento do coeficiente de transferência de massa sólido-liquido com o aumento da agitação do meio reacional. Tal efeito era esperado, uma vez que quanto maior a velocidade de agitação maior será o número de Reynolds. Além disso, uma maior agitação ocasiona o aumento da probabilidade de choques entre as moléculas dos substratos e as partículas do catalisador, aumentando a taxa de reação. Outro ponto que deve ser ressaltado é que partículas menores geraram maiores coeficientes de transferência de massa, uma vez que em menores partículas a resistência à transferência

de massa é menor. Em geral, os valores de efetividade externa e interna demonstraram ser próximos à unidade. Assim, pode-se dizer que tanto a resistência à transferência de massa convectiva (externo) quanto à transferência de massa na partícula sólida (interno) são negligenciáveis. Portanto, é possível afirmar que o mecanismo de cinética enzimática é o fator limitante no processo de reação, e é necessário conhecê-lo.

Assim como no estudo de esterificação de eugenol, neste terceiro passo foi estudada a cinética de reação enzimática com base no modelo de Ping-Pong Bi-Bi. Primeiramente, foi avaliada a possiblidade de inibição pelos substratos, que possibilitou concluir que não há inibição da atividade da enzima nas concentrações testadas. Assim, o modelo de Ping-Pong Bi-Bi sem inibição associado ao balanço de massa para um reator em batelada foi ajustado numericamente. Os resultados demonstraram que, novamente, a enzima tem maior afinidade com o anidrido acético que com o substrato receptor do grupo acil (eugenol ou álcool isoamílico). De maneira geral, o modelo ajustado representou satisfatoriamente a cinética de reação enzimática, porém os parâmetros obtidos somente são válidos para as condições experimentais testadas nesse trabalho.

Por fim, na quarta etapa, a comparação entre os reatores em modo contínuo e batelada foi realizada com base nos resultados de conversão, produtividade e produtividade específica para a mesma condição de temperatura e pressão (40 °C e 15 MPa), além do estudo das variáveis vazão de CO_2 supercrítico e de substratos no reator contínuo. Verificou-se que o aumento das vazões de substratos e de CO_2 supercrítico acarretou uma diminuição da conversão, da produtividade e da produtividade específica de acetato de isoamila. Além disso, mudanças na razão de alimentação dos substratos não ocasionaram aumentos nos parâmetros avaliados. Avaliou-se também a possiblidade de surgimento de duas fases tanto no reator em modo contínuo quanto no separador por simulação computacional, e com os dados de equilíbrio gerados foi possível afirmar que nas condições testadas não houve o surgimento de novas fases no reator contínuo. Porém, no separador a alta pressão o sistema foi composto por duas fases. Tal comportamento já era esperado, uma vez que o separador foi projetado e montado para operar na separação através da mudança de fase do solvente. De maneira geral, notou-se que apesar dos baixos valores de conversão obtidos nas reações em modo contínuo, os valores de produtividade compensam seu desempenho em comparação ao reator em batelada.

O estudo da esterificação de álcool isoamílico demostrou ser um processo alternativo para obter acetato de isoamila, que industrialmente é produzido em reatores de leito agitado acoplados a colunas de destilação ou através de destilação reativa. O processo proposto aplica uma técnica branda em termos de temperatura e solvente, e o catalisador pode ser totalmente removido do meio de reação em um único passo (despressurização e decantação ou centrifugação). Além disso, o catalisador normalmente utilizado na produção industrial é o ácido sulfúrico, o que exige a sua neutralização e separação da mistura final. Ademais, o catalisador empregado nos processos convencionais não pode ser considerado natural como as enzimas aplicadas neste trabalho. Contudo, o produto final obtido no presente trabalho também não pode ser considerado como natural, pois o doador do grupo acil (anidrido acético) não é um substrato natural, como o ácido acético, que pode ser obtido por processos microbiológicos e utilizado na reação estudada. Além disso, o método proposto pode ser aplicado para a esterificação de óleo fúsel, que é um subproduto obtido a partir de usinas sucroalcooleiras, composto por uma mistura de álcoois superiores, rica em álcool isoamílico.

A aplicação da tecnologia supercrítica em reações de síntese de ésteres de aromas, especificamente com CO_2 supercrítico, mostrou-se tecnologicamente viável e é um processo alternativo na obtenção de tais compostos. Cabe salientar que, apesar dos avanços desenvolvidos por este trabalho, mais estudos deverão ser realizados com o intuito de elucidar os mecanismos fenomenológicos, bem como aplicar essa tecnologia a processos industriais e estimar os custos referentes ao processo, o que é necessário quanto se visa à aplicação industrial.

CAPÍTULO 7

CONCLUSÃO GERAL E SUGESTÕES PARA TRABALHOS FUTUROS

7.1 CONCLUSÃO GERAL

O trabalho desenvolvido e apresentado no Capítulo 3 permitiu concluir informações importantes sobre a enzima imobilizada comercial Lipozyme 435 e seu comportamento em CO_2, as quais são listadas a seguir:

1. A exposição da enzima imobilizada comercial Lipozyme 435 ao CO_2 supercrítico reduziu a sua atividade catalítica em todas as condições experimentais testadas;
2. O tratamento a 10 MPa e 40 °C em 1 hora de exposição resultou na maior atividade residual, sendo que os maiores valores de tempo de meia vida e os maiores tempos de redução decimal foram obtidos em tal condição. Além disso, foi demonstrado que a reutilização, ciclos de pressurização e despressurização da enzima imobilizada diminuem sua atividade catalítica em até 64% do seu valor inicial;
3. Análises de espectroscopia de infravermelho revelaram uma mudança na estrutura da lipase imobilizada tratada com CO_2 supercrítico. Além disso, através da análise das imagens obtidas por FESEM foi possível concluir que não houve mudança na estrutura do suporte macroporoso da resina iônica da enzima com o tratamento em CO_2 supercrítico;
4. O estudo da esterificação de ácido oleico mostrou que, apesar da diminuição da atividade catalítica da enzima imobilizada com a exposição ao CO_2 supercrítico, é possível obter altos valores de esterificação e rendimento em condições operacionais específicas;
5. Os resultados obtidos por esse capítulo podem ser relevantes na seleção de condições específicas de processo, nas quais a enzima Lipozyme 435 mantenha a sua maior atividade residual em CO_2 supercrítico. Além disso, a utilização de tal solvente mostrou-se hábil para reações químicas, havendo ainda a possiblidade de sua utilização em uma futura etapa de separação dos produtos e reagentes envolvidos no final do processo, através de uma simples etapa.

Após compreender o comportamento da enzima imobilizada Lipozyme 435 em CO_2 supercrítico, foi realizado o estudo da esterificação de eugenol em acetato de

eugenila em CO_2 supercrítico, conforme exposto no Capítulo 4. Os resultados apresentados permitiram concluir que:

1. A atividade enzimática específica obtida para a Novozym 435 foi aproximadamente 18% maior do que a obtida para a Lipozyme 435. Diferenças também ocorreram na distribuição de partículas e no conteúdo de umidade das enzimas imobilizadas. Além disso, a Novozym 435 apresentou maiores taxas de esterificação de eugenol do que a Lipozyme 435;
2. A melhor condição operacional, com base nos resultados de esterificação e rendimento de acetato de eugenila, foi de 60 °C e 10 MPa. O estudo do comportamento de fases revelou uma região de duas fases nessa condição (liquido/gás);
3. O aumento do número de ciclos de utilização da enzima diminuiu significativamente o percentual de esterificação e rendimento. Além disso, tais ciclos diminuem a quantidade de água disponível na vizinhança da enzima, o que, possivelmente, foi a razão da diminuição na atividade enzimática;
4. Estudos cinéticos sugeriram que o mecanismo de reação pode ser descrito pelo modelo sem inibição de Ping-Pong Bi-Bi, nas condições testadas por este trabalho. Além disso, concluiu-se que a afinidade da enzima com anidrido acético foi maior do que com o eugenol, sendo que tal afinidade aumentou com o acréscimo da temperatura. Dentre as duas etapas de reação, a segunda etapa necessitou de mais energia.

O estudo de esterificação de eugenol levantou questionamentos referentes aos processos de transferência de massa nas reações em CO_2 supercrítico. Além disso, o anseio pela aplicação da tecnologia em modo contínuo levou ao estudo da esterificação de álcool isoamílico, conforme exposto no Capítulo 5 deste trabalho. Os resultados permitiram concluir que:

1. A esterificação do álcool de isoamílico em *n*-hexano foi menor do que em CO_2 supercrítico, evidenciando os benefícios da utilização deste solvente como meio de reação para a produção de ésteres de aromas;
2. Os efeitos da razão molar de substratos, quantidade de enzima e de agitação foram estatisticamente significativos na conversão do álcool isoamílico, enquanto temperatura e pressão tiveram pouca influência sobre tal resultado;

3. Os efeitos de transferência de massa na fase fluida e na fase sólida são negligenciáveis. Portanto, a cinética da reação é independente do diâmetro da partícula e agitação e é controlada pela cinética enzimática.

4. O gráfico de Lineweaver-Burk sugeriu que a reação enzimática segue um mecanismo simples de Ping-Pong Bi-Bi sem inibição, na faixa de concentrações testadas. O modelo cinético descrito para a esterificação de álcool isoamílico com anidrido acético e os parâmetros obtidos indicam que a afinidade da enzima com o anidrido acético é maior do que com o álcool isoamílico.

5. O reator de leito fixo em modo contínuo, apesar da conversão inferior, apresentou uma maior produtividade de acetato de isoamila do que o reator em batelada e provou ser a melhor opção para sintetizar acetato de isoamila em CO_2 supercrítico.

7.2 SUGESTÕES PARA TRABALHOS FUTUROS

Apesar do avanço tecnológico alcançado por este trabalho, questionamentos referentes às reações enzimáticas em meio supercrítico surgiram, e para uma futura aplicação industrial estas questões devem ser abordadas em novos estudos. Assim, são sugestões para trabalhos futuros:

1. Estudar os mecanismos fenomenológicos envolvidos nos processos de esterificação em modo contínuo;
2. Aplicar outro modelo de reator na produção dos ésteres de aromas, como por exemplo, o reator contínuo de leito agitado;
3. Estudar diferentes reações de produção de ésteres de aromas através de catálise enzimática, como por exemplo, butirato de isoamila e acetato de cinamila;
4. Avaliar a seletividade das lipases imobilizadas para diferentes substratos em CO_2 supercrítico;
5. Elucidar o processo de separação do solvente e dos ésteres de aromas, objetivando a melhor separação dos produtos.
6. Aproveitando a versatilidade do equipamento montado, avaliar diferentes geometrias de reatores contínuos;
7. Efetuar o aumento de escala para os diferentes modos de processos e estudar a viabilidade econômica dos mesmos, bem como acoplar a unidade de reação em modo contínuo a um processo de reciclo de CO_2;
8. Aplicar a tecnologia envolvida a processos de reutilização de subprodutos e resíduos indústrias como, por exemplo, o óleo fúsel;
9. Acoplar o processo de extração com o processo de reação enzimática para obtenção de ésteres de ácidos graxos a partir de matrizes vegetais.

CAPÍTULO 8

REFERÊNCIAS

REFERÊNCIAS BIBLIOGRÁFICAS

ANGUS, S.; ARMSTRONG, B. e REUCK, K. M. D. **International Thermodynamic Tables of the Fluid State: Carbon Dioxide**. Oxford: Pergamon Press, 1976.

ASSIS, A. V. R. D. **Montagem, teste e validação de uma unidade de extração supercrítica com reciclo e operação contínua**. 2010. 152 (Doutorado). Departamento de Engenharia de Alimentos, Universidade Estadual de Campinas

AUCOIN, M. e LEGGE, R. Effects of supercritical CO2 exposure and depressurization on immobilized lipase activity. **Biotechnology Letters,** v. 23, n. 22, p. 1863-1870, 2001.

BASRI, M.; KASSIM, M. A.; MOHAMAD, R. e ARIFF, A. B. Optimization and kinetic study on the synthesis of palm oil ester using Lipozyme TL IM. **Journal of Molecular Catalysis B: Enzymatic,** v. 85–86, p. 214-219, 2013.

BIRD, B.; STEWART, W. e LIGHTFOOT, E. **Transport Phenomena, Revised 2nd Edition**. John Wiley & Sons, Inc., 2006. ISBN 0470115394.

BISSWANGER, H. Enzyme Kinetics: Section 2.6–2.12. In: (Ed.). **Enzyme Kinetics**. Weinheim, Germany. : Wiley-VCH Verlag GmbH & Co. KGaA, 2008. p.124-193. ISBN 9783527622023.

BRUNNER, G. **Gas Extraction: An Introduction to Fundamentals of Supercritical Fluids and the Application to Separation Processes**. 1. Steinkopff-Verlag Heidelberg, 1994. 387

BRUNNER, G. Supercritical fluids: technology and application to food processing. **Journal of Food Engineering,** v. 67, n. 1–2, p. 21-33, 2005.

BRUSSEL, V. U. Selection and representativity of the calibration sample subset. Vrije Universiteit Brussel - Departament of Analytical Chemistry and Pharmaceutical Technology, 2015. Disponível em: < http://www.vub.ac.be/fabi/publiek/index.html >. Acesso em: December 2015.

CARRASCO A., H.; ESPINOZA C., L.; CARDILE, V.; GALLARDO, C.; CARDONA, W.; LOMBARDO, L.; CATALÁN M., K.; CUELLAR F., M. e RUSSO, A. Eugenol and its synthetic analogues inhibit cell growth of human cancer cells (Part I). **Journal of the Brazilian Chemical Society,** v. 19, p. 543-548, 2008.

CHAIBAKHSH, N.; RAHMAN, M. B. A.; VAHABZADEH, F.; ABD-AZIZ, S.; BASRI, M. e SALLEH, A. B. Optimization of operational conditions for adipate ester synthesis in a stirred tank reactor. **Biotechnology and Bioprocess Engineering,** v. 15, n. 5, p. 846-853, 2010.

CHAITANYA, V. S. e SENAPATI, S. Self-assembled reverse micelles in supercritical CO2 entrap protein in native state. **J Am Chem Soc,** v. 130, n. 6, p. 1866-70, 2008.

CHEN, B.; MILLER, E. M.; MILLER, L.; MAIKNER, J. J. e GROSS, R. A. Effects of Macroporous Resin Size on Candida antarctica Lipase B Adsorption, Fraction of Active Molecules, and Catalytic Activity for Polyester Synthesis. **Langmuir,** v. 23, n. 3, p. 1381-1387, 2007.

CHENG, K.-W.; KUO, S.-J.; TANG, M. e CHEN, Y.-P. Vapor–liquid equilibria at elevated pressures of binary mixtures of carbon dioxide with methyl salicylate, eugenol, and diethyl phthalate. **The Journal of Supercritical Fluids,** v. 18, n. 2, p. 87-99, 2000.

CHIARADIA, V.; PAROUL, N.; CANSIAN, R. L.; JUNIOR, C. V.; DETOFOL, M. R.; LERIN, L. A.; OLIVEIRA, J. V. e OLIVEIRA, D. Synthesis of eugenol esters by lipase-catalyzed reaction in solvent-free system. **Appl Biochem Biotechnol,** v. 168, n. 4, p. 742-51, 2012a.

CHIARADIA, V.; PAROUL, N.; CANSIAN, R. L.; JÚNIOR, C. V.; DETOFOL, M. R.; LERIN, L. A.; OLIVEIRA, J. V. e OLIVEIRA, D. Synthesis of Eugenol Esters by Lipase-Catalyzed Reaction in Solvent-Free System. **Applied Biochemistry and Biotechnology,** v. 168, n. 4, p. 742-751, 2012b.

CHIOU, S.-H. e WU, W.-T. Immobilization of Candida rugosa lipase on chitosan with activation of the hydroxyl groups. **Biomaterials,** v. 25, n. 2, p. 197-204, 2004.

CHULALAKSANANUKUL, W.; CONDORET, J.-S. e COMBES, D. Geranyl acetate synthesis by lipase-catalyzed transesterification in supercritical carbon dioxide. **Enzyme and Microbial Technology,** v. 15, n. 8, p. 691-698, 1993.

COLLINS, S. E.; LASSALLE, V. e FERREIRA, M. L. FTIR-ATR characterization of free Rhizomucor meihei lipase (RML), Lipozyme RM IM and chitosan-immobilized RML. **Journal of Molecular Catalysis B: Enzymatic,** v. 72, n. 3, p. 220-228, 2011.

COPELAND, R. A. Enzymes: A Practical Introduction to Structure, Mechanism, and Data Analysis. In: (Ed.). **Enzymes**: John Wiley & Sons, Inc., 2002. p.42-75. ISBN 9780471220633.

COUTO, R.; VIDINHA, P.; PERES, C.; RIBEIRO, A. S.; FERREIRA, O.; OLIVEIRA, M. V.; MACEDO, E. A.; LOUREIRO, J. M. e BARREIROS, S. Geranyl Acetate Synthesis in a Packed-Bed Reactor Catalyzed by Novozym in Supercritical Carbon Dioxide and in Supercritical Ethane. **Industrial & Engineering Chemistry Research,** v. 50, n. 4, p. 1938-1946, 2011a.

COUTO, R.; VIDINHA, P.; PERES, C. L.; RIBEIRO, A. S.; FERREIRA, O.; OLIVEIRA, M. V.; MACEDO, E. N. A.; LOUREIRO, J. M. e BARREIROS, S. Geranyl Acetate Synthesis in a Packed-Bed Reactor Catalyzed by Novozym in Supercritical Carbon Dioxide and in Supercritical Ethane. **Industrial & Engineering Chemistry Research,** v. 50, n. 4, p. 1938-1946, 2011b.

DAMODARAN, S.; PARKIN, K. L. e FENNEMA, O. R. **Fennema's food chemistry**. Boca Raton :: CRC Press/Taylor & Francis 2008.

DANNENBERG, F. e KESSLER, H.-G. Reaction Kinetics of the Denaturation of Whey Proteins in Milk. **Journal of Food Science,** v. 53, n. 1, p. 258-263, 1988.

DE LOS RÍOS, A. P.; HERNÁNDEZ-FERNÁNDEZ, F. J.; GÓMEZ, D.; RUBIO, M.; TOMÁS-ALONSO, F. e VÍLLORA, G. Understanding the chemical reaction and mass-transfer phenomena in a recirculating enzymatic membrane reactor for green ester synthesis in ionic liquid/supercritical carbon dioxide biphasic systems. **The Journal of Supercritical Fluids,** v. 43, n. 2, p. 303-309, 2007.

DHAKE, K. P.; DESHMUKH, K. M.; PATIL, Y. P.; SINGHAL, R. S. e BHANAGE, B. M. Improved activity and stability of Rhizopus oryzae lipase via immobilization for citronellol ester synthesis in supercritical carbon dioxide. **J Biotechnol,** v. 156, n. 1, p. 46-51, 2011a.

DHAKE, K. P.; DESHMUKH, K. M.; PATIL, Y. P.; SINGHAL, R. S. e BHANAGE, B. M. Improved activity and stability of Rhizopus oryzae lipase via immobilization for citronellol ester synthesis in supercritical carbon dioxide. **Journal of Biotechnology,** v. 156, n. 1, p. 46-51, 2011b.

DHAKE, K. P.; TAMBADE, P. J.; QURESHI, Z. S.; SINGHAL, R. S. e BHANAGE, B. M. HPMC-PVA Film Immobilized Rhizopus oryzae Lipase as a Biocatalyst for Transesterification Reaction. **ACS Catalysis,** v. 1, n. 4, p. 316-322, 2011c.

DHAKE, K. P.; THAKARE, D. D. e BHANAGE, B. M. Lipase: A potential biocatalyst for the synthesis of valuable flavour and fragrance ester compounds. **Flavour and Fragrance Journal,** v. 28, n. 2, p. 71-83, 2013.

DIAZ, M. D. R.; GÓMEZ, J. M.; DÍAZ-SUELTO, B. e GARCÍA-SANZ, A. Enzymatic synthesis of short-chain esters in n-hexane and supercritical carbon dioxide: Effect of the acid chain length. **Engineering in Life Sciences,** v. 10, n. 2, p. 171-176, 2010.

DONG, H.-P.; WANG, Y.-J. e ZHENG, Y.-G. Enantioselective hydrolysis of diethyl 3-hydroxyglutarate to ethyl (S)-3-hydroxyglutarate by immobilized Candida antarctica lipase B. **Journal of Molecular Catalysis B: Enzymatic,** v. 66, n. 1–2, p. 90-94, 2010.

DORAN, P. M. Bioprocess engineering principles. Waltham, MA, 2013. ISSN 9780080917702 0080917704 9780122208515 012220851X. Disponível em: < http://www.books24x7.com/marc.asp?bookid=50921 >.

DORDICK, J. S.; MARLETTA, M. A. e KLIBANOV, A. M. Polymerization of phenols catalyzed by peroxidase in nonaqueous media. **Biotechnology and Bioengineering,** v. 30, n. 1, p. 31-36, 1987.

DUMONT, T.; BARTH, D.; CORBIER, C.; BRANLANT, G. e PERRUT, M. Enzymatic reaction kinetic: Comparison in an organic solvent and in supercritical carbon dioxide. **Biotechnology and Bioengineering,** v. 40, n. 2, p. 329-333, 1992.

ESCANDELL, J.; WURM, D. J.; BELLEVILLE, M. P.; SANCHEZ, J.; HARASEK, M. e PAOLUCCI-JEANJEAN, D. Enzymatic synthesis of butyl acetate in a packed bed reactor under liquid and supercritical conditions. **Catalysis Today,** v. 255, p. 3-9, 2015.

EUROPEAN FOOD SAFETY AUTHORITY, E. F. S. A. Scientific Opinion on the safety and efficacy of allylhydroxybenzenes (chemical group 18) when used as flavourings for all animal species. EFSA Panel on Additives and Products or Substances used in Animal Feed (FEEDAP). **EFSA Journal,** v. 9, n. 12, 2011.

FERREIRA, M. C.; MEIRELLES, A. J. A. e BATISTA, E. A. C. Study of the Fusel Oil Distillation Process. **Industrial & Engineering Chemistry Research,** v. 52, n. 6, p. 2336-2351, 2013.

FORNEY, L. J.; PENNEY, W. R. e VO, H. X. Scale-up in plug-flow reactors: Laminar feed. **AIChE Journal,** v. 47, n. 1, p. 31-38, 2001.

FRANCISCO, J. D. C.; GOUGH, S. e DEY, E. Use of Lipases in the Synthesis of Structured Lipids in Supercritical Carbon Dioxide. In: POLAINA, J. e MACCABE, A. (Ed.). **Industrial Enzymes**: Springer Netherlands, 2007. cap. 20, p.341-354. ISBN 978-1-4020-5376-4.

GARCÍA- ALLES, L. F. e GOTOR, V. Lipase- catalyzed transesterification in organic media: Solvent effects on equilibrium and individual rate constants. **Biotechnology and bioengineering,** v. 59, n. 6, p. 684-694, 1998.

GIEßAUF, A.; MAGOR, W.; STEINBERGER, D. J. e MARR, R. A study of hydrolases stability in supercritical carbon dioxide (SC-CO2). **Enzyme and Microbial Technology,** v. 24, n. 8–9, p. 577-583, 1999.

GROUP, T. F. World Flavors & Fragrances: Industry Study with Forecasts for 2016 & 2021. Cleveland, OH, 2012. Disponível em: < http://www.freedoniagroup.com/DocumentDetails.aspx?Referrerid=FM-Bro&StudyID=2952 >.

GUAN, W.; LI, S.; HOU, C.; YAN, R. e MA, J. Determination and correlation of solubilities of clove oil components in supercritical carbon dioxide. **CIESC Journal,** v. 58, n. 5, p. 1077-1081, 2007.

GUBICZA, L.; KABIRI-BADR, A.; KEOVES, E. e BELAFI-BAKO, K. Large-scale enzymatic production of natural flavour esters in organic solvent with continuous water removal. **Journal of Biotechnology,** v. 84, n. 2, p. 193-196, 2000.

GUI, F.; WANG, Z.; WU, J.; CHEN, F.; LIAO, X. e HU, X. Inactivation and reactivation of horseradish peroxidase treated with supercritical carbon dioxide. **European Food Research and Technology,** v. 222, n. 1-2, p. 105-111, 2006.

GUPTA, A. e KHARE, S. K. A protease stable in organic solvents from solvent tolerant strain of Pseudomonas aeruginosa. **Bioresource Technology,** v. 97, n. 15, p. 1788-1793, 2006.

GUTHALUGU, N. K.; BALARAMAN, M. e KADIMI, U. S. Optimization of enzymatic hydrolysis of triglycerides in soy deodorized distillate with supercritical carbon dioxide. **Biochemical Engineering Journal,** v. 29, n. 3, p. 220-226, 2006.

GÜVENÇ, A.; KAPUCU, N. e MEHMETOĞLU, Ü. The production of isoamyl acetate using immobilized lipases in a solvent-free system. **Process Biochemistry,** v. 38, n. 3, p. 379-386, 2002.

HABULIN, M. e KNEZ, Ž. Activity and stability of lipases from different sources in supercritical carbon dioxide and near-critical propane. **Journal of Chemical Technology & Biotechnology,** v. 76, n. 12, p. 1260-1266, 2001.

HABULIN, M.; KRMELJ, V. e KNEZ, Ž. Synthesis of Oleic Acid Esters Catalyzed by Immobilized Lipase. **Journal of Agricultural and Food Chemistry,** v. 44, n. 1, p. 338-342, 1996.

HABULIN, M.; PRIMOZIC, M. e KNEZ, Z. Supercritical fluids as solvents for enzymatic reactions. **Acta chimica slovenica,** v. 54, n. 4, p. 667-677, 2007a.

HABULIN, M.; ŠABEDER, S.; PALJEVAC, M.; PRIMOŽIČ, M. e KNEZ, Ž. Lipase-catalyzed esterification of citronellol with lauric acid in supercritical carbon dioxide/co-solvent media. **The Journal of Supercritical Fluids,** v. 43, n. 2, p. 199-203, 2007b.

HABULIN, M.; ŠABEDER, S.; SAMPEDRO, M. A. e KNEZ, Ž. Enzymatic synthesis of citronellol laurate in organic media and in supercritical carbon dioxide. **Biochemical Engineering Journal,** v. 42, n. 1, p. 6-12, 2008.

HAJAR, M. e VAHABZADEH, F. Production of a biodiesel additive in a stirred basket reactor using immobilized lipase: Kinetic and mass transfer analysis. **Korean Journal of Chemical Engineering,** v. 33, n. 4, p. 1220-1231, 2016.

HARI KRISHNA, S.; DIVAKAR, S.; PRAPULLA, S. G. e KARANTH, N. G. Enzymatic synthesis of isoamyl acetate using immobilized lipase from Rhizomucor miehei. **Journal of Biotechnology,** v. 87, n. 3, p. 193-201, 2001a.

HARI KRISHNA, S.; DIVAKAR, S.; PRAPULLA, S. G. e KARANTH, N. G. Enzymatic synthesis of isoamyl acetate using immobilized lipase from Rhizomucor miehei. **J Biotechnol,** v. 87, n. 3, p. 193-201, 2001b.

HEIDARYAN, E.; HATAMI, T.; RAHIMI, M. e MOGHADASI, J. Viscosity of pure carbon dioxide at supercritical region: Measurement and correlation approach. **The Journal of Supercritical Fluids,** v. 56, n. 2, p. 144-151, 2011.

HERNÁNDEZ, F. J.; DE LOS RÍOS, A. P.; GÓMEZ, D.; RUBIO, M. e VÍLLORA, G. A new recirculating enzymatic membrane reactor for ester synthesis in ionic liquid/supercritical carbon dioxide biphasic systems. **Applied Catalysis B: Environmental,** v. 67, n. 1–2, p. 121-126, 2006.

HILDEBRAND, C.; DALLA ROSA, C.; FREIRE, D. M. G.; DESTAIN, J.; DARIVA, C.; OLIVEIRA, D. D. e OLIVEIRA, J. V. Fatty acid ethyl esters production using a non-commercial lipase in pressurized propane medium. **Food Science and Technology (Campinas),** v. 29, p. 603-608, 2009.

HIRATA, H.; HIGUCHI, K. e YAMASHINA, T. Biotechnology in JapanLipase-catalyzed transesterification in organic solvent: effects of water and solvent, thermal stability and some applications. **Journal of Biotechnology,** v. 14, n. 2, p. 157-167, 1990.

HOUSAINDOKHT, M. R.; BOZORGMEHR, M. R. e MONHEMI, H. Structural behavior of Candida antarctica lipase B in water and supercritical carbon dioxide: A molecular dynamic simulation study. **The Journal of Supercritical Fluids,** v. 63, n. 0, p. 180-186, 2012.

HUANG, S. Y.; CHANG, H. L. e GOTO, M. Preparation of Surfactant-Coated Lipase for the Esterification of Geraniol and Acetic Acid in Organic Solvents. **Enzyme and Microbial Technology,** v. 22, n. 7, p. 552-557, 1998.

INCROPERA, F. P. e WITT, D. P. **Fundamentos da transferência de calor e de massa**. 3. LCT, 1992.

JACKSON, M. A.; MBARAKA, I. K. e SHANKS, B. H. Esterification of oleic acid in supercritical carbon dioxide catalyzed by functionalized mesoporous silica and an immobilized lipase. **Applied Catalysis A: General,** v. 310, n. 0, p. 48-53, 2006.

JAEGER, K.-E. e EGGERT, T. Lipases for biotechnology. **Current Opinion in Biotechnology,** v. 13, n. 4, p. 390-397, 2002a.

JAEGER, K. E.; DIJKSTRA, B. W. e REETZ, M. T. Bacterial biocatalysts: molecular biology, three-dimensional structures, and biotechnological applications of lipases. **Annu Rev Microbiol,** v. 53, p. 315-51, 1999.

JAEGER, K. E. e EGGERT, T. Lipases for biotechnology. **Curr Opin Biotechnol,** v. 13, n. 4, p. 390-7, 2002b.

JENAB, E.; TEMELLI, F.; CURTIS, J. M. e ZHAO, Y.-Y. Performance of two immobilized lipases for interesterification between canola oil and fully-hydrogenated canola oil under supercritical carbon dioxide. **LWT-Food Science and Technology,** v. 58, n. 1, p. 263-271, 2014.

KAMAT, S.; BARRERA, J.; BECKMAN, J. e RUSSELL, A. J. Biocatalytic synthesis of acrylates in organic solvents and supercritical fluids: I. Optimization of enzyme environment. **Biotechnology and Bioengineering,** v. 40, n. 1, p. 158-166, 1992.

KERN, D. Q. **Processos de Transmissão de Calor**. Guanabara Koogan S.A., 1987.

KNEZ, Ž. Enzymatic reactions in dense gases. **The Journal of Supercritical Fluids,** v. 47, n. 3, p. 357-372, 2009.

KNEZ, Ž. e HABULIN, M. Compressed gases as alternative enzymatic-reaction solvents: a short review. **The Journal of Supercritical Fluids,** v. 23, n. 1, p. 29-42, 2002.

KNEZ, Ž.; HABULIN, M. e KRMELJ, V. Enzyme catalyzed reactions in dense gases. **The Journal of Supercritical Fluids,** v. 14, n. 1, p. 17-29, 1998.

KNEZ, Ž.; HABULIN, M. e PRIMOŽIČ, M. Enzymatic reactions in dense gases. **Biochemical Engineering Journal,** v. 27, n. 2, p. 120-126, 2005.

KNEZ, Ž.; KAVČIČ, S.; GUBICZA, L.; BÉLAFI-BAKÓ, K.; NÉMETH, G.; PRIMOŽIČ, M. e HABULIN, M. Lipase-catalyzed esterification of lactic acid in supercritical carbon dioxide. **The Journal of Supercritical Fluids,** v. 66, n. 0, p. 192-197, 2012a.

KNEZ, Ž.; KAVČIČ, S.; GUBICZA, L.; BÉLAFI-BAKÓ, K.; NÉMETH, G.; PRIMOŽIČ, M. e HABULIN, M. Lipase-catalyzed esterification of lactic acid in supercritical carbon dioxide. **The Journal of Supercritical Fluids,** v. 66, p. 192-197, 2012b.

KNEZ, Z.; LAUDANI, C. G.; HABULIN, M. e REVERCHON, E. Exploiting the pressure effect on lipase-catalyzed wax ester synthesis in dense carbon dioxide. **Biotechnol Bioeng,** v. 97, n. 6, p. 1366-75, 2007a.

KNEZ, Ž.; LAUDANI, C. G.; HABULIN, M. e REVERCHON, E. Exploiting the pressure effect on lipase-catalyzed wax ester synthesis in dense carbon dioxide. **Biotechnology and Bioengineering,** v. 97, n. 6, p. 1366-1375, 2007b.

KNEZ, Ž.; LEITGEB, M. e PRIMOŽIČ, M. Enzymatic Reactions in Supercritical Fluids. In: FORNARI, T. e STATEVA, R. P. (Ed.). **High Pressure Fluid Technology for Green Food Processing**. Cham: Springer International Publishing, 2015. p.185-215. ISBN 978-3-319-10611-3.

KRISTJANSSON, M. M. e KINSELLA, J. E. Protein and enzyme stability: structural, thermodynamic, and experimental aspects. **Adv Food Nutr Res,** v. 35, p. 237-316, 1991.

KRMELJ, V.; HABULIN, M.; ZNEZ, Ž. e BAUMAN, D. Lipase-catalyzed synthesis of oleyl oleate in pressurized and supercritical solvents. **Lipid / Fett,** v. 101, n. 1, p. 34-38, 1999.

KUMAR, R.; MADRAS, G. e MODAK, J. Enzymatic synthesis of ethyl palmitate in supercritical carbon dioxide. **Industrial & engineering chemistry research,** v. 43, n. 7, p. 1568-1573, 2004.

KUMAR, R.; MODAK, J. e MADRAS, G. Effect of the chain length of the acid on the enzymatic synthesis of flavors in supercritical carbon dioxide. **Biochemical Engineering Journal,** v. 23, n. 3, p. 199-202, 2005.

KUO, C.-H.; JU, H.-Y.; CHU, S.-W.; CHEN, J.-H.; CHANG, C.-M.; LIU, Y.-C. e SHIEH, C.-J. Optimization of Lipase-Catalyzed Synthesis of Cetyl Octanoate in Supercritical Carbon Dioxide. **Journal of the American Oil Chemists' Society,** v. 89, n. 1, p. 103-110, 2012.

LANZA, M.; PRIAMO, W.; OLIVEIRA, J.; DARIVA, C. e DE OLIVEIRA, D. The effect of temperature, pressure, exposure time, and depressurization rate on lipase activity in SCCO2. **Applied Biochemistry and Biotechnology,** v. 113, n. 1-3, p. 181-187, 2004a.

LANZA, M.; PRIAMO, W. L.; OLIVEIRA, J. V.; DARIVA, C. e DE OLIVEIRA, D. The effect of temperature, pressure, exposure time, and depressurization rate on lipase activity in SCCO2. **Applied Biochemistry and Biotechnology - Part A Enzyme Engineering and Biotechnology,** v. 113, n. 1-3, p. 181-187, 2004b.

LAUDANI, C. G.; HABULIN, M.; KNEZ, Ž.; PORTA, G. D. e REVERCHON, E. Immobilized lipase-mediated long-chain fatty acid esterification in dense carbon dioxide: bench-scale packed-bed reactor study. **The Journal of Supercritical Fluids,** v. 41, n. 1, p. 74-81, 2007a.

LAUDANI, C. G.; HABULIN, M.; KNEZ, Ž.; PORTA, G. D. e REVERCHON, E. Lipase-catalyzed long chain fatty ester synthesis in dense carbon dioxide: Kinetics and thermodynamics. **The Journal of Supercritical Fluids,** v. 41, n. 1, p. 92-101, 2007b.

LEE, K.-G. e SHIBAMOTO, T. Antioxidant property of aroma extract isolated from clove buds [Syzygium aromaticum (L.) Merr. et Perry]. **Food Chemistry,** v. 74, n. 4, p. 443-448, 2001.

LI, C.; TAN, T.; ZHANG, H. e FENG, W. Analysis of the conformational stability and activity of Candida antarctica lipase B in organic solvents: insight from molecular dynamics and quantum mechanics/simulations. **J Biol Chem,** v. 285, n. 37, p. 28434-41, 2010.

LIAQUAT, M. e APENTEN, R. Synthesis of low molecular weight flavor esters using plant seedling lipases in organic media. **Journal of food science,** v. 65, n. 2, p. 295-299, 2000.

LIAW, E. T. e LIU, K. J. Synthesis of terpinyl acetate by lipase-catalyzed esterification in supercritical carbon dioxide. **Bioresour Technol,** v. 101, n. 10, p. 3320-4, 2010.

LIONG, K. K.; WELLS, P. A. e FOSTER, N. R. Diffusion of fatty acid esters in supercritical carbon dioxide. **Industrial & Engineering Chemistry Research,** v. 31, n. 1, p. 390-399, 1992.

LIU, K.-J. e HUANG, Y.-R. Lipase-catalyzed production of a bioactive terpene ester in supercritical carbon dioxide. **Journal of Biotechnology,** v. 146, n. 4, p. 215-220, 2010.

LIU, Y.; CHEN, D. e WANG, S. Effect of sub- and super-critical CO2 pretreatment on conformation and catalytic properties evaluation of two commercial enzymes of CALB and Lipase PS. **Journal of Chemical Technology & Biotechnology,** v. 88, n. 9, p. 1750-1756, 2013.

LOWRY, O. H.; ROSEBROUGH, N. J.; FARR, A. L. e RANDALL, R. J. Protein measurement with the Folin phenol reagent. **J Biol Chem,** v. 193, n. 1, p. 265-75, 1951.

LOZANO, P.; ViLLORA, G.; GÓMEZ, D.; GAYO, A. B.; SÁNCHEZ-CONESA, J. A.; RUBIO, M. e IBORRA, J. L. Membrane reactor with immobilized Candida antarctica lipase B for ester synthesis in supercritical carbon dioxide. **The Journal of Supercritical Fluids,** v. 29, n. 1–2, p. 121-128, 2004.

MACEDO, G. A. **Síntese de ésteres de aroma por lipases microbianas em meio livre de solvente orgânico**. 1997. 143 (Doutorado). Faculdade de Engenharia de Alimentos, Universidade Estadual de Campinas, Campinas.

MACEDO, G. A.; PASTORE, G. M. e RODRIGUES, M. I. Optimising the synthesis of isoamyl butyrate using Rhizopus sp. lipase with a central composite rotatable design. **Process Biochemistry,** v. 39, n. 6, p. 687-693, 2004.

MARKETS, M. A. Food Flavors Market by Type (Chocolate, Vanilla, Fruits & Nuts, Others), Origin (Natural, Synthetic), Application (Beverages, Savory & Snacks, Bakery & Confectionery, Dairy & Frozen Products, Others), & by Region - Global Forecast to 2020. September 2015. Disponível em: < http://www.marketsandmarkets.com/Market-Reports/food-flavors-market-93115891.html >.

MARTINEZ, J. L. **Supercritical fluid extraction of nutraceuticals and bioactive compounds.** . Boca Raton-FL: CRC Press, 2008.

MARTY, A.; CHULALAKSANANUKUL, W.; CONDORET, J. S.; WILLEMOT, R. M. e DURAND, G. Comparison of lipase-catalysed esterification in supercritical carbon dioxide and in n-hexane. **Biotechnology Letters,** v. 12, n. 1, p. 11-16, 1990.

MARTY, A.; CHULALAKSANANUKUL, W.; WILLEMOT, R. M. e CONDORET, J. S. Kinetics of lipase-catalyzed esterification in supercritical CO2. **Biotechnology and Bioengineering,** v. 39, n. 3, p. 273-280, 1992.

MARTY, A.; COMBES, D. e CONDORET, J. S. Continuous reaction-separation process for enzymatic esterification in supercritical carbon dioxide. **Biotechnol Bioeng,** v. 43, n. 6, p. 497-504, 1994.

MASSERSCHMIDT, I.; CUELBAS, C.; POPPI, R.; DE ANDRADE, J.; DE ABREU, C. e DAVANZO, C. Determination of organic matter in soils by FTIR/diffuse reflectance and multivariate calibration. **Journal of Chemometrics,** v. 13, n. 3- 4, p. 265-273, 1999.

MATSUDA, T.; HARADA, T. e NAKAMURA, K. Organic synthesis using enzymes in supercritical carbon dioxide. **Green Chemistry,** v. 6, n. 9, p. 440-444, 2004a.

MATSUDA, T.; WATANABE, K.; HARADA, T. e NAKAMURA, K. Enzymatic reactions in supercritical CO2: carboxylation, asymmetric reduction and esterification. **Catalysis Today,** v. 96, n. 3, p. 103-111, 2004b.

MEI, Y.; MILLER, L.; GAO, W. e GROSS, R. A. Imaging the Distribution and Secondary Structure of Immobilized Enzymes Using Infrared Microspectroscopy. **Biomacromolecules,** v. 4, n. 1, p. 70-74, 2003.

MELGOSA, R.; SANZ, M. T.; G. SOLAESA, Á.; BUCIO, S. L. e BELTRÁN, S. Enzymatic activity and conformational and morphological studies of four commercial lipases treated with supercritical carbon dioxide. **The Journal of Supercritical Fluids,** v. 97, n. 0, p. 51-62, 2015a.

MELGOSA, R.; SANZ, M. T.; G. SOLAESA, Á.; BUCIO, S. L. e BELTRÁN, S. Enzymatic activity and conformational and morphological studies of four commercial lipases treated with supercritical carbon dioxide. **The Journal of Supercritical Fluids,** v. 97, p. 51-62, 2015b.

MONHEMI, H. e HOUSAINDOKHT, M. R. How enzymes can remain active and stable in a compressed gas? New insights into the conformational stability of Candida antarctica lipase B in near-critical propane. **The Journal of Supercritical Fluids,** v. 72, n. 0, p. 161-167, 2012.

NAIDU, G. S. N. e PANDA, T. Studies on pH and thermal deactivation of pectolytic enzymes from Aspergillus niger. **Biochemical Engineering Journal,** v. 16, n. 1, p. 57-67, 2003.

NAKAYA, H.; MIYAWAKI, O. e NAKAMURA, K. Determination of log P for pressurized carbon dioxide and its characterization as a medium for enzyme reaction. **Enzyme and Microbial Technology,** v. 28, n. 2–3, p. 176-182, 2001.

NIST. **NIST Chemistry WebBook, NIST Standard Reference Database Number 69**. LINSTROM, P. J. e MALLARD, W. G.: National Institute of Standards and Technology 2005.

OLIVEIRA, D.; FEIHRMANN, A. C.; DARIVA, C.; CUNHA, A. G.; BEVILAQUA, J. V.; DESTAIN, J.; OLIVEIRA, J. V. e FREIRE, D. M. G. Influence of compressed fluids treatment on the activity of Yarrowia lipolytica lipase. **Journal of Molecular Catalysis B: Enzymatic,** v. 39, n. 1–4, p. 117-123, 2006a.

OLIVEIRA, D.; FEIHRMANN, A. C.; RUBIRA, A. F.; KUNITA, M. H.; DARIVA, C. e OLIVEIRA, J. V. Assessment of two immobilized lipases activity treated in compressed fluids. **The Journal of Supercritical Fluids,** v. 38, n. 3, p. 373-382, 2006b.

OLIVEIRA, M. V.; REBOCHO, S. F.; RIBEIRO, A. S.; MACEDO, E. A. e LOUREIRO, J. M. Kinetic modelling of decyl acetate synthesis by immobilized lipase-catalysed transesterification of vinyl acetate with decanol in supercritical carbon dioxide. **The Journal of Supercritical Fluids,** v. 50, n. 2, p. 138-145, 2009.

OLUSESAN, A. T.; AZURA, L. K.; FORGHANI, B.; BAKAR, F. A.; MOHAMED, A. K.; RADU, S.; MANAP, M. Y. e SAARI, N. Purification, characterization and thermal inactivation kinetics of a non-regioselective thermostable lipase from a genotypically identified extremophilic Bacillus subtilis NS 8. **N Biotechnol,** v. 28, n. 6, p. 738-45, 2011.

ORTEGA, N.; DE DIEGO, S.; PEREZ-MATEOS, M. e BUSTO, M. D. Kinetic properties and thermal behaviour of polygalacturonase used in fruit juice clarification. **Food Chemistry,** v. 88, n. 2, p. 209-217, 2004.

OWUSU, R. K.; MAKHZOUM, A. e KNAPP, J. S. Heat inactivation of lipase from psychrotrophic Pseudomonas fluorescens P38: Activation parameters and enzyme stability at low or ultra-high temperatures. **Food Chemistry,** v. 44, n. 4, p. 261-268, 1992.

PAIVA, A. L.; BALCÃO, V. M. e MALCATA, F. X. Kinetics and mechanisms of reactions catalyzed by immobilized lipases. **Enzyme and Microbial Technology,** v. 27, n. 3–5, p. 187-204, 2000.

PATIDAR, P. e MAHAJANI, S. M. Esterification of fusel oil using reactive distillation – Part I: Reaction kinetics. **Chemical Engineering Journal,** v. 207–208, p. 377-387, 2012.

PERES, C.; GOMES DA SILVA, M. D. e BARREIROS, S. Water activity effects on geranyl acetate synthesis catalyzed by novozym in supercritical ethane and in supercritical carbon dioxide. **J Agric Food Chem,** v. 51, n. 7, p. 1884-8, 2003.

PETRY, I.; GANESAN, A.; PITT, A.; MOORE, B. D. e HALLING, P. J. Proteomic methods applied to the analysis of immobilized biocatalysts. **Biotechnol Bioeng,** v. 95, n. 5, p. 984-91, 2006.

POWELL, M. J. D. **Subroutine BOBQYA**: Department of Applied Mathematics and Theorical Physics, Cambrige University 2009.

RANDOLPH, T. W.; BLANCH, H. W. e PRAUSNITZ, J. M. Enzyme-caytalyzed oxidation of cholesterol in supercritical carbon dioxide. **AIChE Journal,** v. 34, n. 8, p. 1354-1360, 1988.

RAVENTOS, M.; DUARTE, S. e ALARCON, R. Application and possibilities of supercritical CO2 extraction in food processing industry: An overview. **Food Science and Technology International,** v. 8, n. 5, p. 269-284, 2002.

RAVENTÓS, M.; DUARTE, S. e ALARCÓN, R. Application and Possibilities of Supercritical CO2 Extraction in Food Processing Industry: An Overview. v. 8, n. 5, p. 269-284, 2002.

RAZAFINDRALAMBO, H.; BLECKER, C.; LOGNAY, G.; MARLIER, M.; WATHELET, J.-P. e SEVERIN, M. Improvement of enzymatic synthesis yields of flavour acetates: The example of the isoamyl acetate. **Biotechnology Letters,** v. 16, n. 3, p. 247-250, 1994.

REIS, P.; HOLMBERG, K.; WATZKE, H.; LESER, M. E. e MILLER, R. Lipases at interfaces: a review. **Adv Colloid Interface Sci,** v. 147-148, p. 237-50, 2009.

REVERCHON, E. e DE MARCO, I. Supercritical fluid extraction and fractionation of natural matter. **The Journal of Supercritical Fluids,** v. 38, n. 2, p. 146-166, 2006.

REZAEI, K.; JENAB, E. e TEMELLI, F. Effects of Water on Enzyme Performance with an Emphasis on the Reactions in Supercritical Fluids. **Critical Reviews in Biotechnology,** v. 27, n. 4, p. 183-195, 2007.

RIBEIRO, A. S.; OLIVEIRA, M. V.; REBOCHO, S. F.; FERREIRA, O.; VIDINHA, P.; BARREIROS, S.; MACEDO, E. A. e LOUREIRO, J. M. Enzymatic production of decyl acetate: kinetic study in n-hexane and comparison with supercritical CO2. **Industrial & Engineering Chemistry Research,** v. 49, n. 16, p. 7168-7175, 2010.

RINNAN, Å.; BERG, F. V. D. e ENGELSEN, S. B. Review of the most common pre-processing techniques for near-infrared spectra. **TrAC Trends in Analytical Chemistry,** v. 28, n. 10, p. 1201-1222, 2009.

ROBERTS, G. W. **Reações químicas e reatores químicos**. Rio de Janeiro: LTC, 2010. 414

ROMERO, M. D.; CALVO, L.; ALBA, C. e DANESHFAR, A. A kinetic study of isoamyl acetate synthesis by immobilized lipase-catalyzed acetylation in n-hexane. **Journal of Biotechnology,** v. 127, n. 2, p. 269-277, 2007.

ROMERO, M. D.; CALVO, L.; ALBA, C.; DANESHFAR, A. e GHAZIASKAR, H. S. Enzymatic synthesis of isoamyl acetate with immobilized Candida antarctica lipase in n-hexane. **Enzyme and Microbial Technology,** v. 37, n. 1, p. 42-48, 2005a.

ROMERO, M. D.; CALVO, L.; ALBA, C.; HABULIN, M.; PRIMOŽIČ, M. e KNEZ, Ž. Enzymatic synthesis of isoamyl acetate with immobilized Candida antarctica lipase in supercritical carbon dioxide. **The Journal of Supercritical Fluids,** v. 33, n. 1, p. 77-84, 2005b.

ROSA, P.; MEIRELES, M. A. A.; BEATRIZ, D.-R.; LOUW, F.; MOTONOBU, G.; ANDRES, M.; MASAAKI, T.; SUSANA, L.; RICHARD, L. S.; COR, P.; HERMINIA, D. N. e JUAN CARLOS, P. Supercritical and Pressurized Fluid Extraction Applied to the Food Industry. In: (Ed.). **Extracting Bioactive Compounds for Food Products**: Boca Raton: CRC Press, 2008. p.269-401. (Contemporary Food Engineering). ISBN 978-1-4200-6237-3.

SAHA, B.; ALQAHTANI, A. e TEO, H. Production of iso-amyl acetate: Heterogeneous kinetics and techno-feasibility evaluation for catalytic distillation. **International Journal of Chemical Reactor Engineering,** v. 3, n. 1, 2005.

SANDLER, S. I. **Chemical, biochemical and engineering thermodynamics**. 4ª. Wiley Series, 2006. 495

SANTOS, P.; REZENDE, C. A. e MARTÍNEZ, J. Activity of immobilized lipase from Candida antarctica (Lipozyme 435) and its performance on the esterification of oleic acid in supercritical carbon dioxide. **The Journal of Supercritical Fluids,** v. 107, p. 170-178, 2016.

SANTOS, P.; ZABOT, G. L.; MEIRELES, M. A. A.; MAZUTTI, M. A. e MARTÍNEZ, J. Synthesis of eugenyl acetate by enzymatic reactions in supercritical carbon dioxide. **Biochemical Engineering Journal,** v. 114, p. 1-9, 2016.

SASSIAT, P. R.; MOURIER, P.; CAUDE, M. H. e ROSSET, R. H. Measurement of diffusion coefficients in supercritical carbon dioxide and correlation with the equation of Wilke and Chang. **Analytical Chemistry,** v. 59, n. 8, p. 1164-1170, 1987.

SEGEL, I. H. **Enzyme Kinetics**. New York: Wiley-Interscience, 1993.

SEHGAL, A. C.; TOMPSON, R.; CAVANAGH, J. e KELLY, R. M. Structural and catalytic response to temperature and cosolvents of carboxylesterase EST1 from the extremely thermoacidophilic archaeon Sulfolobus solfataricus P1. **Biotechnol Bioeng,** v. 80, n. 7, p. 784-93, 2002.

SILVEIRA, R. L.; MARTÍNEZ, J.; SKAF, M. S. e MARTÍNEZ, L. Enzyme Microheterogeneous Hydration and Stabilization in Supercritical Carbon Dioxide. **The Journal of Physical Chemistry B,** v. 116, n. 19, p. 5671-5678, 2012.

SKJOT, M.; DE MARIA, L.; CHATTERJEE, R.; SVENDSEN, A.; PATKAR, S. A.; OSTERGAARD, P. R. e BRASK, J. Understanding the plasticity of the alpha/beta hydrolase fold: lid swapping on the Candida antarctica lipase B results in chimeras with interesting biocatalytic properties. **Chembiochem,** v. 10, n. 3, p. 520-7, 2009.

SOUZA, A. M. D. e POPPI, R. J. Experimento didático de quimiometria para análise exploratória de óleos vegetais comestíveis por espectroscopia no infravermelho médio e análise de componentes principais: um tutorial, parte I. **Química Nova,** v. 35, p. 223-229, 2012.

SOUZA, A. T.; CORAZZA, M. L.; CARDOZO-FILHO, L.; GUIRARDELLO, R. e MEIRELES, M. A. A. Phase Equilibrium Measurements for the System Clove (Eugenia caryophyllus) Oil + CO2. **Journal of Chemical & Engineering Data,** v. 49, n. 2, p. 352-356, 2004.

SOVOVÁ, H.; ZAREVÚCKA, M.; BERNÁŠEK, P. e STAMENIĆ, M. Kinetics and specificity of Lipozyme-catalysed oil hydrolysis in supercritical CO2. **Chemical Engineering Research and Design,** v. 86, n. 7, p. 673-681, 2008.

SRIVASTAVA, S.; MODAK, J. e MADRAS, G. Enzymatic Synthesis of Flavors in Supercritical Carbon Dioxide. **Industrial & Engineering Chemistry Research,** v. 41, n. 8, p. 1940-1945, 2002.

STEINBERGER, D.-J.; GAMSE, T. e MAAR, R. **Enzyme inactivation and prepurification effects of supercritical carbon dioxide (SC-CO2)**. Proceedings of the Fifth Conference on Supercritical Fluids and their Applications. Verona, Italy: A. Bertucco (Ed.)**:** p. 339 p. 1999.

STEYTLER, D.; MOULSON, P. e REYNOLDS, J. Biotransformations in near-critical carbon dioxide. **Enzyme and microbial technology,** v. 13, n. 3, p. 221-226, 1991.

STOYTCHEVA, M.; MONTERO, G.; ZLATEV, R.; A. LEON, J. e GOCHEV, V. Analytical Methods for Lipases Activity Determination: A Review. **Current Analytical Chemistry,** v. 8, n. 3, p. 400-407, 2012.

TRAN, D.-T. e CHANG, J.-S. Kinetics of enzymatic transesterification and thermal deactivation using immobilized Burkholderia lipase as catalyst. **Bioprocess and Biosystems Engineering,** v. 37, n. 3, p. 481-491, 2014.

UPPENBERG, J.; HANSEN, M. T.; PATKAR, S. e JONES, T. A. The sequence, crystal structure determination and refinement of two crystal forms of lipase B from Candida antarctica. **Structure,** v. 2, n. 4, p. 293-308, 1994.

VALIVETY, R. H.; JOHNSTON, G. A.; SUCKLING, C. J. e HALLING, P. J. Solvent effects on biocatalysis in organic systems: Equilibrium position and rates of lipase catalyzed esterification. **Biotechnology and Bioengineering,** v. 38, n. 10, p. 1137-1143, 1991.

VAN ROON, J. L.; JOERINK, M.; RIJKERS, M. P.; TRAMPER, J.; SCHROËN, P.; CATHARINA, G. e BEEFTINK, H. H. Enzyme Distribution Derived from Macroscopic

Particle Behavior of an Industrial Immobilized Penicillin- G Acylase. **Biotechnology progress,** v. 19, n. 5, p. 1510-1518, 2003.

VARMA, M. e MADRAS, G. Synthesis of isoamyl laurate and isoamyl stearate in supercritical carbon dioxide. **Applied Biochemistry and Biotechnology,** v. 141, n. 1, p. 139-147, 2007a.

VARMA, M. e MADRAS, G. Effect of Chain Length of Alcohol on the Lipase-Catalyzed Esterification of Propionic Acid in Supercritical Carbon Dioxide. **Applied Biochemistry and Biotechnology,** v. 160, n. 8, p. 2342-2354, 2010a.

VARMA, M. N. e MADRAS, G. Synthesis of isoamyl laurate and isoamyl stearate in supercritical carbon dioxide. **Appl Biochem Biotechnol,** v. 141, n. 1, p. 139-48, 2007b.

VARMA, M. N. e MADRAS, G. Kinetics of synthesis of butyl butyrate by esterification and transesterification in supercritical carbon dioxide. **Journal of Chemical Technology & Biotechnology,** v. 83, n. 8, p. 1135-1144, 2008.

VARMA, M. N. e MADRAS, G. Kinetics of enzymatic synthesis of geranyl butyrate by transesterification in various supercritical fluids. **Biochemical Engineering Journal,** v. 49, n. 2, p. 250-255, 2010b.

VENY, H.; AROUA, M. K. e SULAIMAN, N. M. N. Kinetic study of lipase catalyzed transesterification of jatropha oil in circulated batch packed bed reactor. **Chemical Engineering Journal,** v. 237, p. 123-130, 2014.

VERGER, R. ‘Interfacial activation’ of lipases: facts and artifacts. **Trends in Biotechnology,** v. 15, n. 1, p. 32-38, 1997.

VERMA, M.; AZMI, W. e KANWAR, S. Microbial lipases: At the interface of aqueous and non-aqueous media. **Acta Microbiologica et Immunologica Hungarica,** v. 55, n. 3, p. 265-294, 2008.

VILLENEUVE, P.; MUDERHWA, J. M.; GRAILLE, J. e HAAS, M. J. Customizing lipases for biocatalysis: a survey of chemical, physical and molecular biological approaches. **Journal of Molecular Catalysis B: Enzymatic,** v. 9, n. 4–6, p. 113-148, 2000.

WEEMAES, C. A.; LUDIKHUYZE, L. R.; VAN DEN BROECK, I. e HENDRICKX, M. E. Effect of pH on Pressure and Thermal Inactivation of Avocado Polyphenol Oxidase: A Kinetic Study. **Journal of Agricultural and Food Chemistry,** v. 46, n. 7, p. 2785-2792, 1998.

WEINGÄRTNER, H. e FRANCK, E. U. Supercritical Water as a Solvent. **Angewandte Chemie International Edition,** v. 44, n. 18, p. 2672-2692, 2005.

WIMMER, Z. e ZAREVÚCKA, M. A Review on the Effects of Supercritical Carbon Dioxide on Enzyme Activity. v. 11, n. 1, p. 233-253, 2010a.

WIMMER, Z. e ZAREVÚCKA, M. A Review on the Effects of Supercritical Carbon Dioxide on Enzyme Activity. **International Journal of Molecular Sciences,** v. 11, n. 1, p. 233-253, 2010b.

YADAV, G. D. e DEVI, K. M. Enzymatic synthesis of perlauric acid using Novozym 435. **Biochemical Engineering Journal,** v. 10, n. 2, p. 93-101, 2002.

YOSHIMURA, T.; FURUTERA, M.; SHIMODA, M.; ISHIKAWA, H.; MIYAKE, M.; MATSUMOTO, K.; OSAJIMA, Y. e HAYAKAWA, I. Inactivation Efficiency of Enzymes in Buffered System by Continuous Method with Microbubbles of Supercritical Carbon Dioxide. **Journal of Food Science,** v. 67, n. 9, p. 3227-3231, 2002.

YOSHIMURA, T.; SHIMODA, M.; ISHIKAWA, H.; MIYAKE, M.; HAYAKAWA, I.; MATSUMOTO, K. e OSAJIMA, Y. Inactivation Kinetics of Enzymes by Using Continuous Treatment with Microbubbles of Supercritical Carbon Dioxide. **Journal of Food Science,** v. 66, n. 5, p. 694-697, 2001.

YU, Z.-R.; CHANG, S.-W.; WANG, H.-Y. e SHIEH, C.-J. Study on synthesis parameters of lipase-catalyzed hexyl acetate in supercritical CO2 by response surface methodology. **Journal of the American Oil Chemists' Society,** v. 80, n. 2, p. 139-144, 2003.

ZABOT, G. L.; MORAES, M. N.; PETENATE, A. J. e MEIRELES, M. A. A. Influence of the bed geometry on the kinetics of the extraction of clove bud oil with supercritical CO2. **The Journal of Supercritical Fluids,** v. 93, p. 56-66, 2014.

ZHANG, D.-H.; LI, C. e ZHI, G.-Y. Kinetic and thermodynamic investigation of enzymatic l-ascorbyl acetate synthesis. **Journal of Biotechnology,** v. 168, n. 4, p. 416-420, 2013.

APÊNDICE

Este apêndice apresenta a metodologia e os materiais utilizados na montagem da unidade de reações químicas a alta pressão. Os desenhos técnicos e esquemáticos, bem como a lista de peças e equipamentos da unidade em modo batelada e em modo contínuo também são apresentados. Além disso, todos os algoritmos (MATLAB software 2014Ra, MathWorks, Natick, MA, USA) envolvidos nos trabalhos elaborados são expostos neste apêndice.

I Montagem da Unidade de Reação Química

Antes da montagem ou construção de qualquer tipo de equipamento industrial, o responsável deve elaborar o projeto do mesmo, ou seja, ele deve responder perguntas básicas, como: Para qual finalidade o equipamento será construído? Quais são as limitações do processo, tais como temperatura, pressão, utilização de solventes, ácidos e/ou água? O equipamento será utilizado para fins alimentícios? Qual a capacidade, taxa de produção ou extração, que o processo requer? Quais materiais serão utilizados? Respondidas estas perguntas, o responsável deverá elaborar o projeto, ou seja, dimensionar e esboçar (desenhar) todos componentes do equipamento.

O desenho técnico do equipamento é uma etapa essencial para dimensionar o tamanho, estrutura, disposição dos componentes e quantidades de material a ser utilizado na montagem. Portanto, deve-se dedicar algum tempo a esta etapa, pois com tais informações o projetista será capaz de prever os custos de construção da futura unidade. Atualmente, alguns programas de desenho técnico são utilizados para projetar e desenhar as unidades que utilizam fluido supercrítico. A Figura 11 apresenta a vista isométrica da unidade de reações químicas em CO_2 supercrítico montada neste trabalho.

Figura 11 - Perspectiva da unidade de reações químicas em CO_2 supercrítico.

Após ter respondido as perguntas essenciais e projetada a unidade, o responsável iniciará a seleção dos equipamentos e acessórios envolvidos em todo o processo, como válvulas de bloqueio e de controle de vazão e pressão, válvulas de segurança, filtros, banhos de refrigeração e aquecimento, totalizadores de vazão, manômetros, termopares, indicadores e controladores de temperatura, tubulações, acessórios (cruzetas, curvas, reduções, etc.), bombas e *boosters*. Todos os equipamentos e acessórios envolvidos na montagem da unidade de reação química estão listados na Tabela 4 e o esquema da unidade de reações químicas a alta pressão, tanto em batelada quanto em modo contínuo, são apresentados nas seções I.I e I.II deste apêndice, respectivamente.

Tabela 4- Materiais e equipamentos da unidade reação química.

Quantidade	Componente	Especificação	Marca
18 m	Tubos de aço inoxidável	TP 316 1/4'', 1/8'' e 1/16''OD	Detroit/Park Corp.
-	Flanges e anilhas de aço inoxidável	TP 316 1/4'', 1/8'' e 1/16''OD	Detroit/Park Corp.
-	Conexões de aço inoxidável	TP 316 1/4'', 1/8'' e 1/16''OD	Detroit/Park Corp.
1	Bomba pneumática	M111-CO_2	Maximator
2	Bomba de HPLC	PU 2080	Jasco
5	Manômetros	Z.10.B+-	Zürich LTDA
1	Banho termostático de refrigeração com circulação	SL152/18	Solab
2	Banho termostático de aquecimento com circulação	MA 126/BD	Marconi
1	Filtro de CO_2	SS-2F-05	Swagelok
1	Filtro de ar comprimido		Norgen
1	Válvula de segurança	SS-4R3A	Swagelok
7	Válvula agulha para bloqueio	10V2071	Autoclave Engineers
1	Válvula micrométrica	8481.40.00	Autoclave Engineers
2	Válvula *back-pressure*	26-1700	Tescom
1	Fluxômetro	PMR1 010423	Cole Parmer
30 m	Perfis de Alumínio	45 x 45mm - DS680	Jartec Automação
1	Totalímetro	ACP G1,0	Itrón
1	Separador	-	Maq'nagua
1	Célula em batelada	-	Maq'nagua
1	Reator Contínuo	-	LAPEA
5	Termopares Tipo J	Bainha de 1/8"	Pyrotec
1	Indicador de Temperatura	T4WM	Autonics
4	Rodízios	GL 512 SPE G	Schioppa
1	Agitador magnético		IKA
1	Sistema de aquecimento válvula micrométrica	MA-152/FEA/2	Marconi

Atualmente, encontram-se no mercado diversos tipos de estruturas metálicas para o uso em equipamentos de processos, nos mais diferentes materiais, tais como aço inox, aço-carbono e alumínio. Para as unidades que operam com fluído supercrítico, utilizam-se perfis de alumínio devido à facilidade de manipulação, corte e perfuração e resistência a intempéries, tais como temperatura e solventes. Dentre os formatos de perfis de alumínio encontrados à venda, pode-se citar o perfil de 45 mm X 45 mm UL (Jartec). A Figura 12 apresenta a estrutura de perfis montada para a unidade de reações químicas em CO_2 supercrítico.

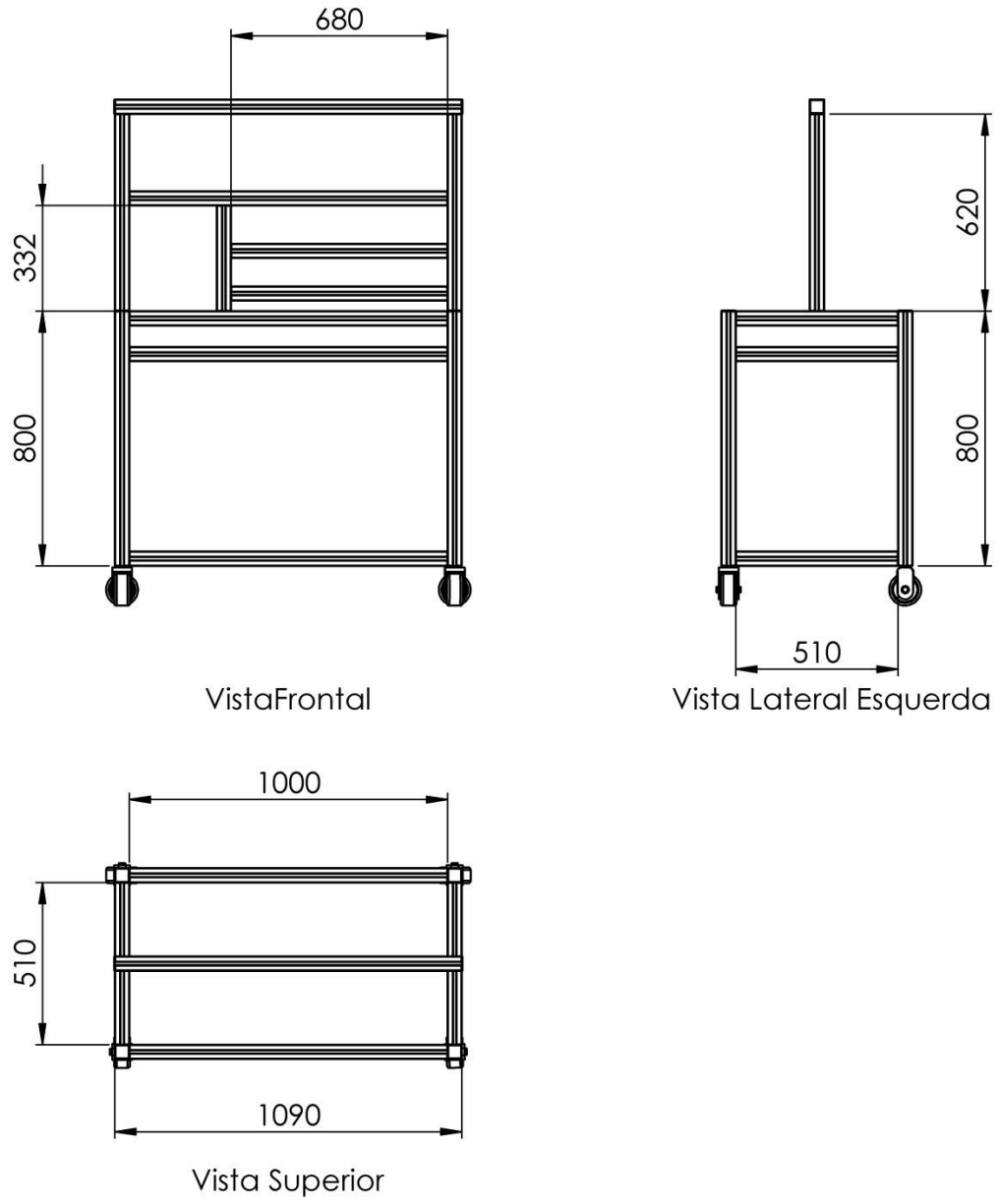

Figura 12 - Dimensões básicas da estrutura com perfis de alumínio da unidade de reações químicas em CO_2 supercrítico.

Todos os equipamentos e acessórios que têm contato direto com os produtos envolvidos nos processos de reação química são de aço inoxidável AISI 316, como, por exemplo, a célula de reação em batelada de 100 mL, o reator contínuo e o separador de 250 mL. As especificações de tais acessórios são detalhadas nas seções I.IV, I.V e I.VI deste apêndice, respectivamente.

Atualmente, no Laboratório de Alta Pressão em Engenharia de Alimentos (LAPEA-DEA/FEA-Unicamp), utiliza-se um *booster* específico para o pressurizar e

movimentar dióxido de carbono. Porém, há a possibilidade de usar o mesmo modelo de *booster*, com especificações diferentes, para deslocar outros fluidos. Tais *boosters* são bombas pneumáticas, ou seja, operam através de uma corrente de ar comprimido. O Modelo M-111 da Maximator, um dos modelos utilizados, tem uma taxa de conversão de 1:130, ou seja, para um psi de pressão fornecido a bomba, a mesma irá converter em 130 vezes mais, portanto 130 psi. As especificações do modelo utilizado no laboratório são: Bomba hidropneumática para CO_2, pressão máxima de trabalho de 18850 psi, Maximator-M111.

Por outro lado, a bomba de HPLC é de fácil operação, pois consiste em uma bomba elétrica de deslocamento positivo. Porém, sua manutenção e custo são mais elevados que dos *boosters*. Atualmente, utilizam-se tais bombas no LAPEA para o deslocamento de cossolventes em extração supercrítica, injeção de soluções em uma célula de formação de partículas e em extração com líquidos pressurizados. Para líquidos, geralmente não há a necessidade de refrigeração do mesmo, pois em temperatura ambiente tais fluídos já são líquidos. Porém, o CO_2 deve ser refrigerado, a fim de garantir que o fluido esteja na fase líquida até a entrada da bomba (*booster*), pois, caso contrário a bomba iria cavitar. Portanto, deve-se montar um sistema de refrigeração adequado para o CO_2.

O sistema de refrigeração de CO_2 é montado com os seguintes componentes: banho ultratermostatizado de refrigeração, serpentina de aço inox AISI 316L, mangueiras de silicone e isolantes térmicos. As Figura 13, Figura 14 e Figura 15 ilustram o sistema de refrigeração, o cabeçote de refrigeração e a serpentina para o CO_2, respectivamente. O cálculo da carga térmica para o sistema de refrigeração é apresentado na secção I.III desse apêndice.

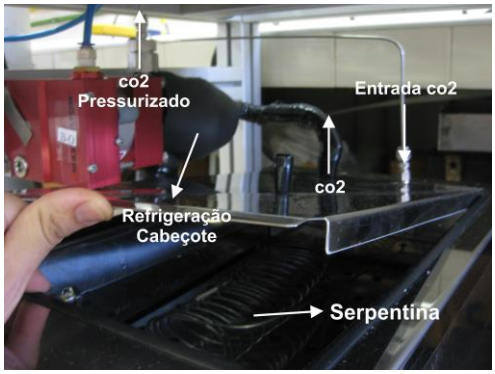

Figura 13 – Sistema de refrigeração.

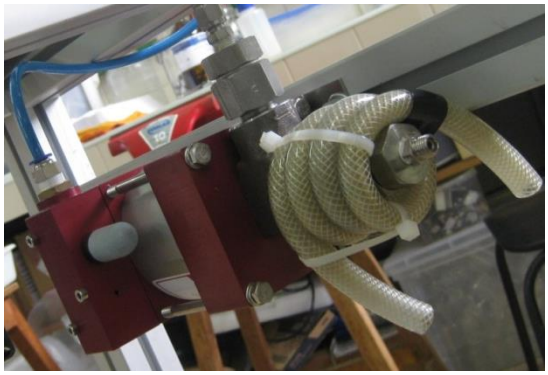

Figura 14 – Cabeçote refrigerado.

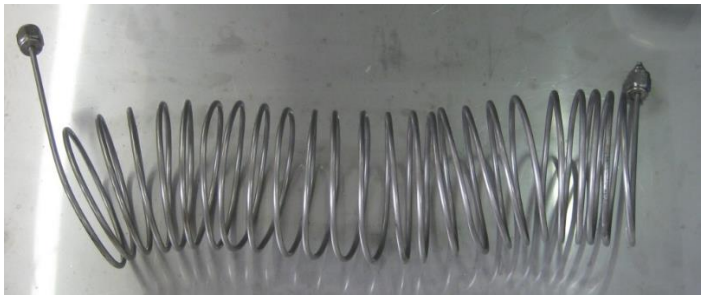

Figura 15 – Serpentina de refrigeração CO_2.

O mesmo sistema foi montado para o aquecimento do CO_2, através de uma serpentina igual à mostrada na Figura 15 e um banho ultratermostatizado de aquecimento e, novamente, procederam-se os cálculos de carga térmica conforme a secção I.III desse apêndice.

I. I Esquema da Unidade Reações Químicas em Modo Batelada

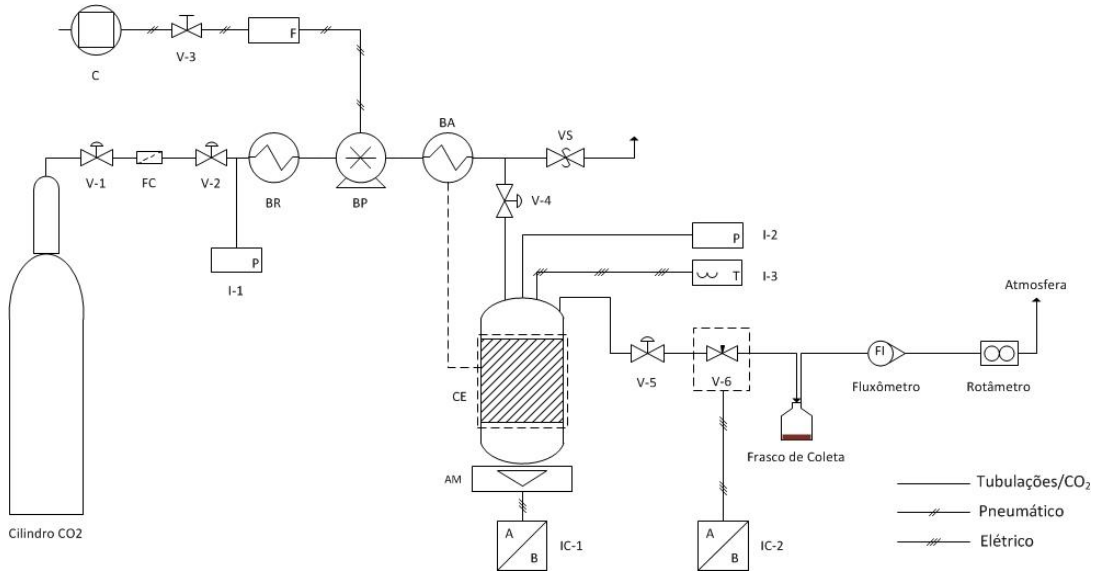

Figura 16 - Esquema da unidade de reações químicas em meio supercrítico: V-1, V-2, V-3, V-4 e V-5– Válvulas de bloqueio; V-7 – Válvula micrométrica; VS – Válvula de segurança (P_{max} = 450 bar); C- Compressor; F-Filtro de ar comprimido; FC – Filtro de CO2; BR – Banho de refrigeração; BP- Bomba pneumática (*Booster*); BA – Banho de aquecimento; I-1 e I-2 – Indicadores de pressão; I-3 Indicador de temperatura; IC-1 – Controlador e indicador do agitador magnético; IC-2 – Controlador e indicador de temperatura da válvula micrométrica; AM – Agitador magnético; CE – Célula de reação química com aquecimento.

I. II Esquema da Unidade Reações Químicas em Modo Contínuo

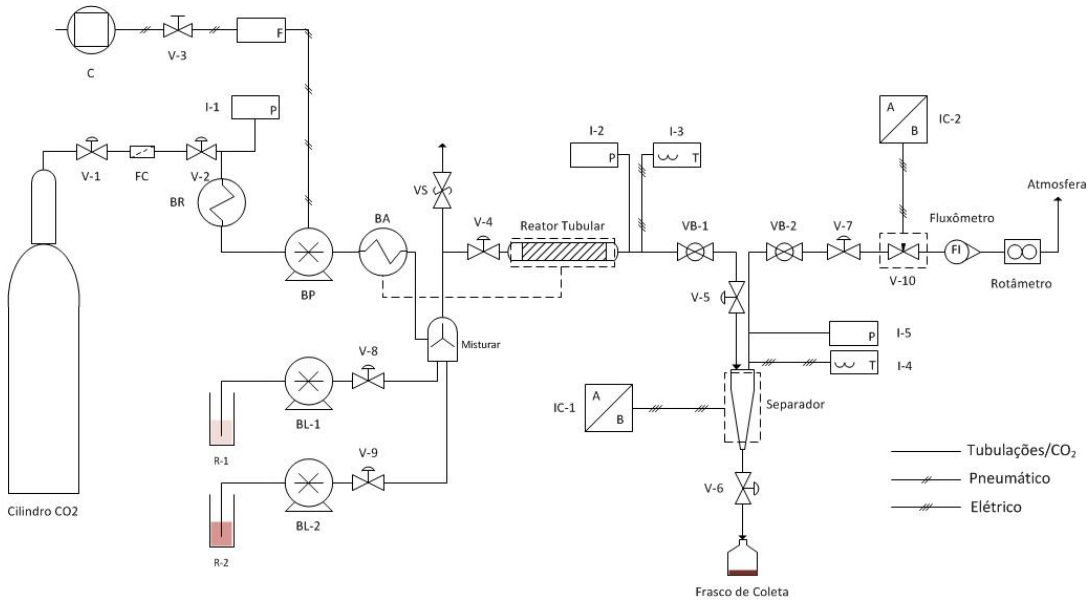

Figura 17 - Esquema da unidade de reações químicas em meio supercrítico: V-1, V-2, V-3, V-4, V-5,V-6,V-7, V-8 e V-9– Válvulas de bloqueio; V-10 – Válvula micrométrica; VS – Válvula de segurança (P_{max} = 450 bar); VB-1 e VB-2 – Válvula *back-pressure*; C-Compressor; F-Filtro de ar comprimido; FC – Filtro de CO2; BR – Banho de refrigeração; BP- Bomba pneumática (*Booster*); BA – Banho de aquecimento; BL-1 e BL-2 – Bomba de liquido (reagentes); I-1, I-2 e I-5 – Indicadores de pressão; I-3 e I-4 - Indicador de temperatura; IC-1 e IC-2 – Controlador e indicador de temperatura do separador e da válvula micrométrica, respectivamente.

I. III Calculo da Carga Térmica do Sistema de Refrigeração e Aquecimento

Para os cálculos de carga térmica dos sistemas de refrigeração e de aquecimento, considerou-se que o CO_2 escoa em um tubo de seção transversal circular de raio (*r*), com vazão mássica é constante ($\dot{m}$), a convecção de calor ocorre na superfície interna do tubo em estado estacionário, sem geração de energia e desconsiderou-se a transferência de calor por condução na direção axial (*x*). O escoamento é completamente limitado ao seu interior. Assim, é possível fazer um balanço de energia para um tubo de comprimento finito (*L*), conforme a Figura 18. O equacionamento foi realizado com base nas discussões teóricas de Kern (1987) e Incropera e Witt (1992) e as aplicações de Assis (2010) em uma unidade de extração supercrítica em modo contínuo.

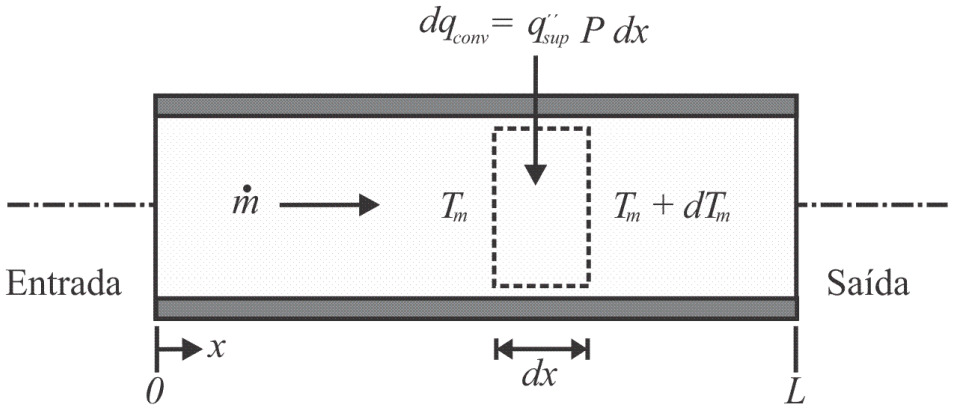

Figura 18 – Volume de controle para o escoamento interno em um tubo.

Considerando o volume de controle um volume infinitesimal de fluído no interior do tubo (*dx*) e a partir da lei de conservação de energia, tem-se que:

$$dq_{conv} = \dot{m} c_p dT_m \tag{1}$$

Ou na forma integrada:

$$q_{conv} = \dot{m} c_p \left(T_{m,e} - T_{m,s}\right) \tag{2}$$

onde:

dq_{conv} - Elemento diferencial de transferência de calor;

c_p - Calor específico do fluido;

dT_m - Elemento diferencial de temperatura;

$T_{m,e}$ - Temperatura média de entrada;

$T_{m,s}$ - Temperatura média de saída;

A taxa de transferência de calor por convecção por unidade de comprimento também pode ser escrita considerando o fluxo de calor na superfície do tubo (q''_{sup}) e o perímetro do tubo (*P*).

$$dq_{conv} = q''_{sup} P dx \tag{3}$$

Igualando as Equações (1) e (3) tem-se:

$$\frac{dT_m}{dx} = \frac{q''_{sup} P}{\dot{m} c_p} \tag{4}$$

Pode-se determinar o fluxo de calor na superfície do tubo (q''_{sup}) através da lei de resfriamento de Newton:

$$q''_{sup} = h_{loc}\left(T_{sup} - T_m\right) \tag{5}$$

onde:

h_{loc} - Coeficiente local de transferência de calor por convecção;

T_{sup} – Temperatura da superfície do tubo;

T_m – Temperatura média do fluído;

Substituindo a Equação (5) em (4) tem-se:

$$\frac{dT_m}{dx} = \frac{h_{loc}\left(T_{sup} - T_m\right) P}{\dot{m} c_p} \tag{6}$$

Considerando que a temperatura superficial do tubo é constante devido ao contato direto com o fluído de refrigeração ou aquecimento, e definindo $\Delta T = \left(T_{sup} - T_m\right)$, tem-se:

$$\frac{dT_m}{dx} = -\frac{d(\Delta T)}{dx} = \frac{P}{\dot{m}c_p} h_{loc} \Delta T \tag{7}$$

Rearranjando e integrando a Equação (7) para a entrada e saída do tubo, tem-se:

$$\int_{\Delta T_s}^{\Delta T_e} \frac{d(\Delta T)}{d\Delta T} = -\frac{P}{\dot{m}c_p} \int_0^L h_{loc} dx \tag{8}$$

$$ln\left(\frac{\Delta T_s}{\Delta T_e}\right) = -\frac{A_{sup}}{\dot{m}c_p} \overline{h_L} \tag{9}$$

onde:

$\overline{h_L}$ – Valor médio do coeficiente local de transferência de calor por convecção em todo o tubo;

A_{sup} – Área superficial do tubo;

Rearranjando a Equação (9):

$$\dot{m}c_p = \frac{A_{sup}\overline{h_L}}{ln\left(\frac{\Delta T_s}{\Delta T_e}\right)} \quad X \quad (\Delta T_e - \Delta T_s) \tag{10}$$

$$\dot{m}c_p(\Delta T_e - \Delta T_s) = -\frac{(\Delta T_e - \Delta T_s)}{ln\left(\frac{\Delta T_s}{\Delta T_e}\right)} A_{sup}\overline{h_L} \tag{11}$$

Expressando a Equação (1) em relação à temperatura da superfície do tubo, em que ΔT_{ml} é a média logarítmica das diferenças de temperatura, tem-se:

$$q_{conv} = \dot{m}c_p\left[\left(T_{sup} - T_{m,e}\right) - \left(T_{sup} - T_{m,s}\right)\right] = \dot{m}c_p(\Delta T_e - \Delta T_s) \tag{11}$$

$$\Delta T_{ml} = \frac{(\Delta T_s - \Delta T_e)}{ln\left(\frac{\Delta T_s}{\Delta T_e}\right)} \tag{12}$$

$$q_{conv} = \overline{h_L} A_{sup} \Delta T_{ml} \tag{13}$$

A Equação (13) representa a taxa total de transferência de calor na superfície do tubo. Neste caso, especificamente, é conveniente utilizar a temperatura do meio (T_∞) ao invés da temperatura da superfície do tubo, logo:

$$\frac{\Delta T_s}{\Delta T_e} = \frac{T_\infty - T_{m,s}}{T_\infty - T_{m,e}} \tag{14}$$

Desta forma, pode-se substituir $\overline{h_L}$ pelo o coeficiente global de transferência de calor (U).

$$Q = UA_{sup}\Delta T_{ml} \tag{15}$$

Após o desenvolvimento do balanço de energia na serpentina, os cálculos para a determinação da carga dos banhos de refrigeração e de aquecimento foram efetuados, conforme as seguintes etapas. Primeiramente, as temperaturas de médias de saída ($T_{m,s}$) e entrada ($T_{m,e}$) do CO_2, temperatura média do CO_2 (T_{m,CO_2}), temperatura de refrigeração e aquecimento (T_∞) e a média logarítmica das diferenças de temperatura do CO_2 (ΔT_{ml}) foram determinadas, conforme apresentado na Tabela 5.

Tabela 5 – Temperaturas utilizadas para o cálculo da carga térmica

Temperatura	Resfriamento	Aquecimento
$T_{m,e}$(ºC)	22	-5,0
$T_{m,s}$(ºC)	-5,0	60
T_{m,CO_2}(ºC)	8,5	27.5
T_∞(ºC)	-8,0	62
ΔT_{ml}(ºC)	11,72	-18.51

A temperatura média e a média logarítmica das diferenças de temperatura foram determinadas conforme as Equações (16) e (17).

$$T_{m,CO_2} = \frac{T_{m,e} + T_{m,s}}{2} \tag{16}$$

$$\Delta T_{ml} = \frac{(\Delta T_s - \Delta T_e)}{ln\left(\frac{\Delta T_s}{\Delta T_e}\right)} \tag{17}$$

Para efetuar os cálculos da carga térmica foi necessária a obtenção das propriedades físico-químicas do CO_2 a 6 MPa e 8,5 °C para a refrigeração e 30 MPa e 27.5 °C para o aquecimento. Considerou-se a pressão de 30 MPa para o aquecimento, pois essa foi a pressão máxima utilizada em todos os ensaios na unidade de reação química, e 6 MPa representa a pressão máxima do cilindro de CO_2. A Tabela 6 apresenta as propriedades físico-químicas para as condições citadas.

Tabela 6 – Propriedades físico-químicas do CO_2 para as temperaturas média na refrigeração (6 MPa) e no aquecimento (30 MPa).

Propriedade[1]	6 MPa e T_{m,CO_2}	30 MPa e T_{m,CO_2}
Calor Específico (c_p) J/kg K	2629,5	1920,4
Viscosidade (μ) cP	0,0899	0,1070
Condutividade Térmica (k) J/h m K	373,82	427,969
Densidade (ρ) kg/m³	892,97	957,29

[1] Valores obtidos no NIST (2005)

A partir das propriedades físico-químicas, da vazão mássica ($\dot{m}$) de CO_2 e da Equação (2) foi possível determinar a quantidade de calor necessária para o fluido atingir a temperatura desejada. O valor obtido foi de 79232 J/h ou aproximadamente 22,0 W e 139310 J/h ou 38,7 W, para a refrigeração e o aquecimento, respectivamente. Como a potência do banho de refrigeração é de 500 W e a do banho de aquecimento é de 200 W, ou seja, superiores às potências necessárias para refrigerar e aquecer o fluido, os equipamentos são capazes de promover tais trabalhos nas condições estabelecidas.

Posteriormente, para o cálculo do comprimento necessário da serpentina (tubo) para resfriar ou aquecer o fluido nas condições desejadas, deve-se determinar o coeficiente global de transferência de calor (U). Para isso são necessárias algumas informações, como as características do tubo e do escoamento do fluído. A Tabela 7 apresenta tais informações.

Tabela 7 – Propriedades para o cálculo do coeficiente global de transferência de calor (U).

Propriedade	Valor
Diâmetro Interno - d_i (m)	0,0068
Diâmetro Externo - d_e (m)	0,0103
Área Transversal - a_t	$3{,}74 \times 10^{-5}$
Superfície por metro - S_{ext} (m²/m)	0,0323

Vazão mássica - $\dot{m}$ (kg/s)	$3{,}1 \times 10^{-4}$
Coeficiente de transferência de calor para a água - h_∞ (J/h m ²K)[1]	$3{,}06 \times 10^{6}$

[1]Descosiderou-se o etilenoglicol no inserido no sistema de refrigeração;

Determinou-se o fluxo mássico (*G*) e o número de Reynolds (*Re*) através das Equações (18) e (19), respectivamente.

$$G = \frac{\dot{m}}{a_t} \tag{18}$$

$$Re = \frac{d_i G}{\mu} \tag{19}$$

onde:

$\dot{m}$ – Vazão mássica (kg/s);

a_t – Área transversal do tubo (m²);

d_i – Diâmetro interno do tubo (m);

μ – Viscosidade na temperatura média T_{m,CO_2} (Pa.s);

Após a determinação do número de Reynolds, deve-se avaliar se esse número é menor ou maior que 2100, para determinar o coeficiente de transferência de calor interno (h_i) pela seguinte equação ($Re > 2100$):

$$\frac{h_i}{\phi} = 1{,}86 \frac{k}{d_i} \left(\frac{d_i c_p G d_i \mu}{\mu k L} \right)^{1/3} \tag{20}$$

onde:

$$\phi = \left(\frac{\mu}{\mu_p} \right)^{0{,}14} \tag{21}$$

k - Condutividade Térmica do fluido (J/h m K);

c_p - Calor Específico (J/kg K);

L – Comprimento do tubo (m);

ϕ – Razão de viscosidade (ad.);

μ_p – Viscosidade na temperatura da parede T_p (K);

A temperatura na parede (T_p) interna do tubo foi determinada conforme a Equação (22).

$$T_p = T_\infty + \frac{{h_i}/{\phi}}{{h_i}/{\phi} + h_\infty}\left(T_{m,CO_2} - T_\infty\right) \tag{22}$$

onde:

T_∞ - Temperatura do fluído externo (K);

h_∞ – Coeficiente de transferência de calor para o fluído externo, água (J/h m² K);

Com o valor da temperatura da parede do tubo foi possível obter a viscosidade do fluido na parede. Assim, através das Equações 20 e 21 foi calculado o valor do coeficiente de transferência de calor interno. Em seguida foi calculado o coeficiente de transferência de calor referente ao diâmetro externo do tubo (h_{io}).

$$h_{io} = h_i \frac{d_i}{d_e} \tag{23}$$

onde:

d_i – Diâmetro interno do tubo (m);

d_e – Diâmetro externo do tubo (m);

Uma vez obtidos os valores dos coeficientes de transferência de calor, e considerando que não há incrustações na tubulação, foi possível calcular o coeficiente global de transferência de calor para o sistema.

$$U = \frac{h_i h_\infty}{h_{io} + h_\infty} \tag{24}$$

A partir do *U*, do calor necessário para atingir a temperatura de trabalho (*Q*) e da média logarítmica das temperaturas (ΔT_{ml}) foi possível determinar área necessária de troca térmica (A_{sup}).

$$Q = U A_{sup} \Delta T_{ml} \tag{25}$$

Com o valor da área de troca térmica e a superfície por metro linear de tubo S_{ext} (m²/m) foi possível determinar o comprimento total do tubo para a troca de calor (Q).

$$L = \frac{A_{sup}}{S_{ext}} \tag{26}$$

Observa-se que, durante os cálculos do comprimento do tubo (L), foi feita (Equação 20) uma estimativa inicial desse parâmetro. Ao termino dos cálculos, novamente, foi determinado outro valor de L, que sendo igual ao primeiro valor estipulado, validaria a estimativa inicial. Caso contrário, se o valor calculado de L fosse maior ou menor que a estimativa inicial, os cálculos deveriam ser novamente efetuados usando o novo valor determinado de L. Desta maneira, por se tratar de um método iterativo, foi proposto um algoritmo para o cálculo do comprimento da tubulação de resfriamento e aquecimento.

A fim de facilitar os cálculos e o método a equação de Sutherland foi utilizada para o cálculo da viscosidade do fluido na temperatura da parede. A Tabela 8 apresenta algumas constantes para a equação de Sutherland.

$$\mu = \mu_0 \left(\frac{a}{b}\right)\left(\frac{T}{T_0}\right)^{3/2} \tag{27}$$

Onde:

μ_0 – Viscosidade de referência (cP);

T_0 – Temperatura de referência (°R);

T – Temperatura do fluido na parede (°R);

$a = 0{,}555T_0 + C$;

$b = 0{,}555T + C$;

C – Constante de acordo com o fluido;

Tabela 8 – Constante de alguns fluidos para a equação de Sutherland.

Fluído	C	T_0 (ºR)	μ_0 (cP)
Oxigênio (O_2)	72	528,93	0,00876
Nitrogênio (N_2)	111	540,99	0,01781
Dióxido de Carbono (CO_2)	240	527,67	0,01480

Algoritmo – Cálculo da Temperatura de Refrigeração e Aquecimento

```
%--------------------------------------------------------------------------
% Determinação da carga térmica dos sistemas de refrigeração e aquecimento
% para unidade de reação química
% Dimensionamento do comprimento da Serpentina;
% Para tubo 1/8'' ASTM A269 TP 316
%--------------------------------------------------------------------------
%1. Definindo as variáveis de entrada
%--------------------------------------------------------------------------
clear all
clc
format short;
Tinf1=input('Temperatura de refrigeração/aquecimento em °C = ');
Tinf=Tinf1+273.15;
Te1=input('Temperatura de entrada do CO2 em °C = ');
Te=Te1+273.15;
Ts1=input('Temperatura de saída do C02 em °C = ');
Ts=Ts1+273.15;
m1=input('Vazão mássica de CO2 em kg/s - Máxima = ');
m=m1*(60*60);
%--------------------------------------------------------------------------
%2. Definindo a temperatura média Tm
%--------------------------------------------------------------------------
Tm=(Te+Ts)/2;
disp('Temperatura média em °C = ');disp(Tm-273.15);
%--------------------------------------------------------------------------
disp('Inserir Cp, u, k e a densidade do CO2 na Tm ')
Cp=input('Calor específico do CO2 (P;Tm) J/kg.K = ');
u=input('Viscosidade do CO2 (P;Tm) cP = ');
k=input('Condutividade térmica do CO2 (P;Tm) J/m.h.K = ');
ds=input('Densidade do CO2 (P;Tm) kg/m³ = ');
%--------------------------------------------------------------------------
di=0.00683;                       %('Diâmetro interno do tubo em m = ');
de=0.01029;                       %('Diâmetro externo do tubo em m = ');
%Coeficiente global de transferência de calor para a água J/h.m².K
hinf=3.0663*10.^6;
%--------------------------------------------------------------------------
%3. Calculo da quantidade de calor para atingir a temperatura Ts
%--------------------------------------------------------------------------
qconv=m*Cp*(Te-Ts);
%--------------------------------------------------------------------------
%4. Calculo da média logarítmica das diferenças de temperatura Tml
%--------------------------------------------------------------------------
Tml=((Tinf-Te)-(Tinf-Ts))/(log((Tinf-Ts)/(Tinf-Te)));
%--------------------------------------------------------------------------
%5. Calculo do coeficiente global de transferência de calor U
%   Para Re menor que 2100;
%--------------------------------------------------------------------------
L=input('Chute inicial para o comprimento da serpentina em m = ');
n=input('Número de Iterações = ');
Tol=0.01;                                   %Tolerância em m
a=0.000037419; %área da seção transversal de escoamento no interior do tubo
G=m/a;                                      %kg/m².s
Re=((di*G)/(u*10^-3*60*60));                % Conversão de cP
disp('Re = ');disp(Re);
for k=1:n;
A=1.86*(k/di)*(((di*G)*(Cp/k)*(di/L))^(1/3));
Tp=Tinf+(A/(A+hinf))*(Tm-Tinf);
%--------------------------------------------------------------------------
% Sutherland's formula
%--------------------------------------------------------------------------
To=527.67;              % Temperatura de referência para o CO2 em R
C=240;                  % Constante para o CO2
uo=0.01480;             % Viscosidade na Temperatura de referência To em CP
Tpr=Tp*(9/5);           % Conversão para Rankine
a=0.555*(To)+C;
b=0.555*Tpr+C;
up=uo*(a/b)*((Tpr/To)^(3/2));   %Equação de Sutherland
%--------------------------------------------------------------------------
fi=(u/up)^0.14;
hi=fi*A;
hie=hi*(di/de);
U=(hie*hinf)/(hie+hinf);
%--------------------------------------------------------------------------
%6. Cálculo da área de troca térmica
```

```
%-------------------------------------------------------------------------
Area=qconv/(U*Tml);
Sext= 0.032309; %input('Superfície por metro linear de tubo em m²/m = ');
Lf=Area/Sext;
D=abs(Lf-L);
    if D>=Tol;
        L=Lf;
    elseif D<=Tol;
      break
    end
end
%-------------------------------------------------------------------------
%7. Saídas
%-------------------------------------------------------------------------
disp('Comprimento(m)= ');disp(Lf);
disp('Número de Iterações'); disp(k);
%-------------------------------------------------------------------------
```

Através dos equacionamentos propostos e o algoritmo desenvolvido foi possível estimar o comprimento das serpentinas de aquecimento e refrigeração para as condições extremas de processo, maior temperatura de aquecimento e maior vazão de CO_2. Os comprimentos calculados para a serpentina de resfriamento e de aquecimento foram de 2,2 e 2,5 m, respectivamente. Como a tubulação é fornecida em barras de 6 m pelas empresas fornecedoras, cada serpentina foi confeccionada com uma barra, ou seja, o comprimento real aproximadamente 2,5 vezes maior que o necessário, garantindo assim que as condições do processo desejadas fossem atingidas.

I. IV Reator em Batelada

O dimensionamento do reator teve como base dados encontrados em trabalhos científicos específicos de reações químicas utilizando CO_2 supercrítico como solvente. Além disso, levou-se em consideração a quantidade de produto obtido em uma operação do reator. Assim, o sistema foi projetado com um volume útil de 100 mL e diâmetro interno de 40 mm, para garantir a inserção do agitador magnético. O reator ainda conta com um sistema de aquecimento tipo camisa, ou seja, o fluido de aquecimento escoa na seção externa do reator, entrando pela parte inferior e saindo pela parte superior. Por sua vez, a vedação do reator ocorre devido à expansão da gaveta de poliuretano (G) anexada à tampa sem rosca. Três furos foram confeccionados na tampa, correspondendo à entrada e à saída do CO_2, um termopar e um manômetro, para a medida da temperatura e da pressão do reator, respectivamente. A Figura 19 mostra a vista frontal do reator em batelada, que opera em pressão e temperatura de, no máximo, 35 MPa e 80 °C, respectivamente.

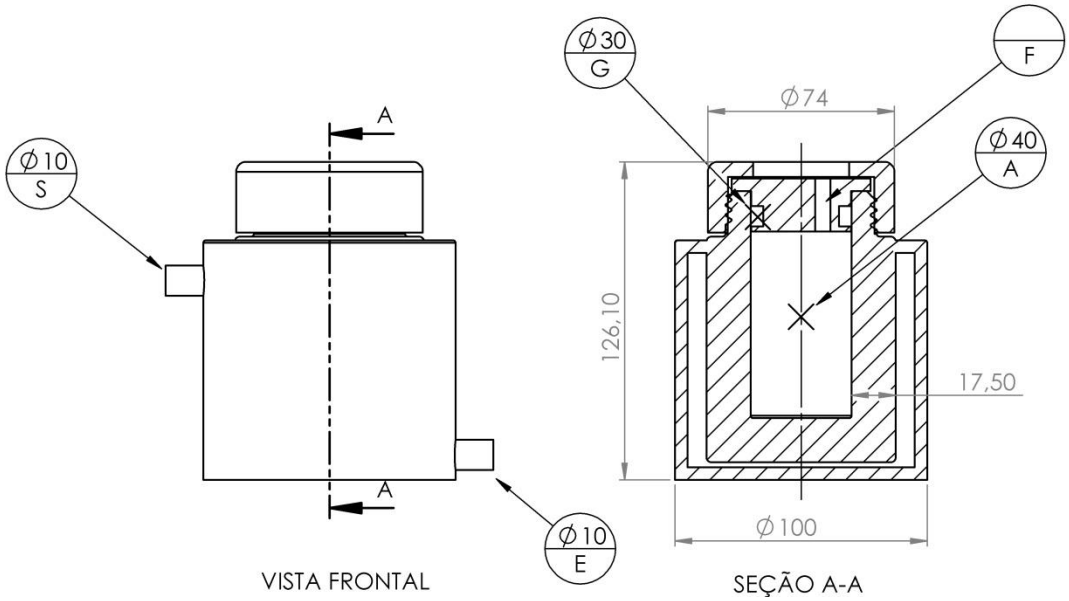

Figura 19 - Vista frontal e corte AA da célula de reação química em modo batelada. A – Volume interno útil de 100 mL; G – Gaxeta de vedação de poliuretano; F – 3 Furos passantes de rosca NPT 1/8’’OD; E e S – Entrada (E) e saída (S) de água na camisa de aquecimento, espigão.

I. V Reator Contínuo

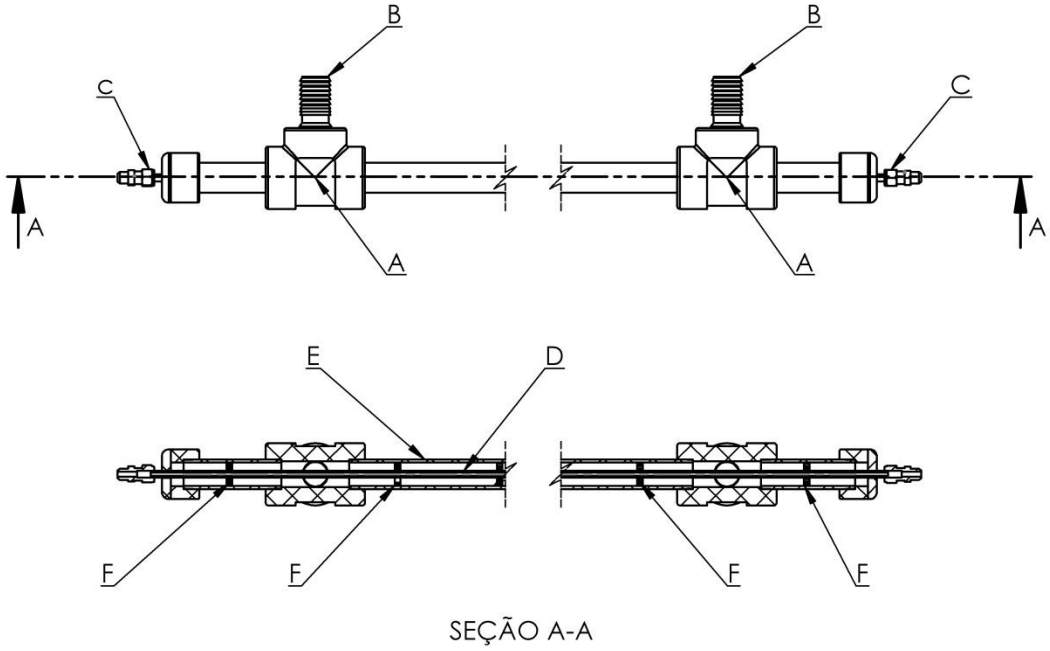

Figura 20 – Vista ortogonal e a seção AA do reator em modo contínuo. A – Conexão em T ¾'' OD PVC; B – Conexão espigão ¾'' OD para ¾''OD em PVC para entrada e saída de água de aquecimento; C- Conexão ¼'' OD tipo flange-luva (Detroit); D – Tubulação aço inox ASTM 316 sem costura ¼'' OD; E – Tubulação ¾'' OD em PVC; F- Chicanas;

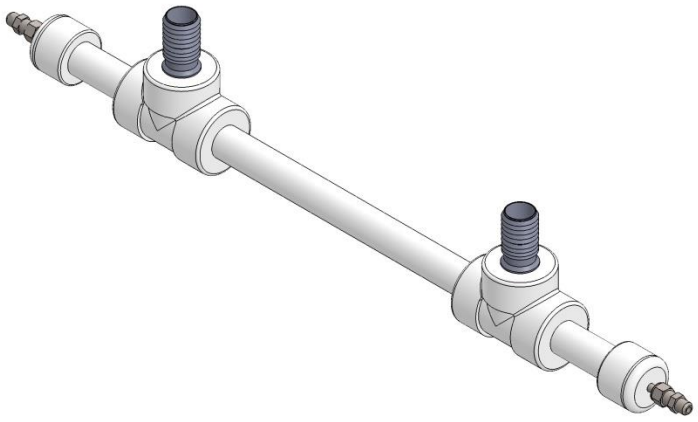

Figura 21 – Vista isométrica do reator tubular em modo contínuo.

I. VI Separador

O separador a alta pressão foi projetado com base nos diagramas de equilíbrio de fases dos compostos utilizados nas reações químicas, encontrados na literatura, levando em consideração as condições de pressão e temperatura. Tais condições foram estipuladas em valores máximos, 20 MPa e 70 °C, respectivamente. O sistema consiste basicamente em um cilindro de 40 mm de diâmetro com a parte inferior cônica e ao final uma saída para a retirada dos produtos e substratos das reações (F). Além disso, o sistema de fechamento, vedação, aquecimento, entrada e saída de CO_2 e a posição do termopar e do manômetro são idênticos aos da célula em batelada.

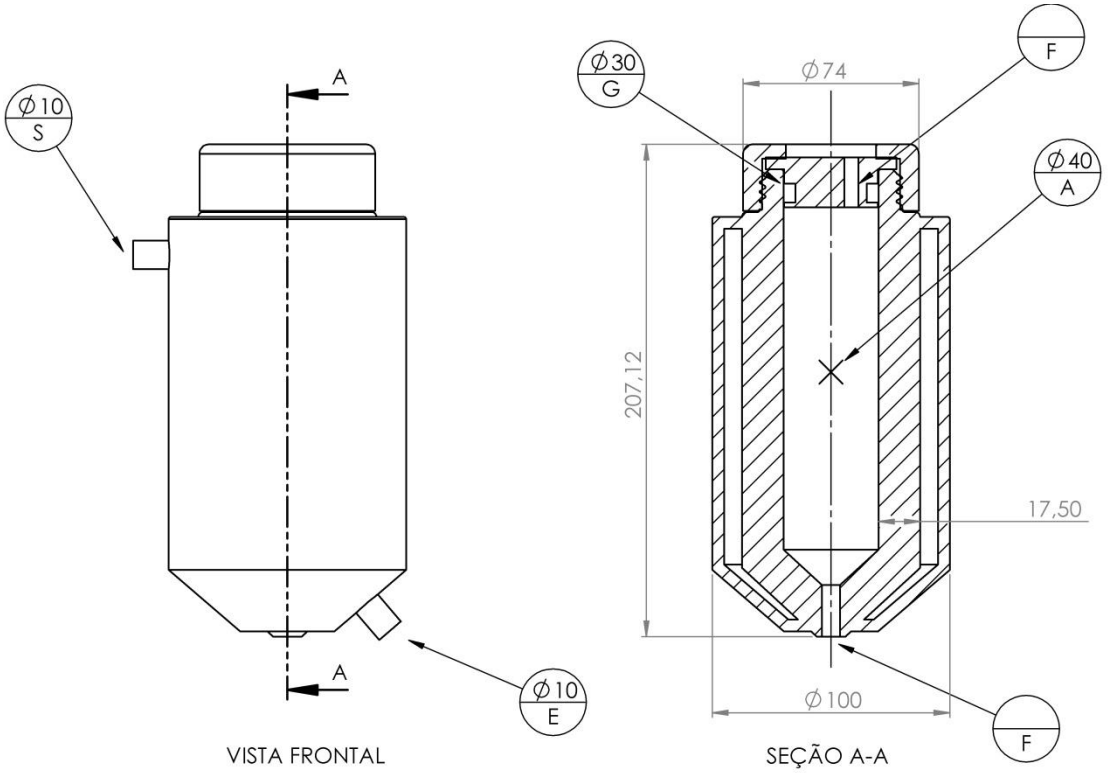

Figura 22 - Vista frontal e corte AA do separador da unidade de reação química. A – Volume interno útil de 250 mL; G – Gaxeta de vedação de poliuretano; F – 4 Furos passantes de rosca NPT 1/8’’ OD; E e S – Entrada (E) e saída (S) de água na camisa de aquecimento, espigão.

II Manual de Operação da Unidade de Reações Químicas

II. I Operação em Modo Batelada

O procedimento operacional padrão do equipamento de reações químicas utilizando CO_2 supercrítico em modo batelada (reator em batelada) é descrito conforme as etapas a seguir:

1) Ligar o banho de refrigeração (-5 °C);
2) Ligar o banho de aquecimento e ajustar a temperatura desejada;
3) Ligar o aquecimento da válvula micrométrica;
4) Ligar o indicador de temperatura;
5) Ligar os manômetros;
6) Manômetro 1: Indica a pressão do reservatório de CO_2;
7) Manômetro 2: Indica a pressão após a bomba pneumática;
8) Manômetro 3: Indica a pressão do reator;
9) Verificar se o compressor de ar está ligado;
10) Inserção das amostras, meio reacional ou catalisadores;
11) Inserir graxa de silicone na vedação do reator (gaxeta azul), em pequenas quantidades;
12) Inserir a tampa do reator;
13) Alinhar as três conexões da tampa;
14) Fechar o reator (sentido horário);
15) Conectar primeiramente o termopar (sentido horário), rosquear com a mão e depois com a chave de boca de ½'. Utilizar uma chave de fenda no sentido oposto para a tampa não rodar.
16) Conectar as demais conexões da mesma maneira que a anterior.
17) Fechar as conexões de entrada e saída ligam-se a linha principal. A primeira conexão utilizar a chave de rosca 3/8' no sentido anti-horário. A segunda conexão utilizar a chave de rosca de 1/2' movimento horário e a chave de rosca de 7/16';
18) Conferir se as válvulas de entrada e saída estão fechadas;
19) Ligar o agitador;
20) Verificar a abertura da válvula micrométrica (pouco aberta) - movimento anti-horário para abrir; Essa válvula nunca deve ser totalmente fechada;

21) Abrir o cilindro de CO_2 (abre no sentido anti-horário e fecha no sentido horário);
22) Abrir a válvula de alimentação;
23) Abrir a válvula de entrada de CO_2 no reator em batelada.
24) Aguardar o equilíbrio entre a pressão do cilindro e do reator;
25) Verificar se tem vazamento nas conexões;
26) Abrir o fluxo de ar comprimido;
27) Abrir a válvula de ar comprimento, válvula de regulagem do *booster* (abre no sentido horário e fecha no sentido anti-horário);
28) Regular a pressão desejada;
29) Fechar a válvula de entrada de CO_2 quando atingir a pressão desejada;
30) Fechar a válvula de ar comprimento;
31) Marcar o tempo desejado;
32) Conectar o frasco de coleta a saída da válvula micrométrica;
33) Após o termino do processo, abrir a válvula de saída de CO_2 do reator;
34) Desligar o agitador;
35) Abrir a válvula de saída, anterior a válvula micrométrica;
36) Regular a válvula micrométrica de acordo a vazão desejada;
37) Aguardar a despressurização do reator;
38) Após a despressurização fechar as válvulas abertas;
39) Efetuar a abertura do reator;
40) Desligar o equipamento;
41) Fechar o cilindro de CO_2;
42) Fechar a o fluxo de ar comprimido;
43) Efetuar a despressurização total do sistema;
44) Desligar os equipamentos e acessórios;
45) Retirar todos os equipamentos dos interruptores;

II. II Operação em Modo Contínuo

O procedimento operacional padrão do equipamento de reação química utilizando CO_2 supercrítico em modo contínuo é descrita conforme as etapas abaixo:

1) Ligar o banho de refrigeração (-5 °C);
2) Ligar o banho de aquecimento do reator e ajustar a temperatura desejada;
3) Ligar o banho de aquecimento do separador e ajustar a temperatura desejada
4) Ligar o aquecimento da válvula micrométrica;
5) Ligar o indicador de temperatura;
6) Ligar os manômetros;
7) Manômetro 1: Indica a pressão do reservatório de CO_2;
8) Manômetro 2: Indica a pressão após a bomba pneumática;
9) Manômetro 4: Indica a pressão do reator;
10) Manômetro 5: Indica a pressão do separador;
11) Ligar as bombas de HPLC e ajustar as vazões desejadas;
12) Verificar se o compressor de ar está ligado;
13) Carregar o reator com a enzima;
14) Estabilizar o sistema somente com CO_2 na pressão do cilindro;
15) Começar a estabilização em uma pressão menor que a de trabalho;
16) Aumentar a pressão do sistema reator aos poucos como o ajuste da válvula *back-pressure* V1 e a válvula de ar comprimento do *booster*;
17) Controlar a pressão do sistema separador através da válvula *back-pressure* V1 e a válvula micrométrica;
18) Ajustar a vazão de CO_2, temperaturas e pressões desejadas;
19) Monitorar a frequência de ciclos da bomba de CO_2 (*booster*), sendo que quanto maior for à frequência maior será a vazão de solvente;
20) Aguardar o tempo de estabilização;
21) Bombear os reagentes para dentro do sistema;
22) Coletar as amostras do separador em tempos pré-determinados através da válvula de saída do separador;
23) Após o termino do tempo de processo parar o bombeamento de substratos;
24) Bombear CO_2 puro para remover os substratos remanescentes na linha;

25) Fechar a válvula de ar comprimento;
26) Fechar a válvula de entrada de CO_2;
27) Aguardar a despressurização do reator e do separador;
28) Após a despressurização fechar as válvulas abertas;
29) Efetuar a abertura do reator;
30) Desligar o equipamento;
31) Fechar o cilindro de CO_2;
32) Fechar a o fluxo de ar comprimido;
33) Efetuar a despressurização total do sistema;
34) Desligar os equipamentos e acessórios;
35) Retirar todos os equipamentos dos interruptores;

III Normalização e Análise dos Dados de FT-IR

Os dados obtidos pela técnica de espectroscopia de infravermelho por transformada de Fourier (FT-IR) foram processados, normalizados e analisados através dos algoritmos apresentados nessa secção.

Algoritmo – Normalização e Análise dos Dados de FT-IR

```
%--------------------------------------------------------------------------
% Abrindo conteudo de um arquivo .spc (FT-IR) no MATLAB
%--------------------------------------------------------------------------
clear all;
clc;
out=tgspcread('n1.spc');
out1=tgspcread('n2.spc');
out2=tgspcread('l1.spc');
out3=tgspcread('l2.spc');
out4=tgspcread('e1.spc');
out5=tgspcread('e2.spc');
x=[out.Y,out1.Y,out2.Y,out3.Y,out4.Y,out5.Y]';
[N,Co]=size(x);
num1=out.X';
% ------------------------------------------------------------------------
% Pre-Processamento e Normalização dos Dados
% ------------------------------------------------------------------------
% Normalização
soma=sum(x');    %soma no comprimento de onda
quad=soma.^2;
B=((quad).^(1/2))';
for i=1:6
    xnor(i,:)=x(i,:)/B(i,:);   %vetor linha / direita
end
%--------------------------------------------------------------------------
soma1=sum(x);       %soma no comprimento de onda
aim=(1/N)*(soma1);
j=length(aim);
for i=1:j
  quad1(:,i)=((x(:,i)-aim(:,i)).^2).^(1/2);
end
soma2=sum(quad1);
for i=1:j
    xnor1(:,i)=x(:,i)/soma2(:,i);
end
%--------------------------------------------------------------------------
%Centrando na média
xm=mean(x);
for i=1:6
    xmc(i,:)=x(i,:)-xm;
end
x1=[out.X,xmc(1,:)',xmc(2,:)',xmc(3,:)',xmc(4,:)',xmc(5,:)',xmc(6,:)'];
x2=x1(x1<2000&x1>1500,:)';
xmca=x2(2:4,:);
num=x2(1,:);
%2° derivada
dx2=deriv(xmc,2,17,2);
%MSC (correção de espalhamento multiplicativo)
xmsc=msc(xnor,1,1932);
%--------------------------------------------------------------------------
%Plotando os resultados
%--------------------------------------------------------------------------
lmi=1200;
lma=1800;
subplot(2,2,1);
plot(out.X,out.Y(:,1),'-b',out1.X,out1.Y(:,1),'-b',out2.X,out2.Y(:,1),'-g'...
    ,out3.X,out3.Y(:,1),'-g',out4.X,out4.Y(:,1),'-r',out5.X,out5.Y(:,1),'-r');
    grid off;
    title('Não-Normalizado')
```

```
    axis([lmi,lma,0,100]);
    set(gca,'XDir','reverse');
    ylabel('Transmitance (%)');
    xlabel('Wavenumbers (cm-1)');
subplot(2,2,2);
plot(num1,dx2(1,:),'-b',num1,dx2(2,:),'-b',num1,dx2(3,:),'-g'...
    ,num1,dx2(4,:),'-g',num1,dx2(5,:),'-r',num1,dx2(6,:),'-r');
    grid off;
    title('Derivative computation by using the Savitsky-Golay');
    axis([lmi,lma,-0.6,0.6]);
    set(gca,'XDir','reverse');
    xlabel('Wavenumbers (cm-1)');
subplot(2,2,3);
plot(out.X,xnor(1,:),'-b',out1.X,xnor(2,:),'-b',out2.X,xnor(3,:),'-g'...
    ,out3.X,xnor(4,:),'-g',out4.X,xnor(5,:),'-r',out5.X,xnor(6,:),'-r');
    grid off;
    legend('N1','N2','L1','L2','E1','E2',4);
    legend('boxon');
    title('Normalizado')
    axis([lmi,lma,0.1e-4,7e-4]);
    set(gca,'XDir','reverse');
    xlabel('Wavenumbers (cm-1)');
subplot(2,2,4);
plot(out.X,xmsc(1,:),'-b',out1.X,xmsc(2,:),'-b',out2.X,xmsc(3,:),'-g'...
    ,out3.X,xmsc(4,:),'-g',out4.X,xmsc(5,:),'-r',out5.X,xmsc(6,:),'-r');
    grid off;
    legend('boxon');
    title('Correção de espalhamento multiplicativo-MSC')
    axis([lmi,lma,0.1e-4,7e-4]);
    set(gca,'XDir','reverse');
    xlabel('Wavenumbers (cm-1)');
%-------------------------------------------------------------------------
%Salvando em .xls(Excel)
%-------------------------------------------------------------------------
A=[out.X,out.Y(:,1),out1.X,out1.Y(:,1),out2.X,out2.Y(:,1),...
    out3.X,out3.Y(:,1),out4.X,out4.Y(:,1),out5.X,out5.Y(:,1)];
C=[out.X,xnor(1,:)',out1.X,xnor(2,:)',out2.X,xnor(3,:)',...
    out3.X,xnor(4,:)',out4.X,xnor(5,:)',out5.X,xnor(6,:)'];
xlswrite('date_FTIR.xls',A);
xlswrite('date_FTIR_norm.xls',C);
```

function [dx] = deriv(x,der,window,order) (BRUSSEL, 2015)

```
%#
%#  function [dx] = deriv(x,der,window,order)
%#
%#  AIM:    Derivative computation by using the Savitsky-Golay
%#      algorithm.
%#
%#  PRINCIPLE:  Differentiation by convolution method.
%#
%#  INPUT:  x   - Data Matrix: (nxm) n spectra m variables
%#      der - (1x1) degree of the derivative;
%#            it must be <= order
%#      window  - (optional), (1x1) the number of points
%#            in filter, it must be >3 and odd
%#      order   - (optional), (1x1) the order of the polynomial
%#            It must be <=5 and <= (window-1)
%#
%#  OUTPUT: dx  - Matrix of differentiated function (nxm)
%#  SUBROUTINE:
%#      weight.m
%#      genfact.m
%#      grampoly.m
%#
%#  AUTHOR:     Luisa Pasti
%#          Copyright(c) 1997 for ChemoAc
%#              FABI, Vrije Universiteit Brussel
%#              Laarbeeklaan 103 1090 Jette
%#      Modified program of
%#      Sijmen de Jong
%#      Unilever Research Laboratorium Vlaardingen
%#
%# VERSION: 1.1 (28/02/1998)
%#
%#  TEST:       Kris De Braekeleer
%#
 function dx = deriv(x,der,window,order)
[nr,nc]=size(x);
if (nargin<4)
  order = 2;
  disp('  Polynomial order set to 2')
end
if (nargin<3)
  window=min(17,floor(nc/2));
  disp(['  Windows size set to ',num2str(window)]);
end
if (nargin<2)
  disp(' function dx = deriv(x,der)')
end

m = fix(window/2);
p = round(window/2);
o=order;

for i=1:window
    i0=i-p;
    for j=1:window,
       j0=j-p;
       w(i,j)=weight(i0,j0,m,o,der);
    end
end
yr(:,1:m)=x(:,[1:window])*w(:,1:m);     % First window
for i=1:(nc-2*m)                 % Middle
    yr(:,i+m)=x(:,[i:(i+2*m)])*w(:,p);
end
a=nc-2*m;                    % Last window
yr(:,(nc-m+1):nc)=x(:,a:nc)*w(:,p+1:window);
dx=yr;


end
```

function [xmsc,me,xtmsc]=msc(x,first,last,xt) (BRUSSEL, 2015)

```
%#
%#  function [xmsc,me,xtmsc]=msc(x,first,last,xt)
%#
%#  AIM:    Multiple Scatter Correction:
%#      To remove the effect of physical light scatter
%#      from the spectrum. (Compensation for particle size
%#      effects.)
%#
%#  PRINCIPLE:  Each spectrum is shifted and rotated so that it fits
%#              as closely as possible to the mean spectrum of the data.
%#      The fit is achieved by LS (first-degree polynomial).
%#      The correction depends on the mean spectrum of the
%#      training set.
%#
%#  INPUT:  x: (m x n) matrix with m spectra and n variables
%#      first: first variable used for correction
%#      last: last variable used for correction
%#       (A segment is selected which is representative for the
%#       baseline of the spectra.)
%#      xt: (mt x nt) matrix for new data (optional)
%#
%#  OUTPUT: xmsc: (m x n) matrix containing the spectra after
%#                correction with msc
%#      me: mean spectrum (1 x n) of x
%#      xtmsc: (mt x nt) matrix containing the new spectra after
%#            correction with msc
%#
%#  AUTHOR:     Andrea Candolfi
%#          Copyright(c) 1997 for ChemoAC
%#              FABI, Vrije Universiteit Brussel
%#              Laarbeeklaan 103 1090 Jette
%#
%# VERSION: 1.1 (28/02/1998)
%#
%#  TEST:       Roy de Maesschalck, Menghui Zhang (2002)
%#

function [xmsc,me,xtmsc]=msc(x,first,last,xt);

if nargin==1;
   first=input('The first variable for the correction: ');
   last=input('The last variables for the correction: ');
end

[m,n]=size(x);
me=mean(x);

for i=1:m,                          % for the x data
  p=polyfit(me(first:last),x(i,first:last),1);          % least square fit between mean
spectrum and each spectrum (first-degree polynomial)
  xmsc(i,:)=(x(i,:)-p(2)*ones(1,n))./(p(1)*ones(1,n));      % each spectrum is corrected
end

if nargin ==4;                          % correction of new data by using the mean
spectrum from x.
[mt,nt]=size(xt);
  for i=1:mt,
    p=polyfit(me(first:last),xt(i,first:last),1);       % least square fit between mean
spectrum and each new spectrum (first-degree polynomial)
    xtmsc(i,:)=(xt(i,:)-p(2)*ones(1,n))./(p(1)*ones(1,n));  % each new spectrum is
corrected
  end
end

end
```

IV Ajuste não-linear do modelo de Ping-Pong Bi-Bi I

Os dados obtidos para taxa de reação de eugenol foram ajustados ao modelo de Ping-Pong Bi-Bi através do algoritmo apresentado a seguir.

Algoritmo – Ajuste não-linear do modelo de Ping-Pong Bi-Bi

```
%%=========================================================================
% Ajuste não-linear do modelo de Ping-Pong Bi-Bi
% Universidade Estadual de Campinas - UNICAMP
% Departamento de Engenharia de Alimentos
% Laboratório de Alta Pressão em Engenharia de Alimentos - LAPEA
% Autor: Philipe dos Santos
% Email: philipe.dsn@gmail.com
%=========================================================================
clear all;clc;clf
format long
global R CS fun             % variaveis globais
data=xlsread('data');       % planilha de dados
R=(data(:,1)');             % taxa de reação para A e B mol/l.g
CS=(data(:,2:3)');          % concenração de substratos [A] e [B] em mmol/l
fun=@ping;                  % define a função a ser ajustada
int=1000000;                 % número de iterações
n=length(R);
%-------------------------------------------------------------------------
%Estimativa inicial dos parametros,
%-------------------------------------------------------------------------
%B0=[Vmax,Kma,Kmb];
B0=[0.0045,0.016,0.1475];
%-------------------------------------------------------------------------
L=[0;-Inf];
U=[];
options = optimset('Diagnostics','on','MaxFunEvals',100000,...
         'MaxIter',int,'TolFun',1e-20,'TolX',1e-20,'Display','iter');
[xsol, fsol]=fmincon(@fobj,B0,[],[],[],[],L,U,'confun',options);
Rcal=fun(CS,xsol);
%-------------------------------------------------------------------------
%Saida - Plotagem
figure(1)
plot(CS(1,:),R,'b*',CS(1,:),Rcal,'bo');
%-------------------------------------------------------------------------
disp('vmax = '); disp(xsol(1));disp('mmol/g.s');
disp('Kmb = ');disp(xsol(3));disp('mmol/l');
disp('Kma = ');disp(xsol(2));disp('mmol/l');
disp('SS = ');disp(fsol);
xlswrite('preditos.xls',[Rcal']);
[y]=fun(CS,xsol);
y1=y;
for i=1:n
arrd=((sum((abs(CS(i)-y(i))/CS(i))))*100/n);
end
disp(arrd);
%=========================================================================
```

function R=ping(y,B)

```
%=========================================================================
% Modelo de Ping-Pong Bi-Bi
% Lipase-catalyzed production of a bioactive terpene ester in supercritical
% carbon dioxide
% Inibição do substrato A
% B(1) = vmax  (mmol/g.min)
% B(3) = KmB   (mmol/l)
% B(2) = KmA   (mmol/l)
% y(1) = concentraçao de substrato [A](mmol)  - Anidrido Acético
% y(2) = concentraçao de substrato [B](mmol)  - Eugenol
%=========================================================================
function R=ping(y,B)
n=length(y);
for i=1:n
R(1,i)=[((B(1)*y(1,i)*y(2,i))/((B(2)*y(2,i)+B(3)*y(1,i)+y(1,i)*y(2,i))))];
end
end
```

function f=fobj(B)

```
%=========================================================================
% Função Objetivo((sum((abs(CS(i)-y(i))/CS(i))))*100/n)
% Soma dos Quadrados sum((R(l,i)-y1(1,i))^2))
%=========================================================================
function f=fobj(B)
global R CS fun
n=length(R);
l=1;
%-------------------------------------------------------------------------
% Solucionando para a estimativa inicial
%-------------------------------------------------------------------------
[y]=fun(CS,B);
y1=y;
f=0;
    for i=1:n
        f=f+sum((R(l,i)-y1(1,i))^2);
    end
end
```

function [c, ceq] = confun(B)

```
function [c, ceq] = confun(B)
% Nonlinear inequality constraints
c = [];
% Nonlinear equality constraints
ceq = [];
end
```

V Ajuste não-linear do modelo de Ping-Pong Bi-Bi II

Os dados obtidos para as concentrações de produtos e reagentes nas reações de acetato de isoamila foram ajustados ao modelo de Ping-Pong Bi-Bi juntamente com a equação diferencial para um reator batelada ideal, através do algoritmo apresentado a seguir.

Algoritmo – Ajuste não-linear do modelo de Ping-Pong Bi-Bi

```
%=========================================================================
% Ajuste não-liner do modelo Ping-Pong Bi-Bi a equação diferencial de um
% reator em modo batelada - Obtenção de paramêtros cinéticos;
% Universidade Estadual de Campinas - UNICAMP
% Departamento de Engenharia de Alimentos
% Laboratório de Alta Pressão em Engenharia de Alimentos - LAPEA
% Autor: Philipe dos Santos
% Email: philipe.dsn@gmail.com
%
% int     = número de iterações [tamanho da matriz da estimativa inicial]
% p       = número de parametros número de parametros do modelo
% lw      = limite inferior dos valores da estimativa inicial
% up      = limite superior dos valores da estimativa inicial
% @ chute = função para o calculo da estimativa inicial
% BOupper = limite superior dos paramêtros no ajuste de BOBYQA
% B0lowe  = limite inferior dos paramêtros no ajuste de BOBYQA
%
% data    = planilha de dados
% time    = tempo em minutos
% x0      = condição inicial (t=0) em mol/l
% CS      = concenração de substratos mol/l
% enz     = massa de enzima em gramas por volume do reator
% fun     = define a função a ser ajustada
%=========================================================================
clear all;clc;clf
format long
close
global time CS enz x0 fun options1 n j
data=xlsread('data');
time=data(:,1)';
x0=data(1,2:5);
CS=(data(:,2:5)');
enz=(1.87);
fun=@ping_4;
%-------------------------------------------------------------------------
%                     OPÇÕES DA RESOLUÇÃO DA DERIVADA
%-------------------------------------------------------------------------
options1 = odeset('RelTol',1e-5,'AbsTol',1e-5,'NormControl','on');
n=length(time);
j=length(x0);
%-------------------------------------------------------------------------
%                    ESTIMATIVA INICIAL/LIMITES/ITERAÇÕES
%-------------------------------------------------------------------------
int=1000;
p=4;
lw=1e-3;
up=1e2;
B0=chute(int,lw,up,p);
%-------------------------------------------------------------------------
%                              BOBYQA-POWELL
%-------------------------------------------------------------------------
for k=1:int
B0upper=up*(1e1).*ones(p,1);
B0lower=(1e-3).*ones(p,1);
svOptions = struct('display', 'none', 'rho_end', 1e-6, 'maxFunEval', 1000);
```

```
[fsol(:,k), xsol(:,k)]=bobyqa(@fobj, B0(k,:), B0lower, B0upper, svOptions);
disp(['Numero de iterações = ',num2str(k),' de ', num2str(int)...
    ,' ----- ',' Fobj = ',num2str(fsol(:,k))]);
end
[min,ind]=min(fsol);
[m,g]=ind2sub(size(fsol),ind);
%--------------------------------------------------------------------------
%   RESOLUÇÃO DA EDO - CALCULO DOS PRODUTOS: BALANÇO DE MASSA/CONVERSÃO
%--------------------------------------------------------------------------
[sol]=ode23s(fun,time,x0,[],xsol(:,g),options1);
y=deval(sol,time);
Conv=((1-((CS(1,:)/x0(1,1))))*100);
Convsol=((1-((y(1,:)/x0(1,1))))*100);
%--------------------------------------------------------------------------
%                   SAÍDA - PLOTAGEM - PLANILHA EXCEL
%--------------------------------------------------------------------------
subplot(1,2,1);
    plot(time,y,'b-',(time),CS,'r*');
    xlabel('Tempo (minutos)');
    ylabel('Concentração (mol/l)');
    title('Simulação Modelo de Ping-Pong Bi-Bi');
subplot(1,2,2);
    plot(time,Conv,'b*',time,Convsol,'b--');
    xlabel('Tempo (minutos)');
    ylabel('Conversão (%)');
    title('Simulação Modelo de Ping-Pong Bi-Bi');
disp('----------RESULTADOS----------');
disp(['vmax = ',num2str(xsol(1,g)),' mol/g.min']);
disp(['Kma = ',num2str(xsol(2,g)),' mol/l']);
disp(['Kmb = ',num2str(xsol(3,g)),' mol/l']);
disp(['Keq = ',num2str(xsol(4,g)),' ad.']);
disp(['SSQ = ',num2str(fsol(:,g))]);
xlswrite('preditos.xls',[time',CS',y']);
xlswrite('preditos_con.xls',[time',Conv',Convsol']);
xlswrite('xsol.xls',[fsol',xsol']);
%==========================================================================
```

function dcdt=ping_4(t,y,B,options1)

```
%=========================================================================
% Modelo de Ping-Pong Bi-Bi
% B(1) = vmax   (mol/g.min)
% B(2) = Kma    (mol/l)
% B(3) = Kmb    (mol/l)
% B(4) = Keq    (mol/l)
% y(1) = concentraçao de substrato [B](mol)  - Alcool Isoamilico
% y(2) = concentraçao de substrato [A](mol)  - Anidrido Acetico
% y(3) = concentraçao de substrato [P](mol)  - Acetato de Isoamila
% y(4) = concentraçao de substrato [Q](mol)  - Acido Acetico
%=========================================================================
function dcdt=ping_4(t,y,B,options1)
global enz
dcdt=zeros(4,1);
dcdt(1)=-enz*((B(1)*((y(1)*y(2))-
((y(3)*y(4))/B(4)))/(B(2)*y(1)+B(3)*y(2)+y(1)*y(2))));
dcdt(2)=-enz*((B(1)*((y(1)*y(2))-
((y(3)*y(4))/B(4)))/(B(2)*y(1)+B(3)*y(2)+y(1)*y(2))));
dcdt(3)=enz*((B(1)*((y(1)*y(2))-
((y(3)*y(4))/B(4)))/(B(2)*y(1)+B(3)*y(2)+y(1)*y(2))));
dcdt(4)=enz*((B(1)*((y(1)*y(2))-
((y(3)*y(4))/B(4)))/(B(2)*y(1)+B(3)*y(2)+y(1)*y(2))));
end
```

function [B0] = chute(int,lw,up,p)

```
%=========================================================================
% Função para calculo da matriz com as estimativas iniciais
% int = Número de iterações [Tamanho da matriz B0]
% lw = Limite inferior para os valores de B0
% up = Limite Superior para os valores de B0
% p = Número de paramêtros do modelo [Tamanho da matriz B0]
%=========================================================================
function [B0] = chute(int,lw,up,p)
% B0=(up-lw).*abs(rand(int,4))+lw;
% B0=randi([lw up],int,4);
B0=(up-lw).*abs(randn(int,p))+lw;
End
```

function [B0] = chute(int,lw,up,p)

```
%=========================================================================
% Função Objetivo
% ARRD
%=========================================================================
function f=fobj(B)
global time CS x0 fun options1 n j
%-------------------------------------------------------------------------
% Solucionando a EDO para a estimativa inicail
%-------------------------------------------------------------------------
[sol]=ode23s(fun,time,x0,[],B,options1);
y1=deval(sol,time);
% Conv=(100-((CS(1,:)/x0(1,1))*100));
% Convsol=(100-((y1(1,:)'/x0(1,1))*100));
f=0;
for l=1:j
   for i=1:n
   f=f+(sum(((CS(l,i)-y1(l,i))^2)));
%f=f+(sum((((abs(CS(l,i)-y1(l,i))/CS(l,i))*(100/n)))));
%f=f+(sum((Conv'-Convsol).^2));
    end
end
end
```

function [nF_opt, vX_opt] = bobyqa(sObjFunName, vX_opt, vX_l, vX_u, svOptions)

```
function [nF_opt, vX_opt] = bobyqa(sObjFunName, vX_opt, vX_l, vX_u, svOptions)
% The BOBYQA algorithm for bound constrained optimization without
% derivatives by M.J.D. Powell
%
%
% ==== License ====
%
% Copyright (c) [2014] [Karlsruhe Institute of Technology
%                       Institute of Engineering Mechanics]
%
% Permission is hereby granted, free of charge, to any person obtaining a
% copy of this software and associated documentation files (the
% "Software"), to deal in the Software without restriction, including
% without limitation the rights to use, copy, modify, merge, publish,
% distribute, sublicense, and/or sell copies of the Software, and to permit
% persons to whom the Software is furnished to do so, subject to the
% following condition:
%
%   * The above copyright notice and this permission notice shall be
%     included in all copies or substantial portions of the Software.
%
% THE SOFTWARE IS PROVIDED "AS IS", WITHOUT WARRANTY OF ANY KIND, EXPRESS
% OR IMPLIED, INCLUDING BUT NOT LIMITED TO THE WARRANTIES OF
% MERCHANTABILITY, FITNESS FOR A PARTICULAR PURPOSE AND NONINFRINGEMENT. IN
% NO EVENT SHALL THE AUTHORS OR COPYRIGHT HOLDERS BE LIABLE FOR ANY CLAIM,
% DAMAGES OR OTHER LIABILITY, WHETHER IN AN ACTION OF CONTRACT, TORT OR
% OTHERWISE, ARISING FROM, OUT OF OR IN CONNECTION WITH THE SOFTWARE OR THE
% USE OR OTHER DEALINGS IN THE SOFTWARE.
%
%
% ==== Preparation ====
%
% This file uses the dlib C++ implementation of BOBYQA.
% To use the algorithm, the mex file has to be compiled for the specific
% archtecture of your computer. Please refer to the official MATLAB help
% for further details.
%
% You need three files to run the algorithm:
%
%   * This file, which executes the mex file, defines default parameters,
%     updates the screen during the iterations and enables the C++
%     algorithm to evaluate MATLAB objective functions.
%   * The file "bobyqa_alg.cpp" which contains the C++ source code defining
%     a gateway between MATLAB and the dlib library containing the
%     algorithm.
%   * The dlib library containing the C++ source files with the BOBYQA
%     algorithm. Successful compilation requires a copy of the (sub)folder
%     "/dlib" in the same directory as the other two files.
%     You can download the dlib library at http://dlib.net
%
% The function will display the necessary commands for compilation in case
% of an error.
%
%
% ==== Execution ====
%
% This file sets defaults for the BOBYQA parameters (if not specified) and
% executes the mex function. The mex function itself calls this file to
% evaluate the MATLAB objective function during the iterations.
%
% Input parameters:
%
%   * sObjFunName   string/function_handle   name of the objective function
%
%   * vX_opt        vector                   initial optimization vector
%
%   * vX_l          vector (optional)        lower bounds for optimization
```

```
%                                                 default: -1e100 (no bound)
%
%   * vX_u          vector (optional)        upper bounds for optimization
%                                                 default:  1e100 (no bound)
%
%   * svOpts        structure                options for display/algorithm
%           .display         display mode:
%                              'none': no output during iterations
%                              'iter': (default) output after every step
%           .npt             number of points for quadratic approximation
%                              default: 2*n + 1
%           .rho_beg         initial trust region radius
%                              default: 10
%           .rho_beg         final trust region radius
%                              default: 1e-6
%           .maxFunEval      maximum number of function evaluations
%                              default: 1000
%
% Output parameters:
%
%   * nF_opt        scalar   value of objective function for final step
%
%   * vX_opt        vector   final optimization vector
%
% If the optional parameters are not specified, the default values are set.
% If only one of the bounds (vX_l or vX_u) is specified, the default is set
% for both bounds!
%
% The file uses a persistent variable to save previous results for display
% purposes. If a critical error occurs during the evaluation and the
% function is not exited properly it could be possible, that the persistent
% variable is not deleted properly. In this case make sure the input
% variable "sObjFunName" is a function handle in the next iteration!
%
%
% ==== Example ====
%
% To test the algorithm you can run the following MATLAB code as example:
%
%     fprintf('\n\n>>> First run:\n\n');
%     fhTestfun = @(vX) norm(vX-[3;5;1;7]);
%     vX_opt = [-4;5;99;3];
%     vX_l = -1e100*ones(4,1);
%     vX_u =  1e100*ones(4,1);
%     svOptions = struct('display', 'iter', 'npt', 9, 'rho_beg', 10, ...
%                        'rho_end', 1e-6, 'maxFunEval', 100);
%     [nF_opt, vX_opt] = bobyqa(fhTestfun, vX_opt, vX_l, vX_u, svOptions)
%     fprintf('\n\n>>> Second run:\n\n');
%     svOptions = struct('display', 'none', 'npt', 9, 'rho_beg', 10, ...
%                        'rho_end', 1e-6, 'maxFunEval', 1000);
%     [nF_opt, vX_opt] = bobyqa(fhTestfun, vX_opt, vX_l, vX_u, svOptions)

narginchk(2, 5);
nargoutchk(0, 2);

% Persistent variable for output during evaluation
persistent svOpts;

try
    if isempty(svOpts) || isa(sObjFunName, 'function_handle') % => first call
to function -> initialization
        %% Call BOBYQA_ALG mex function
        nN = numel(vX_opt);

        % Set default options if necessary
        svOpts = struct('display', 'iter', ...
                        'npt', 2*nN+1, ...
```

```
                        'rho_beg', 10, ...
                        'rho_end', 1e-6, ...
                        'maxFunEval', 1000);
        if nargin == 5
            cOpts = {'display', 'npt', 'rho_beg', 'rho_end', 'maxFunEval';
            for i = 1:numel(cOpts)
                if isfield(svOptions, cOpts{i)
                    svOpts.(cOpts{i) = svOptions.(cOpts{i);
                end
            end
        end

        % Hold display variables
        svOpts.nFunEval = 0;

        if ~exist('vX_l','var') || ~exist('vX_u','var') || isempty(vX_l) ||
isempty(vX_u)
            vX_l = -1e100*ones(nN,1);
            vX_u =  1e100*ones(nN,1);
        end

        if isa(sObjFunName, 'function_handle')
            sObjFunName = func2str(sObjFunName);
        end

        % Call mex function
        try
            [nF_opt, vX_opt] = bobyqa_alg(sObjFunName, vX_opt, nN, svOpts.npt,
vX_l, vX_u, svOpts.rho_beg, svOpts.rho_end, svOpts.maxFunEval);
        catch ME
            fprintf(['\n\n', 'An error occured trying to evaluate the
BOBYQA_ALG mex function.', '\n', ...
                     'If the error perisits try to recompile the mex function
for your system.', '\n', ...
                     'Navigate to', '\n\n' ...
                     '    ', strrep(mfilename('fullpath'), '\', '\\'), '\n\n',
...
                     'and use the command', '\n\n', ...
                     '    mex(strcat(''-I"'',pwd,''"''), ''bobyqa_alg.cpp'')',
'\n\n']);
            rethrow(ME);
        end

    else
        %% Evaluate ojective function if called by BOBYQA_ALG
        if nargout < 2 && nargin == 2
            fhObjFun = str2func(sObjFunName);
            nF_opt = fhObjFun(vX_opt);
            status_display()
            return;
        end
    end
catch ME
    % Clear persistent variable in case of unsuccessful previous run
    clear svOpts;
    rethrow(ME);
end

% Clean up
clear svOpts;

%% Subfunctions
function status_display()
% STATUS_DISPLAY Displays the status in the Matlab command window depending
% on the 'display' option set in the options.
```

```
    switch svOpts.display
        case 'none'
        case 'iter'
            if mod(svOpts.nFunEval, 30) == 0
                fprintf(['\n', 'FunEval        ObjFunVal     Norm of step
Rel norm step', '\n']);
            end
            svOpts.nFunEval = svOpts.nFunEval + 1;
            if isfield(svOpts, 'vX_last')
                sNormStep = sprintf('%12.8e', norm(vX_opt - svOpts.vX_last));
                sRelStep  = sprintf('%12.8e', norm(vX_opt -
svOpts.vX_last)/svOpts.rho_end);
            else
                sNormStep = '            ';
                sRelStep  = '            ';
            end
            fprintf([sprintf('%7.1u', svOpts.nFunEval), '   ', ...
                     sprintf('%12.8e', nF_opt), '   ', ...
                     sNormStep, '   ', ...
                     sRelStep, ...
                     '\n']);
            svOpts.vX_last = vX_opt;
        otherwise
            fprintf('Unknown display setting. Display set to ''none''.');
            svOpts.display = 'none';
    end
end

end
end
```

VI Curvas de Calibração

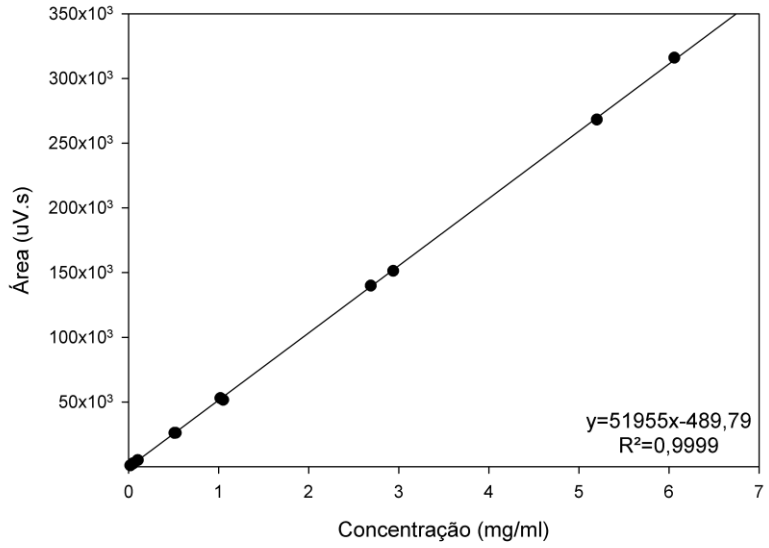

Figura 23 – Curva padrão para a determinação por cromatografia gasosa do composto acetato de eugenila.

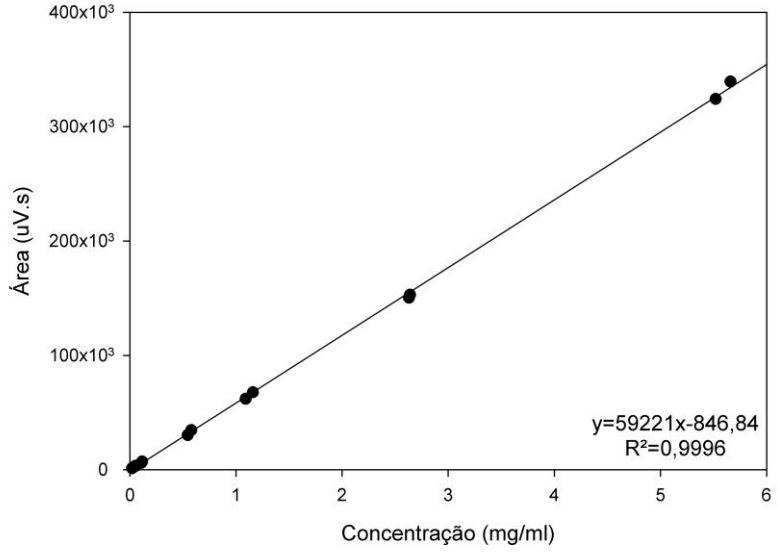

Figura 24 – Curva padrão para a determinação por cromatografia gasosa do composto eugenol.

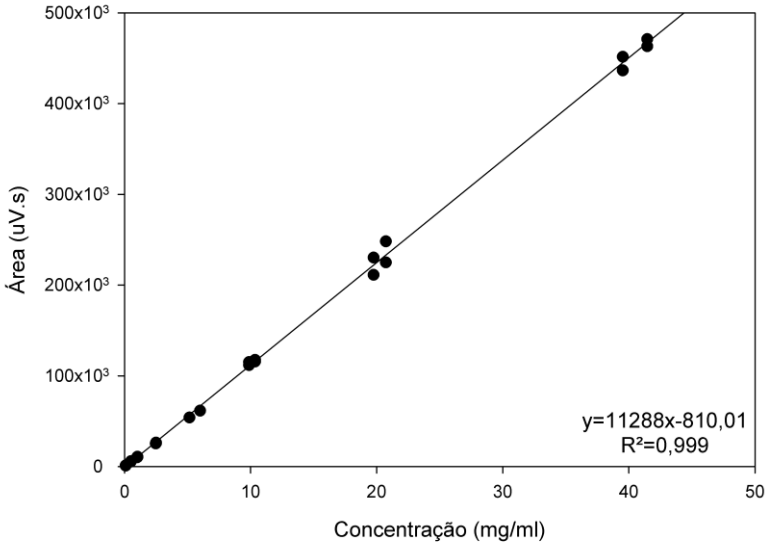

Figura 25 – Curva padrão para a determinação por cromatografia gasosa do composto álcool isoamílico.

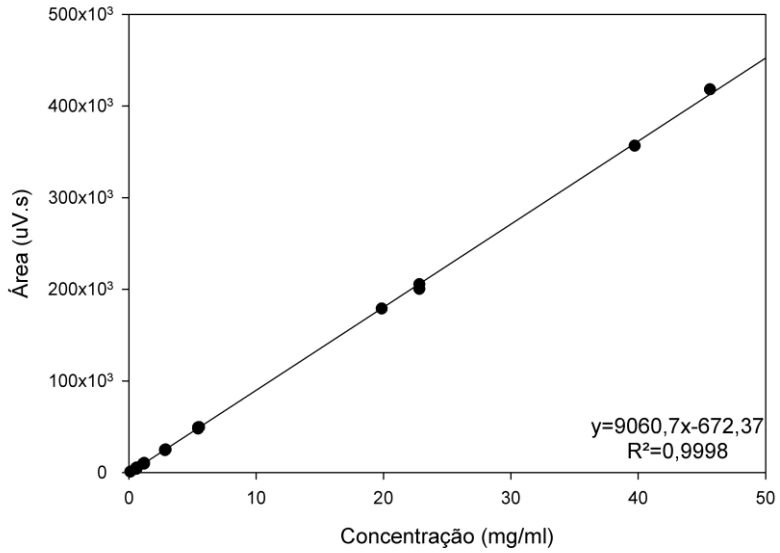

Figura 26 – Curva padrão para a determinação por cromatografia gasosa do composto acetato de isoamila.

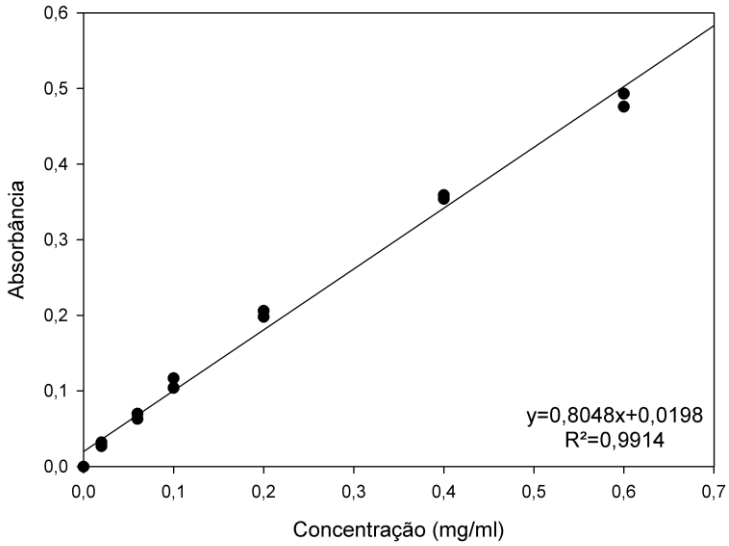

Figura 27 – Curva padrão de albumina para a determinação de proteína nos experimentos de caracterização da enzima imobilizada.

VII Cromatogramas

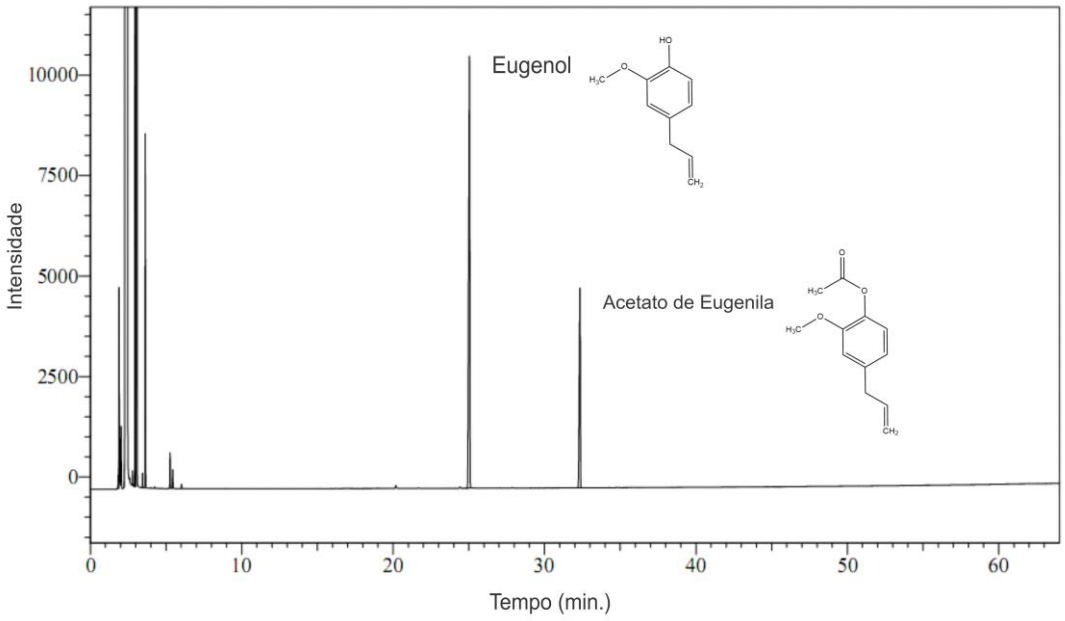

Figura 28 – Cromatograma (CG-FID) típico obtido nas análises de quantificação de eugenol (tempo de retenção de 25 min.) e acetato de eugenila (tempo de retenção de 32,3 min).

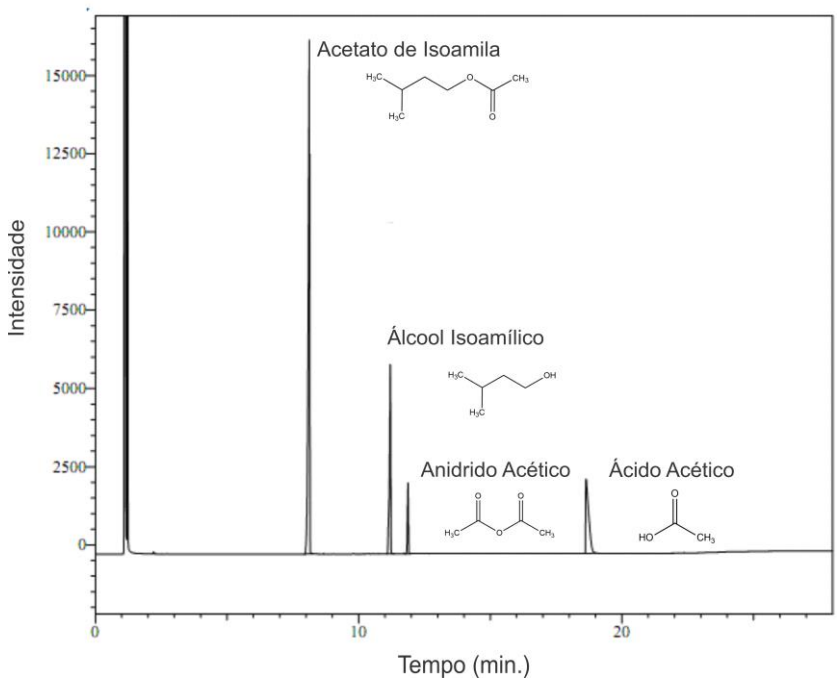

Figura 29 – Cromatograma (CG-FID) típico obtido nas análises de quantificação de acetato de isoamila (tempo de retenção de 8 min.), álcool isoamílico (11,1 min.), anidrido acético (11,8 min.) e ácido acético (18,7 min.).

Referências Bibliográficas

ASSIS, A. V. R. D. **Montagem, teste e validação de uma unidade de extração supercrítica com reciclo e operação contínua**. 2010. 152 (Doutorado). Departamento de Engenharia de Alimentos, Universidade Estadual de Campinas

BRUSSEL, V. U. Selection and representativity of the calibration sample subset. Vrije Universiteit Brussel - Departament of Analytical Chemistry and Pharmaceutical Technology, 2015. Disponível em: < http://www.vub.ac.be/fabi/publiek/index.html >. Acesso em: December 2015.

INCROPERA, F. P. e WITT, D. P. **Fundamentos da transferência de calor e de massa**. 3. LCT, 1992.

KERN, D. Q. **Processos de Transmissão de Calor**. Guanabara Koogan S.A., 1987.

NIST. **NIST Chemistry WebBook, NIST Standard Reference Database Number 69**. LINSTROM, P. J. e MALLARD, W. G.: National Institute of Standards and Technology 2005.

Memorial do Período de Doutorado

O doutorando Philipe dos Santos ingressou no curso de doutorado do Programa de Pós-Graduação em Engenharia de Alimentos da Faculdade de Engenharia de Alimentos da Universidade Estadual de Campinas, em agosto de 2013. Com auxilio financeiro do CNPq, cursou as seguintes disciplinas: TP132 - Métodos Matemáticos na Engenharia de Alimentos; IQ064 - Encapsulação de Agentes Bioativos; TP121- Tópicos em Engenharia de Alimentos; totalizando sete (7) créditos. Além disso, integralizou mais dez (10) créditos referentes à participação no Programa de Estágio Docente. Durante o período de doutorado publicou trabalhos em períodos internacionais e em anais de congressos nacionais e internacionais. As participações no Programa de Estágio Docente e os trabalhos publicados são listados a seguir.

Estágio de Capacitação Docente

Estágio de Capacitação Docente - PED C na disciplina de Instalações Industriais.
Estágio de Capacitação Docente - PED B na disciplina de Instalações Industriais.
Estágio de Capacitação Docente - PED C na disciplina de Instalações Industriais.
Estágio de Capacitação Docente - PED C na disciplina de Operações Unitárias II.

Artigos completos publicados em periódicos:

Santos, P.; Zabot, G. L.; Meireles, M. A. A.; Mazutti, M. A.; Martínez, J. Synthesis of eugenyl acetate by enzymatic reactions in supercritical carbon dioxide. Biochemical Engineering Journal, v. 114, p. 1-9, 2016.

Santos, P.; Rezende, C. A.; Martínez, J. Activity of immobilized lipase from Candida antarctica (Lipozyme 435) and its performance on the esterification of oleic acid in supercritical carbon dioxide. The Journal of Supercritical Fluids, v. 107, p. 170-178, 2015.

Santos, P.; Aguiar, A. C.; Viganó, J.; Boeing, J. S.; Visentainer, J. V.; Martínez, J. Supercritical CO_2 extraction of cumbaru oil (*Dipteryx alata* Vogel) assisted by ultrasound: Global yield, kinetics and fatty acid composition. The Journal of Supercritical Fluids, v. 107, p. 75-83, 2015.

Trabalhos completos publicados em anais de congressos

DIAS, A. L. B.; **Santos, P.**; Aguiar, A. C.; Barbero, G. F.; Martínez, J. Extração de pimenta malagueta (*Capsicum frutescens* L.) a baixa pressão assistida por ultrassom. In: XX Congresso Brasileiro de Engenharia Química, 2015, Florianópolis. Anais do XX Congresso Brasileiro de Engenharia Química. p. 4752.

Resumos publicados em anais de congressos

Santos, P.; Zabot, G. L.; Meireles, M. A. A.; Martinez, J.. Production of Eugenyl Acetate by Enzymatic Reactions in Supercritical Carbon Dioxide (CO_2). In: 11th International Symposium on Supercritical Fluids, 2015, Seoul. ISSF 2015, 2015.

Dias, A. L. B.; Sergio, C. S. A.; **Santos, P.**; Barbero, G. F.; Martinez, J. Supercritical Extraction of Dedo de Moça Pepper (*Capsicum baccatum* L. var. *pendulum*) Assisted by Ultrasound. In: ISSF 2015, 2015, Seoul. 11th International Symposium on Supercritical Fluids, 2015.

Santos, P.; Martínez, J. Production of Isoamyl Acetate By Enzymatic Reactions In Supercritical Carbon Dioxide (CO_2) - Development and Validation of a Reaction Unit. In: XVII World Congress on Food Science and Technology, 2014, Montreal. Proceedings of XVII IUFOST, 2014.

Aguiar, A. C.; **Santos, P.**; Rezende, C. A.; Martinez, J.Design and Assembly of a Laboratory-Scale Supercritical Anti-Solvent System (SAS and SFEE). In: 14th European Meeting On Supercritical Fluids, 2014, Marseille. 14th European Meeting On Supercritical Fluids, 2014.

ANEXOS

I Permissão para o uso do artigo correspondente ao capítulo 3

ELSEVIER LICENSE
TERMS AND CONDITIONS

Aug 10, 2016

This Agreement between Philipe dos Santos ("You") and Elsevier ("Elsevier") consists of your license details and the terms and conditions provided by Elsevier and Copyright Clearance Center.

License Number	3925470879693
License date	Aug 10, 2016
Licensed Content Publisher	Elsevier
Licensed Content Publication	The Journal of Supercritical Fluids
Licensed Content Title	Activity of immobilized lipase from Candida antarctica (Lipozyme 435) and its performance on the esterification of oleic acid in supercritical carbon dioxide
Licensed Content Author	Philipe dos Santos,Camila A. Rezende,Julian Martínez
Licensed Content Date	January 2016
Licensed Content Volume Number	107
Licensed Content Issue Number	n/a
Licensed Content Pages	9
Start Page	170
End Page	178
Type of Use	reuse in a thesis/dissertation
Intended publisher of new work	other
Portion	full article
Format	both print and electronic
Are you the author of this Elsevier article?	Yes
Will you be translating?	No
Order reference number	
Title of your thesis/dissertation	PRODUCTION OF ESTERS BY ENZYMATIC-CATALYZED REACTION IN SUPERCRITICAL CARBON DIOXIDE (CO2)
Expected completion date	Jan 2017
Estimated size (number of pages)	170
Elsevier VAT number	GB 494 6272 12
Requestor Location	Philipe dos Santos Cidade Universitária"Zeferino Vaz", s/n Campinas, other 13083-862 Brazil Attn:
Total	0.00 USD
Terms and Conditions	

INTRODUCTION

1. The publisher for this copyrighted material is Elsevier. By clicking "accept" in connection with completing this licensing transaction, you agree that the following terms and conditions apply to this transaction (along with the Billing and Payment terms and conditions established by Copyright Clearance Center, Inc. ("CCC"), at the time that you opened your Rightslink account and that are available at any time at http://myaccount.copyright.com).

GENERAL TERMS

2. Elsevier hereby grants you permission to reproduce the aforementioned material subject to the terms and conditions indicated.

3. Acknowledgement: If any part of the material to be used (for example, figures) has appeared in our publication with credit or acknowledgement to another source, permission must also be sought from that source. If such permission is not obtained then that material may not be included in your publication/copies. Suitable acknowledgement to the source must be made, either as a footnote or in a reference list at the end of your publication, as follows:

"Reprinted from Publication title, Vol /edition number, Author(s), Title of article / title of chapter, Pages No., Copyright (Year), with permission from Elsevier [OR APPLICABLE SOCIETY COPYRIGHT OWNER]." Also Lancet special credit - "Reprinted from The Lancet, Vol. number, Author(s), Title of article, Pages No., Copyright (Year), with permission from Elsevier."

4. Reproduction of this material is confined to the purpose and/or media for which permission is hereby given.

5. Altering/Modifying Material: Not Permitted. However figures and illustrations may be altered/adapted minimally to serve your work. Any other abbreviations, additions, deletions and/or any other alterations shall be made only with prior written authorization of Elsevier Ltd. (Please contact Elsevier at permissions@elsevier.com)

6. If the permission fee for the requested use of our material is waived in this instance, please be advised that your future requests for Elsevier materials may attract a fee.

7. Reservation of Rights: Publisher reserves all rights not specifically granted in the combination of (i) the license details provided by you and accepted in the course of this licensing transaction, (ii) these terms and conditions and (iii) CCC's Billing and Payment terms and conditions.

8. License Contingent Upon Payment: While you may exercise the rights licensed immediately upon issuance of the license at the end of the licensing process for the transaction, provided that you have disclosed complete and accurate details of your proposed use, no license is finally effective unless and until full payment is received from you (either by publisher or by CCC) as provided in CCC's Billing and Payment terms and conditions. If full payment is not received on a timely basis, then any license preliminarily granted shall be deemed automatically revoked and shall be void as if never granted. Further, in the event that you breach any of these terms and conditions or any of CCC's Billing and Payment terms and conditions, the license is automatically revoked and shall be void as if never granted. Use of materials as described in a revoked license, as well as any use of the materials beyond the scope of an unrevoked license, may constitute copyright infringement and publisher reserves the right to take any and all action to protect its copyright in the materials.

9. Warranties: Publisher makes no representations or warranties with respect to the licensed material.

10. Indemnity: You hereby indemnify and agree to hold harmless publisher and CCC, and their respective officers, directors, employees and agents, from and against any and all claims arising out of your use of the licensed material other than as specifically authorized pursuant to this license.

11. No Transfer of License: This license is personal to you and may not be sublicensed, assigned, or transferred by you to any other person without publisher's written permission.

12. No Amendment Except in Writing: This license may not be amended except in a writing signed by both parties (or, in the case of publisher, by CCC on publisher's behalf).

13. Objection to Contrary Terms: Publisher hereby objects to any terms contained in any purchase order, acknowledgment, check endorsement or other writing prepared by you, which terms are inconsistent with these terms and conditions or CCC's Billing and Payment terms and conditions. These terms and conditions, together with CCC's Billing and Payment

terms and conditions (which are incorporated herein), comprise the entire agreement between you and publisher (and CCC) concerning this licensing transaction. In the event of any conflict between your obligations established by these terms and conditions and those established by CCC's Billing and Payment terms and conditions, these terms and conditions shall control.

14. Revocation: Elsevier or Copyright Clearance Center may deny the permissions described in this License at their sole discretion, for any reason or no reason, with a full refund payable to you. Notice of such denial will be made using the contact information provided by you. Failure to receive such notice will not alter or invalidate the denial. In no event will Elsevier or Copyright Clearance Center be responsible or liable for any costs, expenses or damage incurred by you as a result of a denial of your permission request, other than a refund of the amount(s) paid by you to Elsevier and/or Copyright Clearance Center for denied permissions.

LIMITED LICENSE

The following terms and conditions apply only to specific license types:

15. **Translation**: This permission is granted for non-exclusive world **English** rights only unless your license was granted for translation rights. If you licensed translation rights you may only translate this content into the languages you requested. A professional translator must perform all translations and reproduce the content word for word preserving the integrity of the article.

16. **Posting licensed content on any Website**: The following terms and conditions apply as follows: Licensing material from an Elsevier journal: All content posted to the web site must maintain the copyright information line on the bottom of each image; A hyper-text must be included to the Homepage of the journal from which you are licensing at http://www.sciencedirect.com/science/journal/xxxxx or the Elsevier homepage for books at http://www.elsevier.com; Central Storage: This license does not include permission for a scanned version of the material to be stored in a central repository such as that provided by Heron/XanEdu.

Licensing material from an Elsevier book: A hyper-text link must be included to the Elsevier homepage at http://www.elsevier.com . All content posted to the web site must maintain the copyright information line on the bottom of each image.

Posting licensed content on Electronic reserve: In addition to the above the following clauses are applicable: The web site must be password-protected and made available only to bona fide students registered on a relevant course. This permission is granted for 1 year only. You may obtain a new license for future website posting.

17. **For journal authors:** the following clauses are applicable in addition to the above:

Preprints:

A preprint is an author's own write-up of research results and analysis, it has not been peer-reviewed, nor has it had any other value added to it by a publisher (such as formatting, copyright, technical enhancement etc.).

Authors can share their preprints anywhere at any time. Preprints should not be added to or enhanced in any way in order to appear more like, or to substitute for, the final versions of articles however authors can update their preprints on arXiv or RePEc with their Accepted Author Manuscript (see below).

If accepted for publication, we encourage authors to link from the preprint to their formal publication via its DOI. Millions of researchers have access to the formal publications on ScienceDirect, and so links will help users to find, access, cite and use the best available version. Please note that Cell Press, The Lancet and some society-owned have different preprint policies. Information on these policies is available on the journal homepage.

Accepted Author Manuscripts: An accepted author manuscript is the manuscript of an article that has been accepted for publication and which typically includes author-incorporated changes suggested during submission, peer review and editor-author communications.

Authors can share their accepted author manuscript:

- immediately
    - via their non-commercial person homepage or blog

- by updating a preprint in arXiv or RePEc with the accepted manuscript
- via their research institute or institutional repository for internal institutional uses or as part of an invitation-only research collaboration work-group
- directly by providing copies to their students or to research collaborators for their personal use
- for private scholarly sharing as part of an invitation-only work group on commercial sites with which Elsevier has an agreement

- after the embargo period
  - via non-commercial hosting platforms such as their institutional repository
  - via commercial sites with which Elsevier has an agreement

In all cases accepted manuscripts should:

- link to the formal publication via its DOI
- bear a CC-BY-NC-ND license - this is easy to do
- if aggregated with other manuscripts, for example in a repository or other site, be shared in alignment with our hosting policy not be added to or enhanced in any way to appear more like, or to substitute for, the published journal article.

Published journal article (JPA): A published journal article (PJA) is the definitive final record of published research that appears or will appear in the journal and embodies all value-adding publishing activities including peer review co-ordination, copy-editing, formatting, (if relevant) pagination and online enrichment.
Policies for sharing publishing journal articles differ for subscription and gold open access articles:
Subscription Articles: If you are an author, please share a link to your article rather than the full-text. Millions of researchers have access to the formal publications on ScienceDirect, and so links will help your users to find, access, cite, and use the best available version.
Theses and dissertations which contain embedded PJAs as part of the formal submission can be posted publicly by the awarding institution with DOI links back to the formal publications on ScienceDirect.
If you are affiliated with a library that subscribes to ScienceDirect you have additional private sharing rights for others' research accessed under that agreement. This includes use for classroom teaching and internal training at the institution (including use in course packs and courseware programs), and inclusion of the article for grant funding purposes.
Gold Open Access Articles: May be shared according to the author-selected end-user license and should contain a CrossMark logo, the end user license, and a DOI link to the formal publication on ScienceDirect.
Please refer to Elsevier's posting policy for further information.
18. **For book authors** the following clauses are applicable in addition to the above:
Authors are permitted to place a brief summary of their work online only. You are not allowed to download and post the published electronic version of your chapter, nor may you scan the printed edition to create an electronic version. **Posting to a repository:** Authors are permitted to post a summary of their chapter only in their institution's repository.
19. **Thesis/Dissertation**: If your license is for use in a thesis/dissertation your thesis may be submitted to your institution in either print or electronic form. Should your thesis be published commercially, please reapply for permission. These requirements include permission for the Library and Archives of Canada to supply single copies, on demand, of the complete thesis and include permission for Proquest/UMI to supply single copies, on demand, of the complete thesis. Should your thesis be published commercially, please reapply for permission. Theses and dissertations which contain embedded PJAs as part of the formal submission can be posted publicly by the awarding institution with DOI links back to the formal publications on ScienceDirect.

Elsevier Open Access Terms and Conditions
You can publish open access with Elsevier in hundreds of open access journals or in nearly 2000 established subscription journals that support open access publishing. Permitted third

party re-use of these open access articles is defined by the author's choice of Creative Commons user license. See our open access license policy for more information.

Terms & Conditions applicable to all Open Access articles published with Elsevier:

Any reuse of the article must not represent the author as endorsing the adaptation of the article nor should the article be modified in such a way as to damage the author's honour or reputation. If any changes have been made, such changes must be clearly indicated.

The author(s) must be appropriately credited and we ask that you include the end user license and a DOI link to the formal publication on ScienceDirect.

If any part of the material to be used (for example, figures) has appeared in our publication with credit or acknowledgement to another source it is the responsibility of the user to ensure their reuse complies with the terms and conditions determined by the rights holder.

Additional Terms & Conditions applicable to each Creative Commons user license:

CC BY: The CC-BY license allows users to copy, to create extracts, abstracts and new works from the Article, to alter and revise the Article and to make commercial use of the Article (including reuse and/or resale of the Article by commercial entities), provided the user gives appropriate credit (with a link to the formal publication through the relevant DOI), provides a link to the license, indicates if changes were made and the licensor is not represented as endorsing the use made of the work. The full details of the license are available at http://creativecommons.org/licenses/by/4.0.

CC BY NC SA: The CC BY-NC-SA license allows users to copy, to create extracts, abstracts and new works from the Article, to alter and revise the Article, provided this is not done for commercial purposes, and that the user gives appropriate credit (with a link to the formal publication through the relevant DOI), provides a link to the license, indicates if changes were made and the licensor is not represented as endorsing the use made of the work. Further, any new works must be made available on the same conditions. The full details of the license are available at http://creativecommons.org/licenses/by-nc-sa/4.0.

CC BY NC ND: The CC BY-NC-ND license allows users to copy and distribute the Article, provided this is not done for commercial purposes and further does not permit distribution of the Article if it is changed or edited in any way, and provided the user gives appropriate credit (with a link to the formal publication through the relevant DOI), provides a link to the license, and that the licensor is not represented as endorsing the use made of the work. The full details of the license are available at http://creativecommons.org/licenses/by-nc-nd/4.0.

Any commercial reuse of Open Access articles published with a CC BY NC SA or CC BY NC ND license requires permission from Elsevier and will be subject to a fee.

Commercial reuse includes:

- Associating advertising with the full text of the Article
- Charging fees for document delivery or access
- Article aggregation
- Systematic distribution via e-mail lists or share buttons

Posting or linking by commercial companies for use by customers of those companies.

20. **Other Conditions**:

v1.8

Questions? customercare@copyright.com or +1-855-239-3415 (toll free in the US) or +1-978-646-2777.

II Permissão para o uso do artigo correspondente ao capítulo 4

ELSEVIER LICENSE
TERMS AND CONDITIONS

Aug 10, 2016

This Agreement between Philipe dos Santos ("You") and Elsevier ("Elsevier") consists of your license details and the terms and conditions provided by Elsevier and Copyright Clearance Center.

License Number	3925470754008
License date	Aug 10, 2016
Licensed Content Publisher	Elsevier
Licensed Content Publication	Biochemical Engineering Journal
Licensed Content Title	Synthesis of eugenyl acetate by enzymatic reactions in supercritical carbon dioxide
Licensed Content Author	Philipe dos Santos,Giovani L. Zabot,M. Angela A. Meireles,Marcio A. Mazutti,Julian Martínez
Licensed Content Date	15 October 2016
Licensed Content Volume Number	114
Licensed Content Issue Number	n/a
Licensed Content Pages	9
Start Page	1
End Page	9
Type of Use	reuse in a thesis/dissertation
Intended publisher of new work	other
Portion	full article
Format	both print and electronic
Are you the author of this Elsevier article?	Yes
Will you be translating?	No
Order reference number	
Title of your thesis/dissertation	PRODUCTION OF ESTERS BY ENZYMATIC-CATALYZED REACTION IN SUPERCRITICAL CARBON DIOXIDE (CO2)
Expected completion date	Jan 2017
Estimated size (number of pages)	170
Elsevier VAT number	GB 494 6272 12
Requestor Location	Philipe dos Santos Cidade Universitária"Zeferino Vaz", s/n Campinas, other 13083-862 Brazil Attn:
Total	0.00 USD
Terms and Conditions	

INTRODUCTION

1. The publisher for this copyrighted material is Elsevier. By clicking "accept" in connection with completing this licensing transaction, you agree that the following terms and conditions apply to this transaction (along with the Billing and Payment terms and conditions established by Copyright Clearance Center, Inc. ("CCC"), at the time that you opened your Rightslink account and that are available at any time at http://myaccount.copyright.com).

GENERAL TERMS

2. Elsevier hereby grants you permission to reproduce the aforementioned material subject to the terms and conditions indicated.

3. Acknowledgement: If any part of the material to be used (for example, figures) has appeared in our publication with credit or acknowledgement to another source, permission must also be sought from that source. If such permission is not obtained then that material may not be included in your publication/copies. Suitable acknowledgement to the source must be made, either as a footnote or in a reference list at the end of your publication, as follows:

"Reprinted from Publication title, Vol /edition number, Author(s), Title of article / title of chapter, Pages No., Copyright (Year), with permission from Elsevier [OR APPLICABLE SOCIETY COPYRIGHT OWNER]." Also Lancet special credit - "Reprinted from The Lancet, Vol. number, Author(s), Title of article, Pages No., Copyright (Year), with permission from Elsevier."

4. Reproduction of this material is confined to the purpose and/or media for which permission is hereby given.

5. Altering/Modifying Material: Not Permitted. However figures and illustrations may be altered/adapted minimally to serve your work. Any other abbreviations, additions, deletions and/or any other alterations shall be made only with prior written authorization of Elsevier Ltd. (Please contact Elsevier at permissions@elsevier.com)

6. If the permission fee for the requested use of our material is waived in this instance, please be advised that your future requests for Elsevier materials may attract a fee.

7. Reservation of Rights: Publisher reserves all rights not specifically granted in the combination of (i) the license details provided by you and accepted in the course of this licensing transaction, (ii) these terms and conditions and (iii) CCC's Billing and Payment terms and conditions.

8. License Contingent Upon Payment: While you may exercise the rights licensed immediately upon issuance of the license at the end of the licensing process for the transaction, provided that you have disclosed complete and accurate details of your proposed use, no license is finally effective unless and until full payment is received from you (either by publisher or by CCC) as provided in CCC's Billing and Payment terms and conditions. If full payment is not received on a timely basis, then any license preliminarily granted shall be deemed automatically revoked and shall be void as if never granted. Further, in the event that you breach any of these terms and conditions or any of CCC's Billing and Payment terms and conditions, the license is automatically revoked and shall be void as if never granted. Use of materials as described in a revoked license, as well as any use of the materials beyond the scope of an unrevoked license, may constitute copyright infringement and publisher reserves the right to take any and all action to protect its copyright in the materials.

9. Warranties: Publisher makes no representations or warranties with respect to the licensed material.

10. Indemnity: You hereby indemnify and agree to hold harmless publisher and CCC, and their respective officers, directors, employees and agents, from and against any and all claims arising out of your use of the licensed material other than as specifically authorized pursuant to this license.

11. No Transfer of License: This license is personal to you and may not be sublicensed, assigned, or transferred by you to any other person without publisher's written permission.

12. No Amendment Except in Writing: This license may not be amended except in a writing signed by both parties (or, in the case of publisher, by CCC on publisher's behalf).

13. Objection to Contrary Terms: Publisher hereby objects to any terms contained in any purchase order, acknowledgment, check endorsement or other writing prepared by you, which terms are inconsistent with these terms and conditions or CCC's Billing and Payment terms and conditions. These terms and conditions, together with CCC's Billing and Payment

terms and conditions (which are incorporated herein), comprise the entire agreement between you and publisher (and CCC) concerning this licensing transaction. In the event of any conflict between your obligations established by these terms and conditions and those established by CCC's Billing and Payment terms and conditions, these terms and conditions shall control.

14. Revocation: Elsevier or Copyright Clearance Center may deny the permissions described in this License at their sole discretion, for any reason or no reason, with a full refund payable to you. Notice of such denial will be made using the contact information provided by you. Failure to receive such notice will not alter or invalidate the denial. In no event will Elsevier or Copyright Clearance Center be responsible or liable for any costs, expenses or damage incurred by you as a result of a denial of your permission request, other than a refund of the amount(s) paid by you to Elsevier and/or Copyright Clearance Center for denied permissions.

LIMITED LICENSE

The following terms and conditions apply only to specific license types:

15. **Translation**: This permission is granted for non-exclusive world **English** rights only unless your license was granted for translation rights. If you licensed translation rights you may only translate this content into the languages you requested. A professional translator must perform all translations and reproduce the content word for word preserving the integrity of the article.

16. **Posting licensed content on any Website**: The following terms and conditions apply as follows: Licensing material from an Elsevier journal: All content posted to the web site must maintain the copyright information line on the bottom of each image; A hyper-text must be included to the Homepage of the journal from which you are licensing at http://www.sciencedirect.com/science/journal/xxxxx or the Elsevier homepage for books at http://www.elsevier.com; Central Storage: This license does not include permission for a scanned version of the material to be stored in a central repository such as that provided by Heron/XanEdu.

Licensing material from an Elsevier book: A hyper-text link must be included to the Elsevier homepage at http://www.elsevier.com . All content posted to the web site must maintain the copyright information line on the bottom of each image.

Posting licensed content on Electronic reserve: In addition to the above the following clauses are applicable: The web site must be password-protected and made available only to bona fide students registered on a relevant course. This permission is granted for 1 year only. You may obtain a new license for future website posting.

17. **For journal authors:** the following clauses are applicable in addition to the above:

Preprints:

A preprint is an author's own write-up of research results and analysis, it has not been peer-reviewed, nor has it had any other value added to it by a publisher (such as formatting, copyright, technical enhancement etc.).

Authors can share their preprints anywhere at any time. Preprints should not be added to or enhanced in any way in order to appear more like, or to substitute for, the final versions of articles however authors can update their preprints on arXiv or RePEc with their Accepted Author Manuscript (see below).

If accepted for publication, we encourage authors to link from the preprint to their formal publication via its DOI. Millions of researchers have access to the formal publications on ScienceDirect, and so links will help users to find, access, cite and use the best available version. Please note that Cell Press, The Lancet and some society-owned have different preprint policies. Information on these policies is available on the journal homepage.

Accepted Author Manuscripts: An accepted author manuscript is the manuscript of an article that has been accepted for publication and which typically includes author-incorporated changes suggested during submission, peer review and editor-author communications.

Authors can share their accepted author manuscript:

- immediately
    - via their non-commercial person homepage or blog

- by updating a preprint in arXiv or RePEc with the accepted manuscript
- via their research institute or institutional repository for internal institutional uses or as part of an invitation-only research collaboration work-group
- directly by providing copies to their students or to research collaborators for their personal use
- for private scholarly sharing as part of an invitation-only work group on commercial sites with which Elsevier has an agreement

- after the embargo period
  - via non-commercial hosting platforms such as their institutional repository
  - via commercial sites with which Elsevier has an agreement

In all cases accepted manuscripts should:

- link to the formal publication via its DOI
- bear a CC-BY-NC-ND license - this is easy to do
- if aggregated with other manuscripts, for example in a repository or other site, be shared in alignment with our hosting policy not be added to or enhanced in any way to appear more like, or to substitute for, the published journal article.

Published journal article (JPA): A published journal article (PJA) is the definitive final record of published research that appears or will appear in the journal and embodies all value-adding publishing activities including peer review co-ordination, copy-editing, formatting, (if relevant) pagination and online enrichment.
Policies for sharing publishing journal articles differ for subscription and gold open access articles:
Subscription Articles: If you are an author, please share a link to your article rather than the full-text. Millions of researchers have access to the formal publications on ScienceDirect, and so links will help your users to find, access, cite, and use the best available version.
Theses and dissertations which contain embedded PJAs as part of the formal submission can be posted publicly by the awarding institution with DOI links back to the formal publications on ScienceDirect.
If you are affiliated with a library that subscribes to ScienceDirect you have additional private sharing rights for others' research accessed under that agreement. This includes use for classroom teaching and internal training at the institution (including use in course packs and courseware programs), and inclusion of the article for grant funding purposes.
Gold Open Access Articles: May be shared according to the author-selected end-user license and should contain a CrossMark logo, the end user license, and a DOI link to the formal publication on ScienceDirect.
Please refer to Elsevier's posting policy for further information.
18. **For book authors** the following clauses are applicable in addition to the above:
Authors are permitted to place a brief summary of their work online only. You are not allowed to download and post the published electronic version of your chapter, nor may you scan the printed edition to create an electronic version. **Posting to a repository:** Authors are permitted to post a summary of their chapter only in their institution's repository.
19. **Thesis/Dissertation**: If your license is for use in a thesis/dissertation your thesis may be submitted to your institution in either print or electronic form. Should your thesis be published commercially, please reapply for permission. These requirements include permission for the Library and Archives of Canada to supply single copies, on demand, of the complete thesis and include permission for Proquest/UMI to supply single copies, on demand, of the complete thesis. Should your thesis be published commercially, please reapply for permission. Theses and dissertations which contain embedded PJAs as part of the formal submission can be posted publicly by the awarding institution with DOI links back to the formal publications on ScienceDirect.

Elsevier Open Access Terms and Conditions
You can publish open access with Elsevier in hundreds of open access journals or in nearly 2000 established subscription journals that support open access publishing. Permitted third

party re-use of these open access articles is defined by the author's choice of Creative Commons user license. See our open access license policy for more information.

Terms & Conditions applicable to all Open Access articles published with Elsevier:

Any reuse of the article must not represent the author as endorsing the adaptation of the article nor should the article be modified in such a way as to damage the author's honour or reputation. If any changes have been made, such changes must be clearly indicated.

The author(s) must be appropriately credited and we ask that you include the end user license and a DOI link to the formal publication on ScienceDirect.

If any part of the material to be used (for example, figures) has appeared in our publication with credit or acknowledgement to another source it is the responsibility of the user to ensure their reuse complies with the terms and conditions determined by the rights holder.

Additional Terms & Conditions applicable to each Creative Commons user license:

CC BY: The CC-BY license allows users to copy, to create extracts, abstracts and new works from the Article, to alter and revise the Article and to make commercial use of the Article (including reuse and/or resale of the Article by commercial entities), provided the user gives appropriate credit (with a link to the formal publication through the relevant DOI), provides a link to the license, indicates if changes were made and the licensor is not represented as endorsing the use made of the work. The full details of the license are available at http://creativecommons.org/licenses/by/4.0.

CC BY NC SA: The CC BY-NC-SA license allows users to copy, to create extracts, abstracts and new works from the Article, to alter and revise the Article, provided this is not done for commercial purposes, and that the user gives appropriate credit (with a link to the formal publication through the relevant DOI), provides a link to the license, indicates if changes were made and the licensor is not represented as endorsing the use made of the work. Further, any new works must be made available on the same conditions. The full details of the license are available at http://creativecommons.org/licenses/by-nc-sa/4.0.

CC BY NC ND: The CC BY-NC-ND license allows users to copy and distribute the Article, provided this is not done for commercial purposes and further does not permit distribution of the Article if it is changed or edited in any way, and provided the user gives appropriate credit (with a link to the formal publication through the relevant DOI), provides a link to the license, and that the licensor is not represented as endorsing the use made of the work. The full details of the license are available at http://creativecommons.org/licenses/by-nc-nd/4.0.

Any commercial reuse of Open Access articles published with a CC BY NC SA or CC BY NC ND license requires permission from Elsevier and will be subject to a fee.

Commercial reuse includes:

- Associating advertising with the full text of the Article
- Charging fees for document delivery or access
- Article aggregation
- Systematic distribution via e-mail lists or share buttons

Posting or linking by commercial companies for use by customers of those companies.

20. **Other Conditions**:

v1.8

Questions? customercare@copyright.com or +1-855-239-3415 (toll free in the US) or +1-978-646-2777.